Booklet of Abstracts

"2nd International Conference on Mathematical Modelling in Mechanics and Engineering"

Mathematical Institute of the Serbian Academy of Sciences and Arts
Belgrade, 12.-14. September 2024.

Editor: Ivana Atanasovska

Supported by:

Ministry of Science, Technological Development and Innovation, Republic of Serbia

METALFER STEEL MILL, Serbia

SHIMADZU, Serbia

eCon Engineering Kft, Hungary

SVECOM, Beograd, Serbia

"PROJEKTINŽENJERING TIM", Niš, Serbia

AMING PROJEKT, Knjaževac, Serbia

BREGAVA, Beograd, Serbia

Organized by:

Mathematical Institute of the Serbian Academy of Sciences and Arts

Faculty of Mechanical Engineering, University of Belgrade

Faculty of Mechanical and Civil Engineering in Kraljevo, University of Kragujevac

Scientific Society for Engineering Design, Simulations and Innovations

Belgrade, 2024

Booklet of abstracts of the "2nd International Conference on Mathematical Modelling in Mechanics and Engineering", Belgrade, 12.-14. September 2024.

https://www.mi.sanu.ac.rs/~icme/icme2024/

Editor: Ivana Atanasovska

Publisher: Mathematical Institute of the Serbian Academy of Sciences and Arts, Belgrade

Printed by: CopyPlanet, Belgrade, Serbia

Circulation: 130 copies

ISBN 978-86-80593-77-7

Publishing year: 2024.

CONFERENCE COMMITTEES

International Scientific Committee

Prof. Teodor Atanacković (Academician of the Serbian Academy of Sciences and Arts; Faculty of Technical Sciences, University of Novi Sad, Serbia)

Prof. Miloš Kojić (Academician of the Serbian Academy of Sciences and Arts, Serbia; The Methodist Hospital Research Institute, Houston, USA)

Prof. Miodrag Mihaljević (Academician of the Serbian Academy of Sciences and Arts; Mathematical Institute SANU, Belgrade, Serbia)

Prof. Livija Cvetićanin (Faculty of Technical Sciences, University of Novi Sad, Serbia; Obuda University in Budapest, Hungary)

Prof. Sondipon Adhikari (University of Glasgow, UK)

Dr. Zoran Ognjanović (Mathematical Institute SANU, Belgrade, Serbia)

Prof. Ivana Kovačić (Faculty of Technical Sciences, University of Novi Sad, Serbia)

Prof. Chiara Bisagni (Delft University of Technology, Netherlands)

Prof. Pedro Leal Ribeiro (University of Porto, Portugal)

Prof. Emil Manoach (Institute of Mechanics, Bulgarian Academy of Sciences, Bulgaria)

Prof. Christos Spitas (School of Aerospace Engineering, Department of Mechanical, Materials and Manufacturing Engineering, University of Nottingham, Ningbo, China)

Prof. Vitaly Samsonov (Lomonosov Moscow State University, Russia)

Prof. Aleksandar Obradović (Faculty of Mechanical Engineering, University of Belgrade, Serbia)

Prof. Wei Li (School of Mathematics and Statistics, Xidian University, China)

Dr. Andrea Ianiro (Bioengineering and Aerospace Engineering Department, Carlos III University of Madrid, Spain)

Prof. Mihailo Lazarević (Faculty of Mechanical Engineering, University of Belgrade, Serbia)

Prof. Jelena Andrić (Volvo Group AB, Göteborg, Sweden)

Prof. Mihailo Jovanović (Viterbi School of Engineering, University of Southern California, USA)

Prof. Mile Savković (Faculty of Mechanical Engineering and Civil Engineering in Kraljevo, University of Kragujevac, Serbia)

Prof. Vasilios Spitas (National Technical University of Athens, Greece)

Prof. Miroslav Živković (Faculty of Engineering, University of Kragujevac, Serbia)

Prof. Marina Trajković Milenković (Faculty of Civil Engineering and Architecture, University of Niš, Serbia)

Prof. Saravanan Karuppanan (Mechanical Engineering Department, Universiti Teknologi PETRONAS, Malaysia)

Prof. Miha Brojan (Faculty of Mechanical Engineering, University of Ljubljana, Slovenia)

Prof. Lobna Said (School of Engineering and Applied Science, Nile University, Egypt)

Prof. Victor Roda-Casanova (Department of Mechanical Engineering and Construction, Universitat Jaume I, Spain)

Prof. Nenad Filipović (Faculty of Engineering, University of Kragujevac, Serbia)

Prof. Dongmei Huang (School of Mathematics and Statistic, Xidian University, China)

Prof. Nataša Trišović (Faculty of Mechanical Engineering, University of Belgrade, Serbia)

Prof. Vadim A. Krysko (Yuri Gagarin State Technical University of Saratov, Russia)

Prof. Tatjana Lazović (Faculty of Mechanical Engineering, University of Belgrade, Serbia)

Prof. Mohd. Rizwanullah (Department of Mathematics, Manipal University Jaipur, India)

Dr. Dejan Momčilović (Innovation Center of the Faculty of Mechanical Engineering, University of Belgrade, Serbia)

Prof. Dharmendra Tripathi (National Institute of Technology, Uttarakhand, India)

Prof. Santosh Patil (Manipal University Jaipur, India)

Prof. Radovan Bulatović (Faculty of Mechanical Engineering and Civil Engineering in Kraljevo, University of Kragujevac, Serbia)

Prof. Slaviša Šalinić (Faculty of Mechanical Engineering and Civil Engineering in Kraljevo, University of Kragujevac, Serbia)

Prof. Bojana Rosić (Applied Mechanics & Data Analysis group, University of Twente, Netherland)

Dr. Ana Pavlović (Department of Industrial Engineering, University of Bologna, Italy)

Prof. Milan Bižić (Faculty of Mechanical Engineering and Civil Engineering in Kraljevo, University of Kragujevac, Serbia)

Dr. Hammoudi Abderazek (Mechanics Research Center CRM, Constantine, Algeria)

Dr. Snežana Vulović (Institute of Information Technologies, University of Kragujevac, Serbia)

Prof. Jelena Svorcan (Faculty of Mechanical Engineering, University of Belgrade, Serbia)

Prof. Đorđe Čantrak (Faculty of Mechanical Engineering, University of Belgrade, Serbia)

Dr. Ivana Atanasovska (Mathematical Institute SANU, Belgrade, Serbia)

Reviewers

The received abstracts are reviewed by the International Scientific Committee

Organizing Committee

Dr. Ivana Atanasovska - Chair (Mathematical Institute SANU, Belgrade, Serbia)

Dr. Danilo Karličić (Mathematical Institute SANU, Belgrade, Serbia)

Dr. Milan Cajić (Mathematical Institute SANU, Belgrade, Serbia)

Dr. Dejan Momčilović (Innovation Center of the Faculty of Mechanical Engineering, University of Belgrade, Serbia)

Dr. Andrija Zorić (Faculty of Civil Engineering and Architecture, University of Niš, Serbia)

Dr. Miloš Sedak (Faculty of Mechanical Engineering, University of Belgrade, Serbia)

Dr. Stepa Paunović (Mathematical Institute SANU, Belgrade, Serbia)

Gordana Nastić (Mathematical Institute SANU, Belgrade, Serbia)

Pavle Ljubojević (Faculty of Mechanical Engineering, University of Belgrade, Serbia)

Ivan Simonović (Faculty of Mechanical Engineering, University of Belgrade, Serbia)

Ivana Cvetković (Faculty of Mechanical Engineering, University of Belgrade, Serbia)

Jovana Stojić (Faculty of Mechanical Engineering, University of Belgrade, Serbia)

PREFACE

It's my pleasure to introduce the "2nd International Conference on Mathematical Modelling in Mechanics and Engineering", organized by the Mathematical Institute of the Serbian Academy of Sciences and Arts and co-organized by the Faculty of Mechanical Engineering, University of Belgrade; the Faculty of Mechanical and Civil Engineering in Kraljevo, University of Kragujevac; and the Scientific Society for Engineering Design, Simulations and Innovations. The conference will be held in the hybrid form at the Mathematical Institute of the Serbian Academy of Sciences and Arts, Belgrade, Serbia, from the 12th to the 14th of September 2024.

This conference is planned as the second event in the series of conferences, which is planned to be held every two years and bring together leading academic scientists, researchers, and research scholars to exchange and share experience and research results on various aspects of mathematical modelling in mechanics and engineering. It will keep an interdisciplinary platform for researchers, practitioners and educators to present and discuss the most recent innovations, theories, and algorithms, as well as practical challenges encountered and solutions adopted in the fields of Classical Mechanics, Solid and Fluid Mechanics, Computational Mechanics, Biomechanics, Applied Mathematics and Physics, Structural Mechanics and Engineering. A considerable number of prominent scientists and professors submitted their abstracts and confirmed their attendance at the conference. The scientists and researchers from different countries in Europe and the world (Netherlands, Greece, Spain, Russia, USA, China, Kazakhstan, Italy, India, Malaysia, Slovenia, Bulgaria, Algeria etc.) also have confirmed participation at the conference. The conference presentations will cover development of analytical and numerical methods for effective simulations of different complex problems in mechanical engineering based on multiscale problems, from nano to macro-scales, analytical/numerical and data driven solutions to study complex media, composite aerospace and periodic structures and metamaterials, and capture essential features of linear and nonlinear dynamics that can lead to new designs of such systems. Some presentations will include new experimental setups to study engineering materials and novel control strategies based on classical or fractional derivative models used to control the dynamics of multibody, flexible and/or electromechanical systems. Finally, I believe that the sessions' discussions will have high potential to give significant contributions to the development of new and advanced mathematical models of real-world engineering mechanical systems.

On behalf of the Organizing Committee, I am very proud to announce that the number of accepted contributions to be presented at this Conference is 127, with 7 plenary and 7 invited lecture presentations. We would like to express our gratitude to the institutions that support the conference financially: The Ministry of Science, Technological Development and Innovation, Republic of Serbia; METALFER STEEL MILL, Serbia; SHIMADZU, Serbia; eCon Engineering Kft, Hungary; SVECOM, Beograd, Serbia; "PROJEKTINŽENJERING TIM", Niš, Serbia; AMING PROJEKT, Knjaževac, Serbia; BREGAVA, Beograd, Serbia. We are especially grateful to the members of the International Scientific Committee who contributed to this international scientific meeting with their advices and abstracts' reviews. We also thank the support of the co-organizers of this Conference.

I would also like to express special gratitude to the Department of Technical Sciences SANU, the Scientific Board of the Mathematical Institute of the Serbian Academy of Sciences and Arts, and the family of Academician Prof. Dr. Vladan Djordjevic for their support in organizing the Special session within this conference dedicated to the memory of Academician Prof. Dr. Vladan Djordjevic and establish the "Prof. Vladan Djordjevic" award for young scientists aged up to 35 contributing in the field of fluid mechanics.

I hope that this conference will be successful, at least as the first in this series of international conferences. I wish all participants a successful presentation of their scientific results.

Cordially,

Ivana Atanasovska, Conference Chair

CONTENTS

GENERAL SESSIONS

PLENARY LECTURES

NON-LOCAL ONE DIMENSIONAL ELASTICITY WITH GENERAL FRACTIONAL DERIVATIVES OF RIESZ TYPE

Teodor Atanackovic[1]

[1]*Faculty of Technical Sciences University of Technical Sciences, Novi Sad, Serbia*

[1]atanackovic@uns.ac.rs

[1]ORCID iD: 0000-0002-8714-1388

ABSTRACT

We analyze, spatially one dimensional, non-local elastic body with deformation measure given in the form of General fractional derivative of Riesz type with truncated power-law kernel. It is assumed that stress at the point x and time t depends on the strain at x and time t and weighted strain at point ξ at time $t-\frac{|x-\xi|}{c}$, where c is a constant having dimension of time. Several special linear constitutive equations follow form one that we propose. We formulate equation of motion for such a body and show the influence of the parameter c on the solution for special type of boundary and initial conditions.

MODELING OF A VIBRATION ROBOT WITH AN UNBALANCED ROTOR AND FLYWHEELS

Marat Z. Dosaev[1]

[1]*Institute of Mechanics of Lomonosov Moscow State University, 119192 Moscow, Russia*

[1]*dosayev@imec.msu.ru*

[1]ORCID iD: 0000-0002-3859-4065

Keywords: vibration robot, dry friction, unbalanced rotor, flywheel, control algorithm.

ABSTRACT

A mechanical system with a variable internal configuration is considered. The system is a capsule robot containing flywheels and an unbalanced rotor. The robot body rests on a rough plane at two or three points. The movement of the robot body along the support plane occurs due to the controlled rotation of the internal unbalanced rotor and flywheels, as well as due to dry friction at the support points.

A mathematical model of the system was constructed. The fundamental possibility of controlling the unbalanced rotor is shown, the result of which is the robot jumping and its displacement in the longitudinal direction. The movement of the imbalance is divided into two types of stages: the acceleration stage and the "jump" stage.

With the selected control algorithm, the unbalanced rotor implements a controlled change in the support reactions, and the rotation of the flywheels allows you to maintain the orientation of the body.

With an arbitrary arrangement of internal rotating elements inside the robot body, the value of the control angular acceleration of the flywheels can be large. A robot configuration has been proposed that makes it possible to significantly reduce the magnitude of angular accelerations during the implementation of the control algorithm.

REFERENCES

[1] Dosaev, M., Samsonov, V., Hwang, S. S. (2021) "Construction of control algorithm in the problem of the planar motion of a friction-powered robot with a flywheel and an eccentric weight," Applied Mathematical Modelling, 89. pp. 1517-1527.

[2] Dosaev, M. (2022) "Algorithm for controlling an inertioid robot with a flywheel and an unbalance in conditions of restrictions on the angular acceleration of the unbalance," Applied Mathematical Modelling, 109, pp. 797-807.

SOME COUPLED PROBLEMS IN DYNAMICS OF ELASTIC BODIES

Emil Manoach[1],

[1] *Institute of Mechanics, Bulgarian Academy of Science ,Acad. G. Bonchev Street, bl. 4, 1113 Sofia, Bulgaria*

[1]e.manoach@imbm.bas.bg

[1]ORCID iD: 0000-0002-9571-8618

Keywords: Thermo-elasticity, Fluid-Structures interaction, Energy harvesting.

ABSTRACT

Structural elements and multiple devices are very often subjected to coupled external influences, i.e. bodies are subjected to the action of conjugate fields.. The current work aims to show the complex phenomena that induce coupled fields in dynamically loaded structures. Three different problems will be considered and mathematical description and numerical examples will be presented for each of them.

The first case of coupled fields that will be presented is the problems of thermoelastic oscillations of structures, and the cases of structures with elevated temperature or structures subjected to heat flows will be considered. At the second case full coupling of the elastic and thermal fields will be investigated - the influence of temperature on the dynamic mechanical fields, as well as the influence of mechanical deformations/stresses on the propagation of the temperature (see [1]-[3]).

The second case of coupled interactions that will be presented is the interaction of electric and elastic fields. Here, the goal is to extract energy from external influences - mechanical vibrations - through the piezoelectric properties of materials. An example of energy harvesting device will be presented and the influence of the different parameters of geometry and placement of the PZT on the amount of the collected electrical energy will be shown. (4], [5].

The interaction of rarefied gas flows with elastic structures is the third coupled phenomenon which is studied in this work. A hybrid approach based on DSMC method and finite difference method is used to study the interaction of gas with a cantilever in a micro-channel. Special case for vortex-induced vibration is studied in details. The application of the developed method in micro-electronics and energy harvesting devices is presented. [6]-[8].

REFERENCES

[1] Manoach, E., Ribeiro, P. (2004) Coupled, thermoelastic, large amplitude vibrations of Timoshenko beams. *Int. J. Mechanical Sciences*, vol. 46, pp. 1589-1606

[2] Manoach, E., Warminska, A., Warminski, J., Doneva S. (2019). A reduced multimodal thermoelastic model of a circular Mindlin plate . *International Journal of Mechanical Sciences*, Volumes 153–154, , pp 479-489

[3] Manoach, E., Warminski, J., Kloda, L., Warminska, A., Doneva, S. (2022) Nonlinear vibrations of a bi-material beam under thermal and mechanical loadings. Mechanical Systems and Signal Processing, 177, art. no. 109127

[4] Stoykov, S., Manoach, E. Electro-mechanical coupling of rotating 3D beams, (2016) MATEC Web of Conferences 83:05011

[5] Stoykov, S., Manoach, E., Litak, G. (2015). Vibration energy harvesting by a Timoshenko beam model and piezoelectric transducer.. *European Physical Journal - Special Topics*, 224, Springer, 2015,

[6] Shterev, K., Manoach, E., Stefanov, S. (2019) Hybrid numerical approach to study the interaction of the rarefied gas flow in a microchannel with a cantilever. *International Journal of Non-Linear Mechanics*, 117, art. no. 103239

[7] Shterev, K. Manoach, E. (2020) Geometrically non-ninear nibration of a cantilever interacting with rarefied gas fFlow. *Cybernetics and Information Technologies* (Special Issue on Scalable Methods and Algorithms, Vol. 20, No 6, 126-139

[8] Shterev, K., Manoach E., and Doneva S., (2023) "Vortex induced vibrations of an elastic micro beam with gas modeled by DSMC" *Sensors* 23, no. 4: 1933

2nd International Conference on Mathematical
Modelling in Mechanics and Engineering
Mathematical Institute SANU, 12-14. September, 2024.

SENSITIVITY ANALYSIS OF PROFILE DEVIATIONS OF HIGH-PRESSURE ANGLE SPUR GEARS

Vasilios Spitas[1], A. Mavridis-Tourgelis[2], G. Kaisarlis[3] and G. Vasileiou[4]

[1,2,3,4]*School of Mechanical Engineering, National Technical University of Athen NTUA, Athens, Greece*

[1]vspitas@mail.ntua.gr; [2]amavridis@mail.ntua.gr; [3]gkaiss@mail.ntua.gr; [4]gvasileiou@mail.ntua.gr

[1]ORCID iD: 0000-0003-3999-7752; [2]ORCID iD: 0009-0003-1431-2726;
[3]ORCID iD: 0000-0002-4990-9579; [4]ORCID iD: 0000-0003-3496-0619

Keywords: Spur gears, high pressure angle, tolerancing, profile deviations.

ABSTRACT

This research work presents a methodology for the determination of the required manufacturing accuracy of custom, high-pressure angle gears. The gears examined throughout the present work are constructed using involute segments beyond the 25-degree limit specified in the ISO/TC 60/SC 2 and custom root fillet geometries produced with the employment of 4th order Bezier curves. Due to the existence of extensive undercuts in the root region, production of these geometries cannot be practically achieved by conventional machining, e.g. hobbing; therefore, production methods such as additive manufacturing or powder metallurgy are required.

The root geometry incorporating the 4th order Bezier curves is optimized and described in closed form in terms of the coordinates of the control points. In the context of this study finite element analyses are performed to determine the sensitivity of strength (maximum principal stresses) and functional characteristics (static transmission error - STE) on the surface profile deviations focusing on the root area. Tolerancing of the tooth profile is performed as per ISO 1660:2014, by specifying an unequally disposed tolerance zone with an offset that takes into account the maximum material condition of the theoretically exact feature (TEF) in order to avoid interference at zero backlash nominal tooth geometries and considering nominal center distances. The surface profile tolerance values are calculated using appropriate thresholds for the strength and STE values and can be used as design guidelines for both the production and quality inspection of the gear geometries presented herein. The presented methodology can be applied to any gear pair regardless of the root or flank geometry used.

REFERENCES

[1] ISO 6336-3:2019. Calculation of load capacity of spur and helical gears — Part 3: Calculation of tooth bending strength.

[2] Vasileiou, G., Rogkas, N., Markopoulos, A., & Spitas, V. (2024). Fully ceramic versus steel gears: Potential, feasibility and challenges. Proceedings of the Institution of Mechanical Engineers, Part C: Journal of Mechanical Engineering Science, 238(3), 775-784.

[3] ISO 6336-3:2019. Calculation of load capacity of spur and helical gears — Part 3: Calculation of tooth bending strength.
[4] Vasileiou, G., Rogkas, N., Markopoulos, A., & Spitas, V. (2024). Fully ceramic versus steel gears: Potential, feasibility and challenges. Proceedings of the Institution of Mechanical Engineers, Part C: Journal of Mechanical Engineering Science, 238(3), 775-784.
[5] Kapelevich, A. L., & Shekhtman, Y. V. (2003). Direct gear design: Bending stress minimization. Gear technology, 20(5), 44-47.
[6] Kapelevich, A., & Shekhtman, Y. (2009). Tooth fillet profile optimization for gears with symmetric and asymmetric teeth. Gear technology, 26(7), 73-79.
[7] Kapelevich, A. (2000). Geometry and design of involute spur gears with asymmetric teeth. Mechanism and Machine theory, 35(1), 117-130.
[8] Kumar, V. S., Muni, D. V., & Muthuveerappan, G. (2008). Optimization of asymmetric spur gear drives to improve the bending load capacity. Mechanism and Machine Theory, 43(7), 829-858.
[9] Namboothiri, N. V., & Marimuthu, P. (2022). Influence of drive side pressure angle on fracture characteristics of asymmetric spur gear. Engineering Failure Analysis, 131, 105865.
[10] Shao, N., Ding, X., & Liu, J. (2020). Tolerance analysis of spur gears based on skin model shapes and a boundary element method. Mechanism and Machine Theory, 144, 103658.
[11] Rupal, B. S., Anwer, N., Secanell, M., & Qureshi, A. J. (2020). Geometric tolerance and manufacturing assemblability estimation of metal additive manufacturing (AM) processes. Materials & Design, 194, 108842.
[12] Mohammed, O. D., & Mahmood, Q. (2023). Using powder metal gears in industrial applications-A review. Materials Research Proceedings, 31.
[13] Frech, T., Scholzen, P., Schäflein, P., Löpenhaus, C., Kauffmann, P., & Klocke, F. (2018). Design for PM challenges and opportunities for powder metal components in transmission technology. Procedia CIRP, 70, 186-191.
[14] ISO ISO 1660:2017 (2017). Geometrical product specifications (GPS) — Geometrical tolerancing — Profile tolerancing, International Organization for Standardization (ISO), Geneva.
[15] ISO 1101:2017 Geometrical product specifications (GPS) — Geometrical tolerancing — Tolerances of form, orientation, location and run-out, International Organization for Standardization (ISO), Geneva.

2nd International Conference on Mathematical
Modelling in Mechanics and Engineering
Mathematical Institute SANU, 12-14. September, 2024.

ON COMBINED EXPERIMENTAL AND COMPUTATIONAL FLUID DYNAMICS STUDIES OF THE MULTI-SCALE MULTI-PHYSICS PHENOMENA IN BIO-MEDICAL APPLICATIONS

Saša Kenjereš[1]

[1]*Department of Chemical Engineering, Faculty of Applied Sciences, Delft University of Technology and J. M. Burgerscentrum Research School for Fluid Mechanics, Delft, The Netherlands*

[1]s.kenjeres@tudelft.nl
[1]ORCID iD: 0000-0002-7568-5513

Keywords: blood flow, airflow, left ventricle, aorta, lungs, CFD, finite-volume approach, PIV, MRI, US

ABSTRACT

In this presentation, we provide a comprehensive overview of our recent research activities dealing with combined experimental and numerical studies dealing with the advanced mathematical modeling of parts of the cardiovascular (blood flow) and respiratory (airflow) systems in the human body, [1]. We focus on some important challenges and recent achievements in bio-medical engineering associated with underlying multi-scale multi-physics-based transport phenomena (transport of mass, momentum, energy, species, particles, cells, aerosols, medical drugs) and their role in the formation, progression, and efficient treatment of various health conditions and diseases. These include heart failure, thoracic aorta aneurysm, asthma, lung cancer, respiratory infections, virus transmission, etc.

First, we provide fundamental transport equations (PDEs) based on the conservative laws of mass, momentum, energy, and species, which can be numerically solved. Second, we show details of the developed numerical algorithms based on the fully conservative finite-volume method (FVM) validated against various experimental studies. Third, a comparison with available experimental studies is performed. The experimental studies include our own 4D PIV/PTV (particle image velocimetry/particle tracking velocimetry) measurements, as well as state-of-the-art ultrasound (US) and magnetic imaging resonance (MRI) techniques used in clinical practice.

We will address the following cases: (i) heart failure – analysis of the blood flow patterns in the left ventricle (left heart chamber), where our measurements will be compared with our recently developed CFD simulations that included movement of the left ventricle synchronized with movement of biological mitral and aortic valves (both based on numerically efficient and accurate Radial-Basis Function (RBF) approach), [1-7]; (ii) blood flow and mass transfer in thoracic aorta – where a conjugate mass transfer of the oxygen (O_2) and nitrogen oxide (NO) across the blood vessel interface is simulated for the healthy control and patient-specific groups, [8,9]; (iii) airflow and aerosol transport in the upper and central human airways for the patient-specific geometry, where CFD will be compared with MRI experiments, [1,10]; and finally, (iv) expiratory multi-phase airflow with virus-laden droplets under various surrounding environmental conditions (large eddy simulations, LES) for better understanding of airborne transmission of infectious diseases, [11].

REFERENCES

[1] Kenjeres S. (2016), “On Recent Progress in Modelling and Simulations of Multi-scale Transfer of Mass, Momentum and Particles in Bio-medical Applications“, Flow, Turbulence and Combustion, Vol.96 (3), pp. 837-860.

[2] Khalafvand S. S., Voorneveld J. D., Muralidharan A., Gijsen F. J. H., Bosch J. G., van Walsum T., Haak A., de Jong N., Kenjeres S. (2018), “Assessment of human left ventricle flow using statistical shape modelling and computational fluid dynamics”, Journal of Biomechanics 74, pp.116-125.

[3] Khalafvand S. S., Xu F., Westenberg J., Gijsen F., Kenjeres S. (2019), “Intraventricular blood flow with a fully dynamic mitral valve model”, Computers in Biology and Medicine, Vol. 104, pp.197-204.

[4] Saaid H., Voorneveld J., Schinkel C., Bosch J. G., Westenberg J., Gijsen F., Segers P., Verdonck P., Kenjeres S., Claessens T. (2019), “Tomographic PIV in a Model of the Left Ventricle: 3D Flow Past Biological and Mechanical Heart Valves”, Journal of Biomechanics, Vol. 90, pp.40-49.

[5] Voorneveld J., Saaid H., Schinkel C., Radeljic N., Lippe B., Gijsen F.J.H., van der Steen A. F. W., de Jong N., Claessens T., Vos H. J., Kenjeres S., Bosch J. G. (2020), “4D echo-particle image velocimetry in a left ventricular phantom”, Ultrasound in Medicine & Biology Vol.46 (3), pp.805-817.

[6] Xu F. and Kenjeres S. (2021), “Numerical simulations of flow patterns in the human left ventricle model with a novel dynamic mesh morphing approach based on radial basis function”, Computers in Biology and Medicine, Vol.130, 104184, pp.1-12.

[7] J.J.M. Westenberg, H.C. van Assen, P.J. van den Boogaard, J.J. Goeman, H. Saaid, J. Voorneveld, J. Bosch, S. Kenjeres, T. Claessens, P. Garg, M. Kouwenhoven, H. J. Lamb (2022), “Echo planar imaging- induced errors in intracardiac 4D flow MRI quantification”, Magnetic Resonance in Medicine 87, pp.2938- 2411.

[8] R. Perinajová, J.F. Juffermans, J.J.M. Westenberg, R.L.F. van der Palen, P.J. van den Boogaard, H. J. Lamb, S. Kenjereš (2021), “Geometrically induced wall shear stress variability in CFD-MRI coupled simulations of blood flow in the thoracic aortas”, Computers in Biology and Medicine, Vol.133, 104385, pp.1-19.

[9] Romana Perinajová, Concepción Borrás Álvarez-Cuevas, Joe Juffermans, Jos Westenberg, Hildo Lamb, Saša Kenjereš (2023), “Influence of aortic aneurysm on the local distribution of NO and O2 using image- based computational fluid dynamics”, Computers in Biology and Medicine 160, 106925, pp.1-12.

[10] Kenjeres S. and Tjin J. L. (2017), “Numerical Simulations of Targeted Delivery of Magnetic Drug Aerosols in the Human Upper and Central Respiratory System: A Validation Study”, Royal Society Open Science, Vol.4 (12), Art.No. 170873, pp.1-24.

[11] Kenjeres S., Henry F. S. , Tsuda A. (2021), “Is Current Social Distancing Enough?”, Annals of Biomedical Engineering 49, pp.1973–1974.

THE ORIGIN OF MULTISTABILITY AND ENERGY BARRIERS IN WRINKLING OF ELASTIC FILMS ON ELASTIC HALFSPACE

Miha Brojan[1]

[1]*University of Ljubljana, Faculty of Mechanical Engineering, Aškerčeva 6, SI-1000, Ljubljana*

[1]*miha.brojan@fs.uni-lj.si*

[1]ORCID iD: 0000-0002-3342-9562

Keywords: Multistability; Energy barriers; Wrinkling; Beams.

ABSTRACT

Deformation of layered composites, coatings, drying fruits, biological tissues [1], etc., can be physically described with a relatively simple model of a film that is attached on a soft substrate. Such system releases a part of its strain energy through localized deformation in the form of periodic deformation (wrinkling), which is a result of symmetry breaking, characterized by a pitchfork bifurcation. With the use of the linear bifurcation analysis we can effectively analyze the onset of super-critical bifurcation. However, further deformation evolution is difficult to study, as the strain energy landscape becomes increasingly more non-convex due to the nonlinearity, originating not only from the material nonlinearities (e.g. the substrate) but also from the geometric nonlinearities (membrane strain energy), [2]. This is especially true for the sub-critical bifurcation wrinkling, where the bifurcation point intensely depends on the imperfections and nonlinear nature of the problem, [3]. Due to the nonlinearity and extreme imperfection sensitivity, which results in an undulating non-convex energy landscape, rich in energy barriers and secondary bifurcations, numerical and experimental investigation is remarkably hard.

In this study a theory for the simplest possible case of wrinkling of an elastic film on a planar substrate is presented. This model can used to study the energy landscape of super- and sub-critical bifurcation wrinkling. The theory that builds upon the reduction of dimensionality matches well with the numerical simulations and experiments. To analyze the post-bifurcation energy landscape of wrinkling a relatively simple system of an elastic film on a nonlinear elastic half-space is considered. The film is modeled using large deflection Euler-Bernoulli beam theory, where we additionally consider compressibility of the film. The effect of the nonlinear substrate on the beam is considered through the normal pressure onto the beam, while the shear stresses due to the substrate are neglected. The equilibrium equations take the form

$$D\varphi'''(s) + C\left(\varepsilon - \frac{1}{2}\varphi^2\right)\varphi'(s) - 2\mu i(\varphi + \alpha(\varphi^2 - \langle\varphi^2\rangle) + \beta\varphi^3) = 0 \quad \text{and} \quad C\left(\varepsilon - \frac{1}{2}\varphi^2\right)' = 0,$$

where φ is the rotation of the beam and prime denotes differentiation with respect to the arc-length s of the beam. Additionally, D, C, μ, ε, are the bending stiffness, membrane stiffness of the film, linear shear modulus of the substrate and the longitudinal growth of the beam, respectively. The nonlinearities are characterized by the coefficients α and β, which control the nonlinearities that

can be un-symmetric and symmetric in compression and tension. The system is solved numerically using spectral methods. The influential terms in the potential energy per unit length of the film

$$\mathcal{E} = \frac{D}{2}\left(\frac{A^2k^2}{2} + \frac{B^2g^2}{2}\right) + \frac{C}{2}\left(-\frac{\varepsilon}{2}\left(A^2+B^2\right) + \frac{3}{32}\left(A^4 + 4A^2B^2 + B^4\right)\right)$$
$$+ 2\mu\left(\frac{1}{2}\left(\frac{A^2}{2k} + \frac{B^2}{2g}\right) + \frac{3\beta}{32}\left(\frac{A^4}{k} + \frac{2A^2B^2}{k} + \frac{2A^2B^2}{g} + \frac{B^4}{g}\right)\right),$$

are identified. They may induce strain stiffening or strain softening that creates an energy barrier between deformation modes or a valley in energy landscape that promotes localization of deformations, respectively (see Figs. 1 and 2).

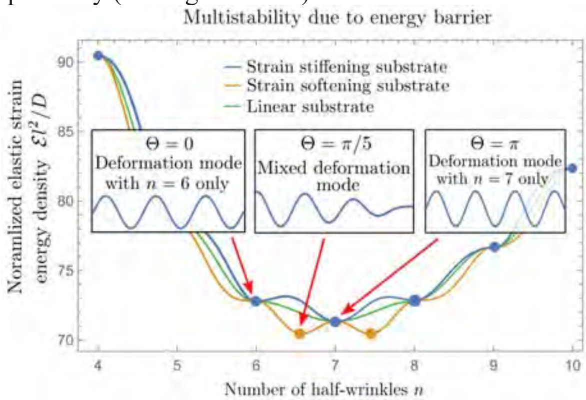

Figure 1. Energy landscape with respect to *n* number of half-wrinkles changes for strain stiffening/softening substrate.

It is shown that the nonlinearities from the membrane strain energy and the substrate critically affect the degree of stability of locally stable solutions, the energy barriers between them, control a secondary loss of stability and promote uni-modal periodical or localized deformation patterns.

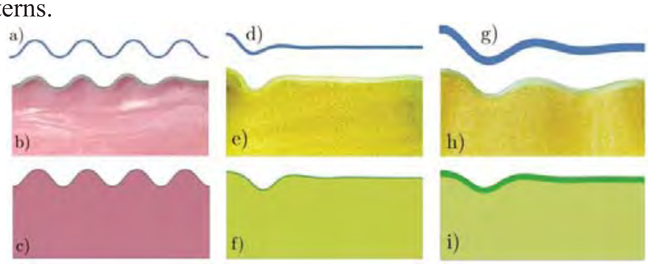

Figure 2. Numerical predictions and experiments exhibiting uni-modal and localized wrinkling patterns.

REFERENCES

[1] Balbi, V., Kuhl, E., Ciarletta, P. (2015) “Morphoelastic control of gastro-intestinal organogenesis: Theoretical predictions and numerical insights”, *J Mech Phys Solids*, vol. 78.

[2] Zavodnik, J., Brojan, M., Kosmrlj, A. (2023), “Rate-dependent evolution of wrinkling films due to growth on semi-infinite planar viscoelastic substrates”, *J Mech Phys Solids*, vol. 173.

[3] Veldin, T., Lavrenčič, M., Brank, B., Brojan, M. (2020), “A comparison of computational models for wrinkling of pressurized shell-core systems”, *Int J Non Linear Mech*, vol. 127.

INVITED LECTURES

2nd International Conference on Mathematical
Modelling in Mechanics and Engineering
Mathematical Institute SANU, 12-14. September, 2024.

TOWARDS HIGH-SPEED ENERGY EFFICIENT SOLUTIONS: HARDWARE ACCELERATION OF HIGH-PERFORMANCE COMPUTATIONAL APPLICATIONS

Lobna A. Said[1], Mohammed H. Yacoub[2]

[1,2]*Nanoelectronics Integrated Systems Center (NISC), Nile University, Giza, Egypt.*

[1]*l.a.said@ieee.org*; [2]*m.hassan2127@nu.edu.eg*

[1]ORCID iD: 0000-0001-8223-4625; [2]ORCID iD: 0009-0005-2056-3817

Keywords: Hardware acceleration, FPGAs, ASICs, GPUs, Fractional Calculus, Nonlinear dynamics, AI.

ABSTRACT

Recently, there has been a rapid increase in computational complexity and massive data processing requirements, mainly due to the surge in artificial intelligence (AI) algorithms. Besides the increased need for better hardware to handle these immense computational requirements, reducing energy consumption becomes inevitable to continue improving such fields at a reasonable cost and minimize the environmental impact of power production related to this advancement. Today's general-purpose processors struggle to obtain the required performance mainly due to the inability to utilize all the chip cores together at their maximum speeds due to the thermal limitations and the upper limit of the number of cores utilizable by most applications [1]. Hence, higher is need for specialized hardware to tackle these requirements as efficiently as possible. In other words, hardware development capable of reaching the maximum possible performance per watt is critically required, especially for high-performance computation (HPC) applications.

Hardware accelerators have gained increased importance due to their ability to handle complex tasks at higher performance and much more efficient energy consumption than general-purpose processors. By relaxing the general-purpose requirements, hardware accelerators allow finer control and optimization of the hardware resources, power consumption, and performance. Graphical Processing Units (GPUs), Application Specific Integrated Circuits (ASICs), and Field Programmable Gate Arrays (FPGAs) are the most common hardware acceleration platforms [2].

Various applications utilized hardware accelerators to improve speed, area utilization, and thermal and power performance. Fractional calculus, an extension of classical calculus that enables modeling systems with memory effects and non-local behavior, employs hardware accelerators due to the complex and iterative nature of the numerical solvers of fractional order differential equations, especially systems with complex orders and systems with function in time orders. Through parallel processing and pipelining, hardware accelerators improve the speed and accuracy at the same energy consumption of differential equations computations. This enhances fractional calculus usage in modeling nonlinear physical systems and aids their employment in designing robust control systems. Furthermore, Accelerators enabled real-time calculations of such complex equations, which allowed the utilization of their results in time-critical applications such as encryption.

Hardware accelerators are also critical in the training and inference of deep learning models. Accelerators are employed to handle the complexity imposed by the increased depth of neural networks, the volume of parameters, data size, real-time computing requirements, and energy

consumption [3]. By leveraging parallel processing and AI-specialized circuitry, Hardware accelerators hugely increase the performance gain per consumed energy, enabling rapid advancement in AI capabilities.

This abstract highlights the growing importance of hardware accelerators in HPC applications. By developing specialized hardware solutions for complex mathematical operations, the maximum performance of various algorithms in several areas, such as fractional calculus, nonlinear systems, and AI. Furthermore, these specialized circuits minimize energy consumption per operation and enable optimal resource utilization, taking advantage of the device's control capabilities.

REFERENCES

[1] Biagio Peccerillo, Mirco Mannino, Andrea Mondelli, Sandro Bartolini, "A survey on hardware accelerators: Taxonomy, trends, challenges, and perspectives, Journal of Systems Architecture," Volume 129, 2022.

[2] Sparsh Mittal, Sumanth Umesh, "A survey on hardware accelerators and optimization techniques for RNNs," Journal of Systems Architecture, Volume 112, 2021,

[3] Kachris, C. (2024). "A Survey on Hardware Accelerators for Large Language Models." ArXiv. /abs/2401.09890

MATHEMATICAL MODELLING OF VIRUS SPREAD VIA BLOOD FLOW

Dharmendra Tripathi[1]

[1] *Department of Mathematics, National Institute of Technology, Uttarakhand*
Srinagar (Garhwal)-246174, Uttarakhand, India.
[1]*dtripathi@nituk.ac.in*
[1]ORCID iD: 0000-0003-4798-1021

Keywords: Mathematical Modelling, Blood, Viruses; Particle Trajectories, BBO Equation.

ABSTRACT

Circulatory system of the human body is one of the major and important physiological systems where blood is flowing throughout the body due to the natural pumping mechanism i.e. heart pump. Blood is having plasma, red blood cells, white blood cells, platelets, and also having many functions like transporting oxygen and nutrients to the lungs and tissues and forming blood clots to prevent excess blood loss. Moreover, blood borne viruses like HIB, HBV, HCB, Covid, etc. are infecting the blood, blood vessels and other parts of the body which further cause the various diseases in the circulatory system. Modeling and simulation of blood flow in circulatory system and tracing the trajectories for the virus spread through blood flow are very complex, however such analysis could be done by using the CFD tools and mathematical approaches under some circumstances. This talk will aim to provide the parametric analysis to examine the effects of various key parameters on the blood flow and viruses movement. This talk will cover the formulation of the blood flow and motion of the viruses through blood flow and their analytical solution under the suitable assumption of low Reynolds number flow. Using BBO equation, velocity and trajectories of viruses are simulated. This talk will also discuss the limitation of the model and future scope in the field of biofluid dynamics, and relate to the emerging technologies in health care.

REFERENCES

[1] Tripathi, D., Bhandari, D. S., & Anwar Bég, O. (2022). Thermal effects on SARS-CoV-2 transmission in peristaltic blood flow: Mathematical modeling. *Physics of Fluids*, 34(6).

[2] Tripathi, Dharmendra, Dinesh Bhandari, Rakesh Kumar, And Yasser Aboelkassem. "Modeling Virus Transport And Dynamics In Viscous Flow Medium." *Journal Of Biological Dynamics* 17, no. 1 (2023): 2182373.

[3] Ram, Daya, Dinesh S. Bhandari, Kushal Sharma, and Dharmendra Tripathi. "Progression of blood-borne viruses through bloodstream: A comparative mathematical study." *Computer Methods and Programs in Biomedicine* 232 (2023): 107425.

PASSIVE WAVE CONTROL IN CELLULAR METASTRUCTURES USING CHAOTICITY OF SOFT-WALLED BILLIARDS

Valery Pilipchuk

Department of Mechanical Engineering, Wayne State University, Detroit, MI, USA

pilipchuk@wayne.edu

ORCID iD: 0000-0001-7051-3539

Keywords: Metastructures, Energy absorption, Wave attenuation, Fermi acceleration.

ABSTRACT

Design of artificial materials with unique properties using structural elements of a relatively small or mesoscale size is a fast-growing field motivating different directions of interdisciplinary studies [1]. A particular interest to soft cellular metamaterials is due to the developing 3D printing technology shortening the path from design to fabrication. Mechanical metamaterials are typically designed to provide acoustic and elastic wave guiding features, and the ability to mitigate excessive loads by redirecting the energy flows. Transitions between different forms of energy is expected to be at frontlines of the academic research, and the industrial R&D due to the developing economic and environmental challenges. Thus, the main objective of the present work is to explore and advance new physical principles of the energy absorption from different forms of environmental disturbances, such as acoustical noise, mechanical impulsive and oscillating loads. The proposed approach emerges from our recent study, which revealed that arrays of oscillating soft-walled cells, if shaped as chaotic billiards, can accelerate their light inclusions through E. Fermi mechanism explaining the acceleration of cosmic particles by electromagnetic waves. The billiard effect appeared to provide thermodynamic energy outflows from global wave modes into inclusions even if each cell has just one inclusion [2]. Our core observation is that the local geometry of cells appeared to have a crucial effect on the global structural dynamics. The important conclusion is that the chaotization of wave itself does not guarantee the energy outflow into inclusions. Whereas the chaoticity of wave shapes is caused by the loss of structural translational symmetry due to impulsive interactions of cells with inclusions, the energy absorption is the result of inclusion' gradual acceleration of inclusions, which is associated with local geometrical specifics of cell boundaries.

REFERENCES

[1] Capolino, F., Khajavikhan, M., Alù, A. (2022), "Metastructures: From physics to application," *Appl. Phys. Lett*. 120 (6), 060401; https://doi.org/10.1063/5.0084696

[2] Pilipchuk, V. (2023), "Oscillators and oscillatory signals from smooth to discontinuous: Geometrical, algebraic, and physical nature," *Springer Nature,* Switzerland, 456 p.

2nd International Conference on Mathematical
Modelling in Mechanics and Engineering
Mathematical Institute SANU, 12-14. September, 2024.

MULTIPHASE FLOW: FROM ACADEMIA TO THE INDUSTRY

Raúl Martínez Cuenca[1], Guillem Monros[2], Javier Climent[3] and Sergio Chiva[4]

[1,2,4]*Group of Multiphase flows, Department of Mechanical Engineering and Construction, Universitat Jaume I, 12071 Castello, Spain*

[3]*Hydrodynamic & Environmental ervices (HYDRENS., Castellón, 12003, Spain*

[1]*raul.martinez@uji.es*; [2]*gmonros@uji.es*; [3]*javier.climent@hydrens.com* ; [4]*sergio.chiva@uji.es*

ORCID iD: [1]0000-0001-5955-3441; [2]0000-0003-4035-0489; [3]0000-0002-6699-0794, [4]0000-0001-6345-2950

Keywords: Multiphase flows, Flow Characterization, CFD simulation, Industrial applications

ABSTRACT

The inherent complexity of multiphase flows has attracted the interest of hundreds of physicists and engineers [1]. Indeed, the dynamics of these flows strongly depends on the structuration of the different phases, giving rise to the so-called multiphase flow-regimes. Every flow regime has its own characteristics and particularities, involving the interaction between the multiple phases across the interfaces, the turbulence for each phase, and the mutual induction of turbulence. The complexity increases when mass/energy transfer takes place across the interphases as well.

This phenomenology provides a powerful tool that can be used for a wide range of industrial applications. Nuclear reactors provide energy thanks to the evaporation of water. At the same time, the water serves for the refrigeration of the nuclear rods and the vapor is a dangerous enemy that can lead to important accidents [1].

Wastewater treatment industry relies on processes that take place thanks to microorganisms that tend to group in flocs [2]. These microorganisms need oxygen which is supplied by aeration systems to remove pollutants from water. [3,4]. Moreover, the tertiary treatment can be performed thanks to the aggregation and settling of particles (flocculation tanks) and then, by applying UV irradiation to pathogenic microorganisms that tend to hide behind dissolved solid particles.

The extraction of petroleum implies the co-existence of liquid (crude oil), solid particles (dragged sand from the seafloor) and the gas that appears as the liquid ascends and loses pressure.

Indeed, the list of industrial applications is huge and has evolved from the classical applications in 20th century (design of boilers, mixers, reactors,…) to modern studies in the 21st century (pollutant dispersion, COVID propagation, preemption of algae blooms).

Of course, the path from the academic knowledge to the industrial applications is plenty of drawbacks and is still under development. In this work, the authors will present the most relevant developments in the field of multiphase flow characterization and modeling. The developments focus mainly in the so-called dispersed flows, but it also has addressed separated flows.

From the point of view of multiphase flow characterization, the use of ultrasound velocimetry (continuous phases) and needle-probe measurements (dispersed phases) have demonstrated a superior performance in industrial environments where dispersed flows play a central role. These flows are composed by a main phase with some components of the

secondary phase dispersed as ‘particles’. Techniques for the characterization of continuous phases, as Particle Image Velocimetry, Laser Doppler Anemometry or hot-wire anemometry, are very complex to implement. The two first are strongly limited when liquid is highly absorbing and for high concentration of particles. The hot-wires tend to break when the particles collide against them and stop working when dissolved solids clog them. The authors provide measurements for the 3D flow characterization of aerobic reactors using ultrasound velocimetry.

The characterization of the dispersed phase is also a cumbersome task. Optical imaging techniques fail again whenever the liquid absorption or the particle concentration are high. The use of conductivity probes is also strongly limited solid particles may clog them. The authors show a novel development based on conductance probes for their application in adverse conditions [5].

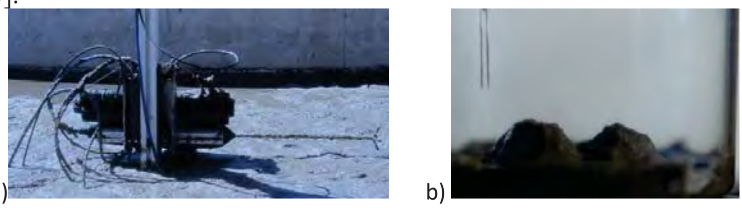

a) b)

Figure 1: Characterization of multiphase flows, a) ultrasound velocimetry, b) conductance probes.

From the point of view of the modelling, Eulerian-Eulerian CFD simulations have provided very interesting results [6]. The authors will introduce the models for the simulation of industrial dispersed flows, usually involving mass transfer and radiation. A baseline model for the Eulerian simulation of multiphase flows will be introduced, with a proper set of submodels for interfacial forces, turbulence induction and population balance (coalescence and break-up) [4, 6, 7].

REFERENCES

[1] Ishii, M. and Hibiki, T. (2011) Thermo-Fluid Dynamics of Two-Phase Flow. 2nd Edition, Springer Verlag, New York.

[2] Samstag R.W., Ducoste J.J., Griborio A., Nopens I., Batstone D.J., Wicks J.D., Saunders S., Wicklein E.A., Kenny G., Laurent J.(2016), “CFD for wastewater treatment: An overview,” Water Science and Technology 74, 549 – 563

[3] Climent J., Martínez-Cuenca R., Basiero L., Berlanga J.G., Chiva S. (2017), “Hydro-swapping: An innovative CFD approach applied to a real bioreactor,” Lecture Notes in Civil Engineering 4, 722 – 726

[4] Climent J., Martínez-Cuenca R., Carratalà P., González-Ortega M.J., Abellán M., Monrós G., Chiva S. (2019), “A comprehensive hydrodynamic analysis of a full-scale oxidation ditch using Population Balance Modelling in CFD simulation,” Chemical Engineering Journal 374, 760 – 775

[5] Monrós-Andreu G., Martinez-Cuenca R., Torró S., Escrig J., Hewakandamby B., Chiva S. (2016), “Multi-needle capacitance probe for non-conductive two-phase flows,” Measurement Science and Technology 27, art. no. 074004

[6] Rzehak R., Krepper E., Liao Y., Ziegenhein T., Kriebitzsch S., Lucas D. (2015), “Baseline Model for the Simulation of Bubbly Flows,” Chemical Engineering and Technology 38, 1972–78.

[7] Yamoah S., Martínez-Cuenca R., Monrós G., Chiva S., Macián-Juan R. (2015), “Numerical investigation of models for drag, lift, wall lubrication and turbulent dispersion forces for the simulation of gas-liquid two-phase flow,” Chemical Engineering Research and Design 98, 17–35.

2nd International Conference on Mathematical
Modelling in Mechanics and Engineering
Mathematical Institute SANU, 12-14. September, 2024.

TIPS AND TRICKS FOR NUMERICAL ANALYSIS OF LOW-VELOCITY IMPACTS ON BIOCOMPOSITES

A. Pavlovic

Department of Industrial Engineering, University of Bologna,40136 Bologna, Italy

ana.pavlovic@unibo.it
ORCID iD: 0000-0003-2158-1820

Keywords: Bio-composites, low-velocity impact, numerical simulation, LS DYNA.

ABSTRACT

The use of unconventional fibers has always attracted some attention. However, there are quite some reasons to prefer glass and carbon as usual reinforcement. Besides cost and availability, the mechanical properties might not be up to par with those of other choices.

This study is meant to investigate the behavior of basalt reinforced composites (BFR) under the action of low-velocity impacts. Basalt was chosen since it offers mechanical properties comparable to those of carbon and glass, although it is a mineral fiber, often assimilated to a ‘natural fiber’. On the other side low-velocity impacts (LVI) was chosen since they possibly represent the dynamic loads of most common interest in everyday life.

This research is not the first to investigate these properties, but the aim is to challenge the issue under a somewhat different angle: predict the behavior of the ‘aged’ material because of salt water and temperature, starting from the knowledge of the initial properties, and modifying the parameters of numerical models.

It was considered as reinforcement a balanced plain weave basalt fiber fabric with a density of 350 g/m^3 and moisture <3% (BASALTEX®, BAS 350.1500). Type and sizing of the fibers also provide a good compatibility with a range of thermoset resin systems. Here it was used a commercial vinyl ester resin (DISTITRON® VEef 220 STZ) with a low styrene content and emission (<35%): this material match ensures the production of a highly sustainable composite material.

The BFR laminates were manufactured by manual lay-up, stacking 8 layers of basalt fabric. Following the indications of the resin’s datasheet, polymerization was achieved by placing the laminates in the autoclave for 24 hours at 23°C and then 3 hours at 100°C. After hardening, the laminates had a thick- ness of 3.95 mm with a 49% volume fraction of reinforcement. Specimens were obtained from the laminates using a diamond blade and some of them were subjected to an accelerated aging process by means of immersion in 35 ppt salt water at 80°C for 912 hours (38 days). Duration and temperature were chosen in agreement with similar experiments that showed how water absorption and degradation of properties decrease significantly after 30 days. Water absorption was monitored by means of weight measurements, showing a variation less than 0.70%.

Impact tests were performed on 150x100 mm rectangular specimens in compliance with the ASTM D7136 regulations. A drop-weight tower was used with a 1.25 kg, hemispherical-tip impactor. The dynamic response was evaluated by means of the trend of contact force and displacement against time. The impactor was released from a height of 2.5 m, corresponding to a theoretical impact energy of 30.65 J and a measured energy of 24.7 J. This height was

chosen to prevent the perforation of the sample. This scenario allows the experimenter to study the combination of the various damage mechanisms, observed by means of scanning electron microscopy (SEM) of the fracture surface, performed with a Zeiss EVO 50 EP SEM.

The measurements performed on the non-aged specimens were used to develop a numerical model aimed at accurately predicting the effect of LVIs on non-aged BFRPPs [1]. Then the measurements on aged samples were used to understand how the model parameters are altered by aging [2].

The aim of the numerical study was simulating the experimental conditions, using LS DYNA to perform an explicit dynamic simulation (Fig.1). Shell-type finite elements for the laminate and solid-type ones for the striker was combined. The stratification of the composite was considered by means of a "stacked-shell" approach reproducing the 8-layer laminate in the form of 4 stacked shells, including two integration points each: in this way very, accurate results were obtained together with a high computational efficiency. Each of the 4 laminate layers was simulated by 19.148 Belytschko Tsai quadrilateral shell elements. It was chosen the "linear orthotropic Chang-Chang" failure criterion as it offers an excellent overall precision by combining the interaction of four different failure mechanisms, i.e. tensile or compression failure in either matrix or fibers.

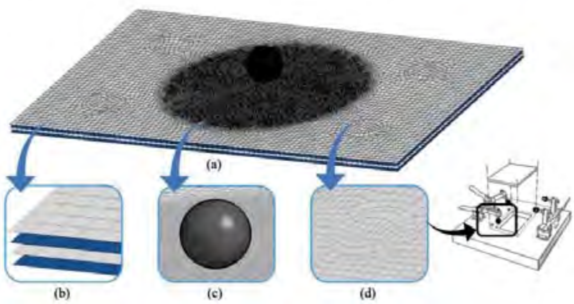

Figure 1: Details of the numerical model: a) impact geometry; b) 4 layers; c) impactor; d) fixing zone.

As a material model of the composite, MAT54 was selected. This advanced model considers a linear orthotropic elastic response in the layer up to failure and a decrease of the longitudinal compression strength of each layer in the case of a failure of the transverse matrix. As in similar cases, several input parameters are required to completely characterize MAT54 with respect to phenomena like erosion, plasticization, and progressive damage. The accuracy of the model prediction is certainly strongly correlated to the value of these parameters, which often do not represent observable physical quantities but rather mathematical concepts and therefore are not measurable in an experiment. These include, for instance, the size of the element, the definition of the contact, the plasticization parameter of the crush front and so on. Consequently, to obtain good results from the simulations one needs a significant effort to calibrate these parameters by trial and error. This research considered all the most important parameters, such as ALPH, BETA, SOFT, FBRT and YCFAC:

• ALPH weighs the nonlinear shear stress in the plane to determine the shear deformation of the laminate in the elastic regime.

• BETA considers the importance of shear in the tensile failure modes of both fibers and matrix within the Chang-Chang failure criterion.

• SOFT is a generic parameter that considers the progressive decrease of tensile and compression strength of elements in the crush front after each numerical iteration.

• FBRT and YCFAC like SOFT in nature. The first parameters reduce the fiber tensile strength only, while the second one reduces the fiber compression resistance.

It is important to notice that since each of these parameters represents a specific mechanism of absorption of the impact energy, they all influence each other. For instance, if shear were more important of LVI failure, BETA should be closer to 1 and more energy would be absorbed by shear instead of other mechanisms such as tensile and compression failure of the matrix (which can increase the final value of SOFT, consequently).

The impactor was simplified as a sphere weighing 1.25 kg, modelled as a rigid body (MAT_20), with a 2-mm mesh, refined to 1 mm in the contact area. The impactor laminate contact condition was simulated using the contact algorithm based on the AUTOMATIC_SURFACE_TO_ SURFACE penalty. In addition to the in-plane tensile stresses considered in the failure criterion adopted here, the out-of-plane tensile stresses can be simulated accurately by means of the TIEBREAK inter-ply contact definition, which takes into account non only compression but also tensile failure during contact, thus reproducing the delamination process. Therefore, the contact definition CONTACT_AUTOMATIC_ONE_WAY_SURFACE_TO_SURFACE_ TIEBREAK was used for the ply-to-ply contact. Edge and clamping system effects were considered by means of suitable constraint and contact conditions.

In the case of the aged BFRP, the results used to calibrate the model parameters are extracted from three impact tests (fig.2). Specifically, it was compared the experimental and simulated trends in the three different stages by which the impact can be described, i.e. loading (I), unloading (II) and relaxation (III) (fig.3).

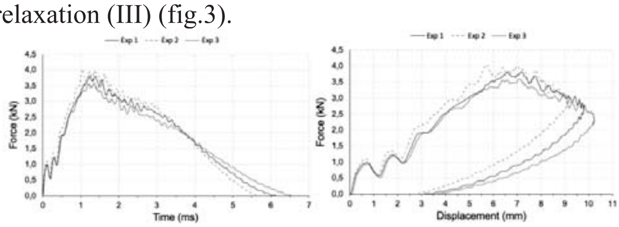

Figure 2: Experimental results: a) force vs time; b) force vs displacement.

This comparison was performed through a total of 11 reference values, related to a set of forces, times, deformations, elastic recovery, linear momenta, and absorbed energies. An in-depth analysis of the results, with a detailed explanation of how the model parameters change, is beyond the scope of this article, but can be found in reference papers [1, 2]. Summarizing, we can say that the force vs time curve reconstructed by means of simulation and calibration of the parameters is a very accurate reproduction of the experiment, with discrepancies always <12%, and even <4% for some fundamental properties such as maximum displacement and time needed to reach it. This predictive precision for the behavior of an aged composite is exceptional itself, and more so if we consider that it was obtained using as a basis the features of the non-aged material. Indeed, it is important to remind the reader that the behavior of aged specimens was used ‘only’ to calibrate the internal parameters of the model (MAT54 with the linear-orthotropic Chang-Chang criterion), while the model itself was set upon the properties of the non-aged material. In this regard, observing the variation of these parameters it is apparent that aging does not alter all of them (just 3 of the 5 parameters), which is a good basis to make further considerations about the general range of applicability of the procedure.

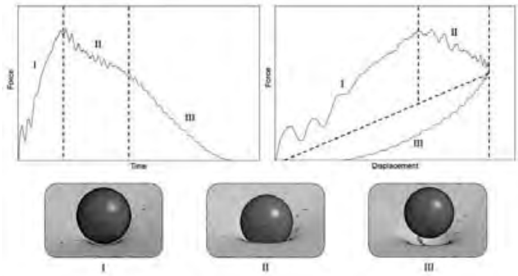

Figure 3: Principal area of interest for the model calibration

The precision shown in the simulation represents a result of great practical importance. Indeed, several studies already confirmed how basalt fibers can significantly affect water absorption by the polymer matrix. This occurs thanks to the rather tight interface bonds that reduce the accumulation of water inside the interface voids, thus preventing the access of water and the following degradation of the mate- rial properties. It is then obvious how important it is to know the behavior of basalt with respect to environmental aging phenomena.

This study paves the way to the proposal of a numerical model that can predict the response of thermosetting basalt laminates to LVIs after high temperature and moisture-induced aging. It is based on the correlation of information and hypotheses obtained from similar works, performed on comparable materials, and loading conditions, filtered through a correct calibration procedure of the main parameters of the constitutive material, that is the ALPH, BETA, SOFT, FBRT and YCFAC parameters of the MAT54 model. In this way, researchers and designers are provided with a computationally efficient tool to accurately predict the response of BFRPP laminates to LVIs, without the need to resort to specific experiments. Furthermore, this model can also provide a valid support in aging conditions that can be foreseen in real life but that are complicated to reproduce in the laboratory.

REFERENCES

[1] Fragassa C, de Camargo FV, Pavlovic A, Minak G (2019). Explicit numerical modeling assessment of a basalt reinforced composite for low-velocity impact. Composites Part B: Engineering. 163, 522-535.

[2] de Camargo FV, Pavlovic A, Schenal EC, Fragassa C. (2020) Stacked-shell finite element approach for explicit modelling aged basalt fiber reinforced polymer composites subjected to low-velocity im- pact. Composite Structures. 256, 113017.

2nd International Conference on Mathematical
Modelling in Mechanics and Engineering
Mathematical Institute SANU, 12-14. September, 2024.

MODELLING SYNCHRONISED CROWD BEHAVIOUR

Vitomir Racić

Faculty of Civil Engineering, University of Belgrade, 11000 Belgrade, Serbia
vracic@grf.bg.ac.rs
ORCID iD 0000-0002-3523-411X

Keywords: crowd dynamics, human-induced vibrations, vibration engineering, external stimuli

ABSTRACT

Many cases of excessive vibrations of footbridges, grandstands and floors induced by active crowds have featured the front pages of newspapers and civil engineering magazines in the last two decades [1]. Predicting structural vibrations at design stage is marked by a great level of uncertainty due to the lack of reliable models of coordinated dynamic loads induced by large groups of people [2].

Quality models of individual loading do exist [3]. But there is a lack of knowledge on how to expand them to multiple people. A key missing element is a model of interaction between individuals, generally known as "synchronization". In the context of dynamic crowd loading, the key aspect of synchronization is the occasional good coordination of their body movements. This is because the source of dynamic loading is in the body motion according to the second Newton's law. So, improved coordination over a longer period of time yields larger amplitudes of the net loading, as illustrated in Figure 1.

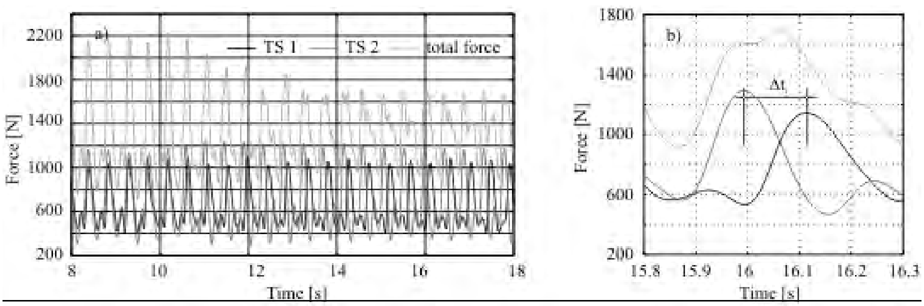

Figure 1: Forces due to a group of two bouncing people (after [4]). Figures a) and b) represent the same data. Δt_i is the time difference between two local peaks.

The model described by Equation (1) features a linear oscillator that generates artificial motion trajectories $x_i(t)$ for each individual i in a group of n people (i=1, …, n). The group is prompted to move by a periodic external stimulus y=y(t) with the angular frequency ω. Examples include a music beat, strobe light and perceptible structural vibration.

$$\ddot{x}_i + \omega^2 x_i + 2\,\varepsilon_i(\delta_i + \sin\omega_i t)(\dot{x}_i - \dot{y}) + (\,\varepsilon_i^{\,2}(\delta_i + \sin\omega_i t)^2 + \omega^2\gamma_i \sin\omega_i t)(x_i - y) = 0 \qquad (1)$$

Here, ε_i weighs the tendency of an individual to synchronise with the given stimulus, $\omega_i>0$ represents the rate by which an individual modifies his/her body motion with respect to the stimulus beat, while γ_i controls the intensity of this variation. Values of ω_i and ω should differ by at least 3% to avoid the resonance. The offset δ_i accounts for the interaction between an individual and others, e.g. a possibility to see and hear people around.

Synchronization is all about the relative timing between the common events in the body motion trajectories or the corresponding loading (Figure 1). A function A(t) of the average lack of synchronization in a group of n people can be expressed as:

$$A(t) = \frac{2}{n(n-1)} \sum_{i,j=1,i<j}^{n} (\ddot{x}_i - \ddot{x}_j)^2 \geq 0 \quad (2)$$

Here, indexes i and j correspond to two individuals in the group. If A(t)=0 all individuals move in unison, while larger amplitudes of A(t) function indicate weaker synchronization. Equation (2) features deliberately acceleration signals $\ddot{x}_i$ and $\ddot{x}_j$ as various accelerometers are the state-of-the-art technology for tracking body motion. This is particularly important for calibrating values of the modelling parameters using the experimental data.

Figure 2a shows A(t) function computed using acceleration records due to two persons bouncing next to each other while prompted by regular metronome beats at 2 Hz. The corresponding A(t) simulation is shown in Figure 2b. Close resemblance is apparent.

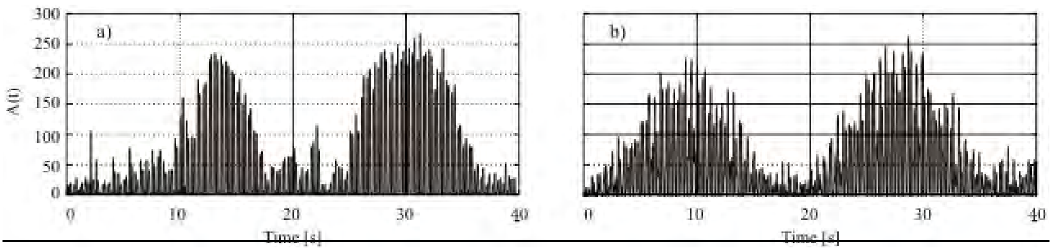

Figure 2: Actual (a-c-e) and simulated (b-d-f) A(t) functions due to two people bouncing.

A comprehensive database of experimentally measured motion trajectories of a large number of individuals moving in groups of various sizes, prompted under a range of different stimuli and performing different actions (e.g. walking, jumping, running), is needed to identify realistic values of the modelling parameters and study their natural variation within the human population.

REFERENCES

[1] Rogers, D. (2000) "Two more 'wobbly' stands", *Construction News*, 17 August.
[2] Gazzola, F., Racic, V. (2018), "A model of synchronisation in crowd dynamics", *Applied Mathematical Modelling* 59, 305-318.
[3] Racic, V. (2023), "Emerging research on vibration serviceability assessment of pedestrian structures", *Building Materials and Structures* 66: 2300001R.
[4] Racic, V., Brownjohn, J.M.W., Pavic, A. (2010), "Reproduction and application of human bouncing and jumping forces from visual marker data" *Journal of Sound and Vibration* 329, 3397-3416.

GENERAL SESSIONS

2nd International Conference on Mathematical
Modelling in Mechanics and Engineering
Mathematical Institute SANU, 12-14. September, 2024.

TWO-STEP-SCALING APPROACH TO SIZE EFFECT MODELING OF FRACTURE TOUGHNESS IN DBT REGION

Sreten Mastilovic[1], Branislav Djordjevic[2] and Aleksandar Sedmak[3]

[1]*University of Belgrade, Institute for Multidisciplinary Research, Belgrade, Serbia*
[2]*Innovation Centre of Faculty of Mechanical Engineering, Belgrade, Serbia*
[3]*University of Belgrade, Faculty of Mechanical Engineering, Belgrade, Serbia*
[1]misko.mastilovic@imsi.bg.ac.rs; [2]brdjordjevic@mas.bg.ac.rs; [3]asedmak@mas.bg.ac.rs
ORCID iD: [1]0000-0002-1856-626X; [2]0000-0001-8595-6930; [3]0000-0002-5438-1895

Keywords: Weibull statistics, Weakest link theory, Fracture toughness, Size effect.

ABSTRACT

This abstract outlines a strategy designed to offer estimates of fracture toughness (J_c) using the Weibull cumulative distribution function (CDF) within the ductile to brittle transition (DBT) region. The size-effect modeling encompasses the dynamic interplay between brittle and ductile damage/fracture micromechanisms, which coexist in varying proportions within the DBT region depending on temperature. The inherent variability is tackled by employing a 3P-Weibull CDF:

$$F\left(J_c \mid \beta, \eta, \gamma\right) = 1 - \exp\left[-\left(\frac{J_c - \gamma}{\eta}\right)^{\beta}\right]; \qquad J_c \geq \gamma;\, \beta, \eta (= \eta_0 - \gamma), \gamma \in \Re^{+} \tag{1}$$

Application of the two-step-scaling (2SS) rest upon the following two scaling conditions along the CDF abscissa and ordinate (governed by the scaling parameters κ and ξ, respectively):

$$\eta \cdot \overline{B}^{\kappa} = \left(\eta_0 - \gamma\right) \cdot \left(B/B_0\right)^{\kappa} = const. = \eta_*; \qquad S \cdot \overline{B}^{\xi} = const. = S_* \tag{2}$$

where B marks specimen thickness (see also Figure for the notation). The two scaling premises (2) define in the scaled space the size-independent Weibull scale parameter (η_*) and the common CDF slope S_* (i.e., the common PDF (probability density function) maxima), respectively [1].

The conditions of constancy (2) stem from the power law, intricately connected to Weibull statistics. This physically plausible power-law scaling is influenced by the traditional concept that the stress at the crack tip increases proportionally to the crack length raised to a power, establishing a connection between weakest link theory (WLT) and the Weibull statistics.

When employing the 2SS scheme (2), the Weibull CDF (1) adopts the Modified WLT form:

$$F\left(J_c \mid \beta, \eta_*, \gamma\right) = 1 - \exp\left\{-\left(\frac{B}{B_0}\right)^{\kappa \cdot \beta}\left(\frac{J_c - \gamma}{\eta_*}\right)^{\beta(B,\xi)}\right\}; \quad (J_c - \gamma) \geq 0;\, \beta, \eta_*, \gamma \in \Re^{+} \tag{3}$$

Finally, temperature-influenced DBT displays resemblances to behavior controlled by strain rates, particularly in scenarios of extreme loading causing shock waves that trigger nearly simultaneous activation of dominant nucleation kernels—an occurrence also witnessed at cryogenic temperatures.

REFERENCES

[1] Mastilovic, S., Djordjevic, B., Sedmak, A., (2022), "A scaling approach to size effect modeling of J_c CDF for 20MnMoNi55 reactor steel in transition temperature region" *Engineering Failure Analysis* 131: 105838.

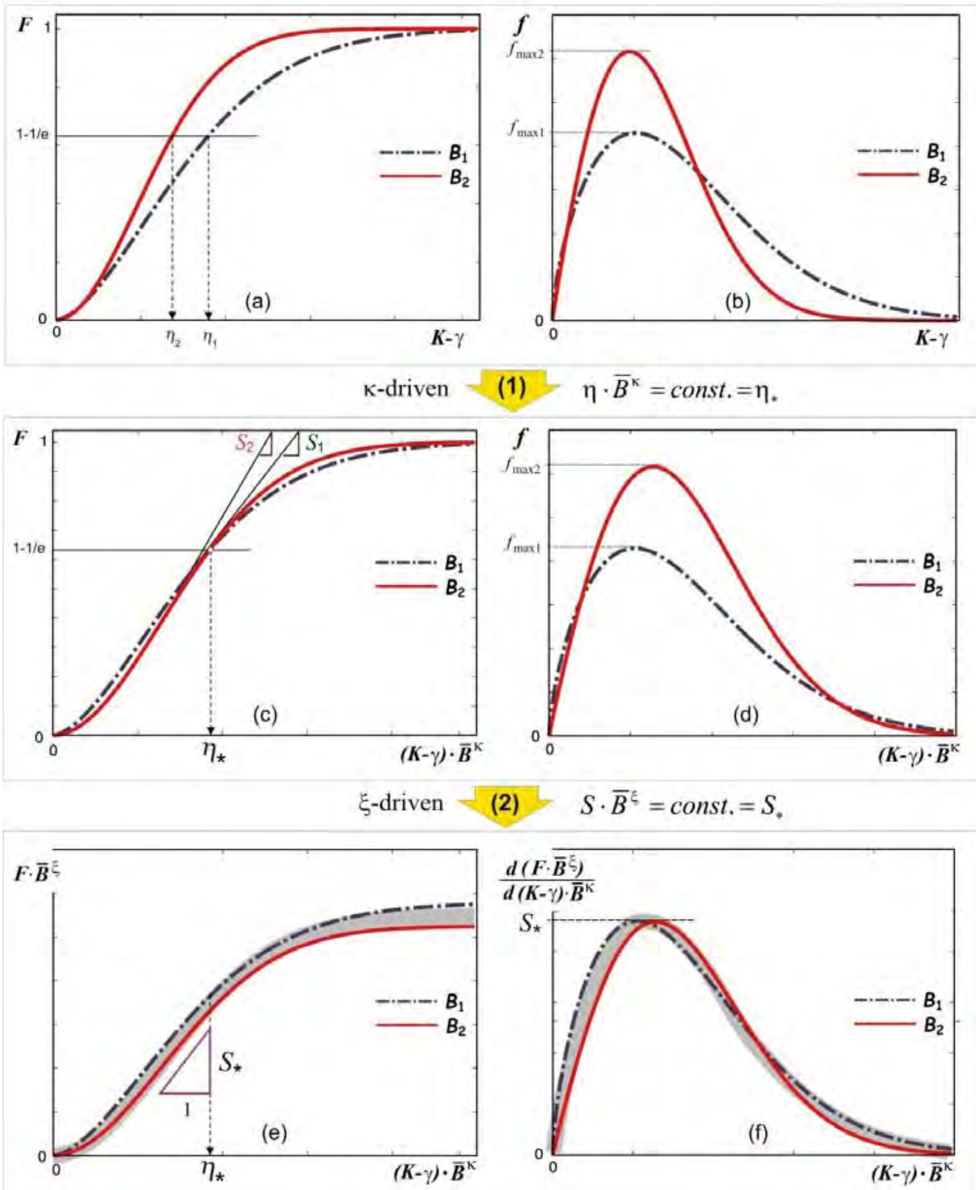

2nd International Conference on Mathematical Modelling in Mechanics and Engineering
Mathematical Institute SANU, 12-14. September, 2024.

COMPARATIVE STUDY OF SOLAR PARABOLIC TROUGH COLLECTOR IN DIFFERENT CLIMATE ZONES OF INDIA

Hemant Raj Singh[1*], Shaurya Verma[2]

[1,2]*Department of Mechanical Engineering, Manipal University Jaipur, Rajasthan 303007, India*

[1*]*hemant.singh@jaipur.manipal.edu*; [2]shaurya.199402045@muj.manipal.edu.

[1]ORCID iD: 0000-0002-1662-4411

Keywords: Solar Concentrator, Parabolic Trough Collector, climatic zone, solar domestic hot water system

ABSTRACT

The utilization of solar energy has gained significant attention as a sustainable alternative to conventional power sources. Among various solar technologies, the solar parabolic trough collector (PTC) stands out as a promising technology for harnessing solar thermal energy. This study presents a comprehensive comparative analysis of the performance of solar parabolic trough collectors across diverse climate zones in India. The research focuses on assessing the efficiency and feasibility of parabolic trough collectors in varying climatic conditions, considering factors such as solar radiation, ambient temperature, and humidity. A set of parabolic trough collector systems has been deployed in representative locations spanning different climatic regions, including arid, semi-arid, tropical, and temperate zones. The study evaluates the influence of climatic parameters on the collector's performance, addressing challenges and opportunities associated with the deployment of solar PTCs in different regions of India. Comparative data analysis enables the identification of optimal conditions for PTC operation and highlights potential modifications required to enhance efficiency in specific climatic contexts. The findings aim to provide valuable insights for policymakers, researchers, and industry stakeholders, aiding in the development of region-specific strategies for the widespread adoption of solar parabolic trough collectors in India.

CONCLUSION

This can form a baseline for designers of solar parabolic trough collector used for solar domestic hot water system.

- **Jaipur** noted the highest temperature of 400K on 21st June at 12 pm and the lowest temperature noted was 315K on 21st December 2 pm. Jaipur is located at 75.7873 E, 26.9124 N and has a semi-arid type of climate. Highest direct solar irradiation over the year was 895.6 W/m^2 on 21st March at 12 pm. Jaipur had the highest temperature achieved between all the cities and climate zones. On the basis of the average temperature achieved, Jaipur as a City/Climate Zone has the highest average temperature of 347.3K.
- **Agumbi** noted the highest temperature of 350K on 21st June at 12 pm and the lowest temperature noted was 308K on 21st September 2 pm. Agumbi is located at 75.0833 E, 13.5 N and has a Tropical Rainforest type of climate. Highest direct solar irradiation over the year was 928.6 W/m^2 on 21st December at 12 pm. On the basis of the average temperature achieved, Agumbi as a City/Climate Zone has the lowest average temperature of 323.3K.
- **Mumbai** noted the highest temperature of 366K on 21st June at 12 pm and the lowest temperature

noted was 311K on 21st September 2 pm. Mumbai is located at 72.8777 E, 19.0760 N and has a Tropical Monsoon type of climate. Highest direct solar irradiation over the year was 914.9 W/m^2 on 21st December at 12 pm. On the basis of the average temperature achieved, Mumbai as a City/Climate Zone has the sixth highest average temperature of 323.3K.

- **New Delhi** noted the highest temperature of 399K on 21st June at 12 pm and the lowest temperature noted was 316K on 21st September 2 pm. New Delhi is located at 77.2090 E, 28.6139 N and is a Sub-Tropical Humid climatic zone. Highest direct solar irradiation over the year was 893.2 W/m^2 on 21st March at 12 pm. On the basis of the average temperature achieved, New Delhi as a City/Climate Zone has the second highest average temperature of 335.62K.
- **Jaisalmer** noted the highest temperature of 375K on 21st June at 12 pm and the lowest temperature noted was 317K on 21st September 2 pm. Jaisalmer is located at 70.9083 E, 26.9157 N and is a Desert climatic zone. Highest direct solar irradiation over the year was 893.8 W/m^2 on 21st March at 12 pm. On the basis of the average temperature achieved, Jaisalmer as a City/Climate Zone has the third highest average temperature of 335.37K.
- **Hyderabad** noted the highest temperature of 353K on 21st December at 12 pm and the lowest temperature noted was 312K on 21st September 2 pm. Hyderabad is located at 78.4867 E, 17.3850 N and is a Savanna climatic zone. Highest direct solar irradiation over the year was 919.8 W/m^2 on 21st December at 12 pm. On the basis of the average temperature achieved, Hyderabad as a City/Climate Zone has the fifth highest average temperature of 330.5K.
- **Gulmarg** noted the highest temperature of 335K on 21st September at 12 pm and the lowest temperature noted was 316K on 21st December 12 pm. Gulmarg is located at 74.3855 E, 34.0494 N and is an Alpine climatic zone. Highest direct solar irradiation over the year was 883.6 W/m^2 on 21st March at 12 pm. On the basis of the average temperature achieved, Gulmarg as a City/Climate Zone has the seventh highest average temperature of 326.37K.
- **Pune** noted the highest temperature of 347K on 21st December at 12 pm and the lowest temperature noted was 316K on 21st March 2 pm. Pune is located at 73.8567 E, 18.5204 N and is a Mediterranean climatic zone. Highest direct solar irradiation over the year was 916 W/m^2 on 21st December at 12 pm. On the basis of the average temperature achieved, Pune as a City/Climate Zone has the fourth highest average temperature of 330.75K.
- **Dras** noted the highest temperature of 347K on 21st March at 12 pm and the lowest temperature noted was 307K on 21st December 2 pm. Dras is located at 76.3189 E, 34.5014 N and is a Subarctic climatic zone. Highest direct solar irradiation over the year was 883.2 W/m^2 on 21st March at 12 pm. Dras had the lowest temperature achieved between all the cities and climate zones. On the basis of the average temperature achieved, Dras as a City/Climate Zone has the second lowest average temperature of 325.62K.

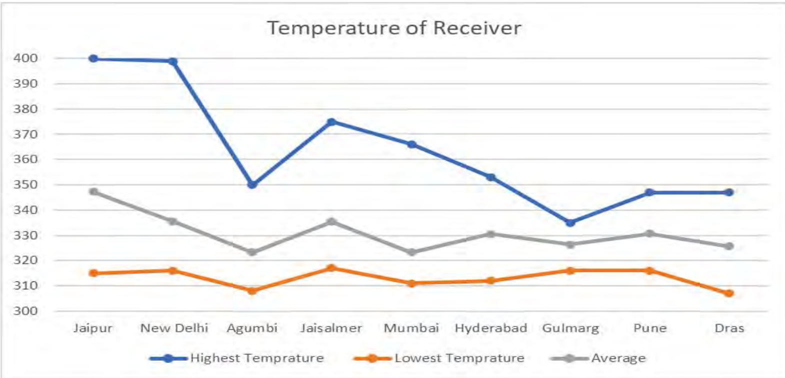

REFERENCES

[1] Arasu, A. & Sornakumar, (2007), Theoretical analysis and experimental verification of parabolic trough solar collector with hot water generation system. Thermal Science - THERM SCI. 11. 119-126. 10.2298/TSCI0701119V.

[2] KR Kumar, KS Reddy , (2009), Thermal analysis of solar parabolic trough with porous disc receiver - Applied energy, 2009 Grena, Roberto.

[3] Xu, JianZhong & Jin, HongGuang & Sui, Jun & Liu, Qibin & Zhang, MingMing, (2012), Recent progress on renewable energy in engineering thermophysics. Chinese Science Bulletin. 57. 10.1007/s11434-012-5532-1.

[4] Singh, Harvinder & Channi, (2023), Harpreet. Performance Analysis of a Parabolic Trough Collector. 10.1007/978-981-99-6774-2_42.

[5] Osorio, Julián & Sensoy, Tugba & Rivera-Alvarez, Alejandro & Patiño, Gustavo & Ordonez, (2023), J.. Influence of Correlations on the Thermal Performance Modeling of Parabolic Trough Collectors. Journal of Solar Energy Engineering. 145. 10.1115/1.4062170.

[6] Alamr, Maiyada & Gomaa, Mohamed, (2023), A Review of Parabolic Trough Collector (PTC): Application and Performance Comparison. 10.37394/232029.2022.1.4.

2nd International Conference on Mathematical
Modelling in Mechanics and Engineering
Mathematical Institute SANU, 12-14. September, 2024.

WEAK STOCHASTIC INTEGRATORS FOR DYNAMICS ON S^2 MANIFOLD

Ankush Gogoi[1*], Satyam Panda[2+], Budhaditya Hazra[2++] and Vikram Pakrashi[1]**

[1]*UCD Centre for Mechanics, School of Mechanical and Materials Engineering, University College Dublin, D04V1W8 Dublin, Ireland*

[2]*Department of Civil Engineering, Indian Institute of Technology Guwahati, 781039 Assam, India*

[1*]*ankush.gogoi@ucdconnect.ie*; [2+]*panda18@iitg.ac.in*; [2++]*budhaditya.hazra@iitg.ac.in*; [1**]*vikram.pakrashi@ucd.ie*

ORCID iD: [1*]0000-0002-2622-434X; [1**]0000-0002-8318-3521

Keywords: Stochastic Integration, Manifold, Exponential Map, Lie Algebra.

ABSTRACT

Stochastic Differential Equations (SDEs) have emerged as a powerful tool to accurately simulate physical systems by incorporating stochastic perturbations in the deterministic dynamics. The theory of SDEs for dynamics on Euclidean space is well established [1]. However, the dynamics of complex systems are often associated with constraints of geometric nature. For example, rigid body rotations are constrained on an abstract mathematical space defined by the collection of special orthogonal groups, or in control theory, the movement of a robot arm is constrained to have a constant length implying that the dynamics evolve on some nonlinear mathematical spaces, commonly known as manifolds [2]. In order to predict the movement or even control such systems, it is necessary to use a numerical integration scheme which can preserve the underlying geometry of the space while considering stochasticity.

To address this, weak stochastic integration schemes for dynamical systems whose dynamics are constrained to move on a manifold is proposed here. The proposed formulation is based on Ito-Taylor expansion for the underlying SDEs and exploiting the relation between the manifold and its Lie Algebra through the exponential map [2]. The geometry preserving weak integrators are appealing for those stochastic dynamical systems where accurate estimation of expected system response and energy is of importance, without the necessity to derive path wise solutions. Numerical illustrations on stochastic systems evolving on S^2 manifold are undertaken to show the efficacy of the weak integrators to provide accurate solutions at coarser step sizes.

REFERENCES

[1] Kloeden PE, Platen E. (1992), “Numerical Solution of Stochastic Differential Equations, First ed., Vol. 23,” *Stochastic Modelling and Applied Probability,* Berlin, Germany, Springer Science & Business Media.

[2] Marjanovic G, Solo V. (2018), “Numerical methods for stochastic differential equations in matrix lie groups made simple,” *IEEE Transactions on Automatic Control,* 63, 4035–4050.

2nd International Conference on Mathematical
Modelling in Mechanics and Engineering
Mathematical Institute SANU, 12-14. September, 2024.

WAVES IN BEAM METASTRUCTURES WITH RIGID BODIES ON INERTER-BASED FOUNDATIONS

Nevena Rosić[1], Milan Cajić[2], Danilo Karličić[3] and Mihailo Lazarević[4]

[1,4]Faculty of Mechanical Engineering, University of Belgrade, 11000 Belgrade, Serbia
[2,3] Mathematical Institute of the Serbian Academy of Sciences and Arts, 11000 Belgrad, Serbia
[1]nrosic@mas.bg.ac.rs; [2]mcajic@mi.sanu.ac.rs; [3]danilok@mi.sanu.ac.rs;
[4]mlazarevic@mas.bg.ac.rs
ORCID iD: [1]0000-0002-9683-3079; [2]0000-0001-5513-0417; [3]0000-0002-7547-9293;
[4]0000-0002-3326-6636

Keywords: Metamaterials, Timoshenko beams, Rigid body, Elastic foundation.

ABSTRACT

This research explores the dynamic behavior of structures encountered in various engineering fields by modeling them as a series of elastic beams interconnected with rigid bodies and supported on an inerter-based elastic foundation. The analytical framework employed enables the derivation of a continuous-mass transfer matrix for arbitrary unit cells, which are tessellated to form a periodic structure (metastructure). Emphasizing the core design of a rigid body suspended between two elastic beams, the study employs Timoshenko beam theory to model the beam segments and performs a thorough analysis of rigid body motion. Dynamical properties of such structures are evaluated by creating band diagrams and analyzing their dispersion properties. The dispersion properties of a supported unit cell are compared to those of a unit cell with free-free boundary conditions, not resting on any foundation. The presence of an elastic foundation increases the system's stiffness, causing the dispersion curves to shift to lower frequencies. This effect is more pronounced with an inerter-based foundation due to inertia amplification.

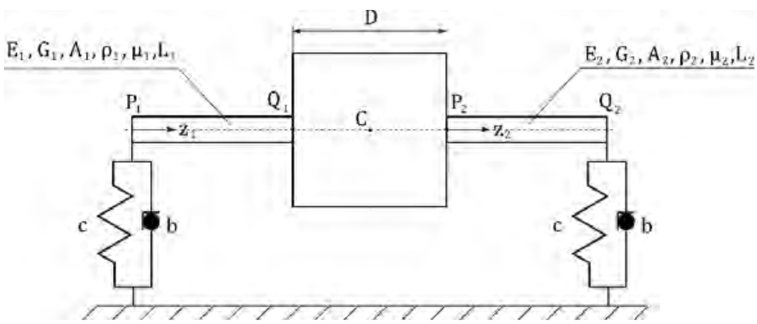

Fig. 1. Unit cell (a rigid body between two elastic beams, with inerter-based elastic foundation)

a) b)

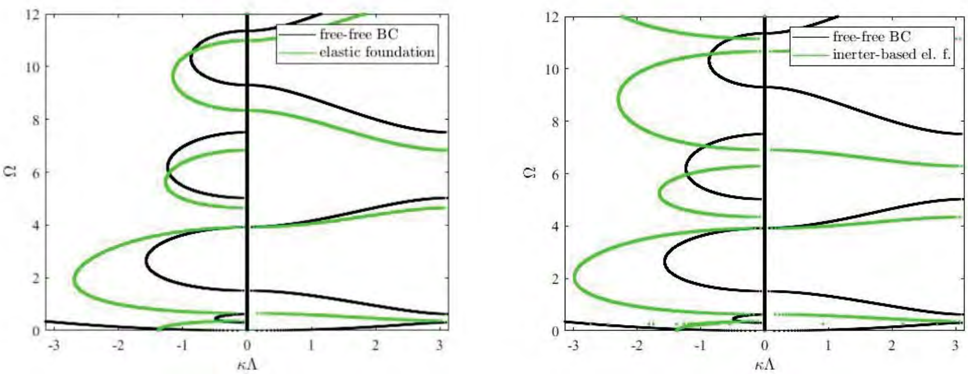

Fig. 2. a) The dispersion curves shift to lower frequencies due to the presence of the elastic foundation. b) This shift is more pronounced with the inclusion of inerters.

ACKNOWLEDGEMENTS

This research was supported by the Serbian Ministry of Science, Technological Development and Innovations, through the Mathematical Institute SANU and grant No. 451-03- 47/2023-01/200105 from 03.02.2023. This support is gratefully acknowledged.

REFERENCES

[1] Obradovic, A., Salinic, S., Trifkovic D.R., Zoric, N., Stokic, Z. (2015) “Free vibration of structures composed of rigid bodies and elastic beam segments”, Journal of Sound and Vibration, 347: 126-138.

[2] Oguamanam, D.C.D., (2003) “Free vibration of beams with finite mass rigid tip load and flexural–torsional coupling”, International Journal of Mechanical Sciences, 45: 963-979.

[3] Heckl, MA., (2002) “Coupled waves on a periodically supported Timoshenko beam”, Journal of Sound and Vibration, 252(5): 849-882.

[4] Younesian, D., Hosseinkhani, A., Askari, H., Esmailzadeh, E. (2019) “Elastic and viscoelastic foundations: a review on linear and nonlinear vibration modeling and applications”, Nonlinear Dynamics, 97: 853-895.

[5] Hussein, M.I., Ruzzene, M., Leamy, M., (2014) “Dynamics of Phononic Materials and Structures: Hystorical Origins, Recent Progress, and Future Outlook”, Applied Mechanics Reviews, 66: 040802.

2nd International Conference on Mathematical
Modelling in Mechanics and Engineering
Mathematical Institute SANU, 12-14. September, 2024.

ALGORITHM FOR PARALLEL COMPUTATIONS OF REACTIVE FLOW WITH PARTICLES – GAINS AND CHALLENGES

Ivan D. Tomanović[1], Srđan V. Belošević[2], Aleksandar R. Milićević[3], Nenad Đ. Crnomarković[4] and Andrijana D. Stojanović[5]

[1,2,3,4,5]*Department of Thermal Engineering and Energy, "Vinca" Institute of Nuclear Sciences – National Institute of the Republic of Serbia, 11000 Belgrade, Serbia*

[1]ivan.tomanovic@vin.bg.ac.rs; [2]v1belose@vin.bg.ac.rs; [3]amilicevic@vin.bg.ac.rs; [4]ncrni@vin.bg.ac.rs; [5]andrijana@vin.bg.ac.rs

ORCID iD: [1]0000-0001-7573-7224; [2]0000-0001-9842-8408; [3]0000-0003-4615-8789; [4]0000-0001-5482-082X; [5]0000-0001-5352-050X

Keywords: CFD, Reactive Flow, Particles, Parallelization, Algorithm.

ABSTRACT

Previously developed parallel CFD code [1] serves as a good foundation for future implementation of more complex codes containing both particle tracking and reactive flows. Initial development of computer code allowed us to estimate potential gains in execution times when moving computationally strongly demanding portions of code to GPU and execute them in parallel.

At the time we have shown that inner portions of code in subroutines that calculate individual scalar or vector fields can be properly restructured to allow significantly shorter calculation times. However, deeper examination of the computer code reveals that some of subroutines do not directly depend on each other, and that they can be executed in parallel. Scaling up this problem to a more complex system such is a model of boiler furnace opens up a new set of opportunities to gain in computation efficiency, but also introduces new challenges.

In this presentation we will discuss algorithm that might lead to optimal parallel implementation of a utility boiler CFD code that would be capable to run on current and upcoming GPUs, providing reliable and fast output. Given that the boiler model introduces subroutines for species in reactive flow, there is an opportunity not only to parallelize their inner structure, but also to execute them in parallel at larger scale. To do this we must first identify if any of reaction subroutines depend on other reactions. Those must be separated from the rest ones and set to wait until their input data is ready for them to run. This is also true for velocity component subroutines which can be executed in parallel, but must wait and synchronize before calling the routine that determines pressure corrections for pressure linked equations.

Aside from additional parallelization opportunities, we discuss the upcoming challenges as well. One of the major challenges will be particle tracking. The code uses Particle Source In Cell coupling between particles and flow field variables. Each particle adds to a source term of a cell as it passes through it. In serial code this is not a major issue, as each source term is updated with new value without the danger of being overwritten by another incoming data. However, going fully parallel opens up a possibility to attempt to write data to the same source term multiple times, effectively causing it to randomly update with data that has been last

written to it, ignoring all other data written before. To overcome this issue, OpenACC allows us to use reductions, creating separate copies of matrices for each new incoming data and keep it until all data is ready, and finally completing the reductions, preventing from any data loss in the code execution process. An alternative approach would be to create a corresponding matrix, and thus create enough space to store data from each time step of each trajectory, without need for reduction at this point. In this matrix one column would store particle coordinates at a given time step during the particle tracking, while the other column would contain particles contribution to the source term in cell with those coordinates.

Overall algorithm, which the CFD code should follow, must break any dependencies between subroutines that would lead their inability to run concurrently, identify portions of code that must wait for data synchronization from different sources, and manage data movements between CPU and GPU in such a way to prevent any unnecessary data transfers that would have significant impact on the code running time.

REFERENCES

[1] Tomanović, I., *et al.* (2022), “Parallel computations in fluid dynamics using multicore/manycore processors,” *Booklet of Abstracts of the 1st International Conference on Mathematical Modelling in Mechanics and Engineering,* Belgrade, Serbia, 08– 10 September, pp. 43-44.

Figure: Flow chart of algorithm for simulations of the particle-laden reactive flow

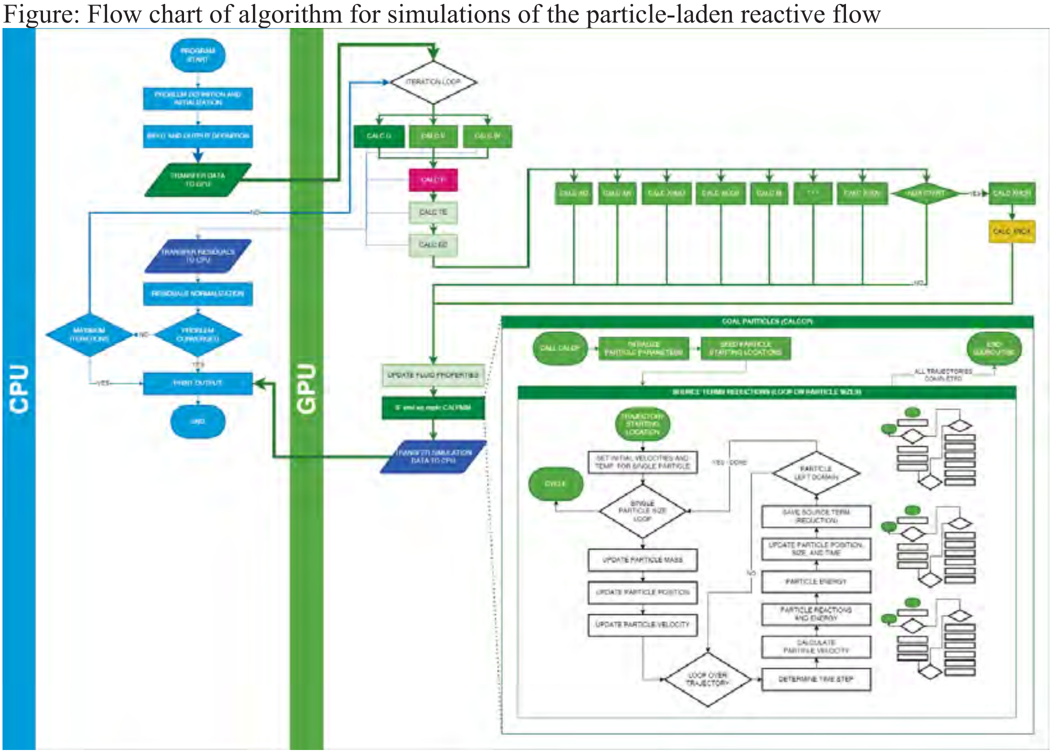

2nd International Conference on Mathematical Modelling in Mechanics and Engineering
Mathematical Institute SANU, 12-14. September, 2024.

INFLUENCE OF ANCHOR ROD BENDING ON THE BEHAVIOR OF COLUMN BASE PLATE CONNECTIONS

M.A Aichouche[1], A. Abidelah[2] and Dj.D Kerdal [3]

[1,2]LMST, Civil Engineering Department, U.S.T.O.M.B., B.P. 1505 El M'Naouer, Oran, Algeria

[3]LM2SC, Civil Engineering Department, U.S.T.O.M.B., B.P. 1505 El M'Naouer, Oran, Algeria

[1]aichoucheamine@hotmail.fr; [2]abidellah@gmail.com;

ORCID iD: [1]0009-0003-5039-8918

Keywords: Column base connection, anchor bolts, Finite element model, Anchor rod bending.

ABSTRACT

Column base plate connections are critical structural elements that transfer axial forces, shear forces, and moments from the superstructure to the foundation in steel frame buildings[1-5]. The failure of these connections can lead to catastrophic collapse of the entire structure [6]. The behavior of column base plate connections is governed by complex interactions between various components, including the column, base plate, anchor rods, and concrete foundation[7]. However, current design codes like Eurocode 3 often oversimplify the behavior of anchor rods by neglecting bending effects, which can lead to inaccurate capacity estimates. This paper investigates the impact of anchor rod bending on the performance of column base plate connections through a validated 3D finite element model developed from existing experimental data, as shown in Fig. (1-2). Under constant axial load followed by monotonic moment loading, the analysis revealed significant combined bending moments and tensile forces acting on the anchor rods, contrary to typical design assumptions (Fig.3). The findings suggest that the Eurocode 3 component method [8], may overestimate anchor rod capacities by disregarding bending moment contributions, underscoring the need for a more comprehensive consideration of anchor rod behavior in the design of these critical connections to ensure structural safety and reliability.

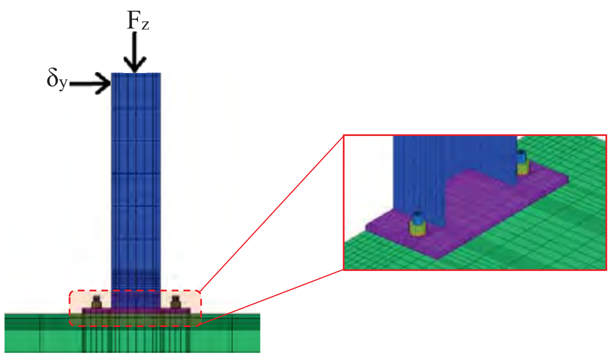

Fig. 1. FEM of Column Base Plate Connection

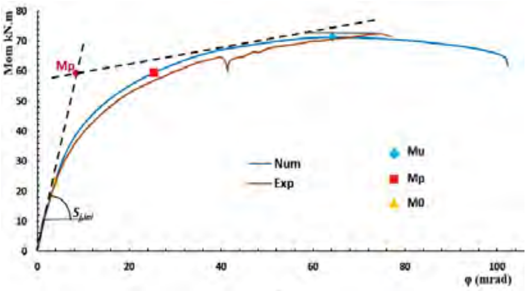

Fig. 2. Numerical and experimental moment-

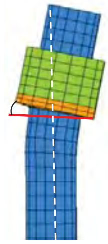

Fig. 3. Deformed shape of the anchor

REFERENCES

[1] Fasaee MAK, Banan MR, Ghazizadeh SJJoCSR. Capacity of exposed column base connections subjected to uniaxial and biaxial bending moments. 2018;148:361-70.
[2] Hassan AS, Torres-Rodas P, Giulietti L, Kanvinde AJES. Strength characterization of exposed column base plates subjected to axial force and biaxial bending. 2021;237:112165.
[3] Kanvinde A, Grilli D, Zareian FJJose. Rotational stiffness of exposed column base connections: Experiments and analytical models. 2012;138:549-60.
[4] Lee D-Y, Goel SC, Stojadinovic BJIJoss. Exposed column-base plate connections bending about weak axis: I. Numerical parametric study. 2008;8:11-27.
[5] Torres-Rodas P, Medalla M, Zareian F, Lopez-Garcia DJES. Cyclic behavior and design methodology of exposed base plates with extended anchor bolts. 2022;260:114235.
[6] Kabir MAB, Hasan AS, Billah AMJES. Failure mode identification of column base plate connection using data-driven machine learning techniques. 2021;240:112389.
[7] Seco LDS, Couchaux M, Hjiaj M, Neves LCJES. Column base-plates under biaxial bending moment. 2021;231:111386.
[8] CEN EJEcfs, Brussels. 1-8 Eurocode 3: Design of Steel Structures–Part 1–8: Design of Joints. 2005.

DEVELOPMENT OF COMPOSITES REINFORCED WITH RAMIE FIBER AND NATURAL RUBBER

Ajith Kuriakose Mani[1*], Abin Varghese Jacob[1], Alen Shibu Paul[1], Anantha Krishnan[1], Akash Krishnan V[1], Sivasubramanian Palanisamy[2*]

[1]*Department of Mechanical Engineering, Saintgits College of Engineering (Autonomous), Pathamuttom, Kottayam, Kerala 686532 India*
[2]*Department of Mechanical Engineering, PTR College of Engineering & Technology, Thanapandiyan Nagar, Madurai-Tirumangalam Road, Madurai Tamil Nadu 625008, India.*
*Corresponding authors: ajith.kuriakose@saintgits.org; sivaresearch948@gmail.com
ORCID iD: [1*]0000-0002-7885-4319; [2*]0000-0003-1926-4949

Keywords: Instructions, Mechanics, Engineering.

ABSTRACT

The pressing issue of global warming has prompted industries to seek sustainable and renewable materials that can reduce the use of petroleum-based products. Natural fibers, as bio-based and environmentally friendly materials, offer a promising solution. In this study, the mechanical properties of natural rubber composites reinforced with ramie fiber were evaluated. The composites were fabricated using a vulcanizing technique at 150°C and the fibers were cut into different lengths (5mm, 10mm & 15mm) and weights (15g, 30g & 60g). Mechanical performance tests, including tensile and tear strength, and hardness were conducted. The results showed that as fiber concentration increased, so did the curing time. Moreover, the composites with higher fiber concentration had higher strength. The composite with 10mm & 60g ramie fiber concentration had the highest tensile strength (10.35MPa) and the composite with 5mm & 60g ramie fiber concentration had the highest tear strength (52.518 KN/m). The specimen with the highest tensile strength was subjected to scanning electron microscope analysis. The SEM analysis revealed that the composite had a ductile type of fracture with appreciable plastic deformation. Overall, the results of this study indicate the potential of using natural rubber composites reinforced with ramie fiber as a sustainable and environmentally friendly alternative to petroleum-based products. Further tests and optimization of the fabrication process are necessary to fully realize the potential of this composite material.

EXPERIMENTAL DETAILS

Materials

The reinforcement material used in this study is Ramie fiber, a plant-based fiber that has been known for its high strength, even when wet. Ramie fiber is purchased from Vruksha Composites, Tenali, Natural rubber (ISNR 5) was purchased from the local market. Ramie fiber has a density of 1.50g/cm^3, fracture load of 0.467N, Tensile Strength of 560MPa, and fracture strain of 0.025%. In contrast, Natural Rubber has excellent resilience, abrasion and surface friction properties, high fatigue resistance, low rolling resistance and hysteresis, and stays flexible even when its temperatures are low. This combination of properties makes it a popular choice for high-performance tires for race buses, trucks, cars, and aircraft, as a result of its high resistance to heat and its high tear strength. The study aims to assess the impact of Ramie fiber reinforced with natural rubber, and its potential as a sustainable alternative for the rubber industry.

Composite Manufacture

Ramie fibers were cut with scissors into different lengths of about 5 mm, 10 mm, and 15 mm and then put into different weight ratios of 15 g, 30 g, and 60g to make the various parts needed for the work. Then, a two-roll mill made a composite at room temperature. Natural rubber (grade ISNR 5) was added to each compound in the mixer to make the composite. The amounts of chemicals required for the mixing process are listed in Table 2.1. The samples were put through the two-roll mixing mill (Fig. 2.2(a)) more than once to ensure the materials were evenly distributed. The total mixing time was 15 to 30 minutes, or until the ramie fibers were completely mixed into the rubber matrix.

In order to determine the ideal curing time, the samples shown in Fig. 2.1 (c) were put through a Rheometer. After determining the ideal curing time, the samples were cured using a hydraulic compression moulding press equipped with electrically heated plates, as shown in Fig. 2.2 (b). This process was carried out at a vulcanizing temperature of 150°C. Curing time characteristics, tensile test, tear test, hardness and Scanning Electron Microscopy fractographic analysis were performed after curing to determine the compound's mechanical properties.

Fig 1. (a) Mixing Mill; (b) Mould Press; (c) Rubber mixed Compound

Characterizing Tests

The following tests are conducted on the composite material and the results are evaluated. The main characterizing tests are (i) Curing Time Test, (ii) Tensile Strength Test, (iii) Tear Strength Test, (iv) Hardness Test, (v) Scanning Electron Microscopy Analysis.

REFERENCES

[1] Du, W., Yu, J., & Chen, L. (2015). Preparation and properties of ramie fiber reinforced natural rubber composites. Polymer Composites, 36(8), 1421-1429.
[2] Shi, Y., Du, W., & Yu, J. (2020). Study on mechanical and dynamic properties of ramie fiber reinforced natural rubber composites. Journal of Natural Fibers, 17(4), 547-559.

APPLYING RODRIGUES' FORMULA FOR KINEMATIC MODELING OF VIBRATORY CONVEYORS

Uroš Lj. Ilić[1], Mihailo P. Lazarević[2]

[1] *Institute Mihajlo Pupin, University of Belgrade, 11000 Belgrade, Serbia*

[2]*Faculty of Mechanical Engineering, University of Belgrade, 11000 Belgrade, Serbia*

[1]uros.ilic@pupin.rs; [2]mlazarevic@mas.bg.ac.rs

ORCID iD: [1]0000-0003-3955-8995; [2]0000-0002-3326-6636

Keywords: Rodrigues' Formula, Serial Kinematics, Mathematical Modelling, Vibratory Conveyers.

ABSTRACT

Vibratory technology is involved in various industries, such as food, metallurgical, arms industry, etc. [1]. Major implementation can be found in material conveyance in the form of vibratory conveyers. Depending on the continuity of the contact of the conveyed particles and vibratory trough's surface, these machines can set material into motion in two ways – hopping and no-hopping motion. Conventional vibratory conveyers (Fig. 1) have an actuator positioned at a certain angle to the ground. This angle defines the force vector that sets the material into forward motion.

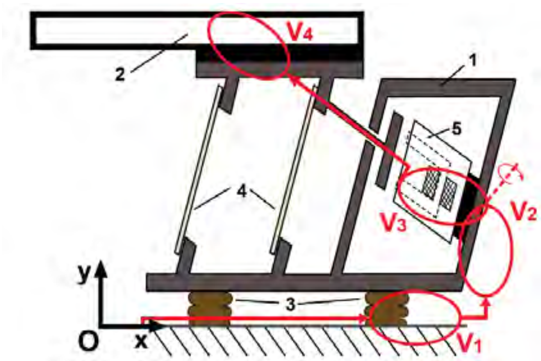

Figure 1 *– A schematics of an electromagnetically driven vibratory conveyer [2] consisting of stationary base (1), vibratory trough (2), dampers (3), leaf springs (4) and electromagnet (5) with a corresponding robotic serial mechanism drawn (red color) over it*

Main goal of this research is to explore a potential design with two orthogonally positioned actuators that can change the direction of the resultant vector. Variation of frequencies, phase differences and amplitude ratios enable different vibratory regimes implemented not only in conveyance, but at fine dosing, shaking and stirring, sifting etc.

Contrary to conventional technological processes that use hopping motion, where a new machine is introduced for various operations, this way only the vibratory trough should be replaced, and the control and actuating system generally remains the same. Additionally, with dual excitation, the no-hopping motion can be achieved in simpler control algorithms. This form of motion is suitable for industries that demand sensitive handling with material (e.g. chemical or military industry).

For this purpose, a mathematical model of a standard vibratory conveyer is defined with segregated upward and sideways displacements of the base. This research explores the kinematics of such vibratory machines from a robotics aspect (Fig. 1). More precisely, the conveyer system (vibratory trough with stationary base) is being analyzed and remodeled as an open serial kinematic chain. The interdependencies of the virtual segments are derived using Rodrigues' formula, that's thoroughly defined in [3].

The analysis starts by defining the relative coordinates of the virtual robotic system. Since the conveyor depicted in Fig 1. can be approximated to perform exclusively planar motion it can be visualized as a robotic system with multiple segments interconnected by means of joints – one for each degree of freedom (DOF). The proposed system will consist of a total of four joints - two linear and one rotational joint to define the absolute movement of the stationary base in the vertical plane and an additional linear joint to define displacement of the trough relative to the base itself.

After the definition of the configuration of the robotic system, absolute radius vectors of centers of inertia of corresponding segments are defined. Furthermore, expressions for angular and translational velocities are obtained for each proposed segment which will be served for setting in an automatic manner of the kinematic model of vibration conveyor.

Acknowledgements

This research has been supported by the research grants of the Serbian Ministry of Science, Technological Development and Innovations, grant No. 451-03-65/2024-03/200105 from 5.2.2024.

REFERENCES

[1] Goncharevich, I. F., Frolov, K.V., Rivin, E.I., (1990) "Theory of vibratory technology", *Hemisphere Publishing Corporation*, New York, pp. 2-45

[2] Despotović, Ž., Urukalo, Đ., Lečić M., et al. (2017) "Mathematical modeling of resonant linear vibration conveyor with electromagnetic excitation: simulations and experimental results", *Applied Mathematical Modelling*, pp. 41:1–24.

[3] Čović, V., Lazarević, M., (2021) „Mehanika robota ", Univerzitet u Beogradu, Mašinski fakultet, Beograd pp. 39-139.

2nd International Conference on Mathematical
Modelling in Mechanics and Engineering
Mathematical Institute SANU, 12-14. September, 2024.

MECHANICAL BUCKLING OF FGM PLATES RESTING ON ELASTIC FOUNDATIONS USING LAYER WISE FINITE ELEMENT

Marina V. Cetkovic[1]

[1]Faculty of Civil Engineering, University of Belgrade, 11 000 Belgrade, Serbia

[1]cetkovicm@grf.bg.ac.rs

ORCID iD: 0000-0001-8595-0424

Keywords: Mechanical buckling, FGM plates, Pasternak elastic foundations, Layer wise Finite element, MATLAB computer program.

ABSTRACT

The concept of FGM was first introduced by a group of material scientists in Japan in mid–1980s. for space plane project [1]. FGMs are microscopically made composites usually from a mixture of metal and ceramic, in which material properties vary continuously in one or three directions. These gradual changes of materials properties overcome the disadvantages of traditional FRP (Fiber Reinforced Polymer) composites, regarding inter and intra laminar failure modes. The variation of material properties is defined by mathematical function, which may be given by: Power Law model, Exponential model, Sigmond law model, Mori Tanaka scheme and others. As FGMs are usually made of two materials, the metal and the ceramic, the ceramic layer serves for thermal resistance, whereas the metal layer gives high toughness. Due to the high heat resistance, FGMs have many practical applications in aerospace industries, defence industries, biomechanics, as well as and civil engineering. Therefore, the buckling problem of FGM plate subjected to in–plane loading and resting on elastic foundations received considerable interest of researchers over the last decades [2].

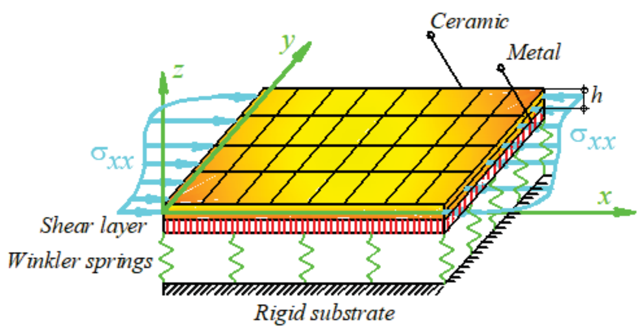

Figure 1. *Geometry of FGM plate resting on Pasternak foundation*

When modelling elastic foundations, many studies have been performed to predict the critical buckling loads of highway and airfield pavement systems as well as foundations of storage tanks, swimming pools, and buildings by employing a plate on an elastic foundation [3]. The surface layer of the pavement (reinforced concrete slab in the rigid pavement and asphalt mixtures in the flexible pavement) is regularly simulated as a rectangular plate, while the underlying layers are modelled using an elastic foundation. For modelling elastic medium and describing the interactions of the plate and foundation, various kinds of foundation models are suggested. The simplest model for the elastic foundation is Winkler or one–parameter model [4], which models the foundation as a series of separated springs without coupling effects between each other. In wish to improve the Winkler model, several researchers tried to more realistically simulate interaction between the spring elements, by connecting upper ends of springs in the Winkler model with an elastic membrane or shear layer. These are so called the two–parameter foundations models, such as Filonenko–Borodich [5], Pasternak [6], generalized [7], and Vlasov [8].

In this study the mechanical buckling analysis of functionally graded plates resting on elastic foundation is modelled using two–parameter Pasternak model. The mathematical model, based on Layer wise theory of Reddy [9], assumes layer wise variation of in plane displacements and constant transverse displacement through the thickness, non–linear strain displacement relations (in von Karman sense) and isotropic nonhomogeneous material properties. The material properties of FGM plates are assumed to be constant in xy–plane and vary through the thickness by a power law function in terms of the volume fraction of the constituents. The effective materials properties are given by the rule of mixture. The principle of virtual displacement (PVD) is used to derive the weak form of linearized buckling problem. The weak form is discretized using nine node Lagrangian isoparametric finite element. The original MATLAB computer program is coded for the FEM solution. The influence of different parameters, such as elastic foundation parameters, in–plane load distribution, side–to–thickness ratio b/h, aspect ratio a/b and power–low index is presented. The accuracy of the numerical model is verified by comparison with the available results from the literature.

REFERENCES

[1] Koizumi M. FGM activities in Japan. Composite part B Eng. 1997; 28: 1–4.
[2] Yaghoobi H, Fereidoon A. Mechanical and thermal buckling analysis of functionally graded plates resting on elastic foundations: An assessment of a simple refined nth–order shear deformation theory. Composites: Part B 2014; 62: 54–64.
[3] Akhavan H, Hashemi H. Taher RD, Alibeigloo A, Vahabi S. Exact solutions for rectangular Mindlin plates under in–plane loads resting on Pasternak elastic foundation. Part I: Buckling analysis. Computational Materials Science 2009; 44: 968–978.
[4] Winkler E. Die Lehre von der elasticitaet und festigkeit. Prag Dominicus 1867.
[5] Filonenko–Borodich MM. Some approximate theories of the elastic foundation, Uchenyie Zapiski Moskovskogo Gosudarstuennogo Universiteta Mechanika 46 (1940) 3–18, (in Russian).
[6] Pasternak PL. On a new method of analysis of an elastic foundation by means of two foundation constants, Gosudarstvennoe Izdatelstvo Literaturi po Stroitelstvu i Arkhitekture, Moscow, 1954, (in Russian).
[7] Kerr AD. J. Appl. Mech. 31 (3) (1964) 491–498.
[8] Vlasov VZ, Leontev U.N. Beams, plates and shells on elastic foundations (translated from Russian), Israel Program for Scientific Translation, Jerusalem, Israel, 1966.
[9] Reddy JN, Barbero EJ, Teply JL. A plate bending element based on a generalized laminated plate theory. International Journal for Numerical Methods in Engineering 1989; 28: 2275–2.

2nd International Conference on Mathematical
Modelling in Mechanics and Engineering
Mathematical Institute SANU, 12-14. September, 2024.

ANALYSIS OF POROUS FUNCTIONALLY GRADED SIZE-DEPENDENT POROUS PLATES ON THE ELASTIC FOUNDATION OF WINKLER-PASTERNAK TAKING INTO ACCOUNT DIFFERENT TYPES OF NONLINEARITY

L.A. Kalutsky[1], T.V. Yakovleva[2], V.A. Krysko[3]

[1-3]*Yuri Gagarin State Technical University of Saratov,*
Politehnicheskaya 77, 410054 Saratov, Russian Federation
[1]leon199703@gmail.com; [2]yan-tan1987@mail.ru; [3]tak@san.ru
ORCID iD: [1]0000-0003-3335-4975; [2]0000-0003-3238-2317; [3]0000-0002-4914-764X

Keywords: Functionally graded porous size-dependent plates, Variational iterations method, Extended Kantorovich method, Elastic Winkler-Pasternak foundation, von Karman nonlinearity, Green-Lagrange nonlinearity.

ABSTRACT

Macro- and microscale plates made of porous functionally graded materials (PFGMs) are widely used in various branches of modern engineering, such as aerospace, automotive, biomedical, optoelectronics, etc.

An analysis of existing studies shows a lack of research on the statics of flexible porous functionally graded size-dependent porous plates on an elastic foundation taking into account Green-Lagrangian nonlinearity.

In this study, a mathematical model of geometrically nonlinear functionally graded porous size-dependent Kirchhoff plates on an elastic Winkler-Pasternak foundation is constructed. Two models are applied to account for geometric non-linearity, the von Karman and the Green-Lagrange models. Size-dependent effects are incorporated by Yang's modified couple stress theory (MCST) [1]. Among the size-dependent theories, MCST has the advantage of using only one material length scale parameter, which makes it convenient to use, better in numerical realisation and representation of elastic properties. At the same time, other non-classical theories have a number of limitations. Note, the nonlocal elasticity theory defined by Eringen leads to a paradox in the results concerning the obtained values of the eigenfrequencies compared to the classical model.

The foundation parameters are considered as functions depending on the x,y coordinates. Plates made of functionally graded material consisting of aluminium and ceramics - zirconium dioxide, as well as of steel SUS304 and ceramics - silicon nitride, etc. are considered. Three porosity patterns are considered: 1) uniform porosity, 2) pore increase at the centre of the plate, and 3) pore increase from the centre to the top and bottom boundaries of the plate.

The system of nonlinear differential equations in displacements is obtained from the Hamilton's principle. The derived system of equations is solved by two methods: the Bubnov-Galerkin method in higher approximations and the Variational Iterations Method (VIM) - extended Kantorovich method (EKM) in first and second approximations. The restrictions of the Fourier hypothesis of separation of variables are not required. The convergence theorems for the VIM method are proved. These two factors allow us to claim that the solutions obtained using the developed methodology provide practically exact solutions to problems involving

both von Karman and Green-Lagrange nonlinearities. This statement is supported by comparisons with solutions obtained by the Bubnov-Galerkin method in higher approximations.

In references [2-6], the accuracy, efficacy and high speed of the Variational Iteration Method (VIM) were demonstrated.

The absence of nonlinear terms associated with the displacement derivatives u, v in the Green-Lagrange expressions for midplane deformation - in particular the transition to the von Kármán model - leads to significant errors in the calculation of stresses and strains.

The study examines the effect of material functionally graded, pore pattern, elastic foundation and size-dependent parameter on the stress-strain state of plates. It is concluded that for the alloys studied, increasing the ceramic content of the plate material increases the strength of the structure. It is also shown that a porosity structure with a maximum distribution of pores in the centre of the plate optimises the load bearing capacity.

The work was supported by the Russian Science Foundation RNF grant No. 22-71-10083.

REFERENCES

[1] Yang J., Liew K. M., Wu Y. F., Kitipornchai S. (2006). Thermo-mechanical post-buckling of FGM cylindrical panels with temperature-dependent properties. *International Journal of Solids and Structures*, 43(2), pp. 307-324.

[2] Awrejcewic, J., Krysko-Jr V. A., Kalutsky L. A., Zhigalov M. V., Krysko, V. A. (2021). Review of the methods of transition from partial to ordinary differential equations: From macro-to nano-structural dynamics. *Archives of Computational Methods in Engineering*, pp. 1-33.

[3] Awrejcewicz J., Krysko Jr, V. A., Kalutsky L. A., Krysko V. A. (2022). Computing static behavior of flexible rectangular von Karman plates in fast and reliable way. *International Journal of Non-Linear Mechanics*, 146, pp. 104162.

[4] Krysko jr V. A., Awrejcewicz J., Kalutsky L. A., Krysko V. A. (2023). Quantification of various reduced order modelling computational methods to study deflection of size-dependent plates. *Computers & Mathematics with Applications*, 133, pp. 61-84.

[5] Krysko A. V., Kalutsky L. A., Krysko V. A. (2024). Stress-strain state of a porous flexible rectangular FGM size-dependent plate subjected to different types of transverse loading: Analysis and numerical solution using several alternative methods. *Thin-Walled Structures*, 196, pp. 111512.

[6] Krysko A. V., Gubaidullin D. A., Kalutsky L. A., Krysko, V. A. (2024). Nonlinear deformations of size-dependent porous functionally graded plates in a temperature field. *International Journal of Solids and Structures*, pp. 112759.

2nd International Conference on Mathematical Modelling in Mechanics and Engineering
Mathematical Institute SANU, 12-14. September, 2024.

DESIGN AND FLOW SIMULATION OF A MORPHING AIRFOIL

Jelena Svorcan[1], Nebojša Lukić[2], Toni Ivanov[3] and Aleksandar Simonović[4]

[1,3,4]*Faculty of Mechanical Engineering, University of Belgrade, 11000 Belgrade, Serbia*
[2]*Technical Testing Center, 11000 Belgrade, Serbia*
[1]*jsvorcan@mas.bg.ac.rs*; [3]*tivanov@mas.bg.ac.rs*;
ORCID iD: [1]0000-0002-6722-2711; [3]0000-0002-8204-4669

Keywords: Morphing airfoil, CFD, Aerodynamic performance.

ABSTRACT

To increase the efficiency of lifting surfaces, such as wings, tails, propeller or wind turbine blades, the concept of morphing (changeable) geometry is gaining popularity and being more and more investigated [1]. With the advances in materials, flexible structures, new production techniques and improved simulations, it is possible to design optimal shapes for particular operating conditions (e.g. low Reynolds numbers), that at the same time have the capability to adapt to a wide range of different working conditions (that are present with small unmanned air vehicles in urban environments). Here, one such airfoil contour is presented in Fig. 1(left), and investigated in more detail. Geometric variations are achieved by vertically sliding three key spinal points (at axial positions corresponding to 20%, 40% and 60% chord length) where fixed-length ribs defining the outer (upper and lower) surfaces are perpendicularly connected. Flow simulations by Reynolds-averaged Navier-Stokes (RANS) equations closed by transition SST turbulence model are employed for the estimation of its aerodynamic performance, example in Fig. 1(right). Very promising results are achieved that justify further research work in this field.

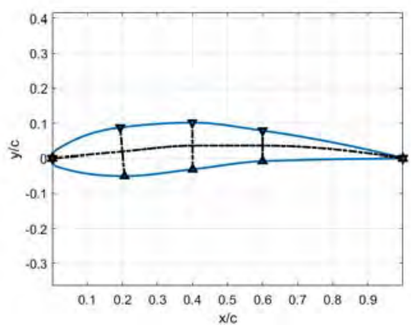

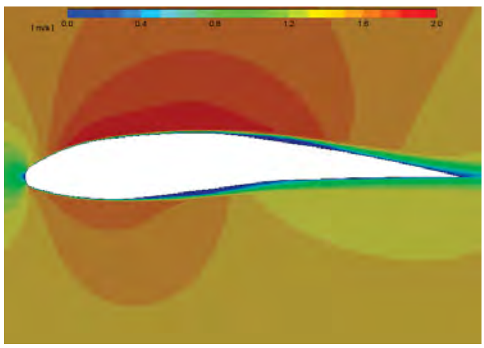

Figure 1. Airfoil contour and key elements (left), Computed velocity field (right).

REFERENCES

[1] Lukić, N., Ivanov, T., Svorcan, J., Simonović, A. (2024), "Numerical Investigation and Optimization of a Morphing Airfoil Designed for Lower Reynolds Number," *Aerospace* 11, no. 4: 252. https://doi.org/10.3390/aerospace11040252

ANALYSIS OF SUB-RESONANCE OF BIO-INSPIRED PAW-LIKE STRUCTURES

Xiaofang Duan, Jimin Ye, Dongmei Huang

[1] *School of Mathematics and Statistics, Xidian University, Xi'an, 710126, China*
[1] *jmye@mail.xidian.edu.cn*; [2] *dmhuang@xidian.edu.cn*;

Keywords: Bio-inspired structure, The method of multiple scales, Vibration isolation

ABSTRACT

Sub-resonances of bionic paw-inspired structure vibration isolation systems are examined in this paper. Amplitude-frequency response functions, stability conditions, and bifurcation sets for subharmonic, ultra-subharmonic, and superharmonic resonances are discussed in detail. Since the equations are nonlinear, the results on the character of subharmonic, superharmonic, and superharmonic resonances may apply to practically all kinds of physical and engineering problems. Based on theoretical derivation, the effect of the structural parameters of the bionic paw-inspired structure on the nonlinear response and bifurcation set is investigated in detail. The effects of subharmonic, superharmonic, and superharmonic resonances on vibration isolation performance have not been discussed for bionic paw-inspired structure. This study can provide a solid foundation for further research in physical and engineering vibration isolation.

REFERENCES

[1] Huang, Dongmei, Shengxi Zhou, and Grzegorz Litak. "Theoretical analysis of multi-stable energy harvesters with high-order stiffness terms.", Communications in Nonlinear Science and Numerical Simulation 69 (2019): 270-286.

2nd International Conference on Mathematical
Modelling in Mechanics and Engineering
Mathematical Institute SANU, 12-14. September, 2024.

ELASTICPLASTIC ANALYSIS OF PERFORATED RECTANGULAR 3D PLATES

Anton Makseev[1], Anton V. Krysko[2], Tatyana V. Yakovleva[3], Ksenia S. Bodyagina[4], Maxim V. Zhigalov[5], Vadim A. Krysko[6]

[1,2,3,4,5,6] *Yuri Gagarin State Technical University of Sarato,v 410054 Saratov, Russian Federation*

[1]*makseevv.anton@mail.ru* ; [2]*anton.krysko@gmail.com*; [3]*yan-tan1987@mail.ru*
[4]*bodksen@mail.ru*; [5]*zhigalovm@yandex.ru*; [6]*krysko1937@gmail.com*
ORCID iD: [1]0000-0003-0181-3460; [2]0000-0002-9389-5602; [3]0000-0003-3238-2317, [4]0000-0002-8822-410X; [5]0000-0002-0642-7211; [6]0000-0002-4914-764X

Keywords: Plate, hole, physical nonlinearity, finite element method, method of variable elasticity parameters.

ABSTRACT

In various engineering applications, structural elements often consist of plates with technological holes. These holes serve essential purposes such as weight reduction and access to specific maintenance areas. The presence of notches and holes in such structures leads to stress concentration, changes in plate stiffness and, consequently, to both changes in the stress-strain state and the appearance of plastic zones. Consequently, the study of 3D plates weakened by holes, taking into account elastoplastic deformations, seems important and relevant. In this study, a mathematical model of elastoplastic deformation is developed based on the deformation theory of plasticity for plates with holes in the center (Fig. 1). The following hypotheses were used to derive the equations:

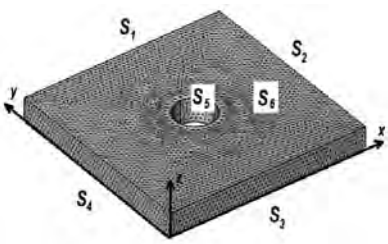

Fig.1.The geometry of the plate

(i) the material of the plate is assumed to be isotropic but inhomogeneous: $E(x,y,z,e_i,e_0)$, $\vartheta(x,y,z,e_i,e_0)$, where e_i is intensities of strain, e_0 is volumetric strain [1];

(ii) the deformation theory of plasticity is applied;

(iii) the von Mises criteria of plasticity is used.

The required differential equations (1), which incorporate the above hypotheses in a 3D formulation for rectangular plates, are derived using Hamilton's principle [2]:

$$(\lambda+\mu)\theta_x+\mu\Delta u+\frac{\partial\lambda}{\partial x}\theta+2\frac{\partial\mu}{\partial x}\frac{\partial u}{\partial x}+\frac{\partial\mu}{\partial y}\left(\frac{\partial v}{\partial x}+\frac{\partial u}{\partial y}\right)+\frac{\partial\mu}{\partial z}\left(\frac{\partial w}{\partial x}+\frac{\partial u}{\partial z}\right)+q_X=0,\quad \overleftrightarrow{(x,y,z)}, \qquad (1)$$

where: $u(x,y,z)$, $v(x,y,z)$, $w(x,y,z)$ – displacement along the axes x,y,z, respectively; $\Delta(\Box)=\frac{\partial^2(\Box)}{\partial x^2}+\frac{\partial^2(\Box)}{\partial y^2}+\frac{\partial^2(\Box)}{\partial z^2}$ - Laplace operator; $\lambda(x,y,z,e_i,e_0)$, $\mu(x,y,z,e_i,e_0)$; - stand for the Lamé constants; $\theta=\frac{\partial u}{\partial x}+\frac{\partial v}{\partial y}+\frac{\partial w}{\partial z}$; $\theta_x,\theta_y,\theta_z$,- partial derivatives θ with regard to x,y,z.

On the areas S_1, S_2, S_3, S_4 we take: $\{u = v = w = 0\}$ and on the area S_5 we take $\{N_p = 0, T = 0\}$, where p is normal to the lateral surface of the hole, $N_p, T-$ the normal and tangential forces, respectively. On the surface S_6, without taking into account the area of the hole S_{hole} a transverse uniformly distributed load q_Z . $q_X = q_Y = 0$ is applied. The material of the plate is pure aluminium and its behaviour has specific dependencies based on its material properties [3].

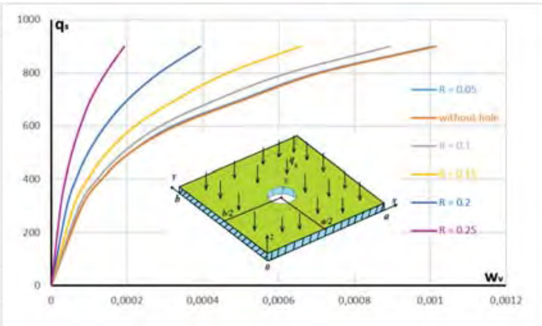

Fig.2. Load-deflection relationship

The solution was carried out using COMSOL Multiphysics software with tetrahedral finite elements. MVEP [4] was used to solve the elastic-plastic problem. The validity of the results is guaranteed by checking the convergence of the finite element method depending on the diameter of holes in the plate, as well as by the MVEP convergence theorem proved by Vorovich and Krasovsky [5]. For each radius of the hole in the plate, the convergence of the finite element method was investigated. Ha Fig.2 shows the dependence of the integral deflection on the distributed surface load for different values of the hole radius. The results show that increasing the hole diameter results in a decrease in deflection and consequently an increase in the flexural stiffness of the plate.

This work has been supported by the Grant RSF No. 22-71-10083.

REFERENCES

[1] Krysko, A.V., Awrejcewicz, J., Bodyagina, K.S. *et al.* (2021), "Mathematical modeling of physically nonlinear 3D beams and plates made of multimodulus materials", *Acta Mech* 232, pp. 3441–3469.

[2] V.A. Krysko-jr., A.D. Tebyakin, M.V. Zhigalov, *et al.*, (2023), Mathematical model of physically non-linear Kirchhoff plates: Investigation and analysis of effective computational iterative methods, *International Journal of Non-Linear Mechanics*, 160, 104346.

[3]. V.A. Krysko- jr, J. Awrejcewicz, M.V. Zhigalov, *et al.*, (2023), Physical nonlinearity in porous functionally graded kirchhoff nano-plates: Modeling and numerical experiment, *Applied Mathematical Modelling*, 123, pp. 39-74.

[4] Awrejcewicz, J., Krysko, V.A., Zhigalov, M.V. *et al.* (2018), Contact interaction of two rectangular plates made from different materials with an account of physical nonlinearity. *Nonlinear Dyn,* 91, pp. 1191–1211.

[5] Vorovich, I. Krasovskii, Yu.P., (1959), "On the method of elastic solutions", *Dokl. Akad. Nauk SSSR*, 126 (4).

TOPOLOGICAL OPTIMISATION METHOD FOR REDUCING STRESS PEAKS AT THE BOUNDARY OF JOINING STRUCTURAL MEMBERS OF MECHANICAL STRUCTURES

Pavel V. Dunchenkin[1], Anton V. Krysko[2], Maxim V. Zhigalov[2], Vadim A. Krysko[2]

[1]*Yuri Gagarin State Technical University of Saratov, Saratov, 410054, Russia*

[2,3,4]*Lavrentyev Institute of Hydrodynamics of SB RAS, Novosibirsk 630090, Russia*

[1]*dunchenkin.pasha@yandex.ru; [2]anton.krysko@gmail.com;[3]zhigalovm@yandex.ru;*
[4]*krysko1937@gmail.com*

ORCID iD: [1]0009-0002-1638-1226; [2]0000-0002-9389-5602; [3]0000-0002-0642-7211;
[4]0000-0002-4914-764X

Keywords: Topological optimization, Shear stresses, Adhesive, Method of sliding asymptotes.

ABSTRACT

Science-intensive industries such as automotive, aerospace and shipbuilding are increasingly seeking to increase the strength and reduce the weight of their structures.

Recently, the manufacture of engineered structures has required the use of multi-layer adhesive joints, which have a number of advantages over traditional bolted or riveted joints. These joints have high rigidity and a high strength-to-weight ratio. They also have improved corrosion and fatigue resistance and excellent damping characteristics. Research in this area is becoming more and more popular. The main defect of adhesive joints is the destruction of the adhesive layer and, as a consequence, the disruption of the structural integrity [1]. In the study [2], the authors identified the cause of the failure of the adhesive layers. This due to the non-uniform distribution of stresses in the structures. They also investigated the effect of adhesive layer thickness on the same strength characteristics. In references [3-6], the authors presented an approach using methods of topological optimisation to design optimal joints, structures and multilayer composites. The present study is a follow-up to the cited works and is characterised by the application of other methods and the development of a more universal optimisation algorithm.

In this study, a mathematical model is constructed to analyse the strength problem of various adhesive bonds in mechanical structures under transverse load. The developed methodology, based on methods of topological optimisation supplemented by finite element methods, is applied as a solution method. In addition, penalty functions for correct optimisation are introduced. Several optimisation methods are used to obtain reliable results. The most popular topological optimisation methods (SIMP and RAMP) are compared. It is shown that the RAMP method is the most optimal. The methodology of topological optimisation is developed based on the RAMP method using finite elements and a penalty function. This combination allows to remove the "checkerboard" effect. Note that a universal methodology is constructed, applicable to a wide class of structures. The penalty function allows to reduce the peak stresses in the adhesive layer, which is the weakest part of the structure and often subject to deformation. The proposed methodology is tested on the optimisation of a multilayer package consisting of two duralumin beams (Figure 1). A comparative analysis is carried out using the example of three engineering structures with Young's modulus $E_1 = 73.1 * 10^6\ Pa$, joined at the top and bottom with silver solder with Young's modulus $E_2 = 2.26 * 10^6\ Pa$.

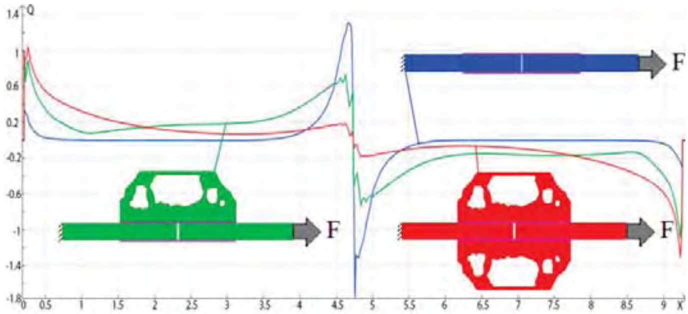

Fig. 1. Shear stresses

There is a slit between the two beams to separate them. Adhesive jointing is applied at the top and bottom. The right side of the cantilever is subjected to a tensile load $F = 1 * 10^5 \frac{N}{m^2}$. The left edge is pinched. The convergence of the finite element method with triangular element approximation of the domain is investigated. The solution obtained by partitioning into 4000 finite elements is optimal. The optimisation is based on the method of sliding asymptotes. The stresses are computed at the centre of the upper adhesive joint. The stress analyses of the adhesive joints show that the main stresses are shear stresses. This is due to the small thickness of the solder. The technique proposed by the authors allowed to reduce the maximum peak tangential stresses by more than 2 times compared to the solutions obtained by the engineering method.

This work has been supported by the Grant RSF No. 22-11-00160.

REFERENCES

[1] Fernandes FJ, Pavanello R. Topology optimization of adhesive material in a single lap joint using an evolutionary structural optimization method and a cohesive zone model as failure criterion. Proceedings of the Institution of Mechanical Engineers, Part L: Journal of Materials: Design and Applications. 2022;236(4):757-778. doi:10.1177/14644207211056945

[2] Edore G. Arhore, Mehdi Yasaee, Iman Dayyani, Comparison of GA and topology optimization of adherend for adhesively bonded metal composite joints, International Journal of Solids and Structures, Volumes 226–227, 2021, 111078, ISSN 0020-7683, doi:10.1016/j.ijsolstr.2021.111078

[3] Dunchenkin, P.V.; Cherekaeva, V.A.; Yakovleva, T.V.; Krysko, A.V. Topological Optimization of Interconnection of Multilayer Composite Structures. Computation 2023, 11, 87. https://doi.org/10.3390/computation11050087

[4] Krysko, A.V., Awrejcewicz, J., Dunchenkin, P.V., Zhigalov, M.V., Krysko, V.A. (2022). Topological Optimization of Multilayer Structural Elements of MEMS/NEMS Resonators with an Adhesive Layer Subjected to Mechanical Loads. In: Altenbach, H., Bauer, S., Eremeyev, V.A., Mikhasev, G.I., Morozov, N.F. (eds) Recent Approaches in the Theory of Plates and Plate-Like Structures. Advanced Structured Materials, vol 151. Springer, Cham. https://doi.org/10.1007/978-3-030-87185-7_13

[5] A.V. Krysko, J. Awrejcewicz, S.P. Pavlov, K.S. Bodyagina, M.V. Zhigalov, (2018) V.A. Krysko,Non-linear dynamics of size-dependent Euler–Bernoulli beams with topologically optimized microstructure and subjected to temperature field, International Journal of Non-Linear Mechanics, 104,75-86, https://doi.org/10.1016/j.ijnonlinmec.2018.05.008.

[6] A.V. Krysko, J. Awrejcewicz, S.P. Pavlov, K.S. Bodyagina, V.A. Krysko,(2019)Topological optimization of thermoelastic composites with maximized stiffness and heat transfer, Composites Part B: Engineering, 158,319-327, https://doi.org/10.1016/j.compositesb.2018.09.047.

COMPRESIVE AND SHEAR WAVE PROPAGATION IN THREE-DIMENSIONAL FRACTIONAL VISCOELASTIC INFINITE SOLID MEDIA

Slađan Jelić[1] and Dušan Zorica[2]

[1,2]*Department of Physics, Faculty of Sciences University of Novi Sad,*
Trg D. Obradovića 4, 21000 Novi Sad, Serbia
[1]sladjan.jelic@df.uns.ac.rs; [2]dusan.zorica@df.uns.ac.rs;
ORCID iD: 0000-0002-0877-6781; [2] 0000-0002-9117-8589

Keywords: wave propagation in three-dimensional isotropic and viscoelastic body, compressive and shear waves, thermodynamically consistent fractional models of viscoelastic body, relaxation moduli as memory functions generalizing Lamé coefficients.

ABSTRACT

In order to consider the wave propagation in three-dimensional homogeneous, isotropic, and viscoelastic body, considered in [1] and to account for results presented this paper, the Cauchy initial value problem on unbounded domain is analyzed for the wave equation written as a system of fractional partial differential equations consisting of equation of motion of three-dimensional solid body

$$\frac{1}{\rho}\operatorname{div}\hat{\boldsymbol{\sigma}}(\boldsymbol{r},t)+\boldsymbol{f}_b(\boldsymbol{r},t)=\partial_{tt}\boldsymbol{u}(\boldsymbol{r},t),$$

that connects stress tensor $\hat{\boldsymbol{\sigma}}$, displacement field $\boldsymbol{u}$, and body forces $\boldsymbol{f}_b$, equation of strain

$$\hat{\boldsymbol{\varepsilon}}(\boldsymbol{r},t)=\frac{1}{2}\Big(\operatorname{grad}\boldsymbol{u}(\boldsymbol{r},t)+\big(\operatorname{grad}\boldsymbol{u}(\boldsymbol{r},t)\big)^{\mathrm{T}}\Big),$$

as well as of the constitutive equation

$$\hat{\boldsymbol{\sigma}}(\boldsymbol{r},t)=\partial_t\left(\left(\sigma_{sr}^{(c)}(t)-2\sigma_{sr}^{(s)}(t)\right)*_t\operatorname{tr}\hat{\boldsymbol{\varepsilon}}(\boldsymbol{r},t)\right)\hat{\boldsymbol{I}}+2\partial_t\left(\sigma_{sr}^{(s)}(t)*_t\hat{\boldsymbol{\varepsilon}}(\boldsymbol{r},t)\right),$$

obtained by generalizing the classical Hooke's law of three-dimensional homogeneous, isotropic, and elastic body by replacing Lamé coefficients with the relaxation moduli $\sigma_{sr}^{(x)}$, $x\in\{c,s\}$, to account for different memory kernels corresponding to the propagation of compressive and shear waves. By the use of method of integral transforms, namely Laplace and Fourier transforms, the displacement field, as a solution of the Cauchy initial value problem, is expressed through Green's functions $G^{(x)}$, $x\in\{c,s\}$, corresponding to both compressive and shear wave propagation. The displacement field is obtained by the action of the resolvent tensor $\hat{\boldsymbol{R}}$ on the known initial conditions $\boldsymbol{u}_0$ and $\boldsymbol{v}_0$, yielding

$$\boldsymbol{u}(\boldsymbol{r},t)=\partial_t\hat{\boldsymbol{R}}(\boldsymbol{r},t)*_r\boldsymbol{u}_0(\boldsymbol{r},t)+\hat{\boldsymbol{R}}(\boldsymbol{r},t)*_r\boldsymbol{v}_0(\boldsymbol{r},t)+\hat{\boldsymbol{R}}(\boldsymbol{r},t)*_{r,t}\boldsymbol{f}_b(\boldsymbol{r},t),$$

for the solution, assuming $\hat{\boldsymbol{R}}(\boldsymbol{r},0)=\boldsymbol{0}$, with $*_{r,t}$ denoting the convolution in space and time, and where the resolvent tensor is given by

$$\hat{\boldsymbol{R}}(\boldsymbol{r},t) = G^{(c)}(r,t)\frac{\boldsymbol{r}\otimes\boldsymbol{r}}{r^2} + G^{(s)}(r,t)\left(\hat{\boldsymbol{I}} - \frac{\boldsymbol{r}\otimes\boldsymbol{r}}{r^2}\right) - \frac{1}{r}\left(\partial_r g^{(s)}(r,t) - \partial_r g^{(c)}(r,t)\right)\left(\hat{\boldsymbol{I}} - 3\frac{\boldsymbol{r}\otimes\boldsymbol{r}}{r^2}\right),$$

with $\otimes$ used to denote the dyadic product. Green's functions are expressed as

$$G_\varepsilon^{(x)}(r,t) = \frac{1}{4\pi^2 r}\int_0^\infty \frac{1}{|\tilde{c}_x^2(\rho \mathrm{e}^{\mathrm{i}\varphi_0})|}\mathrm{e}^{\rho t\cos\varphi_0 - \frac{r\rho}{|\tilde{c}_x(\rho \mathrm{e}^{\mathrm{i}\varphi_0})|}\cos\left(\varphi_0 - \arg\tilde{c}_x(\rho \mathrm{e}^{\mathrm{i}\varphi_0})\right) - \varepsilon\sqrt{\rho}\cos\frac{\varphi_0}{2}} \times \sin\Big(\rho t\sin\varphi_0 - \frac{r\rho}{|\tilde{c}_x(\rho \mathrm{e}^{\mathrm{i}\varphi_0})|}\sin\left(\varphi_0 - \arg\tilde{c}_x(\rho \mathrm{e}^{\mathrm{i}\varphi_0})\right) + \varphi_0 - \arg\tilde{c}_x^2(\rho \mathrm{e}^{\mathrm{i}\varphi_0}) - \varepsilon\sqrt{\rho}\sin\frac{\varphi_0}{2}\Big)\mathrm{d}\rho$$

if $r < c_x t$, with $c_x = \sqrt{\frac{\sigma_{sr}^{(x)}(0)}{\rho}}$, while if $r > c_x t$, then $G_\varepsilon^{(x)}(r,t) = 0$, while function $g^{(x)}$ takes the following form

$$g^{(x)}(r,t) = \frac{1}{4\pi^2 r}\int_0^t \Big(\varphi_0 + \int_0^\infty \frac{1}{\rho}\mathrm{e}^{\rho t'\cos\varphi_0 - \frac{r\rho}{|\tilde{c}_x(\rho \mathrm{e}^{\mathrm{i}\varphi_0})|}\cos\left(\varphi_0 - \arg\tilde{c}_x(\rho \mathrm{e}^{\mathrm{i}\varphi_0})\right)} \times \sin\left(\rho t'\sin\varphi_0 - \frac{r\rho}{|\tilde{c}_x(\rho \mathrm{e}^{\mathrm{i}\varphi_0})|}\sin\left(\varphi_0 - \arg\tilde{c}_x(\rho \mathrm{e}^{\mathrm{i}\varphi_0})\right)\right)\mathrm{d}\rho\Big)\mathrm{d}t'.$$

Compressive wave progresses in the direction of a radius vector, while the shear wave progresses in the plane perpendicular to the direction of a radius vector. Moreover, depending whether $\sigma_{sr}^{(x)}(0)$ has infinite or finite value, the wave propagation speed has either infinite value, as in the case of fractional anti-Zener and Zener models formulated in [2], as well as in the case of the first class of fractional Burgers models, formulated in [3], or has finite value, as in the case of fractional Burgers models of the second class.

REFERENCES

[1] Jelić, S. and Zorica, D. (2024), "Wave propagation in three-dimensional fractional viscoelastic infinite solid body," *arXiv:2401.14774*, pp. 1-38.
[2] Jelić, S. and Zorica, D. (2023), "Fractionalization of anti-Zener and Zener models via rheological analogy," *Acta Mechanica*, pp. 234:313-354.
[3] Okuka, A. S. and Zorica, D. (2018), "Formulation of thermodynamically consistent fractional Burgers models," *Acta Mechanica*, pp. 229:3557-3570.

2nd International Conference on Mathematical
Modelling in Mechanics and Engineering
Mathematical Institute SANU, 12-14. September, 2024.

STORED ENERGY AND DISSIPATED POWER FOR ONE-DIMENSIONAL VISCOELASTIC BODY

Slađan Jelić[1] and Dušan Zorica[2]

[1,2]Department of Physics, Faculty of Sciences University of Novi Sad,
Trg D. Obradovića 4, 21000 Novi Sad, Serbia
[1]sladjan.jelic@df.uns.ac.rs; [2]dusan.zorica@df.uns.ac.rs;
ORCID iD: [1]0000-0002-0877-6781; [2]0000-0002-9117-8589

Keywords: energy balance properties in time domain, stored energy and dissipated power per unit volume, relaxation modulus and creep compliance, thermodynamically consistent fractional anti-Zener and Zener models, response to harmonic excitation.

ABSTRACT

Starting from the power per unit volume

$$P(t)=\sigma(t)\dot{\varepsilon}(t),$$

where σ denotes stress and ε denotes strain, which is posed for one-dimensional solid body and by taking into account the constitutive equation of viscoelastic body, expressed either through relaxation modulus σ_{sr} as

$$\sigma(t)=\frac{d}{dt}\big(\sigma_{sr}(t)*\varepsilon(t)\big),$$

or through creep compliance $\varepsilon_{\mathrm{cr}}$ as

$$\varepsilon(t)=\dot{\varepsilon}_{\mathrm{cr}}(t)*\sigma(t),$$

in [1] the relation

$$P(t)=\frac{\mathrm{d}}{\mathrm{d}t}W(t)+\mathcal{P}(t),$$

is derived, where W can be interpreted as the energy per unit volume stored in viscoelastic body, referring to elastic properties of the material, while $\mathcal{P}$ can be interpreted as dissipated power per unit volume, referring to viscous properties of the material. The explicit forms for stored energy and dissipated power are as follows

$$W(t)=\frac{1}{2}\sigma_{\mathrm{sr}}(t)\varepsilon^2(t)+\frac{1}{2}\int_0^t\big(-\dot{\sigma}_{\mathrm{sr}}(t-t')\big)\big(\varepsilon(t)-\varepsilon(t')\big)^2\mathrm{d}t'>0,$$

$$\mathcal{P}(t)=\frac{1}{2}\big(-\dot{\sigma}_{\mathrm{sr}}(t)\big)\varepsilon^2(t)+\frac{1}{2}\int_0^t\ddot{\sigma}_{\mathrm{sr}}(t-t')\big(\varepsilon(t)-\varepsilon(t')\big)^2\mathrm{d}t'>0,$$

when expressed in terms of strain via relaxation modulus, as well as

$$W(t) = \frac{1}{2}\int_0^t \dot{\varepsilon}_{\mathrm{cr}}(t-t')\sigma^2(t')\mathrm{d}t' > 0,$$

$$\mathcal{P}(t) = \frac{1}{2}\dot{\varepsilon}_{\mathrm{cr}}(t)\sigma^2(t) + \frac{1}{2}\int_0^t \left(-\ddot{\varepsilon}_{\mathrm{cr}}(t-t')\right)\left(\sigma(t)-\sigma(t')\right)^2\mathrm{d}t' > 0,$$

when expressed in terms of stress via creep compliance. Obviously, both stored energy and dissipated power are positive at each time instant $t > 0$ if relaxation modulus (creep compliance) is completely monotonic function (Bernstein function), which holds true in the case of fractional anti-Zener and Zener models if thermodynamical restrictions on model parameters are narrowed.

Moreover, two forms of energy and two forms of dissipated power per unit volume are examined numerically and compared graphically in order to check whether they coincide if the harmonic excitation of a viscoelastic body of fractional anti-Zener and Zener type is prescribed as a sine function, where the stress, as a response to prescribed strain, is also determined in transient regime. These results are presented in [2].

REFERENCES

[1] Jelić, S. and Zorica, D. (2023), "Energy balance for fractional anti-Zener and Zener models in terms of relaxation modulus and creep compliance," *Applied Mathematical Modelling*, pp. 123:688-728.

[2] Jelić, S. and Zorica, D. (2023), "Stress and power as a response to harmonic excitation of a fractional anti-Zener and Zener type viscoelastic body," *arXiv:2311.09798*, pp. 1-29.

2nd International Conference on Mathematical
Modelling in Mechanics and Engineering
Mathematical Institute SANU, 12-14. September, 2024.

VARIOUS LISSAJOUS FIGURES AND THEIR IMPLICATION IN VIBRATORY TECHNOLOGY

Uroš Lj. Ilić[1], Emil A. Veg[2]

[1] *Institute Mihajlo Pupin, University of Belgrade, 11000 Belgrade, Serbia*

[2]*Faculty of Mechanical Engineering, University of Belgrade, 11000 Belgrade, Serbia*

[1]*uros.ilic@pupin.rs*; [2]*eveg@mas.bg.ac.rs*

[1]ORCID iD: 0000-0003-3955-8995; [2]ORCID iD: 0000-0002-6702-6251

Keywords: Lissajous Figures, Computer Simulation, Vibratory Technology.

ABSTRACT

Main component in vibratory machines is the vibratory trough that sets moving material into motion. With the use of different vibratory regimes, the material can move either in hopping or no-hopping motion, depending on the continuity of the contact with the trough's surface [1]. Different vibratory regimes that set material into no-hopping motion are explored, but only vibratory conveyance with biaxial excitation is considered. This form of motion is characterized by the fact that horizontal and vertical components of trough's excitation can be varied independently. When these, mutually orthogonal, oscillations are combined, the trough's center of inertia forms a specific closed-loop path. Combining different vibrational frequencies, amplitudes, and phase shifts between orthogonal components, various Lissajous figures are formed. These figures have a vast spectrum of variations [2]. For example, a regime that's defined with identical drive frequencies and no phase shift and equal amplitudes corresponds to conventional vibratory machines with one actuator inclined at 45°.

This paper focuses on finding the optimal vibratory regime, e.g. corresponding Lissajous figure, for given set of input parameters. SOLIDWORKS® Academia software is used to perform elementary Motion Analysis. For this purpose, a CAD model of vibratory trough with appropriate spring connections is developed. Also, a dummy load of steel cube is used for the purpose of computer experiment. Potential hopping motions of material are left out, so only closed loop and monotonous Lissajous figures are taken into consideration (Fig. 1). This experimental research is conducted in two phases. In first phase only frequencies and phase shifts are varied. When the suitable Lissajous figure is determined it is advanced to second phase, where inclination angle for specific conveyed material is chosen. Inclination angle coincides with figure's orientation in vertical plane. It single-handedly depends on the ratio of amplitudes.

Surface contact's force is plotted in Motion Analysis for each experiment iteration. Given that a no-hopping motion is desired, current iteration is dropped if in any part of the path, the cube loses contact with the surface. Each experiment iteration lasted for a set amount of time after which the distance from starting position is measured and written down in experiment's table of results. In other words, this conveying velocity of the load is quantified value for each iteration and results are analyzed upon it.

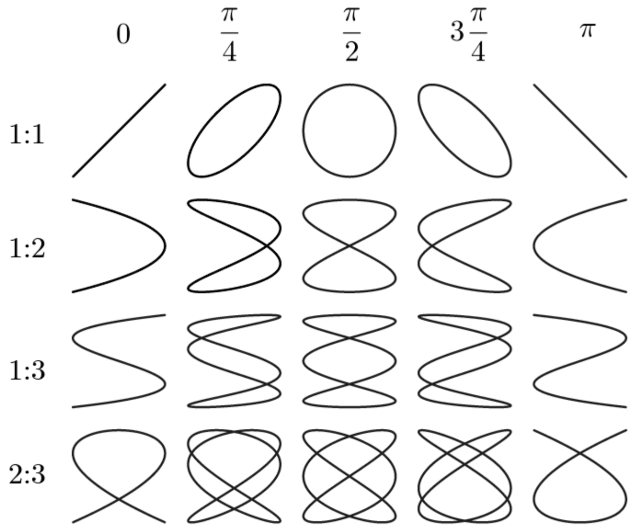

Figure 1 *– Impact of frequency ratio (rows) and phase shifts (columns) of orthogonal components to pathway of trough's center of inertia. Final path is a combination of both movements and represent a Lissajous figure*

Main goal of this research is to serve as a proof of concept of methodology to find optimal vibratory regime for given load, e. g. conveyed material. Obtained results can't be used as a benchmark of optimum regime due to dynamic characteristics of the load (size, mass, contact surface) and other parameters, such as friction coefficient, dynamic reaction forces etc. There are other factors that need to be taken into consideration for future research, such as mechanical model of the whole conveyer, type of actuator and behavior of springs on higher frequencies. Also, the simulation model should be scalable, e.g. multi-particle loads should be put to test. Everything mentioned is part of current and future work on this topic.

Acknowledgements

This research has been supported by the research grants of the Serbian Ministry of Science, Technological Development and Innovations, grants No. 451-03-65/2024-03/200105 from 5.2.2024.

REFERENCES

[1] Goncharevich, I. F., Frolov, K.V., Rivin, E.I., (1990) "Theory of vibratory technology", *Hemisphere Publishing Corporation*, New York, pp. 2-45

[2] Greenslade, T. B. (1993) "All about Lissajous figures" *The Physics Teacher,* American Association of Physics Teachers 31(6), pp. 364–370

2nd International Conference on Mathematical
Modelling in Mechanics and Engineering
Mathematical Institute SANU, 12-14. September, 2024.

NONLINEAR MODELLING OF DC MOTOR USING GA OPTIMIZED ANFIS

Mitra V. Vesović [1], Radiša Ž. Jovanović [2] and Vladimir R. Zarić [3]

[1,2,3] *Faculty of Mechanical Engineering, University of Belgrade, 11000 Belgrade, Serbia*

[1]mvesovic@mas.bg.ac.rs; [2]rjovanovic@mas.bg.ac.rs; [3]vzaric@mas.bg.ac.rs

ORCID iD: [1]0000-0003-0457-1874; [2]0000-0002-8122-756X; [3]0000-0002-0999-0608

Keywords: Nonlinear Modeling, ANFIS, Optimization Algorithms

ABSTRACT

The purpose of this research is to introduce nonlinear methods for identifying the model of DC motor, i.e. for determining velocity of the load shaft ω_l in a direct-current (DC) motor using input voltage signal V_m. These methods comprise three types of fuzzy neural networks. First, before these nonlinear methods, a traditional (linear) model with an actuator gain of A_m, the equivalent damping term of $B_{eq,v}$, and a total moment of inertia of J_{eq} is derived. Unfortunately, this conventional linear model was unable to accurately depict the system in the real-time experiment, neither for the step input signals nor for sinusoidal, Fig. (1). This outcome was expected because the main cause of the linear model's poor behaviour in DC motors - which calls for the use of a nonlinear model - is friction. In order to improve model, Tustin's friction is considered, and the new model is evaluated in terms of the velocity-friction dependency, Eq. (1),

$$J_{eq}\left(\frac{d}{dt}\omega_l(t)\right)+T_{st}(\omega_l(t))+\ B_{eq,n}\,\omega_l(t)=A_mV_m(t). \tag{1}$$

Friction properties are taken to be symmetrical for both positive and negative rotational velocity values [1],

$$T_{st}=\ 0.0174sgn(\omega_l)+0.0087e^{-\frac{\omega_l}{0.064}}\,sgn(\omega_l). \tag{2}$$

There are many other ways to create a DC motor model as well. A few of them employ various models of friction. The nonlinear LuGre friction model incorporates several significant nonlinear phenomena, including stiction, the Stribeck effect, variable break-away force, pre-sliding displacement, and frictional lag. Even though the DC motor model developed using Eq. (1) is producing considerably better results than the linear model, Fig. (1), some control approaches may be extremely difficult or impossible to use because of the discontinuity with the sgn function. Feedback linearization is one of the answers, although it requires approximating this function with a smooth, differentiable one (such as the hyperbolic tangent) [2].

To create a novel model applicable across the entire state space, without any approximations, the three alternative identification methods, utilizing different Adaptive Neuro-Fuzzy Inference Systems (ANFIS) are constructed. Training for all ANFIS models is done using input voltage V_m and velocity ω_l as output from the current and the previous instants (k and k-1). Input signal is normal (Gaussian) distributed random signal with mean equal to 0 and variance equal to 10. The output for all ANFIS models can be defined as follows: $\omega_l(k)=N[V_m(k-1),\omega_l(k-1)]$.

In the first ANFIS, the initial fuzzy model is extracted using grid partitioning (GP) to input-

output data pairs. This method ensures uniformly spaced membership functions (MFs) but can lead to an exponential increase in rules due to the curse of dimensionality, affecting the number of fuzzy rules. The fuzzy C-Means clustering (FCM) algorithm is used to establish the appropriate input-output divisions of the initial MFs for the second and third ANFIS. Many advanced mathematical optimization methods are analyzed and researched [3] and it has been decided that the optimal values of premise and consequent parameters will be determined using genetic algorithm (GA) and particle swarm optimization (PSO).

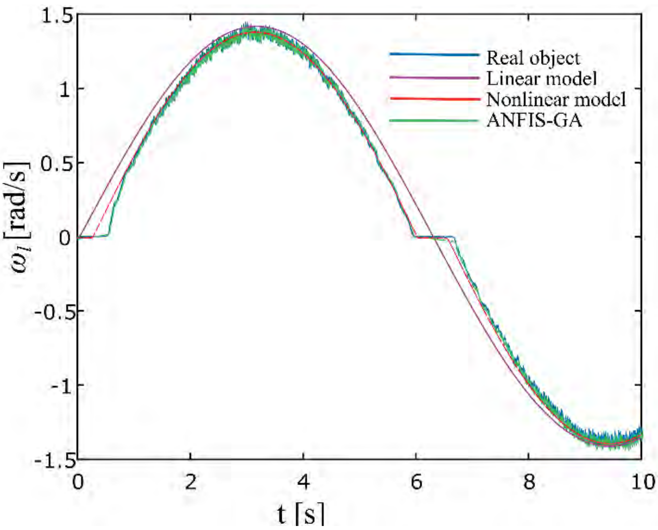

Figure 1. Comparison of models

Each agent in the GA and PSO algorithm contains parameters (premises and consequents) of ANFIS. For these models, the initial agent was obtained using FCM, and the rest of the population was obtained by random arrays from continuous uniform distribution around the initial one. The models were compared after each model was tested (using inputs that had not been utilized during training such as steps, sinusoidal and chirp signals) and each model produced satisfactory results in terms of chosen performance criteria. Because ANFIS-GA provided the best results, output of this model is shown alongside with other models and the real object behaviour in Fig. 1.

The experiment and analysis results show that the response of the object is tracked by the model, indicating a strong possibility of generating an effective control signal through a direct inverse control scheme. This method of creating controllers would rely exclusively on the object behaviour, without the use of any approximations.

REFERENCES

[1] Gruyitch Lj., Bučevac Z., Jovanović R., Ribar Z. (2019), “Structurally variable control of Lurie systems“ *Int J Control*, 93(1), pp. 1-26, doi: 10.1080/00207179.2019.1569764.

[2] Vesović M., Jovanović R., Trišović N. (2022), “Control of a DC motor using feedback linearization and gray wolf optimization algorithm”, *Advances in Mechanical Engineering*, 14(3), doi: 10.1177/16878132221085324.

[3] Atanasovska I., Patil S., Casanova VR. (2024), “Special issue: Advanced mathematical modeling in mechanical engineering”, *Proceedings of the Institution of Mechanical Engineers, Part C: Journal of Mechanical Engineering Science*, 238(3), pp. 621-623, doi: 10.1177/09544062231216509.

2nd International Conference on Mathematical
Modelling in Mechanics and Engineering
Mathematical Institute SANU, 12-14. September, 2024.

VARIABLE STIFFNESS ACTUATOR FOR ACHIEVING 3D MOVEMENT

Nemanja O. Tanasković[1], Mihailo P. Lazarević[2] and Damir Krklješ[3]

[1]*BioSens Institutes, 21000 Novi Sad, Serbia*
[2]*Faculty of Mechanical Engineering, University of Belgrade, 11000 Beograd, Serbia*
[3]*BioSens Institute, 21000 Novi Sad, Serbia*
[1]*nemanja.tanaskovic@biosense.rs* ; [2]*mihailo.lazarevic@gmail.com* ; [3]*dkrkljes@biosense.rs*
[2]ORCID iD: 0000-0002-3326-6636; [3]0000-0003-2279-4545

Keywords: Variable stiffness, Actuators, Stewart platform, Agriculture, Passive compliance, robotics

ABSTRACT

Across various industries, robotics is rapidly transforming how we work and interact with the world around us. These machines, often inspired by biology or mimicking human movement, can perform tasks ranging from delicate assembly to hazardous exploration. From the factory floor to surgical suites, robots are pushing the boundaries of automation and innovation, with applications that continue to expand and evolve. The innovations for robots in agriculture mostly come in the form of big machines for arable field cultivation. Their significance is high as they can be operated by one operator which is important due to the declining workforce in the agricultural field. Besides the arable fields, harvesting fruits in orchards is one of the biggest and the most labour-intensive tasks. In [1] authors proposed a solution for orchard harvesting that uses a robotic arm. Wang et al. [2] proposed a solution for a soft gripper for harvesting delicate fruits. Another type of solution is proposed by Fei and Vougioukas [3] that uses a moving platform for optimal placement of people for harvesting fruit. Zhao et al. [4] proposed a compliant Stewart-like platform. The platform uses electromagnetic springs that provide variable stiffness which provides compliant property. Some solutions have variable stiffness actuators [5], where controlled impedance change adjusts the stiffness. While these solutions offer promise, they face limitations. The high cost and rigidity of some systems, like those using electromagnetic springs [4], pose challenges for practical implementation. Additionally, robotic arms, though offering precise manipulation [1], lack safety features for working alongside humans. By analyzing these approaches, we can see that current solutions for orchard automation often rely on robotic arms for fruit manipulation. However, the safety concerns associated with robotic arms working near humans necessitate alternative approaches.

In this contribution, we are proposing a solution for a variable stiffness actuator, that provides passive compliance for safe operation alongside humans. By using springs as a compliant component and by applying load that is offset from the spring axis we can control spring stiffness as well as use it as a compliant part for shock absorption in case of collision. So far, our solution is purely mechanical. It uses its mass as well as additional spring pretension to achieve variable stiffness. When driven with precise motor movement, it can achieve kinematics like the Stewart platform while still providing compliance. Depending on the load and use case of the actuator spring stiffness can be easily adjusted either by swapping springs or by pre-tensioning the springs.

This actuator's default movement is linear. However, by attaching a suitable rotational joint to the end of the output shaft, we can achieve rotational movement with a linear component. With three actuators placed in a parallel configuration, a Stewart-like platform 3D movement can be achieved.

By incorporating compliant actuation and carefully designed joints, we can create a versatile actuator suitable for agricultural robotics. This actuator can operate safely alongside humans and handle delicate fruits like apples and peaches without risk of damage. This design would ensure smooth, controlled movements while maintaining structural integrity. We utilized SolidWorks for modelling and will showcase the results of simulations alongside some of the design features.

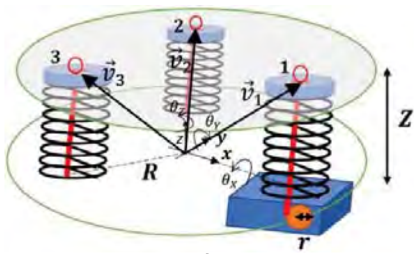

Figure 1. Schematics of the kinematic model for a rotating module within a Stewart platform-like mechanism with compliant actuation

ACKNOWLEDGMENTS

We are grateful to Marko Popović, who was a dedicated researcher at the BioSens Institute, whose insightful contributions and unwavering support have been invaluable throughout this research endeavor. Also, this research has been supported by the research grant of the Serbian Ministry of Science, Technological Development and Innovations, grant No. 451-03-65/2024 03/200105 from 5.2.2024.

REFERENCES

[1] Chen, Mingyou, Et Al. "Dynamic visual servo control methods for continuous operation of a fruit harvesting robot working throughout an orchard." Computers And Electronics In Agriculture 219 (2024): 108774.

[2] Wang, Xing, Et Al. "Geometry-aware fruit grasping estimation for robotic harvesting in apple orchards." Computers And Electronics In Agriculture 193 (2022): 106716.

[3] Fei, Zhenghao, And Stavros G. Vougioukas. "A robotic orchard platform increases harvest throughput by controlling worker vertical positioning and platform speed." Computers And Electronics In Agriculture 218 (2024): 108735.

[4] Zhao, Yong, Et Al. "Design of a parallel compliance device with variable stiffness." Proceedings Of The Institution Of Mechanical Engineers, Part C: Journal Of Mechanical Engineering Science 235.1 (2021): 94-107.

[5] Ramadan, M. A., Awad, M. I., Boushaki, M. N., Niu, Z., Khalaf, K., & Hussain, I. (2023). irisVSA: Infinite-rotation infinite-stiffness Variable Stiffness Actuator towards physical human–robot-interaction. *Mechatronics*, *96*, 103095.

2nd International Conference on Mathematical
Modelling in Mechanics and Engineering
Mathematical Institute SANU, 12-14. September, 2024.

FREE VIBRATION ANALYSIS OF SYMMETRIC ANGLE-PLY LAMINATED PLATES WITH DIFFERENT BOUNDARY CONDITIONS

Marija Stamenković Atanasov[1]

[1]*Department of Mechanical Engineering University of Niš, A. Medvedeva 14, 18000 Niš, Serbia*

[1]marija.stamenkovic.atanasov@masfak.ni.ac.rs

[1]ORCID iD: 0000-0002-1676-9469

Keywords: Free vibration, Laminated plates, Fiber orientations, Fundamental frequency.

ABSTRACT

Because of advantages such as high ratio of stiffness and strength to weight and low maintenance cost, laminated composite plates are widely used in the aerospace, automotive, marine, and other structural applications. Analysis of free vibrations of composite laminated plates based on the Mindlin thin plate theory are developed by the Afshari, P. et al. [1]. Liew [2] analyzed the vibrations of thick symmetric laminates by the Reissner/Mindlin plate theory and the Ritz method where vibrations of laminated plates with various geometric boundary conditions were studied. Very detailed analysis of composite laminated plates is presented in the literature J. N. Reddy [3]. Based on analysis Ni, Z. et al. [4] and Ashour, A. S. [5] idea for investigation of symmetric angle-ply laminated composite plates with different of numbers and thickness of lamella and different fiber orientations are derived.

In this paper a rectangular symmetrically angle-ply laminated plate is considered. The plate consists of N=5 layers (lamella) which are assumed to be made of orthotropic materials. The rectangular symmetrically angle-ply laminated plate with different thickness of lamella (Fig.1a, b and c) and different fiber orientations is presented in Fig.1. For the mentioned plate by applying classical plate theory, differential equation is given to describe the vibrations (small transverse displacements). Ritz solution is applied to solve the presented differential equation of motion for three types boundary conditions plate: simply supported at $x=0,a$ and $y=0,b$; clamped plate at $x=0,a$ and $y=0,b$; clamped plate at x=0,a and simply supported at $y=0,b$. The free vibrations of symmetrically angle-ply laminated plate are studied in detail. For different thickness of lamella and different fiber orientations the paper also provides a detailed analysis of fundamental frequencies.

From Fig. 2 it can be seen five-layer laminate plate with assumed fiber orientations of lamella [45°/- 30 °/ 60 °/- 30°/ 45 °]. Fig. 2 shows the effects of different types of boundary conditions and different thickness of lamella on the fundamental frequencies. The highest value of dimensionless fundamental frequencies was observed for boundary condition clamped plate at $x=0,a$ and $y=0,b$ when is every second lamella twice as thinner.

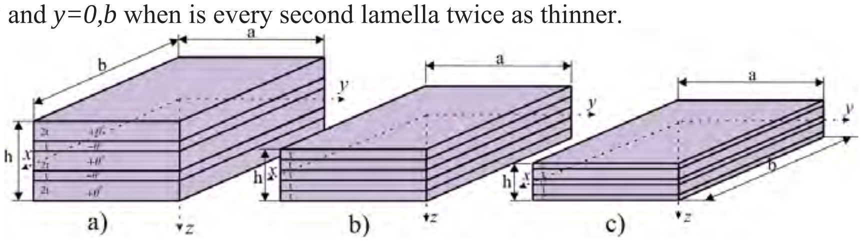

Fig. 1. *Rectangular symmetrically angle-ply laminated plate with number of layers N=5.*

The results of the fundamental frequencies are also comparing with results from literature J. N. Reddy [3].

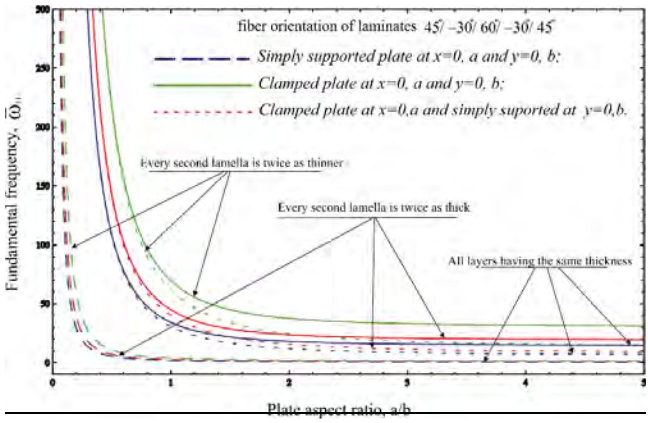

Fig. 2. *Nondimensionalized fundamental frequency ($\overline{\omega}_{11}$) versus plate aspect ratio (a/b)*

This research was financially supported by the Ministry of Science, Technological Development and Innovation of the Republic of Serbia (Contract No. 451-451-03-66/2024-03).

REFERENCES

[1] Afshari, P., and Widera, G. E. O. (2000), Free vibration analysis of composite plates. *J. Pressure Vessel Technol.*, 122(3), pp. 390-398.
[2] Liew, K. M. (1996), Solving the vibration of thick symmetric laminates by Reissner/Mindlin plate theory and thep-Ritz method. *Journal of Sound and Vibration*, 198(3), pp. 343-360.
[3] Reddy, J. N. (2003), *Mechanics of laminated composite plates and shells: theory and analysis*. CRC press.
[4] Ni, Z., Yuan, J., & Chen, B., (2014), Buckling of the SS–C–SS–C symmetrical composite rectangular plate under linear-varying in-plane load. *Composite Structures*, 107, pp. 528-536.
[5] Ashour, A. S., (2006), Vibration of angle-ply symmetric laminated composite plates with edges elastically restrained. *Composite Structures*, 74(3), pp. 294-302.

2nd International Conference on Mathematical
Modelling in Mechanics and Engineering
Mathematical Institute SANU, 12-14. September, 2024.

MODELLING OF THREE-DIMENSIONAL THERMAL-HYDRAULICS OF HORIZONTAL STEAM GENERATOR

Milos Lazarevic[1], Vladimir Stevanovic[2], Sanja Milivojevic[3] and Milan M. Petrovic[4]

[1,2,3,4]*Faculty of Mechanical Engineering, University of Belgrade, 11000 Belgrade, Serbia*

[1]malazarevic@mas.bg.ac.rs; [2]vstevanovic@mas.bg.ac.rs; [3]smilivojevic@mas.bg.ac.rs; [4]mlpetrovic@mas.bg.ac.rs

ORCID iD: [1]0009-0001-4336-3245; [2]0000-0002-7092-4087; [3]0000-0001-5458-2980; [4]0000-0002-3904-4778

Keywords: Numerical Modelling, Thermal-Hydraulics, Two-Phase Flow, Steam Generator, Engineering.

ABSTRACT

The horizontal steam generators (HSGs) are applied in the VVER nuclear power plants equipped with the pressurized water reactor (PWR). The HSG transfers heat from the nuclear reactor coolant to the feedwater, which is heated and evaporated on the HSG shell side. The HSG heat transfer area is composed of the horizontal U-tube bundles connected to the hot inlet header and cold outlet header, which are both positioned vertically. The boiling feedwater flow in the large volume of the HSG shell side is self-organized in complex natural circulations loops. Experimental investigation of the two-phase flow on the HSG shell side is difficult in real operational conditions. However, sophisticated two-phase flow models enable numerical simulation and analyses of these complex conditions, and the obtained results supports design of reliable operation and nuclear power plant safety.

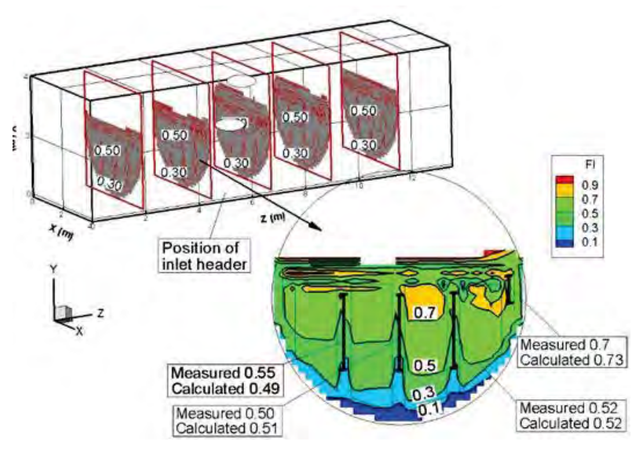

***Figure 1**: Void fraction predictions compared with experimental measurements*

This paper presents a comprehensive numerical modelling approach for simulation of three-dimensional thermal-hydraulics of horizontal steam generator (HSG). The model incorporates governing equations including the continuity equations, momentum conservation equations and energy conservation equations. Two separate fluids are observed: the reactor coolant flowing through the generator tubes and the feedwater on the shell side [1]. For the shell side, a two-phase model is employed to separately account for liquid and steam phases, with closure laws utilized to fulfil governing equations. The numerical simulations are conducted using the in-house program 3D-ANA, which enables detailed analysis and visualization of flow phenomena within the steam generator. Through this approach, the complex interplay between flow dynamics, heat transfer, and phase change phenomena within the steam generator is captured with high fidelity. Results obtained from numerical simulations are verified through comparison with experimental measurements. The proposed numerical framework provides valuable insights into the complex behaviour of horizontal steam generators, facilitating the optimization of design and operational parameters to enhance efficiency and safety in nuclear power plants.

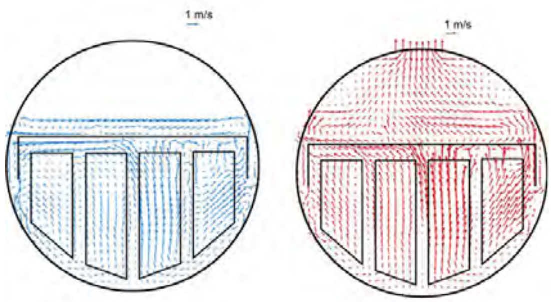

***Figure 2**: Liquid (left) and steam (right) velocity predictions*

The investigation of the three-dimensional thermal-hydraulics of horizontal steam generators has yielded results indicative of notable congruence with experimental data. The calculated predictions demonstrate a high degree of similarity with observed phenomena, suggesting the reliability of the employed modelling techniques (Fig. 1). Crucially, the findings assure the operational safety of the HSG, as evidenced by the absence of local dry-outs within tube bundles and the maintenance of moderate liquid and steam phase velocities that do not lead vibration-induced instabilities (Fig. 2). These outcomes underscore the robustness of the analytical framework employed and emphasize the imperative of rigorous thermal-hydraulic assessments in ensuring the integrity and efficiency of steam generator systems.

REFERENCES

[1] V. Stevanovic, Z. Stosic, M. Kiera, U. Stoll, Horizontal Steam Generator Thermal-Hydraulics at Various Steady-State Power Levels, Proceedings of the 10th Int. Conference on Nuclear Engineering, ICONE-10, Washington, D.C., USA, April 14-18, (2002), paper 22451.

2nd International Conference on Mathematical
Modelling in Mechanics and Engineering
Mathematical Institute SANU, 12-14. September, 2024.

NUMERICAL MODELLING OF POOL AND FLOW BOILING IN TWO-PHASE SYSTEMS OF STEAM GENERATORS

Milan M. Petrovic[1], Vladimir Stevanovic[2] and Sanja Milivojevic[3]

[1,2,3]*Faculty of Mechanical Engineering, University of Belgrade, 11000 Belgrade, Serbia*

[1]mlpetrovic@mas.bg.ac.rs; [2]vstevanovic@mas.bg.ac.rs; [3]smilivojevic@mas.bg.ac.rs
ORCID iD: [1]0000-0002-3904-4778; [2]0000-0002-7092-4087;
[3]0000-0001-5458-2980

Keywords: Pool boiling, Flow boiling, Two-phase flow, Steam generators.

ABSTRACT

Boiling is an effective heat transfer process for cooling surfaces. It has been widely investigated due to its application in thermal and nuclear power engineering, as well as in various equipment in refrigeration and process industry. The complexity of the boiling process is reflected in the fact that multiple bubbles grow at heated wall and different micro/nano conditions affect heat transfer mechanisms in contact of superheated liquid and heated wall. In the literature, numerical modelling of pool boiling is based on common mechanistic wall heat flux partitioning approach, where all boiling mechanisms such as single-phase convection, quenching and evaporation exist in the same control volume. In these models, the exact location of bubbles are not known, so authors cannot predict important boiling quantities such as void fraction distribution in the pool and the wall temperature under the bubble. The pool boiling model presented in this paper overcomes the mentioned shortcomings. This model simulates discrete bubble nucleation sites, a corresponding two-phase mixture pattern over heated wall surface and, due to the applied conjugate heat transfer modelling, enables insight into transient temperature field at the heated wall surface (Figure 1).

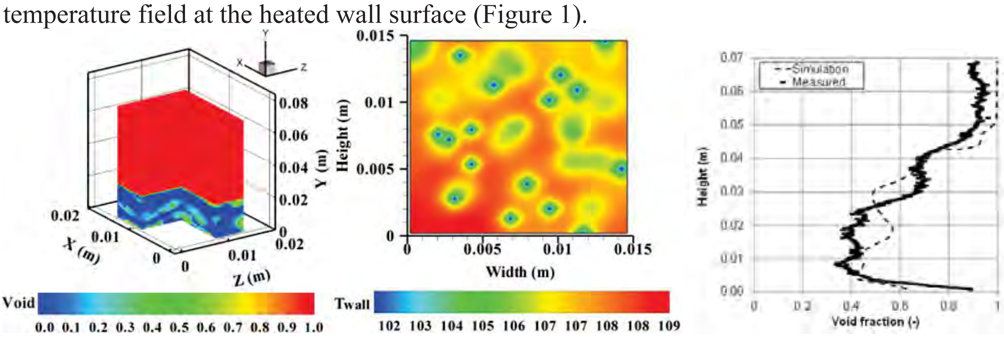

Figure 1. 3D void fraction distribution in the pool boiling at atmospheric pressure (left), 2D temperature distribution of heated wall surface in °C (middle) and comparison of measured and calculated average void fraction distribution with pool height.

The numerical procedure takes into account the conjugate heat transfer coupling [1,2] and it considers the influence of the liquid film thickness in the two-phase mixture at the wall surface on the heat flux. Therefore, the developed method predicts boiling curves and two-phase mixture dynamics in the pool boiling, along with temperature transients in the heated wall. The pool boiling model is validated against experimental conditions and showed that the model can predict the void fraction distribution in the pool as well as the mean wall temperature [1], [2].

The second model presented in this paper is flow boiling model [3]. Numerical simulations of the flow conditions of the two-phase mixture on the secondary side of the steam generator are performed due to the efficiency and safety of different types of the steam generators [4]. Therefore, for its reliable operation, it is necessary to look in detail at all flow and thermal effects that occur. Today, during the development and design of steam generators, more and more complex requirements are set for generating steam on heating surfaces that are exposed to high values of heat flux. Such conditions can lead to a critical heat flux, which is accompanied by thermal and mechanical damage to the heating wall material or dryout and loss of the heat sink on the cold fluid side. Based on computer simulations of boiling, it is possible to investigate complex mechanisms that affect parameters and equipment during steam generation. The model presented here is validated with two experimental installations of vertical steam generators, one with freon as working fluid and the other with water. The void fraction distributions for these two steam generators are presented in Figure 2.

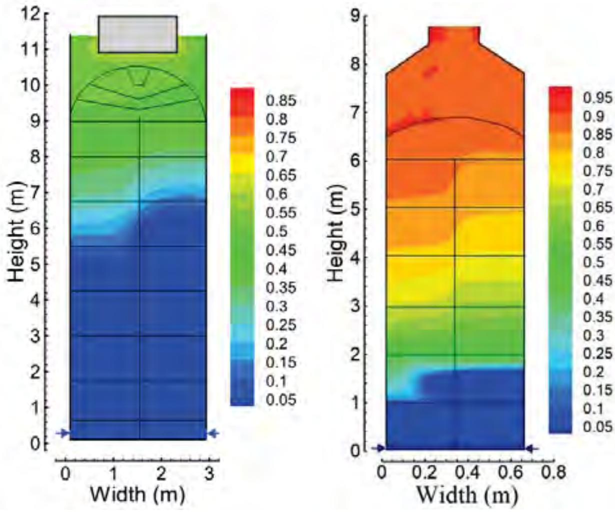

Figure 2. 2D void distribution in vertical steam generator - freon working fluid (left), water working fluid (right).

REFERENCES

[1] Petrovic, M. M., Stevanovic, V. D. (2021), “Pool boiling simulation with two-fluid and grid resolved wall boiling model,” International Journal of Multiphase flow, 144, 103806.

[2] Petrovic, M. M., Stevanovic, V. D. (2021), “Coupled two-fluid and wall heat conduction modeling of nucleate pool boiling, Numerical Heat transfer; Part A: Applications, 80 (3), pp. 63-91.

[3] Petrovic, M. M. (2021), “Dynamics of pool boiling under high heat fluxes in steam generators,” Doctoral dissertation, University of Belgrade Faculty of Mechanical Engineering, Belgrade.

[4] Stevanovic, V. (2006), “Thermal-Hydraulics of Steam Generators – Modelling and Numerical Simulation, Belgrade, Faculty of Mechanical Engineering.

2nd International Conference on Mathematical
Modelling in Mechanics and Engineering
Mathematical Institute SANU, 12-14. September, 2024.

DIMENSIONAL SYNTHESIS OF A HYBRID RIGID-FLEXIBLE FOUR-BAR LINKAGE FOR OPEN-PATH GENERATION

Marina S. Bošković[1], Radovan R. Bulatović[2], Slaviša M. Šalinić[3], Aleksandra M. Nikitović[4], Zorana V. Jeli[5]

[1,2,3]*Faculty of Mechanical and Civil Engineering in Kraljevo, University of Kragujevac, Serbia*
[4]*Faculty of Technical Science Čačak, University of Kragujevac, Čačak, Serbia*
[5]*Faculty of Mechanical Engineering, University of Belgrade, Belgrade, Serbia*
[1]*boskovic.m@mfkv.kg.ac.rs* ; [2]*bulatovic.r@mfkv.kg.ac.rs*; [3]*salinic.s@mfkv.kg.ac.rs;*
[4]*aleksandra.nikitovic@ftn.kg.ac.rs*; [5]*zjeli@mas.bg.ac.rs;*
[1]ORCID iD 0000-0002-3637-2741; [2]ORCID iD 0000-0003-1702-6250; [3]ORCID iD 0000-0002-8146-5461; [4]ORCID iD 0000-0002-7754-700X; [5]ORCID iD 0000-0003-4685-9024

Keywords: Dimensional synthesis, Four-bar linkage, Metaheuristic algorithms, optimization.

ABSTRACT

Hybrid rigid-flexible mechanism is a mechanism composed of rigid and compliant links [1]. Rigid-body joints and flexibility of bendable rods enable the mobility of the hybrid mechanism. In recent years, these mechanisms have gained popularity thanks to safety, easy interaction and a large range of motion. However, research in the area of dimensional synthesis of hybrid rigid-flexible mechanisms are very scarce. This was the motivation for the authors to investigate this problem more deeply and apply modern optimization techniques in order to solve it.

A hybrid rigid-flexible four-bar linkage whose input link is a continuum tendon of constant curvature, described in [2], was considered.

The authors solved the problem of synthesis of a hybrid rigid-flexible four-bar linkage to generate four different types of open paths. The aim of the dimensional synthesis is to design the geometric parameters of this hybrid mechanism whose coupler point should describe the motion that will follow the path defined by the appropriate number of precision points. At the same time, the deviation of the actual path from the desired one, which is defined by precision points, should be as small as possible. Solving the problem of dimensional synthesis was carried out by applying the optimization procedure. Design variables, objective function and constraints were defined for the considered problem, while a modern metaheuristic algorithms [3] were applied in the optimization process. The efficiency of the applied metaheuristic algorithms was confirmed on four examples of an open-path generation in the dimensional synthesis procedure.

REFERENCES

[1] Altuzarra, O., Solanillas, D.M., Amezua, E., Petuya, V. (2021), „Path Analysis for Hybrid Rigid-Flexible Mechanisms“, *Mathematics*, Vol. 9(3), doi: 10.3390/math9161869

[2] Hernandez, A., Munoyerro, A., Urizar, M., Altuzarra O. (2023), “Kinematic Analysis of a Tendon-Driven Hybrid Rigid-Flexible Four-Bar; Application to Optimum Dimensional Synthesis”, *Mathematics,* Vol. 11(19), doi: 10.3390/math11194215

[3] Rajwar, K., Deep, K., Das, S. (2023), „An exhaustive review of the metaheuristic algorithms for search and optimization: taxonomy, applications, and open challenges“, Artificial Intelligence Review, Vol. 56, pp. 13187–13257, doi:10.1007/s10462-023-10470-y

PERTURBED MOTIONS OF A NEARLY DYNAMICALLY SPHERICAL RIGID BODY WITH A MOVING MASS IN A RESISTIVE MEDIUM

D. Leshchenko[1] and A. Rachinskaya[2]

[1]*Odesa State Academy of Civil Engineering and Architecture, 65029 Odesa, Ukraine*

[2]*Odesa I.I.Mechnikov National University, 65082 Odesa, Ukraine*

[1]*leshchenko_d@odaba.edu.ua*; [2]*rachinskaya@onu.edu.ua*

[1]ORCID 0000-0003-2436-221X; [2]ORCID 0000-0003-2430-9603

Keywords: Nearly dynamically spherical rigid body, Movable mass, Resistive medium.

ABSTRACT

The problem of motion of a rigid body about a fixed point is one of the classical problems of mechanics. The interest in the problems of the rigid body dynamics has increased in the second half of the XX century in connection with the development of rocket and space technologies. A spacecraft or satellite, while orbiting about its center of mass, experiences torques from forces of different physical nature. This includes torques generated by the motion of internal masses, which can arise from factors such as presence of rotating components (like rotors or gyroscopes) within the spacecraft or satellite, and the activities of crew members aboard the crew vehicle.

We develop an approximate solution by means of an averaging method to the system of Euler`s equations with additional perturbation terms for a nearly dynamically spherical rigid body containing a viscoelastic element in a resistive medium. The asymptotic approach permits to describe evolution of angular motion using simplified averaged equations and numerical solution. The main objective of this work is to extend the previous results for the problem of motion about a center of mass of a rigid body under the influence of small internal torque (cavity filled with a fluid of high viscosity) or external torques (resistive medium), constant body -fixed torque and viscoelastic element. This work can be considered as mainstreaming of previous papers. The advantage of this work is in receiving the original asymptotic and numerical calculations that describe the evolution of motion a rigid body with moving mass over an infinite time interval with an asymptotically small error.

We present new qualitative and quantitative results of motion in a resistive medium of a nearly dynamically spherical rigid body with a moving mass attached to the body by means of elastic coupling. We obtain the system of motion equations in standard form, which is refined in square approximation by small parameter. The Caushy problem for the system determined after averaging is analyzed. Obtained results made it possible to evaluate the dynamical effects caused by the presence of a moving mass in a resistive medium. The evolution of rigid body motion is described by the solutions obtained asymptotically and numerically. The importance of the gained results is due to its applications such in moving mass control, spinning projectiles, and reentry vehicles.

COMPARISON OF CAPILLARY RISE MODEL IN THE CASE OF CONSTANT AND VARIABLE CROSS-SECTION

Isidora Rapajić [1] and Srboljub Simić [2]

[1]*Mathematical Institute of the Serbian Academy of Sciences and Arts, 11000 Belgrade, Serbia*
[2]*Department of Mathematics and Informatics, Faculty of Sciences, University of Novi Sad, 21000 Novi Sad, Serbia*
[1]isidora.rapajic@turing.mi.sanu.ac.rs; [2]ssimic@uns.ac.rs
ORCID iD: [2]0000-0003-3726-2007

Keywords: capillary rise, viscous flow

ABSTRACT

Washburn's equation is one of the widely used models for describing rise of a liquid column in vertical narrow pipes. Usually, it is derived by applying Newton's second law on a control volume. Our approach was to derive the governing equation using balance laws and clearly imposed assumptions.

In the case of a cylindrical pipe with constant radius R, we start from introducing polar cylindrical coordinates and standard orthonormal basis. The fluid we consider is incompressible with constant density and viscosity. The mass balance law comes down to $\operatorname{div} \boldsymbol{v} = 0$, due to incompressibility. Furthermore, we assume that velocity field is described by $\boldsymbol{v} = v_z \boldsymbol{e}_z$ and Poiseuille flow with no-slip condition at the pipe wall

$$v_z = v(t)\left(1 - \frac{r^2}{R^2}\right).$$

The derivation of the governing equation is conducted by applying the momentum balance law in integral form, taking into consideration the mean velocity $\bar{v}(t) = v(t)/2$. Additionally, the pressure field is assumed to have only z-coordinate, $p = p(z)$. That enables us to balance the difference in pressure with vertical component of the surface tension. In the end, we obtain Washburn's equation

$$\frac{d}{dt}\left[\rho h(t)\frac{dh(t)}{dt}\right] + \rho g h(t) + \frac{8\mu}{R^2} h(t)\frac{dh(t)}{dt} = \frac{2\gamma\cos\theta}{R},$$

where $h(t)$ is height of the meniscus, $dh(t)/dt = \bar{v}(t)$, γ is surface tension coefficient, ρ and μ are density and viscosity, respectively and θ is contact angle of the meniscus and wall of the pipe. After scaling, this equation is suitable for application of fixed-point theorems to prove existence and uniqueness of a solution. It is also proven that equilibrium height is asymptotically stable and that it can be reached either monotonically or oscillatory [1].

In the case of variable radius $R = R(z)$, reduction of the model to a single ordinary differential equation cannot be achieved unless it is assumed $|R'(z)| = |\tan\alpha| \ll 1$, i.e. $|\alpha| \ll 1$. In this case, the mass balance law is satisfied up to $O(\alpha)$, $\operatorname{div} \boldsymbol{v} = O(\alpha)$, by the velocity field $\boldsymbol{v} = v_z \boldsymbol{e}_z + O(\alpha)$, where v_z is described by the Poiseuille flow

$$v_z = v(t)\left(1 - \frac{r^2}{R(z)^2}\right).$$

Extended Washburn's equation is again derived from the momentum balance law in the integral form. Similar problem was studied in [2], but inertial and gravitational effects were neglected. The final governing equation is then

$$\frac{d}{dt}\left[\rho\frac{dh(t)}{dt}\int_0^{h(t)}R(z)^2dz\right]+\rho g\int_0^{h(t)}R(z)^2dz+8\mu h(t)\frac{dh(t)}{dt}=2R\big(h(t)\big)\gamma\cos\theta.$$

This equation reduces to the usual Washburn's equation for $R(z)=\text{const}$. In the case of a converging tube, $R(z)=R_0(1+z/L)^{-0.3}$, it is numerically verified that the equilibrium height can again be reached either monotonically or oscillatory, as in the case of constant radius.

The extended equation is scaled as in [1] and solved numerically for two different values of dimensionless parameter $\omega=\frac{\rho^3R_0^5g^2}{128\mu^2\gamma\cos\theta}$. Namely, for $\omega=0.01$ (left) solution exhibits monotonic approach to equilibrium height, while for $\omega=5$ (right) solution reaches equilibrium in an oscillatory manner.

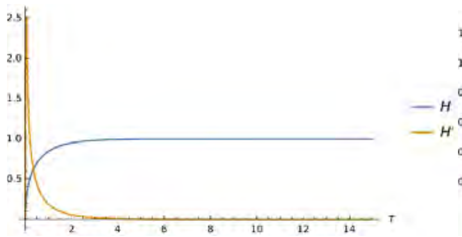

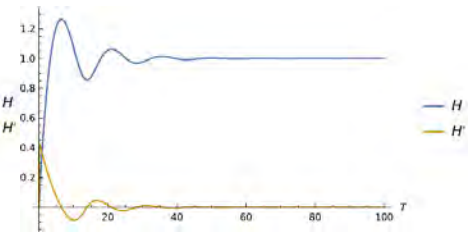

REFERENCES

[1] Plociniczak L. and Switala M.: Monotonicity, oscillations and stability of a solution to a nonlinear equation modelling the capillary rise. *Physica D: Nonlinear Phenomena*, 362:1–8, 2018.

[2] J.-B. Gorce, I.J. Hewitt and D. Vella. Capillary imbibition into converging tubes: beating Washburn's law and the optimal imbibition of liquids. *Langmuir* 32.6 (2016): 1560-1567.

2nd International Conference on Mathematical Modelling in Mechanics and Engineering
Mathematical Institute SANU, 12-14. September, 2024.

STABILITY OF FRACTIONAL-ORDER TIME-DELAY DYNAMICAL SYSTEMS: NEW RESULTS

Mihailo P. Lazarević[1], Stjepko Pišl[2], Darko M. Radojević[3] and Nikola Nešić[4]

[1,2]*Faculty of Mechanical Engineering, University of Belgrade, 11000 Belgrade, Serbia*
[3]*Company Dunav Insurance, 11000 Belgrade, Serbia*
[4]*Faculty of Technical Sciences, University of Priština, Kosovska Mitrovica, Serbia*
[1]*mlazarevic@mas.bg.ac.rs*; [2]*stjepko.pisl@gmail.com* ; [3]*drmasf@yahoo.com;*
[4]*nikola.nesic@pr.ac.rs*
[1]ORCID iD: 0000-0002-3326-6636; [3]ORCID iD: 0000-0001-6237-4735

Keywords: time delay, fractional order, finite time stability, asymptotic stability, neutral time delay system

ABSTRACT

Time delay often appears in many engineering systems and it may lead to bifurcation, chaos and even instability, [1]. Control design and stability issues of time-delay systems (TDS) were widely studied due to the effect of delay phenomena on system dynamics, which often leads to poor performance or even instability. In the biomechanics of humans, a well-known fact is due to the human reaction time, which introduces the effect of a time delay into a control problem. Particularly, it has been obtained that self-balancing models of standing man can be presented in the form of neutral time-delay systems of the integer order, where in solving the stabilization problem, feedback control is introduced that contains a delay (TDTC) and include into account its position, speed, and acceleration [2]. Recently, fractional calculus (FC) has attracted the increased attention of scientific society where fractional operators are often used for complex dynamical systems,[3]. Also, fractional-order dynamical systems have drawn much attention from researchers and engineers over the past few decades, [4,5], particularly for different kinds of stability. Here, we study the problem of human postural balance by applying fractional-order TDFC where the asymptotic stability closed loop of fractional-order neutral time delay systems is studied.

Also, some attention will be devoted to the finite-time stability (FTS)/stabilization problem of nonlinear fractional-order (uncertain) time-delay systems,[6]. By use of the (generalized) Gronwall inequality and its new extended form, new sufficient conditions for FTS of such systems are obtained.

Finally, suitable numerical examples will be given to illustrate the effectiveness and applicability of the proposed theoretical results.

ACKNOWLEDGMENT

This research was supported by the Serbian Ministry of Science, Technological Development and Innovations, grant No. 451-03-65/2024-03/200105 from 5.2.2024. This support is gratefully acknowledged.

REFERENCES

[1] Gu, K., Kharitonov, V., Chen, J. (2003), Stability of Time-Delay Systems. Birkhauser, Boston, MA.

[2] Domoshnitsky, S. Levi, R. H. Kappel, E. Litsyn, R. Yavich, (2021), “Stability of neutral delay differential equations with applications in a model of human balancing”, Math. Model. Nat. Phenom. 16, https://doi.org/10.1051/mmnp/2021008.

[3] Lazarević, M.(2014) “Advanced Topics on Applications of Fractional Calculus on Control Problems, System Stability and Modeling”, Sci. Int. Mon., WSEAS, ID9028, ISBN:978-960-474- 348-3, pp.202.

[4] Lazarević, M. (2022), “Stability of special classes of non-integer and integer order time delay dynamical systems”, Belgrade, Serbia: Faculty of Mechanical Engineering, sci. mon. (in Serbian).

[5] Petráš, I., (2011), Stability of Fractional-Order Systems. In: Fractional-Order Nonlinear Systems. Nonlinear Physical Science. Springer, Berlin, Heidelberg., https://doi.org/10.1007/978-3-642-18101-6_4.

[6] D. Radojević, M. P. Lazarević, (2022), „Further Results on Finite-Time Stability of Neutral Nonlinear Multi-Term Fractional Order Time-Varying Delay Systems”, Filomat 36:5, 1775–1787, https://doi.org/10.2298/ FIL2205775R.

2nd International Conference on Mathematical
Modelling in Mechanics and Engineering
Mathematical Institute SANU, 12-14. September, 2024.

ADVANCING ORTHOTROPIC PLATE STABILITY ANALYSIS THROUGH MACHINE LEARNING

Mirko R. Dinulović[1], Aleksandar Č. Bengin[2], Aleksa M. Maljević[3] and Marta R. Trninić[4]

[1,2,3]*University of Belgrade, Faculty of Mechanical Engineering, 11000 Belgrade, Serbia*

[3]*Vlatacom Institute of High Technologies, 11000 Belgrade Serbia*

[4]*The Academy of Applied Technical Studies, 11000 Belgrade, Serbia*

[1]mdinulovic@mas.bg.ac.rs,[2]abengin@mas.bg.ac.rs,[3]aleksa.maljevic@vlatacom.com,
[4]mtrninic@atssb.edu.rs

ORCID iD: [1]0000-0002-4772-2786, [2]0000-0002-9225-8601, [4]0000-0001-6916-6162

ABSTRACT

Orthotropic plates are widely used in engineering structures due to their ability to efficiently withstand loads while offering flexibility in design. Ensuring the stability of these plates is crucial for maintaining structural integrity and preventing catastrophic failures. Traditional methods for analyzing plate stability rely on complex mathematical formulations and empirical data, often requiring significant computational resources and expertise. However, with the advent of machine learning (ML) techniques, there is an opportunity to revolutionize the stability analysis of orthotropic plates by leveraging data-driven approaches to predict stability characteristics more accurately and efficiently. Integration of Machine Learning in Stability Analysis: Machine learning algorithms can be trained on a vast amount of data generated from simulations, experiments, and real-world observations to learn the complex relationships between various factors influencing plate stability. By incorporating features such as material properties, geometric configurations, loading conditions, and boundary conditions, ML models can effectively capture the nonlinear behavior of orthotropic plates and predict their stability with high accuracy. One of the critical tasks in developing ML-based stability analysis models is the selection and engineering of relevant features. Features that capture the intrinsic properties of orthotropic materials, such as elastic moduli, Poisson's ratios, and fiber orientations, play a crucial role in accurately representing plate behavior. Additionally, incorporating geometric parameters such as plate thickness, aspect ratio, and boundary conditions can further enhance the predictive capabilities of the models.

ML models for orthotropic plate stability analysis can be trained using various algorithms, including neural networks, support vector machines, decision trees, and random forests. Training datasets can be generated through finite element simulations, experimental testing, or a combination of both. Careful validation of the models against independent datasets is essential to ensure their reliability and generalization capability across different scenarios and boundary conditions.

Despite the promising potential of ML in orthotropic plate stability analysis, several challenges remain to be addressed. These include the need for large and diverse datasets, the interpretation of complex ML models, and the integration of uncertainty quantification techniques to account for variability in material properties and loading conditions. Furthermore, ongoing research efforts are focused on developing hybrid approaches that combine physics-based models with data-driven techniques to enhance the robustness and accuracy of stability predictions.

In the present research, the potential use of several algorithms was investigated for the use

in orthotropic plate analysis.

Comparing the Stochastic Dual Coordinate Ascent (SDCA), Limited-memory Broyden-Fletcher-Goldfarb-Shanno (L-BFGS), LightGBM (Light Gradient Boosted Machine), Fast Tree, and Fast Forest algorithms reveals distinct characteristics for each.

Stochastic Dual Coordinate Ascent (SDCA) is an optimization algorithm tailored for large-scale convex problems. It efficiently updates dual variables by randomly selecting coordinates, making it suitable for high-dimensional datasets. However, it requires hyperparameter tuning and is limited to convex problems.

Limited-memory Broyden-Fletcher-Goldfarb-Shanno (L-BFGS) is a quasi-Newton method for unconstrained optimization. It approximates the inverse Hessian matrix without computing it directly and offers fast convergence rates. However, memory requirements increase with the number of variables, limiting its scalability.

LightGBM is a gradient-boosting framework optimized for speed and memory efficiency. It employs histogram-based algorithms for split finding, making it highly scalable. While it offers regularized learning and parallel training, hyperparameter tuning is necessary.

Fast Tree is a decision tree-based ensemble algorithm designed for speed. It supports parallel training and can handle missing data and categorical features without preprocessing. However, it may overfit on noisy data and lacks interpretability compared to simpler models.

Fast Forest is a random forest algorithm known for its speed and scalability. It builds multiple decision trees in parallel, making it robust to overfitting. Despite its flexibility, it may not capture complex interactions between features as effectively as gradient-boosting algorithms.

Conclusion:

Machine learning offers a transformative approach to orthotropic plate stability analysis, enabling engineers to achieve more accurate predictions and faster insights into plate behavior. By leveraging the power of data-driven models, researchers can advance the state-of-the-art in structural engineering and contribute to the development of safer, more resilient engineering structures in various fields ranging from aerospace and automotive to civil infrastructure and marine applications

REFERENCES

[1] Hassanien AE, A Darwish, H El-Askary (2020), Machine Learning and Data Mining in Aerospace Technology, Springer
[2] Dinulović, M.; Benign, A.; Rašuo, B. Composite Fins Subsonic Flutter Prediction Based on Machine Learning. Aerospace,2024, 11, 26.
[3] Shai Shalev-Shwartz, Shai Ben-David - Understanding Machine Learning from Theory to Algorithms-Cambridge University Press (2014).
[4] Dodic, M., Krstic, B., Rasuo, B., Dinulovic, M., Bengin, A., Numerical Analysis of Glauert Inflow Formula for Single-Rotor Helicopter in Steady-Level Flight below Stall-Flutter Limit, Aerospace 2023, 10(3), 238.
[5] Alpaydın, E. (2020), Introduction to Machine Learning, The MIT Press

2nd International Conference on Mathematical
Modelling in Mechanics and Engineering
Mathematical Institute SANU, 12-14. September, 2024.

SOME APPROACHES TO CONSIDERING THE INFLUENCE OF HOMOGENEOUS NUCLEATION ON THE INTENSITY OF HEAT AND MASS TRANSFER DURING EVAPORATION

V. Levashov[1], A. Kryukov[2], I. Shishkova[3], V. Mayorov[4] and V. Tereshkin[5]

[1,2,4,5] *Institute of Mechanisc Lomonosov Moscow State University, Moscow 119192, Russian*

[2,3] *National Research University, Moscow Power Engineering Institute, Moscow 111250, Russian*

[1] *vyl69@mail.ru* ; [2] *kryukovap@mail.ru* ; [3] *in-shishkova@yandex.ru* ;
[4] *mayorovvo@imec.msu.ru* ; [5] i@vtereshkin.ru
ORCID iD: [1] 0000-0002-9488-6636; [4] 0000-0003-0435-0684

Keywords: Evaporation, Homogeneous nucleation, Molecular dynamic, Continuum mechanics, Boltzmann kinetic equation.

ABSTRACT

The problem of unsteady bulk condensation near the evaporation surface is considered using various approaches. As shown in [1], the vapour moving away from the evaporation surface is supersaturated and the degree of supersaturation (ratio of the partial vapor pressure to the saturated vapor pressure) increases significantly with increasing process intensity. Moreover, even at low evaporation rates, the degree of supersaturation (S) is greater than one.

It is well known that homogeneous condensation process can be realized under these conditions [2]. The formation of supersaturated vapor in the process of evaporation was reported in [3] but detail approaches that take into account of homogeneous nucleation influence on evaporation process intensity is absent in the literature. Some approximate approaches that estimate the need to consider nucleation in the description of the evaporation process have been presented in [4].

This study presented different approaches to simulate unsteady evaporation, taking into account the potential formation of droplets (nucleation process):

1) ***Combined solution.*** In this case, the Boltzmann kinetic equation (BKE) was used to describe the non-equilibrium region near the evaporating surface (Knudsen layer). Outside this layer the continuum mechanics equation (CME) was used together with the homogeneous nucleation kinetic equation (HNK). The solution splicing method was used at the boundary of the Knudsen layer;

2) ***BKE approach.*** An approach based on the direct numerical solution of the BKE with a special velocity distribution function transformation procedure (VDFP), which allows to take into account the influence of liquid droplets located in the investigated region [5];

3) ***Molecular dynamics simulation (MD).*** In this case, the time evolution of the system is described on the basis of the equation of motion of each atom (molecule) in the studied system. The condition of minimum energy in the vicinity of the selected point space is used to determine the particles belonging to the cluster [6].

All the approaches presented have some limitations. For example, the "Combined solution" gives the possibility to describe the evaporation problem with nucleation processes in a large region (compare with the mean free path of the vapor molecule). This approach also gives correct boundary conditions for the continuum mechanics equation in the evaporation problem. On the other hand, this approach does not take into account the process of liquid droplet formation in the immediate vicinity in the boundary layer (Knudsen layer). However, this

possibility is given by the "BKE approach". Consequently, the joint application of these approaches can provide more detailed information.

It should be noted that these two approaches may not be valid in the situation where the degree of supersaturation is high. This is due to the fact that both approaches use the classical correlation for the nucleation rate. In the cases where the supersaturation degree is large enough, the radius of the critical droplet calculated on the basis of the classical approach is reduced. As a result, the situation where the critical droplet consists of no more than ten atoms or molecules can be realized. It is obvious that the macroscopic description cannot be used in this case. Also, the classical theory of nucleation also relies on the macroscopic surface tension to describe the formation of a nano-sized embryo, which inevitably causes the model inaccuracy. The "Molecular dynamic simulation" method is free from these limitations.

Some results of the application of the presented approaches are presented in Figure 1.

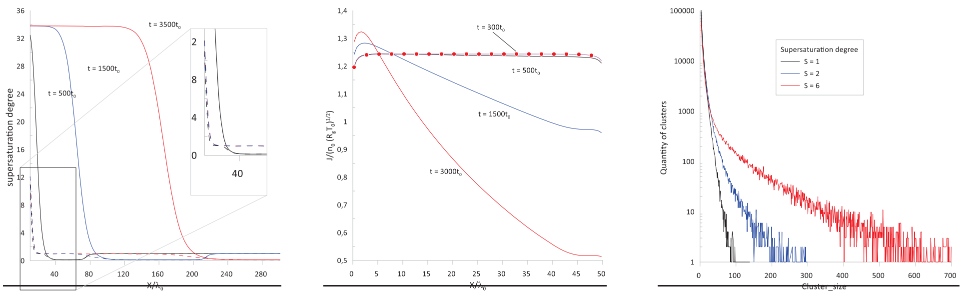

(a) (b) (c)

***Fig. 1** (a) – Supersaturation degree (Combined solution). Dashes lines – with nucleation; (b) – Mass flux density (BKE approach); (c) – MD modeling of cluster distribution*

The research was supported by the Russian Science Foundation (project No. 22-19-00044).

REFERENCES

[1] Labuntsov D.A., Kryukov A.P. (1979), Analysis of intensive evaporation and condensation, Int. J. Heat Mass Transf., 22, 989. DOI: 10.1016/0017-9310(79)90172-8

[2] Kalikmanov V.I. (2013), *Nucleation theory,* Springer, Dordrecht, p. 17.

[3] Anisimov S.I., Imas Ya.A., Romanov G.S., Khodyko Yu.V. (1970) *Deistvie izlucheniya bol'shoi moshchnosti na metally* Nauka, M. (in Russian)

[4] Levashov V. Y., Mayorov V. O., Kryukov A. P. (2023) "Change in evaporation flux due to homogeneous condensation of vapour near the interfacial surface", *Technical Physics Letters*. 49(5), pp. 49-52

[5] Levashov V. Y., Kryukov A. P., Shishkova I.N. (2024), "Influence of homogeneous nucleation on the intensity of evaporation/condensation processes", *Colloid Journal* 86(2), DOI: 10.1134/S1061933X23601361

[6] Zhukhovitskii D. I., Perevoshchikov E.E. (2024), "Nucleation in a non-ideal rapidly cooling vapor", *Journal of experimental and theoretical physics*, V. 138, N 1.

2nd International Conference on Mathematical
Modelling in Mechanics and Engineering
Mathematical Institute SANU, 12-14. September, 2024.

ANALYSIS OF VIBRO-IMPACT PROCESSES OF SINGLE MASS SYSTEM WITH VISCOUS DAMPING AND TWO-SIDED LIMITERS

Ljubiša Garić[1], Nikola Nešić[2], Saša Jovanović[3] and Julijana Lekić[4]

[1,2,3,4] *Faculty of Technical Sciences, University of Priština in Kosovska Mitrovica, 38220 Kosovska Mitrovica, Serbia*

[1] ljubisa.garic@pr.ac.rs; [2] nikola.nesic@pr.ac.rs; [3] sasa.m.jovanovic@pr.ac.rs;
[4] julijana.lekic@pr.ac.rs;

[1] ORCID iD: 0000-0002-4914-8968; [2] ORCID iD: 0000-0001-6237-4735
[3] ORCID iD: 0009-0006-9728-0695; [4] ORCID iD: 0000-0003-1896-6797

Keywords: vibro-impact oscillator, vibro-impact modes, viscous damping, stability analysis.

ABSTRACT

The paper presents an analysis of the horizontal straight-line motion of a single-mass vibro-impact system with two symmetrically placed limiters in the cases when the external coercive force and the viscous damping force are known. This paper investigates the periodic motion of a vibro-impact system, where it is assumed that the period of oscillation is equal to or proportional to the period of the coercive force. The analysis of the mathematical model of the vibro-impact system includes the definition of all possible types of motion, as well as the analysis of the stability of the motion. Obtained results define the areas of existence of periodic vibro-impact regimes, which allows to ensure the stability of the motion of the vibro-impact system.

1. Mathematical model of a single-mass vibro-impact system with two limiters

Figure 1 shows a mathematical model of a horizontal straight-line motion of a single-mass vibro-impact system with two symmetrical limiters.

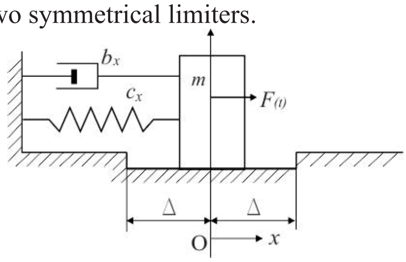

Figure 1. *Mathematical model of a single-mass vibro-impact oscillator with two limiters*

The equation of motion of the system in the interval between two consecutive impacts is:

$$m\ddot{x} + b_x\dot{x} + c_x x = F(t) = \sum_{i=1}^{k} F_i \cos(i\Omega t + \varphi_i) \tag{1}$$

The general solution for the differential equation (1) has the form:

$$x = De^{-nt} \cos\left(\sqrt{\omega_x^2 - n^2}t + \delta\right) + \frac{X_k(1-k^2p^2)}{K_k(p)} \cos(k\Omega t + \varphi_k) + \frac{X_1\frac{\Delta_x}{\pi}pk}{K_k(p)} \sin(k\Omega t + \varphi_k) \tag{2}$$

2. Results

Two cases for stability analysis are investigated - when *l* is odd and when *l* is an even number, where *l* is the multiplicity of the mode.

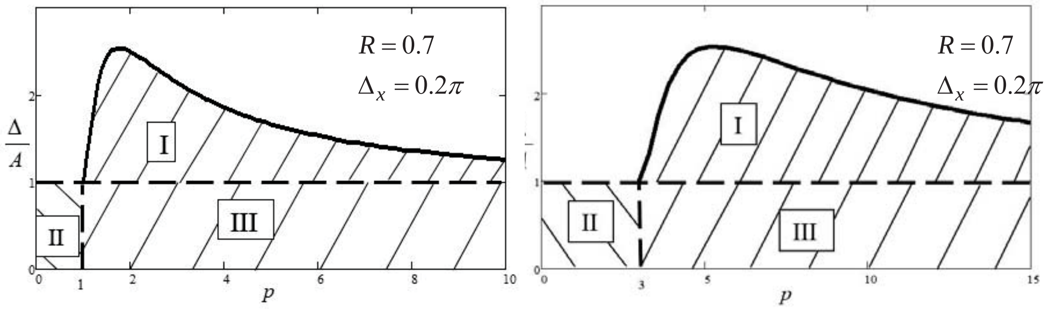

Figure 2. Areas of existence of the vibro-impact modes when l=1 (left) and l=3 (right)

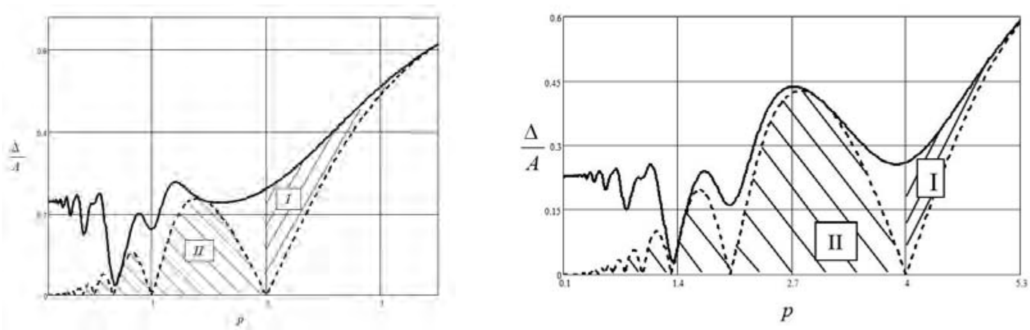

Figure 3. Areas of existence of the vibro-impact modes when l=2 (left) and l=4 (right)

3. Conclusion

Obtained results show the conditions (areas) of the existence of periodic vibro-impact regimes and allow to ensure the stability of the movement of the vibro-impact system. For known distance values, results allow to determine the frequency interval of the implementation of the vibro-impact process. The construction of the vibro-impact system can be realized on the basis of the amplitude-frequency characteristic when *l* is odd (figure 2) and when *l* is even (figure 3). The aim of this research is to increase the efficiency of the periodic vibro-impact systems, based on the results obtained from the analysis of the mathematical model of the system.

REFERENCES

[1] Babicki V. I. (1998), *Theory of Vibro-Impact Systems and Applications*, Springer.
[2] Garić Lj. (2017), *Analysis of Vibro-Impact Processes of a Single-Mass System with Viscous Damping and a Single Limiter*, Transactions of Famena 41(3).
[3] Wang, J. et al. (2017), *Dynamical analysis of a single degree-of-freedom impact oscillator with impulse excitation*, Advances in Mechanical Engineering, 9(7).

2nd International Conference on Mathematical
Modelling in Mechanics and Engineering
Mathematical Institute SANU, 12-14. September, 2024.

A MATHEMATICAL MODEL OF P2P RESOURCE DEFINITION IN UNSTRUCTURED P2P NETWORKS

Vesna Šešum-Čavić

Faculty of Civil Engineering, University of Belgrade, 11000 Belgrade, Serbia

vsesumcavic@grf.bg.ac.rs
ORCID iD: 0000-0002-0759-0686

Keywords: Unstructured Peer-to-Peer overlay networks, Intelligent lookup, Intelligent algorithms

ABSTRACT

Nowadays, distributed systems and their applications are omnipresent (mobile and web applications, etc.). They can be used to model difficult physics and mechanical principles, improve product design, construct complicated structures, create speedier cars, etc. Distributed systems are typically characterized by a huge problem size concerning number of computing devices, clients, requests and size of queries, autonomy and heterogeneity of participating organizations, and dynamic changes of the environment. To cope with unforeseen dynamics and a vast number of unpredictable dependencies on participating components, advanced approaches are demanded. The problems of efficient routing, searching and lookup of incomplete data in complex distributed systems are challenging tasks and, due to dynamic nature of the Internet, require to be updated constantly [1].

In order to properly address such a class of problems, efficient routing, searching and lookup mechanisms in the "underlying" unstructured P2P overlay network should be found. Generally, unstructured P2P overlay networks support very well dynamics and complex queries, but the disadvantage is that they do not scale well, which is the starting point for an improvement. Today P2P services have moved beyond purely internet services. Blockchain technology evolved from early P2P research and might be seen as its continuation.

However, a starting point for plugging adequate and efficient algorithms for routing, searching and lookup is to model and define a P2P resource. Mathematical models are always created with a focus on a particular problem, so that for each problem an applicable model can be developed. Since the created models may present different levels of abstraction from the real system, the required abstraction level can be predefined before the model building [2]. Therefore, a model for P2P resource definition is presented.

A resource in the P2P system is defined as a combination of content and its meta-data [1]. For simplicity, let us suppose that if two resources have the same content, then their meta-data is equal as well, and vice versa.

Let $S = \{D_1, D_2, . . . D_k\}$ be a set of k sets, $k \in \mathcal{N}$, which contain values of different data types. Each set in S contains a zero element, which is denoted as **nil**. A resource is defined as an ordered n-tuple $r = (r_1, r_2, ..., r_n)$, $n \in \mathcal{N}$, $k \leq n$, $r \in D_{i_1} \times D_{i_2} \times ... \times D_{i_n}$, where $D_{i_j} \in S$, and $r_i \neq$ **nil**. The sets in S define the data type of each element in the resource, and the constraints imposed on it. A search query is modeled in exactly the same way, with the only exception that each r_i can be **nil**, but not all of them together. The latter constraint is imposed in order to prevent retrieving all existing resources in the P2P network.

In order to fulfill the requirement that the lookup/search mechanism should be able to find similar objects [1], similarity functions are introduced. The position of each element r_i in a given resource $r = (r_1, r_2, \ldots r_n)$ determines the "meaning" this element has to users, as it can be seen from the example above. Therefore, similarity functions between objects at different positions may differ, even when these objects belong to the same set from S.

Let $r = (r_1, r_2, \ldots, r_n)$, $n \in \mathbb{N}$, $r_i \in D_i$, is a resource. The similarity function δ_i is defined as $\delta_i : D_i \times D_i \rightarrow \mathbb{R}$ and $(\forall r_i)\ \delta_i(\mathbf{nil}, r_i) = 0$. The function itself is normalized, (i.e., the range of δ_i is in the closed interval [0,1]. Without loss of generality, the similarity of objects is inversely proportional to the function's value, hence higher values indicate lower similarity. The similarity between resources and queries are defined as follows. There can be different approaches to that problem. It is possible to use heuristics, and have weights associated with each element in a resource. For the purpose of this research, the similarity function between queries and resources averages the similarity functions associated with each element in the resource:

$$f(q,r) = \frac{\sum_{i=1}^{n} \delta_i(q_i, r_i)}{n}$$

where $q = (q_1, q_2, \ldots q_n)$ is a query, $r = (r_1, r_2, \ldots r_n)$ is a resource, $n \in N$, and δ_i is a similarity function, defined for position i. It follows, from the definition of f, that $f \in [0, 1]$.
Further, a parameter $\varepsilon > 0$, $\varepsilon \in R$ determines the quality of the found data. Three result types can be defined [1] for query q and resource r:

- no data: $f(q, r) \geq \varepsilon$
- acceptable data: $0 < f(q, r) < \varepsilon$
- exact data: $f(q, r) = 0$

If a peer node has multiple resources, then all resources which are evaluated by applying the given query as acceptable, or exact, can be part of the result set. There exists a similarity function for each domain. Following the model described, arbitrary number of parameters can be added to the resource definition. On the top of this, different intelligent algorithms (e.g. swarm–inspired algorithms) for lookup and search or routing can be plugged.

REFERENCES

[1] Šešum-Čavić, V., Kühn, E., Fleischhacker, L. (2020), "Efficient Search and Lookup in Unstructured P2P Overlay Networks inspired by Swarm Intelligence," *IEEE Transactions on Emerging Topics in Computational Intelligence*, 4(3):351-368.

[2] Kotchourova, I. (2008), "Evaluation and Extension of Mathematical Models of P2P Systems," *Grin Verlag,* ISBN: 978-3640219872.

DIRECT AND INVERSE KINEMATICS FOR 6DOF ROBOT BASED ON SCREW THEORY

Vuk Todorović[1], Nikola Nešić[2] and Mihailo Lazarević[3]

[1,2]*Faculty of Technical Sciences, University of Priština in Kosovska Mitrovica, 38220 Kosovska Mitrovica, Serbia*

[3]*Faculty of Mechanical Engineering, University of Belgrade, 11000 Belgrade, Serbia*

[1]vuk.todorovic01@gmail.com; [2]nikola.nesic@pr.ac.rs; [3]mlazarevic@mas.bg.ac.rs

[2]ORCID iD: 0000-0001-6237-4735; [3]ORCID iD: 0000-0002-3326-6636

Keywords: Robotic manipulator, screw theory, Lie group, Lie algebra, Paden-Kahan subproblems, Newton-Raphson method, Niryo One.

ABSTRACT

In the modern age, robotics is gaining an ever-increasing role in shaping modern life, hence why innovations are increasingly more directed towards this interdisciplinary scientific field. The structure of a robot is complex and with a plethora of different ways to construct and control it, here we provide an elegant geometric approach for achieving the desired task by using screw theory [1].

As proved by the Chasles-Mozzi theorem, all motion can be obtained by a rotation around a fixed screw axis and a translation along the same which lends itself naturally to the representation of motion by screws. This is attained by an exponential coordinate representation where given a screw axis and an angle we may find a matrix defining our motion from a given coordinate frame. But why stop there? Not only motion, spatial velocities and forces are defined within screw theory as twists and wrenches that act on inertial coordinate frames attached that are instantaneously coincident to a fixed or even possibly moving frame.

However, unlike other ways of describing a robot's motion such as the Denavit-Hartenberg method which has an excessive amount of coordinate frames, or the use of Euler angles (in combination with position vectors) which have singularities at points, screw theory uses a less cumbersome mathematical apparatus and uses implicit representations thereby avoiding singularities. The mathematical foundation of screw theory lies on the foundation of the $SO(3)$ and $SE(3)$ Lie groups and their algebras $so(3)$ and $se(3)$ which represent rigid body rotations and motions in three-dimensional space respectively.

By far, the largest part of screw theory is rooted in linear algebra which ties in nicely to implementation in practice. Everything described in this paper will be implemented using Python and the Robot Operating System (ROS) on a six-degree-of-freedom robot manipulator Niryo One. In Fig. 1(a) we have the basic geometric description of the Niryo One robot where we have the position of each joint and its direction of rotation. Next, we define a fixed space frame at the bottom of the robot and a moving body frame at the end-effector. Putting this all together we have a kinematic diagram as shown in Fig. 1(b).

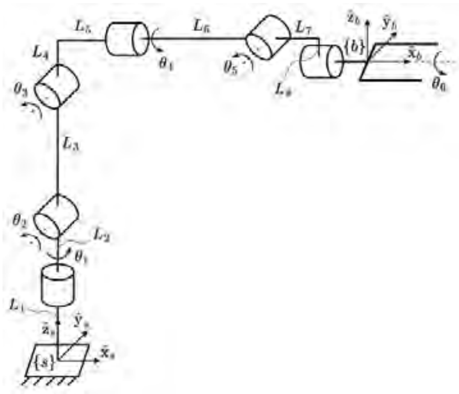

a) b)

Fig. 1: *Niryo One manipulator: a) Position and direction of rotation of the joints where J_i is the i-th joint, b) Kinematic diagram*

In robot kinematics, we use the Product of Exponentials to determine the forward kinematics of a robot-given a set of joint angles, find the representation of the end-effector. While this is straightforward, a more interesting problem which has garnered a lot of interest and is being actively researched is the inverse kinematics-given a representation of the end-effector, find the joint angles that correspond to it. There are two main ways of solving this problem, analytically and numerically, both of which have their advantages and drawbacks. The Paden-Kahan subproblems [2] seek to break apart the inverse kinematics into subproblems that have a known analytical solution. On the other hand, fundamental to numerical nonlinear root-finding is the Newton-Raphson method which can find approximate solutions within a given tolerance. But analytical solutions, if they exist, may not always have a closed-form solution or their computation may be quite involved. The numerical approach, while usually efficient and precise to a practically arbitrary degree, may not always converge with a given initial value. Here we suggest a synergetic approach for robots that do not yield to Paden-Kahan subproblems by a slight amount. It involves finding an approximate analytical solution using the Paden-Kahan subproblems and using that as an initial value for the Newton-Raphson method.

REFERENCES

[1] Lynch, K. M., & Park, F. C. (2019), *Modern robotics: mechanics, planning, and control*, Cambridge University Press.
[2] Murray, R. M., Li, Z., & Sastry, S. S. (2017), *A mathematical introduction to robotic manipulation*, CRC press.

RECENT SWARM INTELLIGENCE TECHNIQUES FOR OPTIMAL SPUR GEAR DESIGN

Hammoudi Abderazek[1], Aissa Laouissi[2], Mourad Nouioua[3] and Ivana Atanasovska[4]

[1,2,3] *Mechanics Research Center CRM, Po. Box 73B, Constantine,25000, Algeria*

[4] *Mathematical Institute of Serbian Academy of Sciences and Arts, Kneza Mihaila 36, 11000 Belgrade, Serbia*

[1]*hammoudiabderazek@gmail.com*; [2]*aissou_011@yahoo.fr*; [3] *nouioua.mo@gmail.com;*
[4] *iviatanasov@yahoo.com*

ORCID iD: [1]0000-0001-8911-348X; [2]0000-0002-5723-3863; [3] 0000-0003-0439-2112;
[4]0000-0002-3855-4207

Keywords: Tooth profile, Profile shift, Spur gear, Meta-heuristics, Swarm intelligence algorithms.

ABSTRACT

Gear tooth profile has a substantial impact on the main operating parameters of gear pairs. By the suitable modification of the tooth profile, the vibration and noise of the gear system can be reduced greatly. In the present study, four recent smart methods are employed to select the optimal geometry parameters of a cylindrical spur gear. The optimization problem is prepared for three mixed design variables consisting of the profile shift coefficients and the normal pressure angle. There are three objectives including the maximum specific sliding, velocity sliding, and nominal tooth root stress of the pinion. The kinematics, as well as the geometric conditions such as contact ratio, the thickness of the tooth, and the interferences, are taken into account to grant an optimum design of the spur gear. The simulation results reached in this paper indicate clearly that the utilized algorithms are very competitive in precision gear design optimization.

REFERENCES

[1] Abderazek, H., Ferhat, D., Atanasovska, I., & Boualem, K. (2015). A differential evolution algorithm for tooth profile optimization with respect to balancing specific sliding coefficients of involute cylindrical spur and helical gears. *Advances in Mechanical Engineering*, 7(9)

[2] Abderazek, H., Ferhat, D., & Ivana, A. (2017). Adaptive mixed differential evolution algorithm for bi-objective tooth profile spur gear optimization. *The International Journal of Advanced Manufacturing Technology*, 90, 2063-2073.

A PREDICTIVE MODEL FOR WEAR IN MISALIGNED HELICAL GEAR CONTACT UNDER CONDITIONS OF BOUNDARY LUBRICATION

Maksat Temirkhan [1] and Christos Spitas [2]

[1]*Department of Mechanical and Aerospace Engineering, Nazarbayev University, 010000 Astana, Kazakhstan*

[2]*School of Aerospace Engineering, Department of Mechanical, Materials and Manufacturing engineering, University of Nottingham, Ningbo, China*

[1]*maksat.temirkhan@nu.edu.kz* ; [2]*cspitas@gmail.com* ;

[1]ORCID iD: 0000-0001-6283-3401

Keywords: Novel TCA method, Contact stress, Helical gear wear, Misalignment.

ABSTRACT

In this work, gear tooth wear under conditions of lubricant starvation is modeled using Archard's equation, employing predictions of the contact stress field for the generalized case of misaligned triaxial ellipsoids corresponding to the localized contact of the gear teeth. The kinematic and geometric analysis is based on a generalized exact tooth contact model, which provides rapid unconditional convergence of the numerical solution. Using this model for the case of a pair of helical gears, tooth wear is predicted under an approximation of quasi-static conditions and thermal steady-state. The effect of different lubrication conditions within the boundary lubrication hypothesis is considered in a parametric study.

REFERENCES

[1] Litvin, F., & Fuentes, A. (2011). Gear geometry and applied theory. New York: Cambridge University Press.

[2] M. Temirkhan, C. Spitas and D. Wei, "A computationally robust solution to the contact problem of two rotating gear surfaces in space". Meccanica, vol. 58, pp. 2455–2466. 2023.

[3] M. Temirkhan, H.B. Tariq, V. Spitas and C. Spitas, "Parametric design of straight bevel gears based on a new tooth contact analysis model". Archive of Applied Mechanics, vol. 93, pp. 4181–4196, 2023.

[4] Bracci, A., Gabiccini, M., Artoni, A., and Guiggiani, M. (2009). Geometric contact pattern estimation for gear drives. Computer Methods in Applied Mechanics and Engineering, 198(17), 1563–1571.

[6] Lin, C. H., & Fong, Z. H. (2015). Numerical tooth contact analysis of a bevel gear set by using measured tooth geometry data. Mechanism and Machine Theory, 84, 1–24.

[7] Temirkhan, M., Tariq, H. B., Kaloudis, K., Kalligeros, C., Spitas, V., & Spitas, C. (2022). Parametric quasi-static study of the effect of misalignments on the path of contact, transmission error, and contact pressure of crowned spur and helical gear teeth using a novel rapidly convergent method. Applied Sciences, 12(19), 10067.

[8] Temirkhan, M., Amrin, A., Spitas, V., & Spitas, C. (2023). Convergence and accuracy problems of the conventional TCA model – critical analysis and novel solution for crowned Spur Gears. Proceedings of the Institution of Mechanical Engineers, Part C: Journal of Mechanical Engineering Science.

2nd International Conference on Mathematical
Modelling in Mechanics and Engineering
Mathematical Institute SANU, 12-14. September, 2024.

TAYLOR-COUETTE FLOW OF A VISCOELASTIC FLUID DURING THE PHOTOPOLYMERIZATION INDUCED PHASE TRANSITION

Enej Istenič[1], Miha Brojan[2]

[1]*University of Ljubljana, Faculty of Mechanical Engineering, 1000 Ljubljana, Slovenia*
[2]*University of Ljubljana, Faculty of Mechanical Engineering, 1000 Ljubljana, Slovenia*
[1]*enej.istenic@fs.uni-lj.si*; [2]*miha.brojan@fs.uni-lj.si*
[1]ORCID iD: 0009-0001-3827-1629; [2]ORCID iD: 0000-0002-3342-9562

Keywords: Taylor-Couette flow, Viscoelasticity, Variable-order calculus, Polymerization.

ABSTRACT

Taylor-Couette flows designate flows in the gap between rotating cylinders or spheres and appear in diverse settings, such as in various industrial processes, water, oil and gas wellbores, or in meteorological, geophysical and astrophysical systems. The stability of these types of flows is an issue of considerable importance and the subject of a great number of theoretical and experimental investigations [1]. In recent times, a number of contributions have been published which treat Taylor-Couette flows of viscoelastic fluids while assuming various types of constitutive laws [2].

In this contribution, we will present the theoretical treatment of the Taylor-Couette flow of a viscoelastic fluid undergoing solidification caused by photopolymerization due to irradiation by an external light source. This phase transition causes the mechanical response to evolve from a purely viscous to a purely elastic. We will assume the extent of polymerization to be a function of both position and time. In doing so, we will adapt the treatment presented in one of our previous contributions concerning plane Poiseuille flow of a variable-order viscoelastic fluid [3]. We will assume photopolymerization to be a simple addition reaction unaffected by mechanical response, with the luminous flux driving the reaction consisting of a radial and axial component while being governed by the Beer-Lambert law. We will assume a variable-order model of viscoelastic response resembling the model relevant for polymer solutions derived by Bagley and Torvik [4], with the term determining the position- and time-dependent component of the response proportional to a variable-order Caputo-type temporal derivative acting upon the strain [5]. The order parameter appearing in the Caputo-type operator is directly related to the extent of polymerization. A model of this type requires fewer experimentally determined material constants compared to the integer-order models of viscoelasticity and enables clear coupling between the process of phase transition and the mechanical response.

We solve the problem with a semi-analytical approach which involves performing the Laplace transform over variable-order terms, and obtain physically sound solutions. This means that the tangential velocity component exhibits characteristics of viscous flow in the part of the domain where the extent of polymerization is low and diminishes in magnitude where it is high. We also conjecture that the flow exhibits viscoelastic instabilities whose dependence on time and position depends on the direction in which the luminous flux propagates in relation to the axis of rotation.

REFERENCES

[1] Lueptow, R. M. et al. (2023), "Taylor-Couette and related flows on the centennial of Taylor's seminal Philosophical Transactions paper: part 1," *Philosophical Transactions of the Royal Society*, A381(2243), 20220140.

[2] Bai, Y. et al. (2023), "Viscoelastic instabilities of Taylor-Couette flows with different rotation regimes," *Philosophical Transactions of the Royal Society A,* 381(2246), 20220133.

[3] Istenič, E., Brojan, M. (2023), "Fluid flow during phase transition: From viscous fluid to viscoelastic solid via variable-order calculus," *Physics of Fluids*, 35(12).

[4] Bagley, R. L., Torvik, P. J. (1983), "A theoretical basis for the application of fractional calculus to viscoelasticity," *Journal of rheology*, 27(3), pp. 201-210.

[5] Caputo, M. (1967), "Linear models of dissipation whose Q is almost frequency independent – II," *Geophysical journal international*, 13(5), pp. 529-539.

2nd International Conference on Mathematical Modelling in Mechanics and Engineering
Mathematical Institute SANU, 12-14. September, 2024.

NONEQUILIBRIUM MODELLING OF KORTEWEG FLUIDS

Zagorka Matić[1] and Srboljub Simić[2]

[1]*Faculty of Technical Sciences, University of Novi Sad, 21000 Novi Sad, Serbia*
[2]*Faculty of Sciences, University of Novi Sad, 21000 Novi Sad, Serbia*
[1]zagorka.mat@uns.ac.rs; [2]ssimic@uns.ac.rs
[2]0000-0003-3726-2007

Keywords: Korteweg fluids, nonequilibium, Liu method.

ABSTRACT

Korteweg fluids are the prototypical models which provide appropriate continuum description of diffuse interfaces or capillary effects [1]. Nonlocal interactions of the molecules in the interface are modelled by the mass density derivatives in the equilibrium (reversible) part of the stress tensor, which capture capillary effects.

Derivation of a thermodynamically consistent model for Korteweg fluids is a challenge due to the presence of capillary stresses. It may be approached using classical Coleman-Noll procedure [1] or some of its variants [2]. Another possibility is to apply the Liu method of multipliers [3] which requires certain generalization due to the presence of density gradients. It is shown that these two approaches are equivalent [4] and recent study [5] presented one possible solution to this problem. In this study we present derivation of the nonequilibrium model of Korteweg fluids using Liu method of multipliers.

Governing equations for Korteweg fluids consist of the conservation laws for mass, momentum and energy, and the additional conservation law for the density gradient derived from the mass conservation law (summation with respect to repeated indices is assumed):

$$\frac{\partial \rho}{\partial t} + \frac{\partial}{\partial x_j}(\rho v_j) = 0, \qquad \frac{\partial}{\partial t}(\rho v_i) + \frac{\partial}{\partial x_j}(\rho v_i v_j - t_{ij}) = 0,$$

$$\frac{\partial}{\partial t}\left(\frac{1}{2}\rho|\boldsymbol{v}|^2 + \rho e\right) + \frac{\partial}{\partial x_j}\left[\left(\frac{1}{2}\rho|\boldsymbol{v}|^2 + \rho e\right)v_j - t_{ij}v_i + q_j\right] = 0,$$

$$\frac{\partial}{\partial t}\frac{\partial \rho}{\partial x_i} + \frac{\partial}{\partial x_j}\left(\frac{\partial \rho}{\partial x_i}v_j + \rho\frac{\partial v_j}{\partial x_i}\right) = 0.$$

These equations have to be compatible with the entropy balance law:

$$\frac{\partial}{\partial t}(\rho s) + \frac{\partial}{\partial x_j}(\rho s v_j + \varphi_j) = \Sigma \geq 0.$$

Liu method of multipliers treats the governing equations as constraints and absorbs them into extended entropy balance law by means of multipliers:

$$\frac{\partial}{\partial t}(\rho s) + \frac{\partial}{\partial x_j}\left(\rho s v_j + \varphi_j\right) - \Lambda^{\rho}\left\{\frac{\partial \rho}{\partial t} + \frac{\partial}{\partial x_j}(\rho v_j)\right\} - \Lambda^{v_i}\left\{\frac{\partial}{\partial t}(\rho v_i) + \frac{\partial}{\partial x_j}\left(\rho v_i v_j - t_{ij}\right)\right\}$$
$$- \Lambda^{e}\left\{\frac{\partial}{\partial t}\left(\frac{1}{2}\rho|\boldsymbol{v}|^2 + \rho e\right) + \frac{\partial}{\partial x_j}\left[\left(\frac{1}{2}\rho|\boldsymbol{v}|^2 + \rho e\right)v_j - t_{ij}v_i + q_j\right]\right\}$$
$$- \Lambda_i^{\nabla\rho}\left\{\frac{\partial}{\partial t}\frac{\partial \rho}{\partial x_i} + \frac{\partial}{\partial x_j}\left(\frac{\partial \rho}{\partial x_i}v_j + \rho\frac{\partial v_j}{\partial x_i}\right)\right\} = \Sigma$$

Extensive analysis of the generalized entropy balance law yields the set of equations–compatibility conditions–which determine the multipliers:

$$\Lambda^{e} = \frac{1}{\theta}, \quad \Lambda_i^{\nabla\rho} = \frac{1}{\theta}\alpha(\rho,\theta)\frac{\partial \rho}{\partial x_i}, \quad \Lambda^{v_i} = -\frac{v_i}{\theta}, \quad \Lambda^{\rho} = -\frac{1}{\theta}\left(e - \theta s + \frac{p}{\rho} - \frac{1}{2}|\boldsymbol{v}|^2\right).$$

The remaining part–residual inequality–first yields the entropy flux which inherits capillary effects:

$$\varphi_j = \frac{1}{\theta}\left(q_j + \rho\alpha(\rho,\theta)\frac{\partial \rho}{\partial x_j}\frac{\partial v_k}{\partial x_k}\right).$$

Minimization of the entropy production Σ in equilibrium leads to the equilibrium stress tensor (and heat flux) which recovers the capillary stresses:

$$t_{ij}^{eq} = -\left[p + \rho\frac{\partial \alpha(\rho,\theta)}{\partial \rho}\frac{\partial \rho}{\partial x_k}\frac{\partial \rho}{\partial x_k} + \rho\alpha(\rho,\theta)\frac{\partial^2 \rho}{\partial x_k \partial x_k}\right]\delta_{ij} + \alpha(\rho,\theta)\frac{\partial \rho}{\partial x_i}\frac{\partial \rho}{\partial x_j}; \quad q_k^{eq} = 0_k.$$

Nonnegativity of the entropy production in nonequilibrium yields linear constitutive relations, which recover viscous stress tensor and generalized form of the heat flux:

$$q_k = -\kappa\frac{\partial \theta}{\partial x_k} - \rho\left[\alpha(\rho,\theta) - \theta\frac{\partial \alpha(\rho,\theta)}{\partial \theta}\right]\frac{\partial v_j}{\partial x_j}\frac{\partial \rho}{\partial x_k}.$$

Liu method of multipliers for the first time led to the recovery of nonequilibrium model of Korteweg fluids in generalized form presented above. Material parameters are determined by the function $\alpha(\rho,\theta)$ which can be chosen to adapt to a particular fluid, which is also a new result.

REFERENCES

[1] Anderson, D.M., McFadden, G.B., Wheeler, A.A. (1998), "Diffuse-Interface Methods in Fluid Mechanics," *Annu. Rev. Fluid Mech.*, **30**:139-165.
[2] Heida, M., Málek, J. (2010), "On compressible Korteweg fluid-like materials," *International Journal of Engineering Science*, **48**:1313-1324.
[3] Liu, I-S. (1972), "Method of Lagrange Multipliers for Exploitation of the Entropy principle," *Arch. Rational Mech. Anal.*, **46**:131-148.
[4] Cimmelli, V.A., Oliveri, F., Pace, A.R. (2011), "On the Thermodynamics of Korteweg Fluids with Heat Conduction and Viscosity," *J. Elast*, **104**:115-131.
[5] Ván, P. (2023), "Holographic fluids: A thermodynamic road to quantum phyisics," *Physics of Fluids*, **35**, 057105.

2nd International Conference on Mathematical
Modelling in Mechanics and Engineering
Mathematical Institute SANU, 12-14. September, 2024.

CROSS SECTION DESIGN OF AN AUTO CRANE ARTICULATED BOOM USING METAHEURISTIC OPTIMIZATION ALGORITHM FOR SET DEFLECTION

Marko Todorović[1], Nebojša Zdravković[2], Goran Marković[3], Mile Savković[4], Predrag Mladenović[5], Goran Pavlović[6]

[1,2,3,4,5]*Faculty of mechanical and civil engineering in Kraljevo, University of Kragujevac, 36000 Kraljevo, Serbia*

[6]*Faculty of Electronic Engineering, University of Niš, 18104 Niš, Serbia*

[1]*todorovic.m@mfkv.kg.ac.rs* ; [2]*zdravkovic.n@mfkv.kg.ac.rs*; [3]*markovic.g@mfkv.kg.ac.rs*; [4]*savkovic.m@mfkv.kg.ac.rs*,[5]*mladenovic.p@mfkv.kg.ac.rs*

ORCID iD: [1]0000-0003-3684-2819; [2]0000-0001-6387-2816; [3]0000-0002-0957-0718; [4]0000-0002-4501-9149, [5]0000-0002-3315-4642, [6]0000-0002-7230-1908

Keywords: Metaheuristic optimization algorithms, cross section design, auto crane, articulated boom.

ABSTRACT

Picking the right geometric parameters for the cross section of an auto crane articulated boom is a complex and tedious iterative process. These geometric parameters, such as type, width, height, and plate thickness of the cross section influence the behavior of the articulated boom, especially deflection. Metaheuristic optimization algorithms can be employed to accelerate this process. The optimization algorithm was used for picking geometric characteristics of the members of a three-segment articulated boom (Figure 1), where each segment is consisted of a box cross section with different parameters (Figure 2). Constraints were defined in such way the height of the cross section cannot exceed the triple width of the cross section, and the whole structure should not exceed the set value of deflection. The mathematical model for calculating the deflection was derived using the second Castigliano's theorem in function of the weight of the payload. The position of the structure in which the deflection takes the highest value was detected (Figure 3), and for that position the optimization was conducted. The goal of the optimization process was to find geometric characteristics of the cross sections of minimal total mass for the set maximal deflection value. Two optimization algorithms were used: Differential Evolution algorithm (DE)[1], and Search and Rescue optimization algorithm (SAR)[2]. The value of set maximal deflection was 5 cm, the payload was set to be 2 kN, the material was set to be structural steel for all three segments. The results of the optimization are shown in Table 1. The verification of the results was completed using finite element method.

Table 1. Results of the optimization

	k	B_1	δ_1	B_2	δ_2	B_3	δ_3	Max. deflection	Total mass
	-	mm	mm	mm	mm	mm	mm	mm	kg
DE	2,958	174,6	3	167,4	3	150	3	≈ 50	565,6141
SAR	2,986	173,5	3	165,7	3	150	3	≈ 50	565,4616

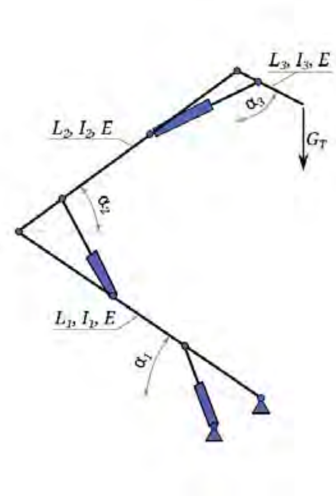

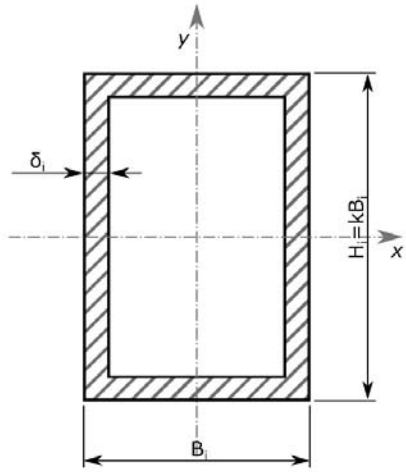

Figure 1. Auto crane articulated boom model

Figure 2. Cross section with important geometric characteristics

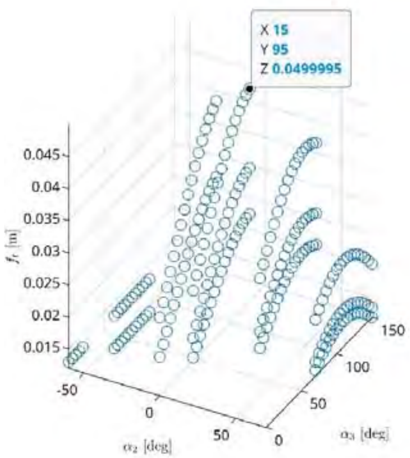

Figure 3. Deflection of the auto crane articulated boom for the optimized cross section

REFERENCES

[1] Storn, R., Price, K., "Differential evolution – a simple and efficient heuristic for global optimization over continuous spaces", *Journal of Global Optimization* 1997; 11(4); 341-359, doi: 10.1023/A:1008202821328

[2] Shabani, A., Asgarian, B., Gharebaghi, S.A., Salido, M., Giret, A., "A New Optimization Algorithm Based on Search and Rescue Operations", *Mathematical problems in Engineering* 2019; doi: 10.1155/2019/2482543

2nd International Conference on Mathematical
Modelling in Mechanics and Engineering
Mathematical Institute SANU, 12-14. September, 2024.

QUALITATIVE INTERPRETATION OF ENTROPY-LIKE MEASURES IN STUDY OF HIGHER ORDER GROUPING IN COMPLEX NETWORKS

Miroslav Andjelković[1] and Slobodan Maletić[2]

[1,2] *"Vinča" Institute of Nuclear Sciences - National Institute of the Republic of Serbia, University of Belgrade, Mike Alasa 12-14, 11351 Vinča, Belgrade, Serbia*

[1]mandjelkovic@vinca.rs; [2]supersloba@vinca.rs

[1]ORCID iD: 0000-0002-4449-8934; [2]ORCID iD: 0000-0001-7642-8271

Keywords: Information entropy, Topological data analysis, Q-analysis, Higher-order analysis, Complex networks

ABSTRACT

How do we obtain purposeful information from the data representing a complex system in order to unravel and interpret information about its hidden substructure and complexity? Research areas such as physics, social, biological, and informational sciences struggle with the same question. Answering this question can help us get closer to resolving relevant problems about extracting the most important properties and degree of complexity of a complex system.

Studying the Shannon information entropy [1] and entropy-like measures combined with the apparatus of algebraic topology [2] can be one way of characterizing the dissimilarity of hidden substructures embedded in a complex network.

Concepts of algebraic topology and information theory are applied in various complex systems. In order to resolve the problem, different entropy-like measures are proposed: for the cohomological nature of information [3], topological entropy [4], higher-order spectral entropy [5], persistent entropy [6,7], and multilevel integration entropies [8,9]. A few of the proposed entropies are given as vectors to capture the distinguishability of different layers of the substructure of a complex network.

A simplicial complex, mathematical object originating from algebraic topology, is used to analyze and extract information on hidden substructures of a complex network. Simplices in simplicial complexes merge elements from the underlying complex network in sets using a meaningful relation depending on the information we want to obtain from the system.

This work presents an overview of the importance of entropy-like measures derived within the algebraic topology used in complex systems analysis and a qualitative interpretation of what they represent. The other part concerns meaningful information that can be obtained by combining the rich methodology from algebraic topology and the study of information entropy.

REFERENCES

[1] Shannon, C.E. (1948), "A mathematical theory of communication", Bell Syst. Tech. J, 27, 379-423.

[2] Munkres, J.R. (1984), "Elements of Algebraic Topology", Addison-Wesley Publishing: Menlo Park, CA, USA.

[3] Baudot, P., Bennequin, D. (2015), "The Homological Nature of Entropy", Entropy, 17, 3253-3318.

[4] Andjelković. M., Gupte, N., Tadić, B. (2015), "Hidden geometry of traffic jamming", Phys. Rev. E, 91, 052817.

[5] Maletić, S., Rajković, M., (2012), "Combinatorial Laplacian and entropy of simplicial complexes associated with complex networks.", Eur.Phys. J, 212, 77-97.

[6] Chintakunta, H., Gentimis, T., Gonzales-Diaz, R., Jimenez, M.-J., Krim, H. (2015), "An entropy-based persistence barcode", Pattern Recognit., 48, 391-401.

[7] Merelli, E., Rucco, M., Sloot, P., Tesei, L. (2015) "Topological Characterization of Complex Systems: Using Persistent Entropy", Entropy, 17, 6872-6892.

[8] Maletić, S., Zhao, Y., (2017), "Multilevel Integration Entropies: The Case of Reconstruction of Structural Quasi-Stability in Building Complex Dataset", Entropy, 19(4), 172.

[9] Maletić, S., Andjelković. M. (2024), "Higher-order clustering patterns in simplicial financial systems", Chaos, 34, 013144.

2nd International Conference on Mathematical
Modelling in Mechanics and Engineering
Mathematical Institute SANU, 12-14. September, 2024.

AN INTELLIGENT METHOD FOR HYPERPARAMETER OPTIMIZATION IN DEEP LEARNING MODEL FOR SOIL ORGANIC CARBON ESTIMATION FROM SPECTRAL MEASUREMENTS

Slobodan Jelić[1], Vesna Šešum-Čavić[2]

Faculty of Civil Engineering, University of Belgrade, 11000 Belgrade, Serbia

[1]sjelic@grf.bg.ac.rs ; [2]vsesumcavic@grf.bg.ac.rs

ORCID iD: [1]0000-0002-2134-3112; [2]0000-0002-0759-0686

Keywords: Soil Organic Carbon, Machine learning, Swarm-based algorithms.

ABSTRACT

Finding inexpensive but reliable ways to measure Soil Organic Carbon (SOC) is essential for maintaining costs of Carbon Credit implementation low. Reflectance spectroscopy has emerged as an important rapid and low-cost complement to traditional wet chemical analysis. The advent of low-cost, portable and handheld spectrometers operating in the visible and near-infrared (VNIR) range and realized using micro-electromechanical systems enables the rapid and non-destructive measurement of a soil's reflectance spectrum. The VNIR spectrum of a soil sample portrays the physical and chemical chromophores present within. Machine learning (ML) techniques can infer from a VNIR spectrum key physical and chemical parameters with good levels of accuracy which are instrumental for the health of the soil ecosystem, including: soil organic carbon, particle size distribution, electrical conductivity, pH, total nitrogen and more.

The main objective is to fit calibration models and/or adopt the standard international models to assist with the conversion of soil spectroscopy data to analysis-ready soil data. ML techniques are extensively used to produce digital soil maps in recent times. Since the sample of the target variable is the basis for mapping, its size and spatial pattern play a key role in the resulting soil map accuracy. A sample used for fitting training a machine learning algorithm is referred to as a calibration sample [1, 2].

While modern deep learning methodologies predominantly rely on feature extraction through convolutional and pooling layers, prior problem-specific feature extraction techniques offer notable advantages. These techniques enhance model accuracy and concurrently diminish model complexity by directing the learning process towards pertinent covariates [3]. However, recent studies [5] have proved the superior performance of Convolutional Neural Networks (CNNs) over traditional methodologies such as ratio indexed-based linear regression, partial least squares regression and CUBIST.

A diverse array of measurement techniques yields datasets characterized by varying probability density functions across specific signal channels. This variability stems from the in-situ driven labeling procedure inherent to spectral measurements, resulting in datasets that differ not only in size but also in accuracy. Consequently, the architecture of a deep neural network cannot be universally tailored to accommodate all datasets and use cases a priori.

In this study, we propose leveraging swarm intelligence [4,6] for hyperparameter optimization within deep neural networks tasked with estimating soil organic carbon levels. By contrast, we compare our approach to conventional methods such as random and grid search

hyperparameter optimization techniques. Our methodology targets the optimization of several critical parameters, including the number of convolutional and fully connected layers, dimensions of convolutional and max-pooling filters, channel quantities, dropout rates, and the number of hidden units within fully connected layers.

REFERENCES

[1] W. Ng, B. Minasny, S. H. Jeon, and A. McBratney, “Mid-infrared spectroscopy for accurate measurement of an extensive set of soil properties for assessing soil functions,” *Soil Security,* vol. 6, p. 100043, 2022.

[2] I. Greenberg, M. Seidel, M. Vohland, H. J. Koch, and B. Ludwig, “Performance of in situ vs laboratory mid-infrared soil spectroscopy using local and regional calibration strategies,” *Geoderma*, vol. 409, p. 115614, 2022.

[3] Z. Bai et al., “Estimation of Soil Organic Carbon Using Vis-NIR Spectral Data and Spectral Feature Bands Selection in Southern Xinjiang, China,” *Sensors*, vol. 22, no. 16, 2022.

[4] K. Liu, M. Shahria Alam, J. Zhu, J. Zheng, L. Chi, “Prediction of carbonation depth for recycled aggregate concrete using ANN hybridized with swarm intelligence algorithms,” *Construction and Building Materials*, vol. 301, 124382, 2021.

[5] Hong, Y.; Sanderman, J.; Hengl, T.; Chen, S.; Wang, N.; Xue, J.; Zhuo, Z.; Peng, J.; Li, S.; Chen, Y.; Liu, Y.; Mouazen, A. M.; Shi, Z. Potential of Globally Distributed Topsoil Mid-Infrared Spectral Library for Organic Carbon Estimation. CATENA 2024, 235, 107628.

[6] Yeh, W.-C.; Lin, Y.-P.; Liang, Y.-C.; Lai, C.-M.; Huang, C.-L. Simplified Swarm Optimization for Hyperparameters of Convolutional Neural Networks. Computers & Industrial Engineering 2023, 177, 109076. https://doi.org/10.1016/j.cie.2023.109076.

2nd International Conference on Mathematical
Modelling in Mechanics and Engineering
Mathematical Institute SANU, 12-14. September, 2024.

NEURAL NETWORK MODEL FOR PREDICTING THE EFFICIENCY OF A STEAM BOILER USING NATURAL GAS AS FUEL

Milica M. Ivanović[1], Mitra V. Vesović[2], Stamenić S. Mirjana[3] Radiša Ž. Jovanović[4] Srbislav B. Genić[5]

Faculty of Mechanical Engineering, University of Belgrade, 11000 Belgrade, Serbia
mvesovic@mas.bg.ac.rs; mivanovic@ mas.bg.ac.rs; mstamenic@mas.bg.ac.rs;
rjovanovic@mas.bg.ac.rs; sgenic@mas.bg.ac.rs
ORCID iD: [1]0000-0001-6239-703X, [2]0000-0003-0457-1874, [3]0000-0002-7163-8584,
[4]0000-0002-8122-756X, [5]0000-0001-7792-2386

Keywords: modelling, neural network, steam boiler, steam boiler efficiency.

ABSTRACT

Predicting the performance of steam boilers is important to enable efficient operational monitoring and appropriate control strategies. The operation of such plants can be both steady-state and transient, with operating parameters changing according to the requirements of the technological process. The establishment of accurate mathematical models to predict boiler efficiency encounters a variety of problems related to the degradation of certain operating parameters and changes in steam production. Due to the inherent flexibility, adaptability, and robustness of neural network models, developers can take advantage of these benefits to create more accurate predictive models for boiler efficiency over time, that achieve comparable or even higher accuracy than conventional techniques. The aim of the neural network model presented in this paper is to predict the directly calculated boiler efficiency based on experimental data from existing steam boiler running on natural gas as fuel.

To overcome this challenge, two well-known machine learning techniques are compared: Feedforward 3-Layered Neural Network (2-5-2) with Levenberg-Marquardt algorithm and Adaptive Neuro-Fuzzy Inference Systems (ANFIS) with hybrid algorithm. The input datasets are the temperature of the generated steam and the steam production (mass flow rate). The data set is divided as follows: 70% of the data is used for training, 15% for validation and the last 15% is used for testing. The training set is used to train a machine learning model by exposing it to examples with known outcomes. The validation set is used to fine-tune the model parameters and to avoid overfitting, while the test set evaluates the model's performance on unseen data.

Error histograms and high correlation coefficients — which have been shown to be greater than 0.9 even for the test data sets — were used to evaluate the effectiveness of the presented machine learning techniques. In addition, thorough analyzes and justifications of the results obtained are provided, offering important new perspectives for the practical implementation of these methods. In order to predict operating costs, one must be able to determine the actual efficiency of steam boilers with a reasonable degree of accuracy.

REFERENCES

[1] Maddah, Heydar, Milad Sadeghzadeh, Mohammad Hossein Ahmadi, Ravinder Kumar, and Shahaboddin Shamshirband. 2019. "*Modeling and Efficiency Optimization of Steam Boilers*

by Employing Neural Networks and Response-Surface Method (RSM)" *Mathematics* 7, no. 7: 629. https://doi.org/10.3390/math7070629.
[2] Rusinowski H., Stanek W., *Neural modelling of steam boilers*, Energy Conversion and Management 48 (2007) 2802–2809, https://doi.org/10.1016/j.enconman.2007.06.040
[3] Smrekar J., Assadi M., Fast M., Kuštrin I., De S., *Development of artificial neural network model for a coal-fired boiler using real plant data,* Energy 34 (2009) 144–152, 10.1016/j.energy.2008.10.010
[4] Jovanović R., Sretenović R., Živković B., *Ensemble of various neural networks for prediction of heating energy consumption,* Energy and Buildings 94 (2015) 189-199, 10.1016/j.enbuild.2015.02.052

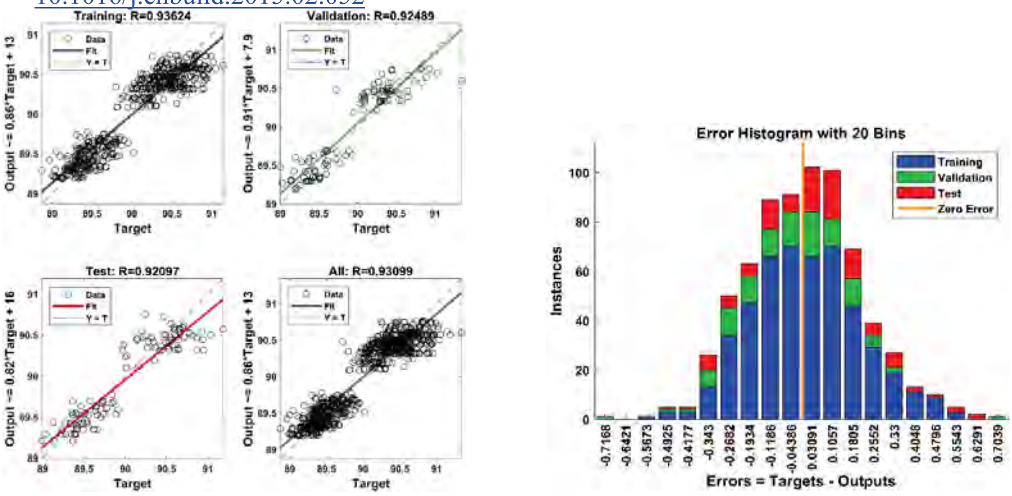

Figure 2. Neural network results: Regression plot and error histogram

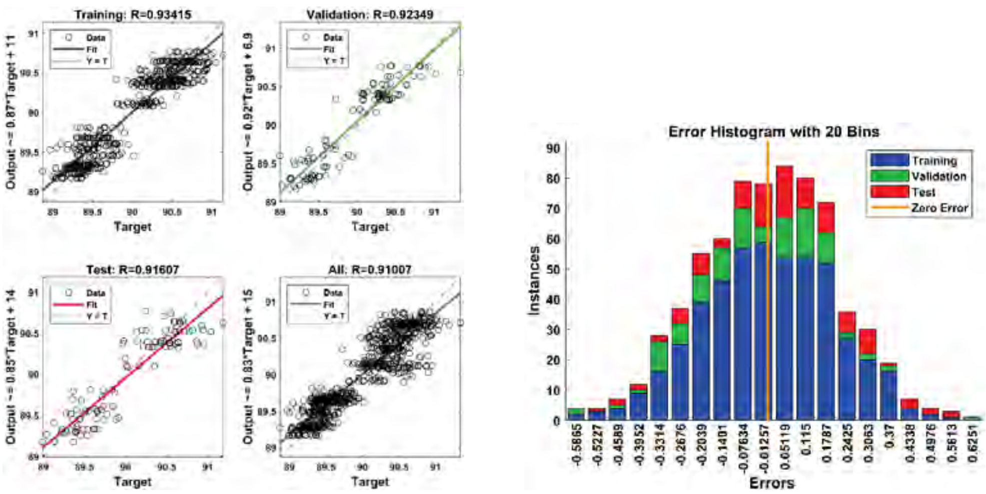

Figure 3. ANFIS results: Regression plot and error histogram

2nd International Conference on Mathematical
Modelling in Mechanics and Engineering
Mathematical Institute SANU, 12-14. September, 2024.

STRUCTURAL OPTIMIZATION OF A COMPOSITE STRUCTURE OF A VERTICAL TAKE-OFF AND LANDING (VTOL) UNMANNED AIR VEHICLE (UAV)

Milica Milić[1], Jelena Svorcan[2]

[1,2]*Faculty of Mechanical Engineering, University of Belgrade, 11000 Belgrade, Serbia*

[1]*mmilic@mas.bg.ac.rs*; [2]*jsvorcan@mas.bg.ac.rs*;

ORCID iD: [1]0000-0003-4505-6086; [2]0000-0002-6722-2711

Keywords: FEM, Composites, Optimization.

ABSTRACT

In order to design the optimal composite structure of a contemporary unmanned air vehicle (UAV) with vertical take-off and landing (VTOL) capability, a finite element (FE) model was developed and incorporated into an optimization cycle. Structure is assumed as a layered carbon-fiber shell, whose lay-up sequence (defined by layer thicknesses and orientations) is optimized by genetic algorithm (GA). As illustrated in Fig. 1 (left) the beam is constrained at places corresponding to connections with the wing, and forces are introduced at one end, simulating worst-case scenario (e.g. a sudden impact). The goal function is the minimal mass, whereas different constraints (such as failure criterion, or maximal strain) are imposed. The population is made up of 100 individuals, that are matched and crossed for 50 generations, until converging to the optimal solution, as represented in Fig. 1 (right). The proposed methodology can significantly facilitate and accelerate the design process of composite structures present in aerospace engineering.

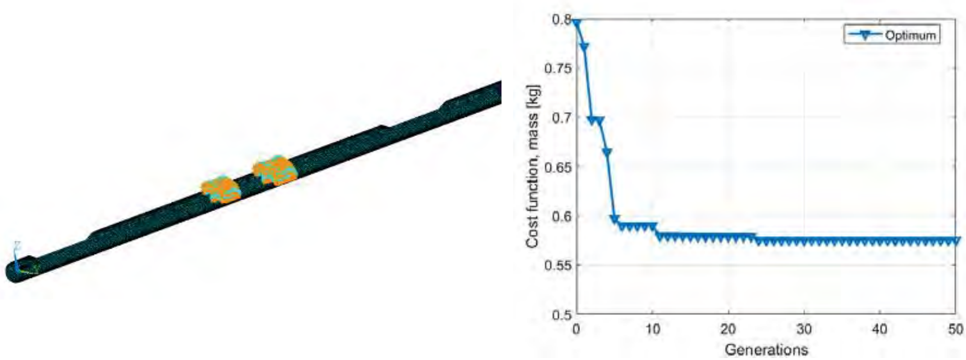

Figure 1. FE model (left), Convergence towards optimal solution (right)

REFERENCES

[1] Malott B, Averill RC, Goodman ED, Ding Y, Punch WF. Use of genetic algorithms for optimal design of laminated composite sandwich panels with bending–twisting coupling. AIAA J 1996;37:1874–81.

[2]Venkataraman S, Haftka TR. Optimization of Composite Panels - AReview. In: Proc of the 14th Annual Tech Conf of the American Society of Composites. Dayton, OH, September 1999. pp. 27–29.

2nd International Conference on Mathematical
Modelling in Mechanics and Engineering
Mathematical Institute SANU, 12-14. September, 2024.

EXPERIMENTAL VALIDATION OF THE FE MODEL OF A COMPOSITE BEAM

Milica Milić[1], Jelena Svorcan[2], Dejan Momčilović[3], Ivana Atanasovska[4]

[1,2]Faculty of Mechanical Engineering, University of Belgrade, 11000 Belgrade, Serbia

[3]Innovation Center of the Faculty of Mechanical Engineering, University of Belgrade, 11000 Belgrade, Serbia

[4]Mathematical Institute of the Serbian Academy of Sciences and Arts, 11000 Belgrade, Serbia

[1]mmilic@mas.bg.ac.rs; [2]jsvorcan@mas.bg.ac.rs; [3]dbmomcilovic@mas.bg.ac.rs; [4]iatanasovska@turing.mi.sanu.ac.rs

ORCID iD: [1]0000-0003-4505-6086; [2]0000-0002-6722-2711; [3]0000-0001-9728-6022; [4]0000-0002-3855-4207

Keywords: FEM, Composites, Experiment.

ABSTRACT

In order to design a composite beam of a contemporary unmanned air vehicle with vertical take-off and landing capability, a finite element (FE) model was developed. Structure is assumed as layered carbon-fiber shell, and is supposed to endure aerodynamic and gravitational loads. The composite beam was manufactured and experimentally tested in accordance with the expected operational load regimes (corresponding to 30%, 50%, 70% and 100% throttle). Static forces, simulating two thrust forces generated by propellers connected to electric engines and loads from the tail surfaces, were introduced as illustrated in Fig. 1 (left). Strain was measured at six locations distributed along the beam. A very good comparison between numerical and experimental results is achieved. Slight discrepancies can be attributed to manufacturing omissions, insufficient knowledge of mechanical properties of the laminas making-up the composite structure, and simplifications and idealizations of the numerical model.

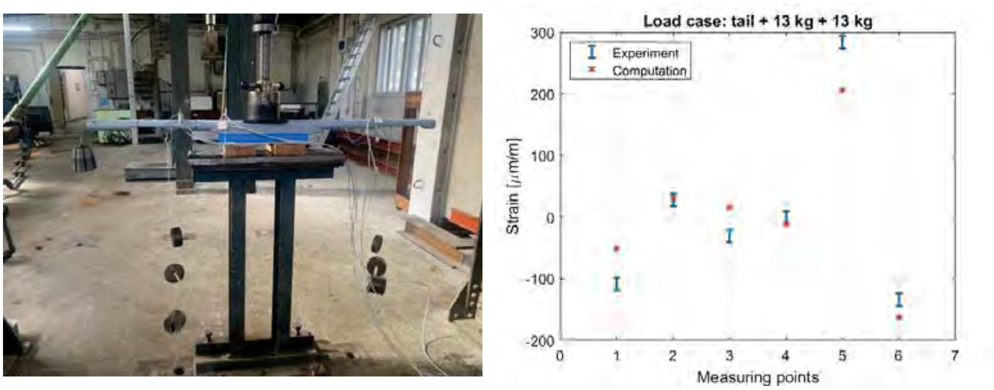

Figure 1. Experimental set-up (left), Obtained results (right)

REFERENCES

[1] Hashim S, Berggreen C, Tsouvalis N, et al. Fabrication, testing and analysis of steel/composite DLS adhesive joints. Ships Offshore Struc 2011; 6: 115−126. doi: 10.1080/17445302.2010.522019

[2] Momčilović D, Odanović Z, Mitrović R, et al. Failure analysis of hydraulic turbine shaft. Eng Fail Anal 2012; 20: 54−66. doi: 10.1016/j.engfailanal.2011.10.006

2nd International Conference on Mathematical
Modelling in Mechanics and Engineering
Mathematical Institute SANU, 12-14. September, 2024.

COMPUTATION MECHANICS IN SERBIA – HOMAGE TO MLADEN BERKOVIĆ

Aleksandar Sedmak[1]

[1] *Faculty of Mechanical Engineering, University of Belgrade, 11000 Belgrade, Serbia*
[1] *asedmak@mas.,bg.ac.rs*
ORCID iD: [1]0000-0002-5438-1895

Keywords: Computational Mechanics, Finite Element Method, Continuum Mechanics.

ABSTRACT

This paper describes development of computational mechanics, inevitably related to Prof. Dr. Mladen Berković (1936-1999). Due to his early efforts and achievements in 1970-ies, computational mechanics has been established in Serbia as sound scientific discipline, based on continuum mechanics and mathematical modelling of engineering problems by using the finite element method. His main contributions have been in solving linear and non-linear static and dynamic problems, especially thin plates and shells, as well as thermomechanical and fracture mechanics problems. His untimely death in 1999 prevent him from introducing the extended finite element method to simulate fatigue crack growth, which would have made the complete tool to solve all common structural engineering problems.

REFERENCES

[1] BerkoviC, M., (1975) GeneraL membane isoparametric elements, Proc. World Conf. Finite EIement Meth Structural Mech. Boumemouth
[2] Berković, M, (1977), "Membrane finite element" (in Serbian), doctoral thesis, University of Belgrade, Faculty of Mathematics.
[3] Berković, M, (1979), On the nonlinear transient analysis of the coupled thermomechanical phenomena, Computers and Structures, 10(1-2), 195-202 DOI 10.1016/0045-7949(79)90087-7
[4] In memory of Mladen Berković (1984), reprints from Proc. Int. Fracture Mechanics Summer Schools, Special Issue, Structural Integrity and Life, 4(2)

MANEUVERS FOR SELECTION A LANDING SITE WITH MINIMAL FUEL CONSUMPTION

O. Cherkasov[1], N. Orel[1]

[1] *Lomonosov Moscow State University, 119991 Moscow,Russia*

[1] oyuche@yandex.ru

ORCID iD: [1] 0000-0003-1435-1541

Keywords: Fuel consumption, Phase portrait, Quadratic drag.

ABSTRACT

When performing a landing site selection mission, the vehicle performs hovering and moving maneuvers at a constant altitude and hovering to inspect a potential destination. In [1], the problem was studied in a close formulation for the choosing of a landing site on the surface of the Moon. It was shown that the problem reduces to the Brachystochrone problem with restrictions on the angle of inclination of the trajectory.

The equation of motion are as follows: $\dot{x} = v$, $\dot{v} = c\mu - kv^2$, $\dot{\xi} = g\sqrt{1+\mu^2}$,

where x is the horizontal distance, v is the velocity of the vehicle, ξ is the fuel expenditures, μ is the thrust, c, k, g are constants. Initial and final conditions for variables are given except the value of $\xi(T)$. Control function is subjected to inequality $|\mu| \le \bar{\mu}$, where $\bar{\mu}$ is positive constant. The aim of the control is to minimize the value of $\xi(T)$ at a given final moment.

The Pontryagin maximum principle application allows to reduce the optimal control problem to a boundary value problem for a system of nonlinear differential equations. The research of the system is carried out by methods of qualitative analysis. The number of the extremal arcs with boundary and intermediate control and the sequence of these arcs are established. The methodology of the study using the phase portrait analysis and the analysis of the first integral was previously used in [2] for the Brachystochrone problem with constraints on the angle of inclination of the trajectory in a medium with resistance.

REFERENCES

[1] R.K. Cheng, D.A. Conrad, (1964) "Optimum translation and the brachistochrone", *Aerospace sciences meeting*, New York, January 20-22, pp.2845-2847.

[2] O.Yu. Cherkasov, N.V. Smirnova, (2022) "On the Brachistochrone problem with state constraints on the slope angle" *International Journal of Non-Linear Mechanics*, V.139.pp. 10.1016/j.ijnonlinmec.2021.103871.

2nd International Conference on Mathematical
Modelling in Mechanics and Engineering
Mathematical Institute SANU, 12-14. September, 2024.

IMPROVEMENT OF A PHYSICAL FIELD IN FEA BY APPLYING A SMOOTHING METHOD

Marija M. Rafailović[1], Miroslav M. Živković[2], Vladimir P. Milovanović[3], Jelena M. Živković[4] and Gordana R. Jovičić[5]

Faculty of Engineering, University of Kragujevac, 34000 Kragujevac, Serbia
[1]marija.rafailovic@kg.ac.rs; [2]zile@kg.ac.rs; [3]vladicka@kg.ac.rs; [4]jelena.zivkovic@kg.ac.rs; [5]gordana.jovicic@kg.ac.rs
ORCID iD: [1]0009-0001-2132-9249; [2]0000-0002-0752-6289; [3]0000-0003-3071-4728; [4]0000-0002-4398-7365; [5]0000-0002-9799-5555

Keywords: Finite element method, Extended finite element method, Strain smoothing, Smoothed finite element method (S-FEM), Strain-smoothed element (SSE) method, Low-order elements.

ABSTRACT

Due to its reliability and efficacy, the finite element method (FEM) is considered to be one of the most successful numerical methods, which is widely applied in science and engineering for structural analysis. Besides its wide application in engineering practice, the standard FEM has certain limitations. Linear triangular and tetrahedral finite elements result in very stiff behavior and a very low rate of convergence which stems from the constant stress field. In addition, the FEM model exhibits sensitivity to distorted isoparametric elements, during the use of which the Jacobian matrix is badly conditioned, leading to poor solutions and even the breakdown of the computation process. Moreover, considering the C^0 continuity of shape functions, the stress field across the element boundaries is discontinuous.

Great efforts have been invested to develop numerical strategies that may be used to overcome the abovementioned problems. In this manner, the smoothed finite element method (S-FEM) [1] is created, and it is used to modify the compatible strain field, by applying the gradient smoothing approach in the FEM, originally employed to stabilize the nodal integrated Galerkin meshfree methods [2]. Depending on the applied scheme for creating smoothing domains on top of the element mesh, a series of S-FEM methods has been developed [1]. Integration in the S-FEM methods has significantly been simplified by applying Gauss's divergence theorem, by means of which the domain integration is transformed into the boundary integration. The formulation of S-FEM methods requires the shape function values only, not their derivatives. Therefore, the Jacobian matrix is not needed, due to which isoparametric mapping is avoided. Significant properties of the S-FEM methods complete with their diverse application were discussed thoroughly in [1].

Bearing in mind all the advantages of the S-FEM methods, including the ones related to enhancing the convergence behaviour of 3-node triangular and 4-node tetrahedral finite elements [1], the only elements the mesh of which can be automatically generated even when it comes to extremely complex geometry, the S-FEM methods are expanded to solve problems involving discontinuous and singular physical fields. Coupling the strain smoothing with the partition of unity enrichment led to the formation of a series of new methods [3,4], which exploit the advantages of not only the S-FEM method, but the extended finite element method

(X-FEM) as well. By transforming the internal integration into the boundary integration, the subdivision of elements intersected by discontinuities was not found to be necessary [3]. In addition, since the derivatives of shape functions in the S-FEM method are replaced by the shape functions multiplied by the component of the outward unit vector on the boundary, the singular term integration $1/\sqrt{r}$, which occurs in the derivatives of near-tip enrichment functions (branch functions), is eliminated during the computation of the stiffness matrix in the fracture mechanics.

To improve the accuracy of 3-node triangular and 4-node tetrahedral finite elements, a new strain smoothing method, coined the strain-smoothed element (SSE) method [5], has recently been proposed. The strain field of such elements is constant, whereas by applying the S-FEM methods the piecewise constant strain fields are constructed through smoothing domains. In the context of the SSE method, a linear strain field is constructed in the elements themselves, by utilizing the constant strains of the adjacent elements. A significant characteristic of the SSE method is the lack of creation of special smoothing domains. Therefore, the standard FEM framework is maintained. To the best of the authors' knowledge, the SSE method has been successfully developed for the polygonal finite elements at last [6].

A numerical analysis was conducted within this particular research in order to provide a comparative presentation of the accuracy of linear and quadratic tetrahedral finite elements, implemented within the PAK and Nastran program packages, compared to the 4-node tetrahedral finite element of the corrected strain field [5]. The 3D problem, known as the Lame problem in the literature [5], was analyzed. The obtained results demonstrated that the corrected elements, even in case of extremely coarse mesh, were achieving a considerably higher level of accuracy compared to the linear elements. When comparing the quadratic and corrected tetrahedral finite elements, a slightly enhanced convergency of the quadratic element was observed. Since the shape functions of these two elements were not in the same range, the elements were described as the ones with various degrees of freedom, meaning that it was completely expected to see the quadratic element converging in a slightly faster manner towards the reference solution. The results of the program packages were well-aligned.

REFERENCES

[1] Zeng, W., Liu, G.R. (2018), "Smoothed Finite Element Methods (S-FEM): An Overview and Recent Developments," *Arch. Comput. Methods Eng.,* 25(2), pp. 397-435.

[2] Chen, J.S., Wu, C.T., Yoon, S., You, Y. (2001), "A stabilized conforming nodal integration for Galerkin mesh-free methods," *Int. J. Numer. Methods Eng.,* 50(2), pp. 435-466.

[3] Chen, L., Rabczuk, T., Bordas, S.P.A., Liu, G.R., Zeng, K.Y., Kerfriden, P. (2012), "Extended finite element method with edge-based strain smoothing (ESm-XFEM) for linear elastic crack growth," *Comput. Methods Appl. Mech. Eng.,* 209-212, pp. 250-265.

[4] Jiang, Y., Tay, T.E., Chen, L., Zhang, Y.W. (2015), "Extended finite element method coupled with face-based strain smoothing technique for three-dimensional fracture problems," *Int. J. Numer. Methods Eng.,* 102(13), pp. 1894-1916.

[5] Lee, C., Lee, P.S. (2018), "A new strain smoothing method for triangular and tetrahedral finite elements," *Comput. Methods Appl. Mech. Eng.,* 341, pp. 939-955.

[6] Jung, H., Lee, C., Lee, P.S. (2023), "Strain-smoothed polygonal finite elements," *Struct. Eng. Mech.,* 86(3), pp. 311-324.

2nd International Conference on Mathematical
Modelling in Mechanics and Engineering
Mathematical Institute SANU, 12-14. September, 2024.

PHASE-FIELD FATIGUE MODELING IN SHAPE MEMORY ALLOYS

Vladimir Lj. Dunić[1] and Miroslav M. Živković[1]

[1] *University of Kragujevac, Faculty of Engineering, 34000 Kragujevac, Serbia*

[1]dunic@kg.ac.rs; miroslav.zivkovic@kg.ac.rs

ORCID iD: [1]0000-0003-1648-1745; [2]0000-0002-0752-6289

Keywords: fatigue, phase-field modeling, shape memory alloys.

ABSTRACT

Shape Memory Alloys (SMA) are smart materials that can exhibit superelasticity and shape memory effects. The same alloy can show both responses depending on the environment's temperature. The superelasticity occurs at a temperature above the austenitic finish. In practical applications like actuators and sensors, superelasticity is mainly exploited where many cycles can be expected. The investigation of SMA device failure is essential for the application, especially for responsible parts such as coronary stents or actuators in airplanes.

Fatigue is the primary mechanism behind fracture occurrence in structures exposed to cyclic loading. This is particularly true for SMA devices operating in the superelasticity regime, which are subjected to several thousands of cycles. Cracks are initiated from micro-voids and micro-cracks in the material, and due to the repeated loading-unloading, the fracture occurs. This underscores the urgent need to address fatigue in SMA devices. Phase-field damage modeling (PFDM) can be a powerful tool in this regard, as it allows for the simulation of crack initiation, evolution, and propagation in various materials. SMA modeling, widely known in literature [1], offers promising solutions, with the Lagoudas model being one of the most popular constitutive models, modified and extended for application to large strain theory and thermo-mechanical coupling conditions by Dunić [2].

One of the recent papers [3] covers the subloop loading condition of SMA and damage, which increases mainly during elastic loading. In contrast, martensitic transformation does not increase it and can be neglected. As it is presented in that paper, the evolution law of the damage phase-field needs to be modified as follows [3]:

$$f\left(\bar{\alpha}\right)G_V\left[d-l_c^2\nabla^2 d\right]+g'\left(d\right)\psi=0, \tag{1}$$

where l_c is the characteristic length, d is the damage variable, $g'(d)$ is the derivative of the damage function, ψ is the strain energy density, and $f\left(\bar{\alpha}\right)$ is the fatigue function [3,4]:

$$f\left(\bar{\alpha}\right)=\begin{cases} 1 & \text{if} \quad \bar{\alpha}\le\alpha_T \\ \left(\dfrac{2\alpha_T}{\bar{\alpha}+\alpha_T}\right)^2 & \text{if} \quad \bar{\alpha}>\alpha_T \end{cases}. \tag{2}$$

In previous equation, α_T represents a value of fatigue history variable $\bar{\alpha}$, below which the fracture energy G_V remains unaffected [5]:

$$\alpha_T=\frac{G_V}{12}. \tag{3}$$

The fatigue history variable increases only during the loading and it can be computed as [3-5]:

$$ {}^{t+\Delta t}\bar{\alpha} = {}^{t}\bar{\alpha} + \int_{t}^{t+\Delta t} H\left(\alpha\dot{\alpha}\right)\left|\dot{\alpha}\right| d\tau \tag{4} $$

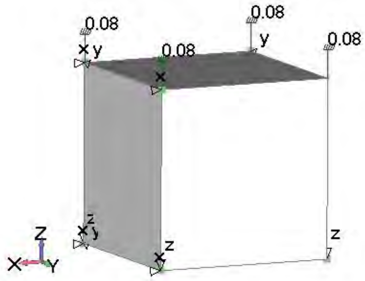

Fig. 1 Boundary and loading conditions – Unit cube

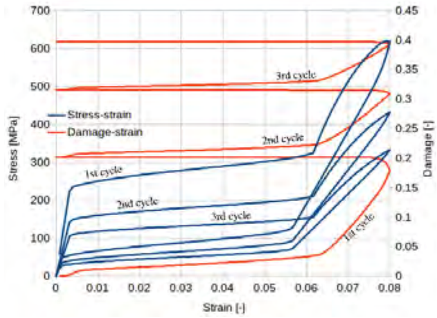

Fig. 2 Stress vs. Strain and Damage vs. Strain for three loading – unloading cycles

As shown in Fig. 2, the strong influence of damage increase can be noticed. The stress-strain curve decreases after each cycle, while the damage value increases in the loading branch and is kept constant during unloading. The presented example is simulated using general material constants from the literature [1] to show the possibility of simulating phenomena.

The research was supported by the Science Fund of the Republic of Serbia, #GRANT No 7475, Prediction of damage evolution in engineering structures - PROMINENT and by the University of Kragujevac project for young scientist Developing the procedure for damage simulation in metallic structures due to cyclic loading - DEEDS.

REFERENCES

[1] Lagoudas D. (2010) “Shape Memory Alloys: Modeling and Engineering Applications,” *Springer*

[2] Dunić V. (2015) “Development and implementation of thermo-mechanical constitutive model for numerical analysis of shape memory alloys,” *PhD thesis, Faculty of Engineering, University of Kragujevac, Serbia*

[3] Dunić V., Matsui R., Takeda K., Živković M. (2024) “Phase-Field Damage Simulation of Subloop Loading in TiNi SMA,” *International Journal of Damage Mechanics*, doi:10.1177/10567895241245859

[4] Carrara P., Ambati M., Alessi R., Lorenzis, L.D. (2020) “A framework to model the fatigue behavior of brittle materials based on a variational phase-field approach,” *Computer Methods in Applied Mechanics and Engineering*, 361:112731

[5] Simoes M., Martínez-Pañeda E. (2021) Phase field modelling of fracture and fatigue in shape memory alloys,” *Computer Methods in Applied Mechanics and Engineering*, 373:113504

2nd International Conference on Mathematical
Modelling in Mechanics and Engineering
Mathematical Institute SANU, 12-14. September, 2024.

DESIGN AND DEVELOPMENT OF AN AUTONOMOUS ROBOT FOR LINEMAN ASSISTANCE

Uttam Kumar[1], Hemant Raj Singh[2] and Krishna Kant Pandey[3,*]

[1] *School of Engineering Ajeenkya D.Y Patil University, Pune, India*

[2]*Mechanical Engineering, Manipal University Jaipur, Jaipur, India 303007*
[3]*Mechatronics Engineering, Manipal University Jaipur, Jaipur, India 303007*

[1]*uttam.kumar@adypu.edu.in*; [2]*hemant.singh@jaipur.manipal.edu*; [3,*]*kknitrkl@yahoo.in*
ORCID iD: [1]0000-0002-7591-9754; [2]0000-0002-1662-4411; [3]0000-0002-5669-5951

Keywords: Lineman Assistance, Robot, PID Control, DIP based Algorithm.

ABSTRACT

Workers engaged in outdoor maintenance and inspection, tasked with identifying and reporting mechanical failures in high-tension electrical wires carrying lethal voltages, frequently encounter high-risk factors that pose physical or electrical health hazards. This requires regular or semi-regular maintenance cycles that cost a lot of money and time. The most widely used means to transmit electricity is through transmission lines. These power lines are susceptible to adverse weather conditions in various locations. Workers climb the poles and manually check if any faults occur in power lines, and this makes their lives riskier. It also interrupts the power supply. A robot-based inspection makes this task easier, more efficient, foolproof, and safe. By operating in both day and night cycles, the robot reduces maintenance time by 6 months. The robot will detect any breakdowns, transmit the breakdown parameters to the store, and process them on the cloud with the assistance of the Digital Image Processing (DIP) based algorithm. A comparative study between published work with proposed work has been projected. Based on comparative study results are depicted. The results of the proposed work have less error as compared to existing work and it is recorded as less than 8%. Increase in efficiency of the proposed system has been increased by 20%.

REFERENCES

[1] A. G. Bitancor et al., "*Distribution Line Inspection Using a Microcontroller Based Quad-Copter Drone with an Integrated Non-contact Voltage Detector and Infrared Thermal Temperature Sensor for Thermal Imaging*," 2023 15th International Conference on Computer and Automation Engineering (ICCAE), Sydney, Australia, 2023, pp. 204-208, doi: 10.1109/ICCAE56788.2023.10111366.

[2] A. S. Surya, B. B. S. D. A. Harsono, H. B. Tambunan and K. G. H. Mangunkusumo, "*Review of Aerial Vehicle Technology for Transmission Line Inspection in Indonesia*," 2020 10th Electrical Power, Electronics, Communications, Controls and Informatics Seminar (EECCIS), Malang, Indonesia, 2020, pp. 49-54, doi: 10.1109/EECCIS49483.2020.9263423.

[3] J. Wang, Y. Su, L. Shen and K. Li, "*Real-Time Automatic Route Generation for Unmanned Aerial Vehicle Based Patrol Inspection in Power Distribution System*," 2022 IEEE 6th Advanced Information Technology, Electronic and Automation Control Conference (IAEAC), Beijing, China, 2022, pp. 1584-1588, doi: 10.1109/IAEAC54830.2022.9929755.

[4] D. -Q. Chen, X. -H. Guo, P. Huang and F. -H. Li, "*Safety Distance Analysis of 500kV Transmission Line Tower UAV Patrol Inspection*," in IEEE Letters on Electromagnetic Compatibility Practice and Applications, vol. 2, no. 4, pp. 124-128, Dec. 2020, doi: 10.1109/LEMCPA.2020.3040878.

BUILDING INFORMATION MODELING'S (BIM) INTEGRATION WITH SUSTAINABLE BUILDING DESIGN

Karam I. ABDULAMEER[1]

[1]*General Company for Electric Power Production / Central Region, Ministry of Electricity, Baghdad, Iraq*

[1]karam.abdulameer@gmail.com

Keywords: Sustainable Building, Quality management, Building Information Modeling (BIM).

ABSTRACT

This paper presents an improving quality management system for sustainable modern building integrating with BIM (building information modelling). The approach to the environmental quality of buildings, initiated since the 1990s by the actors of the construction sector, is currently undergoing a paradigm shift towards an assessment of the building's environmental performance. Due to global environmental concerns, increasing sustainable design has become a main building design goal in recent years. Sustainable development is even more urgent in the light of global climate change. This thesis aims to examine the contributions that building information modelling (BIM) can make to the production of sustainable building designs. Mainly, the case study consists of transforming the energy resource based on coal to another resource of renewable energy like photovoltaic with heat pump which is not only economic but also protects the environment. Therefore, a BIM tool is needed, Revit and Archicad Structures were selected. BIM is found to be ideally suited to the delivery of information needed for improved design and building performance. The two most significant benefits of BIM for sustainable building design are: integrated project delivery (IPD) and design optimization. However, there are also barriers to adopting BIM for sustainable design. Indeed, to continue to be more ambitious in my project, it is now necessary to examine the entire Building cycle and other environmental and health issues. There are four parts in this paper:

1- The first part of this research is to conduct a field survey, which concerns the acceptance of the design sector worldwide to the principles of sustainability in buildings and quality management system in sustainable buildings design.

2- The second part is to study the effect of application of sustainable energy technologies system in buildings; in this case, we mentioned techniques of application of the sustainable building design with BIM in projects.

3- In the third part, we proposed a new approach for integrating sustainable building design with building information modelling (BIM) is proposed which is presented as a case study.

4- In the fourth part the results by integrating sustainable building design with BIM are included.

REFERENCES

[1] Salman Azhar, Wade A. Carlton, Darren Qlsen, Irtishad Ahmed (2011). Building information modelling for sustainable design and LEED rating analysis. Automation in construction. Volume 20. Issue 2, pages 217-224.

[2] Jalaei, F., & Jrade, A. (2014). Integrating Building Information Modeling (BIM) and Energy Analysis Tools with Green Building Certification System to Conceptually Design Sustainable Buildings. Journal of Information Technology in Construction (ITcon), 19(29), 494-519.

[3] Narayanan, S. (2015). Principles of Sustainable Building Design. In Green Building with Concrete: Sustainable Design and Construction, Second Edition (pp. 35-88). CRC Press.

[4] Plank, R. (2008). The principles of sustainable construction. The IES Journal Part A: Civil & Structural Engineering, 1(4), 301-307.

[5] Burnett, J. (2007). Sustainability and sustainable buildings. HKIE Transactions, 14(3), 1-9.

[6] Diesendorf, M. (2000). Sustainability and sustainable development. Sustainability: The corporate challenge of the 21st century, 2, 19-37.

[7] Csefalvay, E., Akien, G. R., Qi, L., & Horváth, I. T. (2015). Definition and application of ethanol equivalent: sustainability performance metrics for biomass conversion to carbon-based fuels and chemicals. Catalysis Today, 239, 50-55.

[8] Griggs, D., Stafford-Smith, M., Gaffney, O,Rockstrom, J, Ohman, M. C., Shyamsundar, P& Noble, I. (2013). Policy: Sustainable development goals for people and planet. Journal: Nature, 495(7441), 305-307.

[9] Dalton, Jennifer; and Fossum, Ernest, (2005), "INL Green Building Strategy", Report, Prepared for the U.S. Department of Energy under Department of Energy Idaho Operations Office, USA.

[10] Kawneer. Kimberly-Clark. Kohler. Kyocera, (2011). Green Building Education Services – GBES. Green Building and LEED fundamentals, Revision 1.29, December 19, (2011).

[11] Cole, R. J. (2005). Building environmental assessment methods: redefining intentions and roles. Building Research & Information, 33(5), 455-467.

2nd International Conference on Mathematical
Modelling in Mechanics and Engineering
Mathematical Institute SANU, 12-14. September, 2024.

MODELLING OF NON-NEWTONIAN INTERSTITIAL FLUID FLOW THROUGH LACUNO-CANALICULAR SYSTEM OF A BONE

Rakesh Kumar[1], Siddhanth Das[2] and Santosh Patil[3*]

[1,2,3]*Deparment of Mechanical Engineering, Manipal University Jaipur, Jaipur, 303007Rajasthan, India*

[*]*Corresponding Author:* santosh045@gmail.com

Keywords: Interstitial Fluid motion, Lacunar canalicular system, Osteoporosis, Axial loading, Streamlines, Jeffery fluid

ABSTRACT

Osteoporotic bone loss is a serious health concern for the clinicians as it changes the bone architecture and also reduces the bone strength which promotes bone fractures risk. Physical exercise such as normal/daily stress/strain and interstitial fluid flow within the bone tissue is found beneficial in inhibiting osteoporotic bone loss. Interstitial fluid flow through the lacuno-canalicular channel acts as a primary stimulus for cortical bone adaptation. In vivo studies have shown that mechanical loading in the form physical exercise improves the interstitial fluid flow within the LCS of bone tissue. Nevertheless, the exact mechanism which enhances the fluid motion essential for osteogenesis in response to mechanical loading remains unclear. Accordingly, present study attempts to compute the uniaxial loading induced non-Newtonian canalicular fluid flow in a complex 2D lacunar-canalicular channel. Present study also considers canalicular fluid as a Jeffery fluid model, that can easily be reduced to Newtonian fluid as a special case. Result shows that the mechanical loading modulates the canalicular fluid flow, wall shear stress and streamline in bone tissue. Interstitial fluid flow and wall shear stress increases with increase in non-dimensional frequency and non-Newtonian parameter (Jeffery fluid parameters). The outcomes of the present study may provide new insights in field of orthopedics by improving the understanding of bone physiology and for preventing or treating bone loss related conditions.

REFERENCES

[1] Kumar, Rakesh. "Computer model of non-Newtonian canalicular fluid flow in lacunar canalicular system of bone tissue." Computer Methods in Biomechanics and Biomedical Engineering (2024): 1-15.
[2] Fan L, Pei S, Lucas Lu X, Wang L. A multiscale 3D finite element analysis of fluid/solute transport in mechanically loaded bone. Bone Research 2016;4:16032.
[3] Sansalone V, Kaiser J, Naili S, Lemaire T. Interstitial fluid flow within bone canaliculi and electro-chemo-mechanical features of the canalicular milieu. Biomechanics and Modeling in Mechanobiology 2013;12:533–53

ON THE LIMITATIONS OF BEAM THEORIES TO PREDICT THE TRANSVERSE DEFLECTION AND VIBRATION OF STEPPED SHAFTS

V. Roda-Casanova[1*], R. Sadik[2], J.L. Iserte-Vilar[3] and F.J. Andrés-Esperanza[4]

[1]*Department of Mechanical Engineering and Construction, Universitat Jaume I, Spain*

*vroda@uji.es

ORCID iD:[*]0000-0002-6430-6119

Keywords: Timoshenko beam theory, Euler-Bernoulli beam theory, deflection, vibration.

ABSTRACT

Euler-Bernoulli and Timoshenko beam theories are widely used in machine design to predict the transverse deflection and vibration of axles and shafts. The applicability of these beam theories depends on the fulfillment of a set of assumptions, which are mainly related to the displacement field of the cross section of the beams: Timoshenko beam theory assumes that cross sections remain plane throughout the deformation of the beam, while Euler-Bernoulli beam theory assumes that cross sections remain plane and perpendicular to the neutral axis of the deformed beam.

Both Timoshenko and Euler-Bernoulli beam theories have proven valid to predict the transverse deflection and vibration of shafts that can be modeled as slender prismatic beams. In contrast, for short prismatic shafts that cannot be modeled as slender beams, one can only rely on Timoshenko beam theory, because in these cases the assumptions of Euler-Bernoulli beam theory are not fulfilled, and it could lead to inaccurate results.

There are some other scenarios where the assumptions of these beam theories are not fulfilled. One of them is the presence of abrupt changes of section along the shafts modeled as beams, because the cross section of the deformed beam does not remain plane nor perpendicular to its neutral axis in the vicinity of an abrupt change of section. Thus, in these cases, applying any of these theories to predict the transverse deflection or vibration of the shafts will yield inaccurate results, which may lead to premature failures or invalid machine designs.

Unfortunately, machine shafts often present these abrupt changes of sections, either because of the geometrical design of the shafts (stepped shafts) or because of the presence of gears, pulleys, etc. assembled over them. For this reason, in this work the limitations of the beam theories to predict transverse deflection and vibration of stepped shafts are explored, aiming to find simple ways to overcome them.

REFERENCES

[1] Sanchez-Marin, F. (2018), "A new analytical model to predict the transversal deflection under load of stepped shafts," *International Journal of Mechanical Sciences,* 146-177, pp. 91-104.

2nd International Conference on Mathematical
Modelling in Mechanics and Engineering
Mathematical Institute SANU, 12-14. September, 2024.

DYNAMIC CHARACTERIZATION OF A FIBRE-REINFORCED HIGH-STRENGTH CONCRETE PEDESTRIAN FOOTBRIDGE BASED ON NUMERICAL-EXPERIMENTAL TECHNIQUES

R. Sadik, C. Rodrigo-Vilar, V. Roda-Casanova*, M.D. Martínez-Rodrigo, J.L. Sancho-Bru and D. Hernandez-Figueirido

Department of Mechanical Engineering and Construction, Universitat Jaume I, Spain

*vroda@uji.es

ORCID iD:*0000-0002-6430-6119

Keywords: Footbridges, vibration, finite element modelling.

ABSTRACT

Pedestrian bridges are rather slender and light structures susceptible to experience important vibrations under serviceability conditions. This contribution focuses on the dynamic characterization and numerical modelling of a recently opened pedestrian bridge made of ultra-high strength concrete. Due to the mechanical characteristics of this rather new material, the footbridge is slender and its performance on the long term is not well known. Two experimental programs are conducted on the bridge to determine its main modal parameters. The first natural frequencies, modes and associated damping are identified from ambient vibration and hammer testing, applying operational and experimental modal analysis techniques. On the other hand, a detailed finite element model of the footbridge is implemented and updated from the dynamic identified properties. The vibration serviceability of the structure is assessed based on current codes. Also, from the numerical-experimental comparison, preliminary conclusions are extracted related to the general state of the footbridge and the behavior of the boundary conditions for different amplitude levels.

2nd International Conference on Mathematical
Modelling in Mechanics and Engineering
Mathematical Institute SANU, 12-14. September, 2024.

TENSOR CALCULUS APPLIED IN CLASSICAL MECHANICS

Nenad Vesić

Mathematical Institute of the Serbian Academy of Sciences and Arts, 11000 Belgrade, Serbia

n.o.vesic@outlook.com

ORCID iD: 0000-0002-7598-9058

Keywords: Riemannian space, perturbations, infinitesimal deformations, invariants

ABSTRACT

This discussion is composed of an introduction and two sections. The paper presents a tensorial approach to computations in classical mechanics.

The introduction provides definitions of tensors in index and operator forms. The first section of the paper is devoted to matrices and their representation in tensorial form. Unlike classical mechanics, where investigations are based on matrices and matrix multiplication and addition, the tensor calculus presented in this paper focuses on determining individual elements of the mentioned matrices. Furthermore, in this section, we demonstrate the matrix representation of indexed quantities with more than two indices. All these quantities are transformed based on the transformation of initial quantities. Subsequently, laws of transformation of various derived quantities are obtained. In these transformation laws, we will illustrate special cases in which the products of two or more quantities determining the transformation are vanished.

In the second part of the paper, we will rely on the invariants determined by transformations of geometric objects used in classical mechanics. The invariants derived based on these transformation laws will be obtained in this part of the paper. In obtaining the invariants, we will use the methodology presented in the work (Vesic, 2020), where, from invariants obtained based on the transformation laws of simpler geometric objects, invariants based on the transformation laws of more complex geometric objects are derived. Following the definitions presented in (J. E. Marsden, T. J. R. Hughes, 1983), these invariants will, in special cases - characteristic of classical mechanics - correspond to the laws of conservation.

The Ministry of Science, Technological Development, and Innovation of the Government of the Republic of Serbia, through the Mathematical Institute of the Serbian Academy of Sciences and Arts, has financially supported this work.

EXPERIMENTAL AND NUMERICAL WEAR ANALYSIS OF POLYMER GEARS

Puneeth M. L.[1], Santosh Patil[2], Deepankar Saini[3], Mohit Jain[4] and Daing Nafiz[5]

[1]*Lead engineer, General Electric, 560066, Bengaluru, India*
[2,3,4]*Department of Mechanical Engineering, Manipal University Jaipur, Jaipur, 30300, Rajasthan, India*

[5]*Faculty of Mechanical & Automotive Engineering, University Malaysia Pahang, 26600 Pekan, Pahang, Malaysia*

[1]*geardyn.1@gmail.com; [2]santosh045@gmail.com; [3]deepankarsaini07@gmail.com; [4]daingnafiz@umpsa.edu.my*

Keywords: Asymmetric gears, Dynamic contact, Explicit analysis, LSDYNA, Polymer, Nylon6, Wear.

ABSTRACT

Polymer gears are increasingly being used in various industries due to their unique properties such as low noise, corrosion resistance, and high strength-to-weight ratio. However, one of the major concerns with the use of polymer gears is their wear behavior, which can significantly affect their performance and service life. Ke Feng [1] shows promise for identifying and evaluating gear wear is vibration-based gear wear monitoring. While, M Karimpour [2] study showed polymeric gears are less rigid than metallic gears, they behave differently kinematically. Larger tooth deflections and longer contact areas result from this, and they can contribute to excessive wear, early contact, and higher bending and contact stresses. Ye Zhang [3] examined the production of nylon polymer gears using 3D printing. Out of the five 3D printing materials examined, Nylon 618 showed the best wear performance, according to the study. Additionally, the study discovered that the wear behavior of injection-molded and 3D printed gears differs. Jadwiga Pisula [4] examined the wear resistance of spur gears constructed from thermoplastic materials using additive manufacturing techniques. According to the study, PEEK, ABS M-30, and Ultem 9085 were the materials with the highest wear resistance. The operating temperature had an impact on the gears' wear resistance as well; the maximum wear happened at the highest temperature. Futher, M.L. Puneeth [5] provides research on the involute asymmetric gear pair's dynamic contact behavior. Analysis is done on the impact of the pressure angle was noticed to get changed on the driving side. The gear teeth in the study are generated using MATLAB, and the dynamic analysis is carried out using LS-DYNA. Therefore, wear analysis of polymer gears is crucial for their design and optimization. This study presents an experimental and numerical investigation of the wear behavior of polymer gears under different operating conditions. The experimental setup involved testing of polymer gears in a specially designed test rig to simulate actual operating conditions. In addition to the experimental study, a numerical simulation using Finite Element Analysis (FEA) was also performed to understand the wear behavior of polymer gears. The numerical method involves using finite element analysis to simulate the gear contact and wear behavior. The simulation model is validated using experimental data, and the wear behavior is analyzed using wear rate, contact pressure, and contact stress. The results show that the wear rate increases with increasing load and speed,

while decreasing with increasing temperature. The wear mechanisms include abrasion, adhesion, and fatigue. The numerical results show good agreement with the experimental data, indicating that finite element analysis can be a reliable method for predicting the wear behavior of polymer gears. The study provides insights into the wear behavior of polymer gears and can aid in the design of more durable and reliable polymer gear systems. Overall, the study provides insights into the wear behavior of polymer gears and can be used to optimize their design for improved performance and longer service life. The combination of experimental and numerical methods offers a comprehensive understanding of the wear behavior of polymer gears under different operating conditions, which can help in the development of reliable polymer gears for various applications. The findings of the study highlight that the performance of gear pairs is influenced by factors such as applied load, gear geometry, and material properties. The observed deformation, weight loss, temperature difference, and debris formation indicate the dynamic behavior of gears under different conditions. Further research is necessary to gain a deeper understanding of how these factors interact and impact the overall performance and durability of gear pairs. Such knowledge can contribute to the improvement of gear design, material selection, and optimization of gear systems in various applications.

REFERENCES

[1] Feng, Ke & Ji, J.C. & Ni, Qing & Beer, Michael. (2023). A review of vibration-based gear wear monitoring and prediction techniques. Mechanical Systems and Signal Processing. 182. 109605. 10.1016/j.ymssp.2022.109605.

[2] Karimpour, Morad & Dearn, Karl & Walton, D. (2010). A kinematic analysis of meshing polymer gear teeth. Proceedings of The Institution of Mechanical Engineers Part L-journal of Materials-design and Applications - PROC INST MECH ENG L-J MATER. 224. 101-115. 10.1243/14644207JMDA315.

[3] Zhang, ye & Mao, Ken & Leigh, Simon & Shah, Akeel & Chao, Zhiming & Ma, Guotao. (2020). A parametric study of 3D printed polymer gears. The International Journal of Advanced Manufacturing Technology. 107. 1-12. 10.1007/s00170-020-05270-5.

[4] Pisula, Jadwiga & Budzik, Grzegorz & Turek, Paweł & Cieplak, Mariusz. (2021). An Analysis of Polymer Gear Wear in a Spur Gear Train Made Using FDM and FFF Methods Based on Tooth Surface Topography Assessment. Polymers. 13. 1649. 10.3390/polym13101649.

[5] ML, Puneeth & Goud, Mallesh. (2021). Dynamic contact behavior of asymmetric spur gear. Materials Today: Proceedings. 44. 10.1016/j.matpr.2020.12.125.

ANALYSIS OF TENSILE AND BUCKLING BEHAVIOUR OF CARBON/BASALT EPOXY COMPOSITE LAMINATES WITH DIFFERENT HOLE ARRANGEMENTS

Santosh Patil[1*], P. S. Shivakumar Gouda[2], Vinayak S. Uppin[2] and Ashu Yadav[1]

[1]*Department of Mechanical Engineering, Manipal University Jaipur, Jaipur, 30300, Rajasthan, India*

[2]*Research Center, Department of Mechanical Engineering, SDM College of Engineering & Technology,*
Dharwad, Visvesvaraya Technological University, Belagavi, Karnataka, India.

[1,*]santosh045@gmail.com

Keywords: Carbon fiber, Basalt fiber, Hole arrangement, Tensile, Buckling, Stacking.

ABSTRACT

Fiber Reinforced composites acquire extensive utilization across industries such as Automotive, Aerospace, Civil engineering, and other crucial research areas. The favorable attributes, such as a high strength-to-weight and stiffness ratio, make them the preferred choice for numerous aircraft structural components, including the cockpit, wings, and empennage etc. However, it's worth noting that the drilled holes used for composite joints represent a significant vulnerability and are a primary cause of structural failure in aircraft structures. Numerous experiments have demonstrated the sensitivity of FRP components to such holes and cutouts, resulting in noticeable strength decrements [1-5]. Hence, it is imperative to consider the sensitivity towards holes/cutouts and the notched strength of FRP components as crucial parameters in the design process. The present study focuses on the effect of hole(s) arrangement and stacking sequence on the tensile and bucking behavior of carbon/basalt epoxy composite laminates through experimental tests. The composite laminates were developed (as shown in Figure 1) using hand layup technique and tensile and buckling tests were performed following ASTM standards.

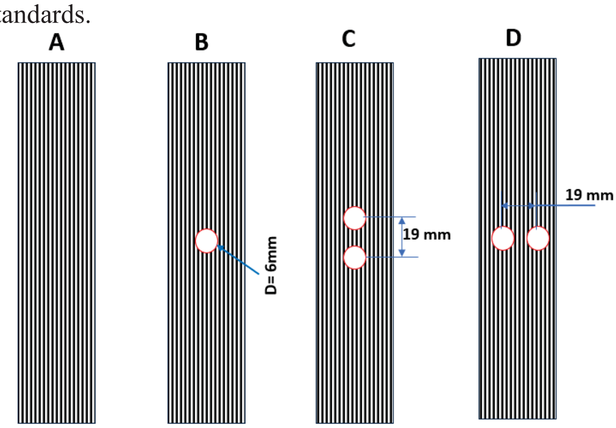

Figure 1. Different hole configuration (a) No-hole (NH) (b) One hole(1H) (c) Two horizontal holes (TB) (d) Two side by side holes (SBS)

Through these tests, it was observed that the position of hole and stacking sequence has a significant effect on tensile and buckling behavior in composite laminates. However, in two-hole arrangement particularly for side by side and top and bottom, in which top- and bottom-hole arrangement has revealed a better tensile strength but in case of buckling side by side hole arrangement gives better buckling resistance. Hence a proper combination and as per the load type the stacking of fiber and hole arrangement are to be proposed. Further, the SEM results presented the failure type under tensile and buckling loading, thus providing the surface morphology of the laminate failure.

REFERENCES

[1] Gupta, S., Pal, S., & Ray, B. C. (2023). An overview of mechanical properties and failure mechanism of FRP laminates with hole/cutout. Journal of Applied Polymer Science, 140(20), e53862.

[2] K. Hadi, B., & K. Rofa, B. (2018). Experimental tensile strength analysis of woven-glass/epoxy composite plates with central circular hole. In Journal of Physics: Conference Series (Vol. 1005, No. 1, p. 012001). IOP Publishing.

[3] Shaari, N., Wahab, M. A., Shaari, N. S., & Jumahat, A. (2021). Unhole and open hole tensile properties of hybrid Kevlar/glass fiber polymer composites with different stacking sequence. Materials Today: Proceedings, 46, 1595-1599.

[4] Ram, T. S., & Kumar, A. Influence of hole-hole distance and orientation on strength of composite laminae.

[5] Eugene, D. J., Russel, K., Wen, S. C., & Selvaraj, S. (2009). Strength of composite laminate with multiple holes. University of Texas at Arlington, The Boeing Company, 1-9.

2nd International Conference on Mathematical
Modelling in Mechanics and Engineering
Mathematical Institute SANU, 12-14. September, 2024.

OPTIMIZATION OF AN IMPELLER BASED ON STRENGTH ASPECTS

Szilveszter Tóth[1]

[1]*eCon Engineering Kft., 1163 Budapest, Hungary*
[1]szilveszter.toth@econengineering.com

Keywords: Optimization, Mechanics, Pareto front, Ansys, optiSLang.

ABSTRACT

Optimization within the context of finite element modeling (FEM) is indispensable for several compelling reasons. It serves as a means to enhance the performance and efficiency of engineered structures and processes by systematically refining design parameters, such as material properties, geometric configurations, and loading conditions. Present work introduces a multi-objective geometry optimization with which there was possible to reach significant stress reduction while the mass and inertia moment's limits were satisfied.

INTRODUCTON

The subject of present study is an impeller that works in a cooling system, installed in a centrifugal turbo. The shape and the blade angles were designed up-front and served as fixed geometrical boundary conditions for this problem. It means that only the backside profile could be modified. The impeller operates under very high rotational speed during the turning on process that served as the dominant load on the Finite element representation. (68 000 [rpm]) Because of that very high stress values appeared on bottom surfaces of the impeller's blades and in the hole. [Figure 1] In order to avoid the high stress values on the blades, increasing the flange thickness was a sensible option. However, it causes an increase in mass leading to higher stress utilization in the hole as well. Thus, it was necessary to apply a multi-objective optimization to minimize both of the high stress values.

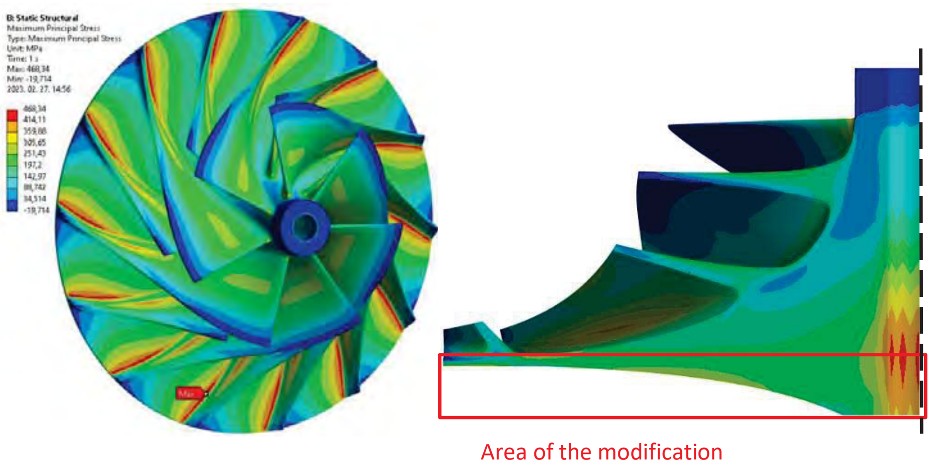

Figure 1: Areas of the high stress values

PARAMETERS OF THE SYSTEM AND THE CONSTRAINT EQUATION

Regarding the height two distinct dimensions were specified to control the profile shape in direction Z. The surface of the backplate was generated by a spline curve. (rotation around the axis Z) This spline has two control points with which it was possible to modify the shape of the spline. All in all, there were created five different parameters to describe the shape of the backside which are the following. [Figure 2]

$p1$: Thickness of the flange
$p2$: Height of the backside
$p3$: Spline 1st controlpoint x coordinate
$p4$: Spline 2nd controlpoint z coordinate
$p5$: Spline 2nd controlpoint x coordinate

The height and the global diameter of the backplate were always normalized with their own actual size. Thus, the parameter $p3$,$p4$,$p5$ coordinate z of the first can only have values between 0 and 1. The control point (CP1) must be 0 because of the tangential connection. One more constraint equation was necessary to provide CP1 always positioned above CP2 which is: $p5 \leq p3(1-p4)$.

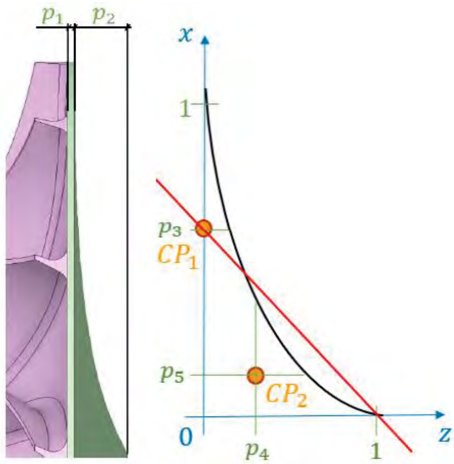

Figure 2: Visualization of Parameters

RESULTS

The entire simulation project was developed within the Ansys framework. To facilitate geometry modifications, a dedicated script was employed in SpaceClaim, enabling dynamic adjustments based on parameter values. For the optimization phase, the optiSLang environment was utilized. Within this environment, parameter ranges, two objective functions, and a constraint equation to control parameter relationships were defined. An evolutionary algorithm was chosen as the optimization method due to its ability to comprehensively map the design space, rendering initial parameter values inconsequential to the solution. Upon completion of the optimization process, results were presented via a 2D diagram, illustrating the formation of the Pareto front that highlights the set of optimum solutions in terms of both objectives. Subsequently, the design chosen for implementation is as follows. [Table 1]

	Original Design	Optimized Design
Hole Max Principal Stress [MPa]	376.5	365.2
Blades Max Principal Stress [MPa]	468.3	369.9

Table 1: Comparison the stress values between the original and the optimized designs

As shown in the hole area there was possible to decrease the stress by 11.3 MPa and significant improvement was observed at the blades, with an almost 100 MPa reduction in stress level.

POROSITY OF PERVIOUS CONCRETE FLAGS – PREDICTION AND MEASUREMENTS

Marina M. Škondrić[1], Ognjen R. Govedarica[2], Aleksandar R. Savić[3] Branislava M. Lekić[4]

[1,2,3,4]*University of Belgrade, Faculty of Civil Engineering, 11000 Belgrade, Serbia*
[1]amarina@grf.bg.ac.rs; [2]ogovedarica@grf.bg.ac.rs; [3]sasha@grf.bg.ac.rs; [4]blekic@grf.bg.ac.rs
ORCID iD: [1]0000-0002-8911-5028; [2]0000-0002-4995-3932; [3]0000-0002-1777-6775; [4]0000-0002-3360-2118

Keywords: pervious concrete, porosity, ultrasonic pulse velocity.

ABSTRACT

Pervious (porous) concrete differentiates from ordinary concrete by the lack of the fine aggregate fraction, which makes it permeable for water, due to the formation of larger open pores. It can be produced on site, or as prefabricated pervious concrete flags. It's main application is in paving the pedestrian and bicycle paths, and when possible parking lots.

The pore diameter in pervious concrete, which is sufficient for the effective passage of water, ranges between 2 and 8 mm, while its' compressive strength usually ranges between 2.8 MPa and 28 MPa [1]. Total porosity of pervious concrete often includes 10-20% closed pores and 80-90% effective, i.e. connected pores. Larger pores increase stress concentration, with reduced toughness of the material, which leads to the failure of the concrete structure [2]. In order to achieve the best performance, pervious concrete must be designed using the optimum cement paste content and aggregate of sufficient size and amount.

Pervious concrete is typically designed for a void content in the range of 15 to 30%. Since the final porosity of the samples is greately influenced by the level of compaction, Ridengaoqier and Shigemitsu [3] have proposed a method for prediction of porosity of pervious concrete. According to their results, relation between measured ultrasonic pulse velocity and porosity for pevious concrete prepared with crushed stone aggregates with particle size between 2.5 mm and 5 mm, and water to cement ratio of 0.25 was $v=-1.9\times p^2+4675$ (m/s) as shown in Figure 1.

Taking into account all stated above, in this research two types of pervious concrete flags were produced, one with designed 15% (PC15) and the second with designed 20% (PC20) of void content. Mixture design was performed according to the steps described by [4]. Cement (CEM I 52.5 R) and crushed andesite aggregate (2/4 mm) were used in both mixtures. The amount of aggregate was the same for both mixtures, while the amount of cement paste was higher for mixture PC15. Water/cement ratio was 0.3 for both mixtures, since lower values between 0.27 to 0.30 are advisable when superplastisizers are applied.

Pervious concrete flags of nominal dimensions 200×200×60 mm were produced with vibropress and cured under laboratory conditions (temperature 20°C, relative humidity 65%) up to the age of 28 days. After reaching the testing age samples were dried at the temperature of 60°C until reaching the constant mass. Measurements of dimensions (a, b and h) and mass in dry state (m_0) were performed on the three samples per mixture. Then these samples were gradually immersed in water, and their mass was again measured after 48 hours (m_{0v}). Using the hidrostatic scale, underwater mass of these samples was also determined (m_{0v}'), leading to

the calculation of the volume without open pores (V_a). According to these measurements water absorption and open porosity were calculated, as presented in Figure 2.

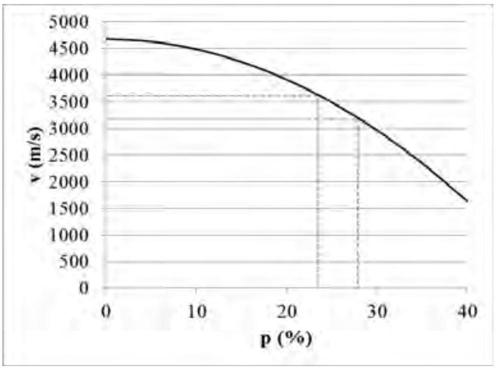

Figure 1. Model proposed by [3] compared with the results of ultrasonic pulse velocity test

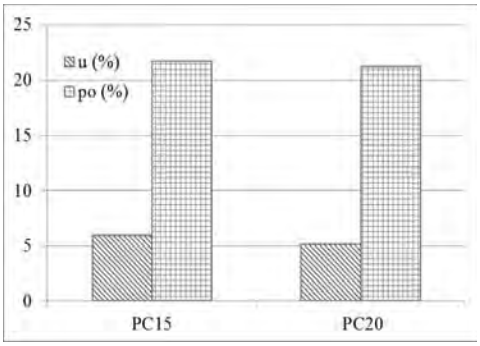

Figure 2. Water absorption and open porosity of tested pervious concrete samples

If the average measurement of the ultrasonic pulse velocity tests performed on the specimens cut from the pervious concrete flags PC15 and PC20 are compared with the relation presented by Ridengaoqier and Shigemitsu [3], porosity of 28.2% (for mixture PC15) and 24.2% (for mixture PC20) can be calculated (Figure 1).

From the presented results it can be concluded that the compaction index has an extremely important role in the formation of the porosity of pervious concrete samples. The mixture designed for the porosity of 15% reached 40% higher open porosity according to the hydrostatic scale method, and 88% according to the ultrasonic pulse velocity method. It was also shown that proposed model offers very good complience with the obtained results, having in mind that it was developed based on the mixtures prepared with lower w/c ratio, and coarser aggregate grain sizes.

ACKNOWLEDGMENT

This research was supported by UNDP, project number 00139323/00129089/2023/3, “Zero-waste porous pavement alternatives for flood resilient cities” .

REFERENCES

[1] Bhavana, T.D.; Koushik, S.; Kumar, K.U.M.; Srinath, R.(2017) “Pervious Concrete Pavement: Integrated Laboratory and Field Study”. *Transp. Res. Rec.* 13–21.

[2] Seeni S. M., Madasamy M.,(2021) “Factors influencing performance of pervious concrete”, *Građevinar* 73, 10,1017-1030

[3] Ridengaoqier E., Shigemitsu, H. (2021) “Prediction of porosity of pervious concrete based on its dynamic elastic modulus”, *Results in Materials,* 10, 100192,

[4] “Pervious Concrete: Guideline to Mixture Proportioning“ (2009), *NRMCA Engineering Division,* 2PE001

2nd International Conference on Mathematical
Modelling in Mechanics and Engineering
Mathematical Institute SANU, 12-14. September, 2024.

TRUNCATION RESONANCES IN ZIG-ZAG PHONONIC CRYSTALS WITH COUPLED LONGITUDINAL AND FLEXURAL WAVES

Bartłomiej Piwowarczyk[1], Michael J. Leamy[2] and Paweł Paćko[3]

[1,3]*Department of Robotics and Mechatronics, Faculty of Mechanical Engineering and Robotics, AGH University of Krakow, Krakow, 30-059, Poland*
[2]*G.W.W. School of Mechanical Engineering, Georgia Institute of Technology, Atlanta, GA, 30332, USA*
[1]*bartlomiej.piwowarczyk@agh.edu.pl*; [2]*michael.leamy@me.gatech.edu*; [3]*pawel.packo@agh.edu.pl*
[1]ORCID 0009-0005-8432-2852; [2]ORCID 0000-0002-9914-640X; [3]ORCID 0000-0002-8962-9969

Keywords: Elastic metamaterials, phononic crystals, wave-based vibration approach, truncation modes.

ABSTRACT

Metamaterials, also known as architected materials, are typically constructed using periodic arrangements of material parameters and/or locally-resonant attachments. These materials exhibit novel response such as frequency bandgaps, localized modes, and topological states. The one- dimensional setting allows for straight-forward investigation of structural properties arising from their periodic structure, and from finite system effects, such as localized truncation modes. The dynamic properties of infinite structures (e.g., dispersion curves) for rods and beams with periodic variation have been well-studied [1]. Studies of finite-size structures focusing on mode localization at edges, and avoided crossing of modes while varying model parameters [2], have also been carried out. Recent research has established a theoretical foundation for the study of truncated modes in bi-layered rods and beams, for either longitudinal or flexural motions [2,3]. The coupling effect between longitudinal and flexural waves, achieved using vibrating attachments [4] or beam junctions [5], has been separately studied. However, to date, no study has investigated truncation modes in structural systems where junctions couple longitudinal and flexural waves.

There is a wide range of analytical and numerical tools available for studying the response characteristics of phononic crystals composed of periodic media, including the transfer matrix method and the wave-based vibration approach [5]. These methods enable exact determination of band structure in monocoupled phononic crystals, for both flexural and longitudinal motions. Computational approaches, such as the finite element method [3], have also been widely used to approximate the band structure. More recently, machine learning techniques [6] have been applied towards determining band structure.

In this research we analyze one-dimensional phononic crystals in the form of zig-zag adjoined beams. The joint between each pair of beams induces coupling between longitudinal and flexural wave modes. We apply a parametrized truncation to one of the edges and an extension to the other end, as shown in Fig.1a. Such a configuration allows for studying truncation modes while keeping the length of the structure constant, similar to [3], where the parameter modifying the unit cell is termed a *phason*. We employ the wave-based vibration approach to derive the exact model of the considered structure. This method allows for straight-forward, exact treatment of joints and end conditions arising at truncations. Figure 1b depicts natural frequencies of the zig-zag structure computed using the wave-based approach. The horizontal axis tracks the unit cell shift associated with the phason (i.e., the change of the

truncation parameter) for a structure consisting of 10 zigzag unit cells. Frequency ranges of densely packed modes correspond to passbands of the structure associated with the infinite phononic crystal. Bandgaps are present between the passbands where edge-localized modes appear (i.e., truncation modes). An important feature is the spectral flow of the modes between the neighbor passbands, which is known to have a topological origin [3]. Details of this spectral flow and its implications will be discussed during the conference presentation.

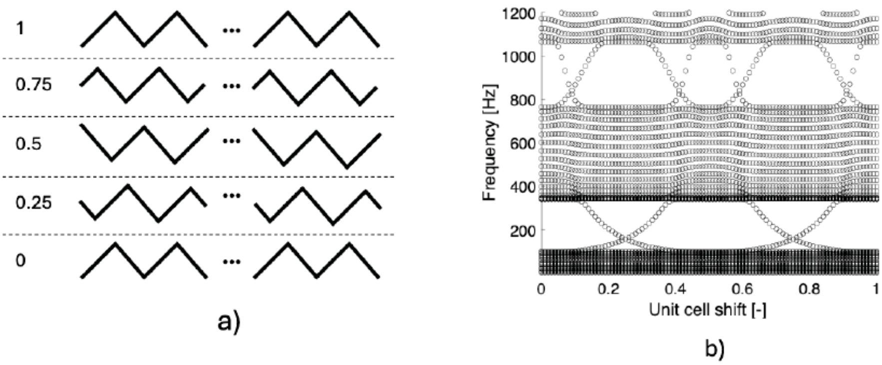

Fig. 1. Phononic crystal with coupled longitudinal and flexural waves: a) phononic crystal with different values of shift (truncation parameter) modifying the boundaries, and b) natural frequencies of the system consisting of 10 unit cells.

REFERENCES

[1] Goto, Adriano and Nóbrega, Edilson and Pereira, Flavio and Dos Santos, J. (2020). Numerical and experimental investigation of phononic crystals via wave-based higher-order rod models. International Journal of Mechanical Sciences. 181. 105776. 10.1016/j.ijmecsci.2020.105776.

[2] H. B. Al Ba'ba'a, C. L. Willey, V. W. Chen, A. T. Juhl, M. Nouh, Theory of Truncation Resonances in Continuum Rod-Based Phononic Crystals with Generally Asymmetric Unit Cells. Adv. Theory Simul. 2023, 6, 2200700. https://doi.org/10.1002/adts.202200700.

[3] Rosa, Matheus I. N. and Davis, Bruce L. and Liu, Liao and Ruzzene, Massimo and Hussein, Mahmoud I. (2023). Material vs. structure: Topological origins of band-gap truncation resonances in periodic structures. Phys. Rev. Mater. 10.1103/PhysRevMaterials.7.124201.

[4] D.J. Mead, Š. Markuš. (1983). Coupled flexural-longitudinal wave motion in a periodic beam. Journal of Sound and Vibration. https://doi.org/10.1016/0022-460X(83)90399-1.

[5] Michael J. Leamy. (2012). Exact wave-based Bloch analysis procedure for investigating wave propagation in two-dimensional periodic lattices. Journal of Sound and Vibration. https://doi.org/10.1016/j.jsv.2011.11.023.

[6] Muhammad, John Kennedy, C.W. Lim. (2022). Machine learning and deep learning in phononic crystals and metamaterials – A review. Materials Today Communications. https://doi.org/10.1016/j.mtcomm.2022.104606.

2nd International Conference on Mathematical
Modelling in Mechanics and Engineering
Mathematical Institute SANU, 12-14. September, 2024.

USE OF MULTIPLE SCATTERING OF ELASTIC WAVES FOR DEVELOPMENT OF ACOUSTIC LOGIC GATES

Jacek Filar[1] and Paweł Paćko[2]

[1,2]*Department of Robotics and Mechatronics, Faculty of Mechanical Engineering and Robotics, AGH University of Krakow, Krakow, 30-059, Poland*
[1]*jacek.filar@agh.edu.pl*; [2]*pawel.packo@agh.edu.pl*
[1]ORCiD 0009-0003-7988-2850; [2]ORCiD 0000-0002-8962-9969

Keywords: Wave-based vibration approach, multiple scattering, elastic wave manipulation, impedance, reflector cluster, acoustic logic gates, micro electro-mechanical systems.

ABSTRACT

Micro Electro-Mechanical Systems (MEMS) are increasingly important in modern technology. These systems execute operations utilizing various signals, differing by type (i.e. analogue or discrete) or propagation medium (e.g., electromagnetic, elastic waves). This study explores elastic waves' multiple scattering to design metamaterial systems capable of logical operations, namely logic gates. To perform such calculations, we employ information encoded in flexural elastic waves propagating in beam metamaterial structures. The latter are equipped with specifically engineered metaclusters of resonators, that allow for achieving desired reflection and transmission properties in these one-dimensional systems. Combining multiple propagation paths with metaclusters leads to the system's capability of reproducing the truth tables of logical gates, hence resembling an elastic analogy of the well-known MEMS-type electronic logical gates.

The developed analysis and design methodology is composed of two stages: design of a cluster of scatterers and implementing them into a two-dimensional frame structure. The first stage evolves from the Euler-Bernoulli beam with a single attachment, through metaclusters composed of multiple scattering elements, and leads to the second-stage two-dimensional frame structures based on the Timoshenko beam theory – with distributed metaclusters. The first model, based on the Euler-Bernoulli beam theory, allows for calculation of transmission and reflection coefficients of individual reflectors, i.e. point impedances placed on a beam, and reflector clusters[1], while the latter – based on the Timoshenko beam theory – extends the analysis to transmission and reflection coefficients for coupled longitudinal-flexural wavefields as well as to the scattering coefficients for beam joints[2] (e.g. in a system of beams connected in a truss).

Based on the models developed earlier, we employ optimization techniques for the design of scatterer clusters of different number of attachments, i.e. ranging from single- to four-reflector setups, each optimized to achieve desired reflection and transmission coefficients. Noting that the signal phase is critical for performing logical operations on elastic waves, we design clusters inducing significant phase shifts on propagating waves, while ensuring minimal amplitude loss. The design process leads to multiple scattering setups of various number of scattering elements, and allows for imposing a 180-degree phase shift compared to the input signal, with approximately 90% of the original amplitude retained in the output signal. The most recent analysis aimed at achieving XOR and AND logical gate

functionalities in a dual-beam system. In this latter case, each beam is equipped with a four-reflector cluster, which parameters were optimized in the design process.

After designing metaclusters for achieving desired scattering properties, we employ the wave-based vibration approach (WBV) to build a complementary model to build on the prior analyses. By integrating WBV with the metaclusters, we account for joint transmissions and reflections in addition to the clusters' scattering coefficients, allowing for the control of mechanical energy flow through a structure. Initially, we developed simplistic models to conduct modal analyses of diverse beam-based truss systems, spanning from cantilever beams to H-shaped frames. These initial models were validated through comparisons with the finite element-based models. With the foundational model validated, we proceeded to derive formulas enabling the incorporation of point scatterer placement in the system. By integrating the WBV theory with the Euler-Bernoulli wave propagation analyses, we proposed a refined model capable of optimizing scatterer parameters for the entire wave propagation system. Finally, we present analysis results on incorporating a reflector cluster, which was tuned to a specific normal mode frequency, within the frame and designing the whole beam system logical functionality.

REFERENCES

[1] Norris, A. N., Paćko, P. (2019), "Non-symmetric flexural wave scattering and one-way extreme absorption" The Journal of the Acoustic Society of America, Vol. 146, Issue: 1, July, pp. 873-883.

[2] Mei, C. (2008), "Wave Analysis of In-Plane Vibrations of H- and T-shaped Planar Frame Structures" Journal of Vibration and Acoustics, Vol. 130, December.

2nd International Conference on Mathematical
Modelling in Mechanics and Engineering
Mathematical Institute SANU, 12-14. September, 2024.

DECODING RECEPTION DIRECTIVITY PATTERNS OF ULTRASONIC TRANSDUCERS FROM RANDOM GUIDED WAVE EXPERIMENTS

Siddhesh Raorane[1], Tadeusz Stepinski[2] and Pawel Packo[3]

[1,2,3]*Department of Robotics and Mechatronics, Faculty of Mechanical Engineering and Robotics, AGH University of Krakow, Krakow, 30-059, Poland*
[1]siddhesh.raorane@agh.edu.pl, [2]tadeusz.stepinski@agh.edu.pl, [3]pawel.packo@agh.edu.pl
ORCID iD: [1]0000-0002-1847-7830; [2]0000-0002-0067-7308; [3] 0000-0002-8962-9969

Keywords: guided waves, wavemode identification, numerical modeling, parameter identification.

ABSTRACT

Owing to the multi-modal and dispersive characteristics of guided waves (GWs), reliable application of GW-based techniques requires *apriori* knowledge of the propagating wavemodes. In this work, a novel strategy for wavemode identification in GWs is proposed. This strategy, being based on random excitations, enables the identification of wavemodes generated by any arbitrary excitation. Furthermore, this strategy can be employed to determine the reception directivity patterns of ultrasonic transducers, enhancing their applicability across various fields.

INTRODUCTION

Guided waves serve as vital tools in non-destructive testing (NDT) and structural health monitoring (SHM), particularly for long-range inspections in civil, mechanical and aerospace engineering [1]. The effectiveness of GWs stems from their high sensitivity to defects and their capacity to scan large areas. GWs are inherently multi-modal, with each mode exhibiting dispersive characteristics, especially in plate-like structures [2]. Consequently, the effective utilization of GWs in NDT and SHM necessitates precise identification of the modal content of the wavefield and evaluation of transmission and reception sensitivity of transducers to different guided wavemodes.

This work presents a novel strategy for identifying wavemodes induced by GWs propagation. The approach involves utilizing a series of experiments with various random excitations being applied to a substrate with a piezoelectric transducer. Subsequently, identification equations are formulated and solved based on the responses of the substrate and the transducer, enabling the identification of wavemodes generated by any arbitrary excitation. The concept is presented using examples with numerical experiments based on finite element models. To ensure computational efficiency, harmonic excitations are used in numerical experiments, although transient simulations are also viable.

METHODOLOGY AND RESULTS

The strategy reported in this work entails applying the excitation at one of the boundaries of the substrate with the excitation remaining constant along the length but varying randomly in the plane normal to the wave propagation direction. This random spatial distribution forms a coding sequence for the identification process, ensures the procedure's adaptability to diverse excitation types and maximizes the probability of the identification matrix being invertible, hence the process being unique.

Next, harmonic simulations are run at the required frequency, and the responses of the substrate – at multiple points along the propagation path – and the transducer are recorded and used to formulate the identification equation as

$$\mathbf{AM} = \mathbf{V}, \tag{1}$$

where **A** is a matrix of modal coefficients extracted from the responses of the substrate, **V** is a vector containing the responses of the transducer and **M** is a vector of directional mode-dependent coefficients. Subsequently, the identification process is carried out by inverting the coefficient matrix. The proposed procedure can be repeated for multiple angles of the transducer for the experimental identification of mode- and direction-dependent reception patterns of ultrasonic transducers.

CONCLUSIONS

This study presents a novel strategy for identification of wavemode-dependent directional characteristics of ultrasonic transducers. The proposed approach utilizes a random excitation procedure, enabling the identification of wavemodes generated by arbitrary excitations. Through this strategy, mode-specific reception directivity patterns of ultrasonic transducers can be precisely determined. Consequently, the work proposed here facilitates the application of GW transducers across diverse fields such as non-destructive testing, structural health monitoring, energy manipulation, and beyond.

REFERENCES

[1] Cawley, P. (2023), "Guided waves in long range nondestructive testing and structural health monitoring: Principles, history of applications and prospects," NDT & E International, 103026.

[2] Rose, J. L. (2014), "Ultrasonic guided waves in solid media," Cambridge university press.

PHYSICAL AND THERMAL CHARACTERISTICS OF LLDPE-MINERAL BLEND FOR ROTATIONAL MOULDING

Prashant Khanna[1] and PL. Ramkumar[2]

[1]*Mechanical Engineering Department, Parul University, Vadodara, Gujarat, India*
[2]*Department of Mechanical and Aerospace Engineering, Institute of Infrastructure Technology Research and Management, Ahmedabad, India*
[1]*prashantkhanna2003.pk@gmail.com*; [2]*plramkumarno1@gmail.com*

Keywords: Rotational moulding, polymers, fibres, chrysotile, LLDPE

ABSTRACT

Polymer matrix composites, which combine fibers with a polymer matrix, offer a unique blend of high strength and lightweight properties, making them highly suitable for various industrial applications. Rotational molding, a technique used to create seamless, hollow parts from polymers, is especially notable for its ability to produce complex shapes by melting and coating the interior of a rotating mold [1,2]. Linear low-density polyethylene (LLDPE) is a common material used in this process due to its moldability and cost-effectiveness, although it sometimes requires fillers to enhance its mechanical and thermal properties [3,4].

In this study, we explored the potential of using chrysotile powder as a filler for LLDPE in rotational molding. Chrysotile, recognized for its superior mechanical and thermal characteristics, has not been extensively examined in this context [5,6]. Our aim was to identify the optimal blend of LLDPE and chrysotile to improve the performance of the composite material in rotational molding applications. For the experimental procedure, we used LLDPE powder with a melt flow index (MFI) of 4.67 g/10 min and chrysotile powder. We prepared samples by dry blending various proportions of chrysotile (ranging from 5% to 50% by weight) with LLDPE. The tests conducted included Fourier-transform infrared spectroscopy (FTIR), Melt flow index (MFI), differential scanning calorimetry (DSC), thermogravimetric analysis (TGA), and water absorption tests.

FTIR analysis revealed significant peaks corresponding to both LLDPE and chrysotile, helping to determine the optimal blending range of 15% to 40% chrysotile. MFI testing showed that blends with 15% to 25% chrysotile retained acceptable flow properties for rotational molding. DSC analysis indicated a slight increase in melting points with the addition of chrysotile, while crystallinity decreased at higher chrysotile content, suggesting improved heat transfer within the composite. TGA analysis demonstrated increased thermal stability and higher residual mass with greater chrysotile content, indicating enhanced thermal resistance. Water absorption tests showed that chrysotile reduced the water absorption capacity of the composites, thereby improving their moisture resistance.

In conclusion, adding chrysotile to LLDPE enhances its thermal stability, reduces water absorption, and maintains acceptable flow properties for rotational molding. The optimal range for chrysotile content was found to be 15% to 25%, providing a balance between improved properties and processability. These findings suggest that chrysotile can be an effective filler for LLDPE in rotational molding, potentially enhancing the mechanical strength and thermal resistance of the final products.

REFERENCES

[1] Crawford RJ, Kearns MP. Practical Guide to Rotational Moulding. 2012. 18 pp.
[2] Ogila KO, Shao M, Yang W, Tan J. Rotational molding: A review of the models and materials. Express Polym Lett. 2017;11(10):778–98.
[3] Ramkumar PL. Study on Mechanical and Fracture Behaviour of Linear Low Density Polyethylene for Rotational Moulding. 2015;188.
[4] Gupta N, Ramkumar PL. Experimental investigation of linear low density polyethylene composites based on coir for rotational molding process. Polymers and Polymer Composites. 2021;29(8):1114–25.
[5] Zholobenko V, Rutten F, Zholobenko A, Holmes A. In situ spectroscopic identification of the six types of asbestos. J Hazard Mater [Internet]. 2021;403(July 2020):123951. Available from: https://doi.org/10.1016/j.jhazmat.2020.123951
[6] Balducci D, Valerio F. Qualitative and Quantitative Evaluation of Chrysotile and Crocidolite Fibers with Ir-Spectroscopy: Application to Asbestos-Cement Productst. Int J Environ Anal Chem. 1986;27(4):315–23.

MODELING THE MECHANICAL BEHAVIOR OF A TRIGGER FINGER TENDON-LIGAMENT APPARATUS

Anfisa S. Rezanova[1], Marat Z. Dosaev[2] and Vitaly A. Samsonov[2]

[1]*Faculty of Mechanics and Mathematics, Moscow State University,119991 Moscow, Russia*

[2]*Institute of Mechanics of Lomonosov Moscow State University, 119192 Moscow, Russia*

[1]*anfisa.rezanova@math.msu.ru*; [2]*dosayev@imec.msu.ru*

[2]ORCID iD 0000-0002-3859-4065; [3]ORCID iD 0000-0002-8930-171X

Keywords: Trigger Finger, Biomechanics.

ABSTRACT

A mechanical model of the contact between flexor tendons and ligaments in Knott's disease was constructed. The problem is solved numerically using the finite element method in the ANSYS package. The inflamed tendon is modeled by a linear elastic cylinder with a hemisphere, the ligament is modeled by a linear elastic cylinder, one face of which is fixed. The minimum axial force applied to the tendon sufficient to cause slippage through the pulley is calculated. An assessment is made of the conditions under which finger snapping occurs depending on the stiffness of the tissues, friction in the contact area and the geometry of the contacting bodies.

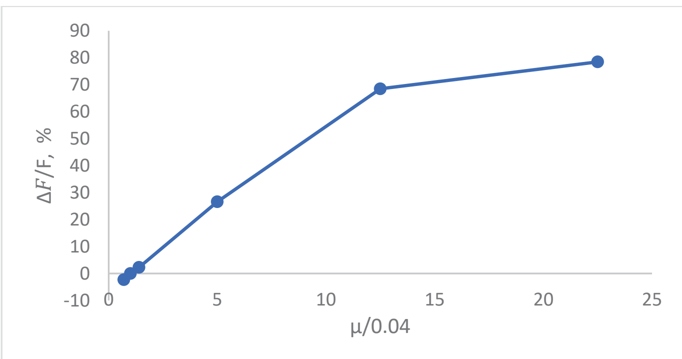

Fig.1. Change in ultimate force relative to $F_{\mu=0.04}$ depending on friction coefficient μ.

REFERENCES

[1] Y.S. Cheng, H.F. Chieh, CJ Lin, L.C. Kuo, K.N. An, F.C. Su (2018), "Comprehensive simulation on morphological and mechanical properties of trigger finger - A cadaveric model" *J. of Biomechanics, Vol. 74, 187-191, 2018*. https://doi.org/10.1016/j.jbiomech.2018.03.043

2nd International Conference on Mathematical
Modelling in Mechanics and Engineering
Mathematical Institute SANU, 12-14. September, 2024.

THE FRACTIONAL ZENER WAVE EQUATIONS

Snežana Gordić[1], Ljubica Oparnica[2] and Dušan Zorica[3]

[1,2]*Faculty of Education in Sombor, University of Novi Sad, Podgorička 4, 25000 Sombor, Serbia*

[3]*Department of Physics, Faculty of Sciences, University of Novi Sad, Trg Dositeja Obradovića 4, 21000 Novi Sad, Serbia*

[1]snezana.gordic@uns.ac.rs; [2]ljubica.oparnica@uns.ac.rs; [3]dusan.zorica@df.uns.ac.rs

ORCID iD: [1]0000-0001-8039-0456; [2]0000-0001-8547-339X; [3]0000-0002-9117-8589

Keywords: wave equation, fractional constitutive equations, fundamental solutions, well-possedness.

ABSTRACT

The fractional Zener wave equation is derived and analysed on three-dimension unbounded domain. The fundamental solution for the Cauchy problem is shown to exist in the space of distributions, and a priori energy estimates are derived yielding well possednes of the problem.

The wave propagation in viscoelastic 3-dimensional unbounded media is modeled by a system of three basic equations of continuum mechanics of solid body: the equation of motion, the constitutive law for a viscoelastic body giving relation between the stress tensor and the strain tensor assumed in the form of fractional Zener law, and the symmetric displacement gradient giving relation of the strain and the displacement. This system is equivalent to a single equation called *fractional Zener wave propagation equation* which could be decomposed in two different ways, both yielding equations of same type referred as *the fractional Zener wave equations*. In first approach the unknowns in the fractional Zener wave equations are the dilatation and the rotation vector, while in the second approach the unknowns in the fractional Zener wave equations are the irrotational and the divergence free vectors.

For the homogeneous medium, using Laplace and Fourier transforms, we show existence of the fundamental solution for the fractional Zener wave operator giving two representations of the unique solution to original fractional Zener wave propagation equation. Further, we analyse regularity of the obtained solution and derive a priori energy estimates which also holds for an inhomogeneous medium. Finally, we show existence of the weak solution of the fractional Zener wave propagation equation in the case of inhomogeneous medium.

This work generalize previous results from [1, 2, 3].

REFERENCES

[1] Konjik, S., Oparnica, L., Zorica, D. (2010) Waves in fractional Zener type viscoelastic media, *Journal of Mathematical Analysis and Applications*, 365(1), 259-268

[2] F. Broucke, Lj. Oparnica, (2022) Micro-local and qualitative analysis of the fractional Zener wave equation. *Journal of Differential Equations* 321: 217-257

[3] Oparnica, Lj., Suli, E. (2020) Well-posedness of the fractional Zener wave equation for heterogeneous viscoelastic materials. *Fractional Calculus and Applied Analysis*, 23(1), 126-166

2nd International Conference on Mathematical
Modelling in Mechanics and Engineering
Mathematical Institute SANU, 12-14. September, 2024.

ENGINEERING TECHNOLOGY FOR CALCULATION OF RESIDUAL PHENOMENA DURING ARC WELDING OF GENERAL PURPOSE STRUCTURES (SPECIAL CASE: THE MODELS OF THE THIN PLATES)

M. Zhukavets[1]

[1]-*The United Institute of Informatics Problems of the National Academy of Sciences of Belarus (UIPI NAS of Belarus), 220012 Minsk, Belarus*

[1]mikhailzhukavets@gmail.com,
ORCID iD: [1]0009-0007-5008-6577

Keywords: Engineering technology, Deformation, Welded structures, Stress-strain state.

ABSTRACT

The abstract shows the description and testing of engineering technology for calculating welding stresses and deformations of thin plate models. The presented technology is aimed at facilitating the work of designers of welded structures, so that design services get an idea of the stress-strain state of structures after welding.

In accordance with the force method proposed in this abstract for determining welding stresses σ and deformations ε [1, 2], the volume of the weld pool, we will call it the fusion zone (FZ), where phase transformations occur, is less than the other temperature zone, namely, the one where temperature plasticity sets in and the metal's yield strength and tensile strength sharply drop, – this zone is limited by an isotherm of 600...650 °C – we will call it the heat-affected zone (HAZ).

The essence of the force method is the application of fictitious forces to create in the FZ and HAZ the same deformations ε and stresses σ as from the actual longitudinal and transverse shrinkage of the welded construction. According to experiments, the main factor influencing the shrinkage force is welding energy input – H_i (the amount of heat entering the metal per weld length) [3]:

$$Hi = q / v, \text{ where}$$

q – part of the source power that getting in the metal of the plates being welded;

v – welding speed.

In the force method, in computer modeling using the finite element method (FEM), a simplification is introduced: welding speed is very large and simultaneous heating is assumed along the entire length of the plates being welded. In this case, the initial condition when modeling plates is single-pass welding, which means the absence of initial stresses, the two plates are not stressed or deformed before welding. In the process welding, the seam is laid symmetrically. The planes of the plates are adiabatic boundaries (there is no exchange of heat with the surrounding space).

The force method replaces the thermomechanical problem, therefore the parameters that are important when modeling thermal processes are replaced by forces (pressure equal to the metal's yield strength of the metal) applied to the ends of the FZ and HAZ to recreate the longitudinal shrinkage force, and to recreate the transverse force, a pressure equal to the metal's yield strength is applied at the boundary of the FZ and HAZ, and the HAZ and the base metal

– this creates the effect of tension of the zone and compression of the HAZ [1, 2]. The stresses along the thickness of thin plates are so small that they can be neglected in calculations. The diagram for applying pressure for thin plates is shown in Fig. 1.

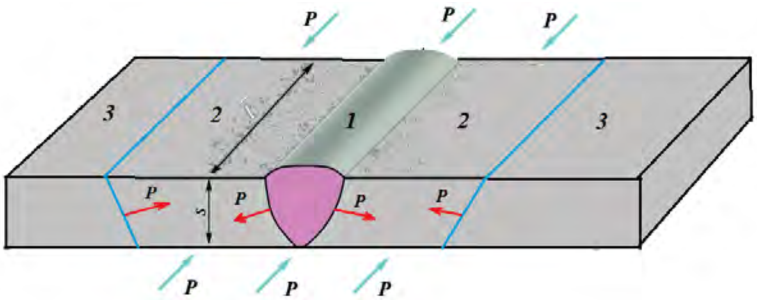

Fig. 1. Scheme of applying pressure equal to the yield strength on a model of welded plates using the force method: 1 – fusion zone (FZ); 2 – heat affected zone (HAZ); 3 – base metal.

The engineering technology presented in the abstract is intended for design bureaus to quickly determine the stress-strain state of welded structures of thin plates based on a limited amount of data: I – welding current, U – voltage of the welding source, η – arc efficiency, v – welding speed. If the designer does not have the exact values of the above data, the technology makes it possible to get by with the value of the deposition volume of the FZ. In addition, the technology, unlike the thermo-mechanical problem, is much less resource-intensive and allows you to quickly determine the stress-strain state of welded structures of thin plates on almost any desktop computer, which affects the speed of design. The use of technology can be automated and added, at the request of designers, as an additional option to some graphics package.

REFERENCES

[1] Medvedev, S.V. (2001), “Computer modeling of residual welding deformations in technological design of welded structures”, Welding Production, 8, pp. 10–18. [In Russian]
[2] Medvedev, S.V., Zhukavets M.V. (2022), “Computer technologies for predicting residual welding phenomena in arc welding of general-purpose structures”, Current issues and advanced welding technologies in science and industry: a collection of articles from the First International Scientific and Technical Conference, ISBN 978-985-492-284-3., pp. 159–163. [In Russian]
[3] Kurkin, A.S., Lukyanov, V.F. (2021), “Welded structures. Calculation and design”, Textbook for universities, p. 264. [In Russian]

2nd International Conference on Mathematical
Modelling in Mechanics and Engineering
Mathematical Institute SANU, 12-14. September, 2024.

INFLUENCE OF RAIL FOOT MODIFICATION ON SOLIDIFICATION STRESS OF RAILWAY ALUMINOTHERMIC WELDING BY CASTING SIMULATION

Gvozden B. Jovanović[1], Vaso D. Manojlović[2], Stefan M. Dikić[3], Miroslav D. Sokić[4], Dejan B. Momčilović[5], Alen Š. Delić[6], and Milorad P. Gavrilovski[7]

[1,4]*Institute for Technology of Nuclear and Other Mineral Raw Materials, 11000 Belgrade, Serbia*
[2,3]*Faculty of Technology and Metallurgy, University of Belgrade, 11000 Belgrade, Serbia*
[5]*Innovation Center, Faculty of Mechanical Engineering, 11000 Belgrade, Serbia*
[6]*TTU energetik d.o.o., 75000 Tuzla, Bosnia and Herzegovina*
[7]*Innovation Center, Faculty of Technology and Metallurgy, 11000 Belgrade, Serbia*
[1]*g.jovanovic@itnms.ac.rs*;[2]*v.manojlovic@tmf.bg.ac.rs*;[3]*sdikic@tmf.bg.ac.rs*;[4]*m.sokic@itnms.ac.rs*
ORCID iD [1]0000-0002-9754-2230; [2]0000-0002-3009-2909; [3]0000-0003-2700-0628;
[4]0000-0002-4468-9503; [5]0000-0001-9728-6022

Keywords: aluminothermic welding, simulation modeling, Novacast, welded joint, preheating influence, residual stress.

ABSTRACT

Aluminothermic welding has been used to connect railway rails for over a century. This method has several advantages, including its versatility, the tightness of the weld it creates, and its ease of execution. To complete the procedure, no further power source is necessary.

The NovaFlow & Solid CV software suite [1] was used to simulate casting thermite steel in the mold cavity or weld joint for the 49E1 rail. As a result, costly experimental techniques in industrial settings lead to ever-changing mould design. The design of the mould with the pouring system, which should ensure even pouring of thermal steel without turbulence, then even heat dissipation or cooling to obtain an appropriate micro and macro structure of steel free of internal and external defects, is one of several factors that contribute to a quality welded joint [2].

Initialy, a crude design of the casting was developed and compared with the real-life results [3], later, preheating was introduced to the simulation [4] and lastly, with the addition of side rails and mould to the casting simulation the design was close to real life conditions. With the final version of the mould design and simulation, stress and strain modeling were performed on the preheated model to provide a more complete understanding of how shrinkage is related to stress [5].

In this paper, the foot of the rail casting was modified to determine how best to eleveate the solidification stress, since the foot is the most compressed part of the rail during explotation.

The steel used for simulation is commercial railway steel R260 or EN 1.0623, the molten metal flow was injected in a circle of 10 mm in diameter. Gravity casting was chosen for the filling parameters with a pressure height of 300 mm, making the flow 1.149 kg/s and the casting temperature was set at 2200 ºC.

Unfortunately, due to the limitations of the software, it was not possible to move the burner heat source outside of the casting cavity (40 cm above the gating hole); however, the shape of

the air flow and temperature were adjusted to reproduce real-life circumstances, but the position of the source remained below the divider.

Software programs are being used to simulate conventional casting procedures that may be used in the casting of thermite steel during the fabrication of welded railway connections in order to prevent costly and time-consuming industrial experimentation. Even though some concave shape modifications of the rail foot proved to be better than others, we will continue to work on developing the simulation conditions and, in the future, compare the most satisfactory with the final weld product experiments.

REFERENCES

[1] NovaCast Systems AB: NovaFlow&Solid 6.0, Ronneby, 2015.
[2] Manojlović, V.D. et al. (2021) 'Unapređenje tehnologije aluminotermijskog zavarivanja železničkih šina različitog poprečnog preseka', Tehnika, 76(6), pp. 756-761. doi:10.5937/tehnika2106756M.
[3] Delić, A.Š. et al. (2022) 'Optimizacija dizajna kalupa za ulivanje termitnog čelika kod aluminotermijskog zavarivanja železničkih šina softverskom simulacijom', Tehnika, 77(3), pp. 311-317. doi:10.5937/tehnika2203311D.
[4] Jovanović, G.B. et al (2022). 'Simulation of the impact of preheating temperature on railway aluminothermic welding', Proceedings of in XIV Conference of Chemists, Technologists and Environmentalists of Republic of Srpska, Banja Luka, Bosnia and Herzegovina, October 21-22, pp. 284-290.
[5] Jovanović, G.B. et al. (2023) 'Razvoj modela za simulaciju livenja pri aluminotermijskom zavarivanju šina', Tehnika, 78(4), pp. 425-430. doi:10.5937/tehnika2304425J.

2nd International Conference on Mathematical
Modelling in Mechanics and Engineering
Mathematical Institute SANU, 12-14. September, 2024.

ACTIVE SURROGATE-BASED APPROACH TO SEISMIC FRAGILITY CURVE ESTIMATION FOR NONLINEAR STRUCTURES

Victor R. Medina[1], Younes Aoues[2] and Didier Lemosse[3]

[1,2,3]*Normandie Université, INSA Rouen Normandie St-Étienne-du-Rouvray, France*
[1]vmedinamordan@insa-rouen.fr; [2]younes.aoues@insa-rouen.fr; [3]didier.lemosse@insa-rouen.fr

Keywords: Fragility Curve; Vulnerability; Active Learning; Polynomial Chaos; Kriging.

ABSTRACT

Seismic fragility curves are essential for evaluating the vulnerability of buildings during earthquakes. However, traditional methods for deriving these curves often employ a lognormal distribution, which introduces significant epistemic uncertainty. This is because these methods neglect various sources of uncertainty, such as material properties and structural parameters. Nonparametric approaches offer a solution to this limitation but typically require Monte Carlo simulations to estimate the probability of exceedance of the limit state. This leads to prohibitive computational demands for complex structures. To overcome this, we propose an innovative active surrogate modeling-based method that significantly reduces the computational expense of nonlinear dynamic analyses while maintaining high accuracy in estimating fragility curves.

The application of active learning in the context of reliability analysis represents a significant advancement in the methodology of seismic fragility assessments. Active learning strategies optimize the selection of sample points for evaluation, concentrating computational resources on areas near the limit state where uncertainty is highest and information gain is maximized. This targeted approach contrasts sharply with traditional Monte Carlo simulations. Our study demonstrates that incorporating active learning substantially reduces computational time compared to conventional Monte Carlo methods. These efficiency gains accelerate the assessment process and enhance the practicality of performing detailed nonlinear analyses on complex structures. This makes it feasible to conduct comprehensive seismic evaluations that were previously too computationally expensive to consider, thereby improving the efficiency and accuracy of seismic risk assessment in practice.

The effectiveness of this approach is demonstrated by developing a site-dependent fragility curve for a two-story steel frame structure subjected to various acceleration levels and situated in four hypothetical locations with different seismic characteristics from Eurocode classification. Using Winkler's model, the modeling incorporates soil-structure interaction effects, which account for shear wave velocity impacts through an elastic beam supported by densely spaced, independent springs [4]. Additionally, the analysis considers uniform corrosion degradation across the structure's surface, with corrosion depth modeled by a power function [3]. This study advances the precision of seismic vulnerability assessments and enhances the efficiency of structural analysis for seismic risk management, accommodating the complex behaviors of highly nonlinear structures.

REFERENCES

[1] Fadzli Mohamed Nazri. "*Seismic Fragility Assessment for Buildings Due to Earthquake Excitation*." *Springer briefs in applied sciences and technology*. 2018.

[2] Schöbi, Roland & Sudret, Bruno & Wiart, Joe. (2015). *"A Polynomial-Chaos-Based Kriging." International journal of uncertainty quantification.*

[3] J. R. Kayser and A. S. Nowak, *"Reliability of Corroded Steel Girder Bridges*," Structural safety, vol. 6, no. 1, pp. 53-63, 1989.

[4] G. Gazetas, *"Formulas and Charts for Impedances of Surface and Embedded Foundations," Journal of Geotechnical Engineering,* vol. 117, no. 9, pp. 1363-1381, 1991.

2nd International Conference on Mathematical
Modelling in Mechanics and Engineering
Mathematical Institute SANU, 12-14. September, 2024.

DYNAMICS OF BIMORPH BEAM-CHAIN WITH PERIODICALLY CHANGING FRACTIONALLY DAMPED COUPLING LAYER

Stepa M. Paunović[1], Milan Cajić[2] and Danilo Karličić[3]

[1,2,3]Mathematical Institute of the Serbian Academy of Sciences and Arts, 11000 Belgrade, Serbia

[1]stepa.paunovic@mi.sanu.ac.rs; [2]mcajic@mi.sanu.ac.rs; [3]danilok@mi.sanu.ac.rs

ORCID iD: [1]0000-0001-9785-4851; [2]0000-0001-5513-0417; [3]0000-0002-7547-9293

Keywords: energy harvesting, fractional damping, multi beam system, band structure analysis.

ABSTRACT

In the last few decades reaching sustainable development has become of paramount importance. Much research has been conducted in the field of alternate energy sources and energy harvesting devices. One possible way to transform mechanical energy into usable electric energy is the through the use of the direct piezoelectric effect in piezoelectric materials. Most often used devices of this type are bimorph beams, consisting of one metallic bearing layer in the middle and two piezo-ceramic layers attached to it from both sides. Beam vibrations cause its deformations, and these induce electric polarization in piezo-plates, so that when they are connected in an electric circuit, electric current flows through the circuit [1]. However, although these devices could produce sufficient amount of electricity to power some sensors or MEMS, this can be done mainly if they operate near their resonant regime. One way to overcome this limitation is to connect several bimorph beams into a chain – a single system with unique dynamic properties that can be designed according to particular needs. Moreover, in order to improve energy harvesting performance of this kind of systems, contemporary specially designed materials can be used to connect the beams. These materials often need to be described by constitutive equations with fractional-order derivatives to accurately model their behavior.

In this contribution, governing equations are derived which describe the motion of a system of connected cantilever bimorph beams with fractionally damped coupling layers. These equations are solved by first homogenizing the boundary conditions and then applying spatial discretization with Galerkin method. The fractional derivatives were approximated by the method proposed by Evangelatos and Spanos [2], and the thus obtained system of equations is solved in time domain by the accelerated Newmark iterative procedure [2], and in frequency domain the solution was derived by assuming the steady state regime. All the piezoelectric layers are connected in parallel, and the electric circuit equation is derived by the Gauss' law, Ohm's law and Kirchhoff's rules.

In addition, the phononic-like properties are added to the bimorph beam-chain by introducing the periodicity in material properties of the coupling layer. Namely, the fractional damping parameters, i.e. fractional derivative order and the relaxation time, are set to vary periodically, with every other having twice as high derivative order and relaxation time value. In such a setup, the system develops particular dynamic behavior that resembles the phononic lattice [3]. This can be observed when analyzing the system band structure on the frequency response function diagrams.

In the present contribution, the frequency band structure of the described system is presented, both for the case of cantilever bimorph beams, and for the case of the simply supported bimorph beams. It will be shown that introducing the phononic-like properties to the bimorph beam-chain improves its energy harvesting capabilities by comparing the generated electric power under the forced vibration conditions.

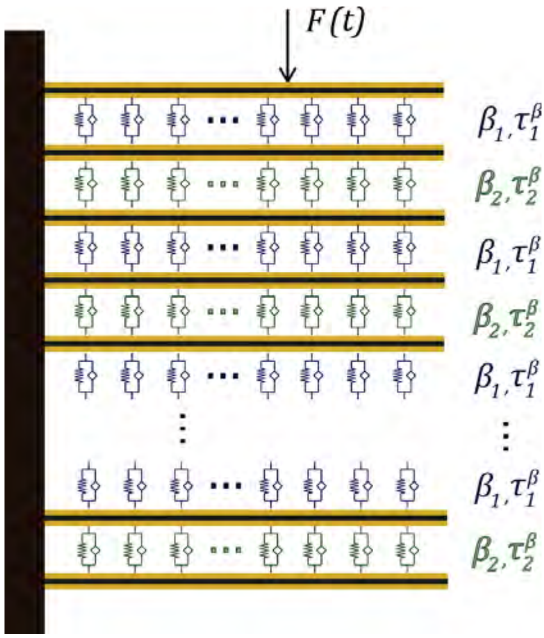

REFERENCES

[1] Erturk, A., & Inman, D. J. (2011). “Piezoelectric energy harvesting”. *John Wiley & Sons*.

[2] Evangelatos, G. I., & Spanos, P. D. (2011). “An accelerated Newmark scheme for integrating the equation of motion of nonlinear systems comprising restoring elements governed by fractional derivatives”. In *Recent Advances in Mechanics: Selected Papers from the Symposium on Recent Advances in Mechanics, Academy of Athens, Athens, Greece, 17-19 September, 2009, Organised by the Pericles S. Theocaris Foundation in Honour of PS Theocaris, on the Tenth Anniversary of His Death* (pp. 159-177). Springer Netherlands.

[3] Cajić, M., Karličić, D., Paunović, S., & Adhikari, S. (2020). A fractional calculus approach to metadamping in phononic crystals and acoustic metamaterials. *Theoretical and Applied Mechanics*, *47*(1), 81-97.

2nd International Conference on Mathematical Modelling in Mechanics and Engineering
Mathematical Institute SANU, 12-14. September, 2024.

COMPARISON OF NUMERICAL SIMULATION RESULTS AND EXPERIMENTAL MEASUREMENTS OF SWIRLING FLOW IN THE PIPE BEHIND THE AXIAL FAN IMPELLER

Mina D. Mirović[1], Danijela S. Srećković[2], Dániel Laki[3], Đorđe S. Čantrak[4] and Novica Z. Janković[5]

[1,2,3]eCon Engineering Kft. Budapest, Kondorosi út 3, 1116 Hungary
[4,5]Faculty of Mechanical Engineering, University of Belgrade, 11000 Belgrade, Serbia

[1]mina.mirovic@econengineering.com; [2]danijela.sreckovic@econengineering.com;
[3]daniel.laki@econengineering.com; [4]djcantrak@mas.bg.ac.rs; [5]njankovic@mas.bg.ac.rs
ORCID iD: [4]0000-0003-1841-9187, [5]0000-0003-2645-8602

Keywords: Axial fan, Turbulent swirl flow, Numerical simulation, Experimental measurements.

ABSTRACT

This study investigates turbulent swirl flow in a pipe induced by an axial fan. The objective is to compare results obtained from numerical simulations in Ansys® CFX software with results from measurements conducted at the Faculty of Mechanical Engineering, University of Belgrade. The industrial axial fan model used for both the numerical simulations and measurements is the W30 axial fan from Minel, Serbia, with seven blades and an outer diameter of 0.397 m (Figure 1). The blade angle of the fan was set to 30° at the outer diameter. The test rig length is 27.35 times the average inner diameter (approximately 0.4 m). Measurements were taken at two downstream measuring sections (z/D = 3.35 and z/D = 26.31), and after the simulation was completed, the same cross-sections were analyzed to ensure the comparison of results was relevant.[1]

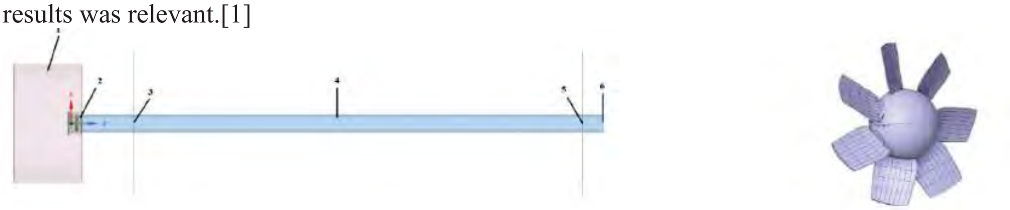

Figure 1. Simulation model (a) Experimental test rig prepared in Ansys® SpaceClaim: 1 – Inlet, 2 – Rotating domain with impeller, 3 – Measuring section 1, 4 – Laser pipe, 5 – Measuring section 3, 6 – Outlet (b) Impeller 3D model [1]

The geometric domain was divided into three distinct sections: an inlet, a rotating domain and laser pipe with an outlet. The physical attributes and dimensions of each domain segment exerted a direct influence on the mesh generation process. The mesh was generated using Ansys® Mesher, resulting in a total cell count of 6 279 730. A boundary layer was applied to the inlet walls in close contact with the impeller, the rotating domain, and the walls of the laser pipe, comprising a total of five layers. The fan model was developed by professors from the Department of Hydropower Engineering at the Faculty of Mechanical Engineering, University of Belgrade

The airflow in the fan was simulated under steady-state conditions using the Shear

Stress Transport (SST) turbulence model, which combines the k–ω model near the wall with the k–ε model in the bulk flow. The numerical results are later compared to the experimental data presented in this study [2].

TABLE 1.1 – Measurement results [1]

Section	Q [m³/s]	Um [m/s]	Re
1	1.178	9.14	254010
3	1.190	9.47	255558

TABLE 1.2 – Simulation results

Section	Q [m³/s]	Um [m/s]	Re
1	1.194297	9.50389	246032
3	1.194307	9.50397	246034

Tables 1.1 and 1.2 compare the results of the main flow parameters. The measurement results indicate larger deviations between sections 1 and 3, unlike the simulation results, which show minimal deviations due to the ideal conditions downstream of the laser pipe, which do not account for interactions with pipe walls, vibrations, and other dynamic effects present in the actual environment.

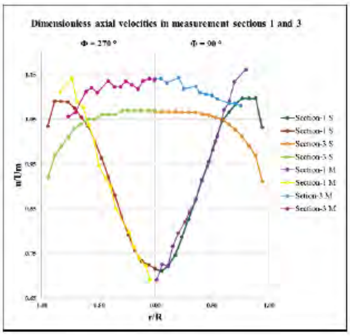

In Figure 2, the comparison results of dimensionless axial velocity in two measured planes are presented. In plane 1, dimensionless axial velocity values diverge for larger dimensionless diameters (r/R > 0.70), attributed to behavior near the pipe walls, which are idealized in the simulation, unlike real measurement conditions. In plane 3, discrepancies in dimensionless axial velocity are more significant between experimental and simulation results due to differences in the averaged axial velocity between measured and simulated results in plane 3; the measured value is lower than the simulated value. (Table 1.1 and Table 1.2)

Figure 2. Comparison of the dimensionless axial velocities between experimental and simulation results in measurement sections 1 and 3 for upper (90°) and lower (270°) halves

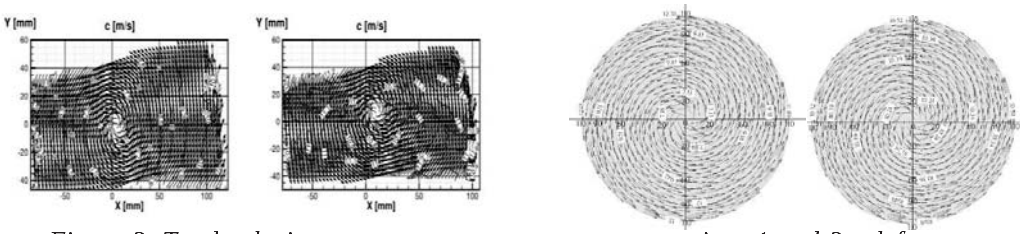

Figure 3. Total velocity vectors at cross-measurement sections 1 and 3 – left: measurement results, right: simulation results.

REFERENCES

[1] Čantrak Đ., Janković N., Ilić D., "Investigation of the turbulent swirl flow in the pipe generated by axial fans using PIV and LDA methods," *Theoretical and applied mechanics Volume 42 (2015) Issue 3,* 211-222.

[2] Menter, F.R., "Zonal Two Equation k-ω Turbulence Models for Aerodynamic Flows", *AIAA Paper*, 93-2906, 1993.

A COMPUTER AIDED APPROACH TO DESIGN OF WELDING ROBOTIC SYSTEMS

M. Kazheunikau[1], M. Zhukavets[2]

[1]*Faculty of Mechanical Engineering, Belarusian State University of Food and Chemical Technologies, 212027 Mogilev, Belarus*

[2] *The United Institute of Informatics Problems of the National Academy of Sciences of Belarus (UIPI NAS of Belarus), 220012 Minsk, Belarus*

[1]kmmk@mail.ru ; [2]mikhailzhukavets@gmail.com
ORCID iD: [1]0009-0000-1108-8210; [2]0009-0007-5008-6577

Keywords: Robotic systems, Design, Welding.

ABSTRACT

Computer aided design of welding robotics systems is a fundamental task of industrial robotics. A basic problem in this area is that a welding system must have a high degree of flexibility with frequent changes of welded constructions and corresponding welding tools. The computer aided design process of the welding robotic system involves searching the appropriate welding technology, including a rational sequence of welding, directions of welding and the order of applying welds [1, 2]. The tasks of computer-aided design of the welding system and its elements have many solutions. Not all criteria used in the computer-aided design can be formalized in advance and taken into account in the implementation of design algorithms. Limitations also depend on the specific design situation.

To implement such tasks, the following models is used in the proposed computer-aided approach to design welding robotic systems: industrial robots, welding tools, positioners, welding equipment, devices for changing and storing welding tools, off-programming systems for robots. The opportunities of the proposed approach includes checking the availability of a welding tool to the seams, selecting the most suitable welding tool for a given set of the welding seams (from those available in the database), training an industrial robot to weld a given welded construction, developing a technological welding program in an industrial robot programming language, graphical modeling of a technological program.

At all stages of design, three-dimensional modeling of objects of a welding system, as well as the movements of an industrial robot and positioners with the welded construction, is performed. The information created and used by the developed approach can be divided into several groups: about welded constructions, about robots, about welding tools, about elements of welding tools, about positioners, about additional components of a welding system. Each group contains three-dimensional graphic models of the objects. A set of graphic models of the welded constructions is stored in a database. The example of the developed graphics models of the robotic system is presented on Fig. 1.

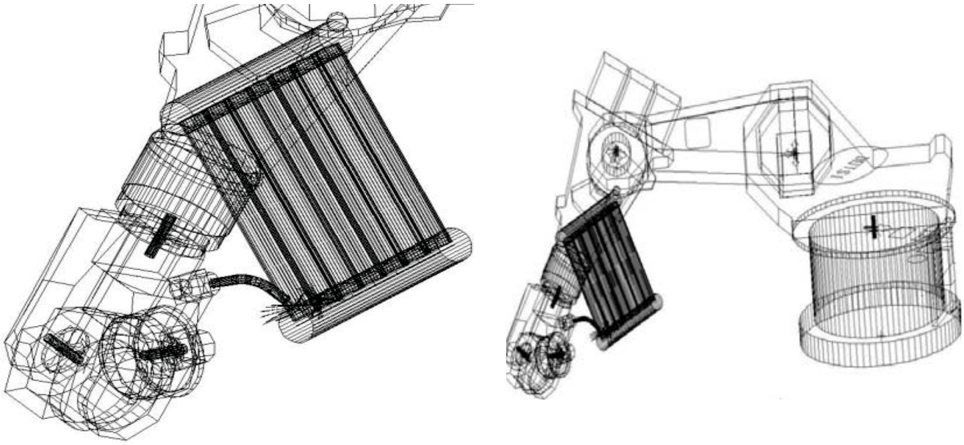

Fig. 1. Graphic models of the robotic system

The first stage of the modeling a welded structure is the creation of its graphic image. At the next stage, the lines of the welds are drawn in accordance with the required type of segment (linear, arc). When creating a new weld, the position of the weld start and end frames is entered. For circular seams, an intermediate frame is used. The orientation of each frame can be controlled visually. Next, enter information about the type of welded joints (butt, fillet, lap), wire extension, position and size of welded areas for intermittent welds. A similar procedure is used for each of the main and auxiliary seams. In accordance with a certain technology for the welding a construction, the sequence of application of main and auxiliary seams welds, as well as the direction of seams welding is set.

At the second stage, welding tools and robots are prepared. The three-dimensional image of the welding tool is supplemented with information about the position of the tools operating point and the position of the tools attachment point to the robot flange.The assembly of robots and positioners is carried out by a special procedure, which also automatically generates data files used by calculation programs.

At the third stage, modeling of the welding system is performed. The components of the welding system can be robotic manipulators, positioners, welding tools, welded construction, as well as additional components. The layout procedure of the welding system allows to sequentially include the necessary components in the model.

Using the proposed approach the effective software package is developed. This package implements all proposed types of procedures for welding systems design.

REFERENCES

[1] Medvedev, S.V. (2022), “Structural and technological design and modeling of welded structures in distributed supercomputer environments”, *Welding Production*, 5, pp. 24–29 (*in Russian*).

[2] Pashkevich, A., Kazheunikau, M., and Ruano, A.E. (2006), “Neural network approach to collision free path planning for robotic manipulators” *International Journal of Systems Science,* 37(8), pp. 555−564.

2nd International Conference on Mathematical Modelling in Mechanics and Engineering
Mathematical Institute SANU, 12-14. September, 2024.

TECHNOLOGICAL FORMS OF PRISMATIC WORKPIECES AND THE SELECTION OF NECESSARY AXES FOR MACHINE TOOLS

Marina Ivanović[1], Aleksandra Petrović[2], Vladan Grković[3], Katarina Mitrović[4] and Nedeljko Dučić[5]

[1,2,3]*Faculty of Mechanical and Civil Engineering in Kraljevo, University of Kragujevac, 36000 Kraljevo, Serbia*

[4,5]*Faculty of Technical Sciences Čačak, University of Kragujevac, 32102 Čačak, Serbia*

[1]*ivanovic.m@mfkv.kg.ac.rs*; [2]*petrovic.a@mfkv.kg.ac.rs*; [3]*grkovic.v @mfkv.kg.ac.rs*; [4]*katarina.mitrovic@ftn.kg.ac.rs*; [5]*nedeljko.ducic@ftn.kg.ac.rs*;

ORCID iD: [1]0000-0002-1576-7613; [2]0000-0002-5732-3578; [3]0000-0003-1229-4678; [4]0000-0002-3328-8739; [5]0000-0003-3336-8867

Keywords: Workpiece, Technological Form Recognition, 3D Convolutional Neural Networks, Machine Tool Configuration.

ABSTRACT

The development of numerous devices, technologies, and industries has resulted in a large number of various metal parts being produced. Each metal part, workpiece, used either independently or as part of an assembly, has characteristic surfaces that are processed using some metal cutting method. For easier and quicker identification of surfaces that need to be processed on a workpiece with complex geometry, it is necessary to form certain classes of typical technological forms that are most commonly encountered in workpieces. Each technological form has corresponding characteristics related to cutting diameter, cutting depth, appropriate radius, and a range of other parameters. The paper analyzes a total of 27 different classes of technological forms, and for each of these forms, 1000 different 3D CAD models are generated. The obtained 3D CAD models serve as input for training and testing 3D Convolutional Neural Networks (3D-CNNs) in recognizing various technological forms. Excellent results were achieved through testing the 3D Convolutional Neural Network.

Based on the data regarding workpieces, or the classes of technological forms that the workpiece possesses, it becomes possible to define the necessary axes for machining on machine tools, namely two, three, and five-axis machine tools. Based on the number of required machining axes, an appropriate configuration of machine tools is proposed and formed from the database of machine tool module models.

APPLICATION OF HYBRIDIZATION OF GWO-PUMA ALGORITHMS FOR IDENTIFICATION OF NON-ACOUSTIC PARAMETERS OF THE JCA

Tanja Dulović[1], Branko Radičević[1], Goran Miodragović[2] and Mišo Bjelić[1]

[1]*Faculty of Mechanical and Civil Engineering in Kraljevo, University of Kragujevac, 36000 Kraljevo, Serbia*

[2]*Academy of Applied Study Šumadija, Department Trstenik, 37240 Trstenik, Serbia*

[1]*dulovic.t@mfkv.kg.ac.rs ; [2]radicevic.b@mfkv.kg.ac.rs; [3]gmiodragovic@asss.edu.rs ; [4]bjelic.m@mfkv.kg.ac.rs*

ORCID iD: [1]0000-0003-3265-5661; [2]0000-0002-4182-4095; [4]0000-0002-6148-1982

Keywords: Sound absorption coefficient, Grey Wolf algorithm, Puma algorithm, Non-acoustic parameters, Polyurethane foam.

ABSTRACT

The paper presents the identification of the non-acoustic parameters of the JCA model for determining the sound absorption coefficient of open-cell polyurethane foams using hybridization of the Grey Wolf (GWO) and Puma (PUMA) algorithms. The main advantage of hybridization is the combination of the excellent search of the space of possible solutions of the GW algorithm with the fast convergence of the PUMA algorithm. This prevents falling into the traps of local minima and enables the identification of the optimal parameters of the JCA model. For method validation, the sound absorption coefficient of the polyurethane foam was measured using an impedance tube according to the transfer function method (EN ISO 10534-2:2001). Then, the hybridized GWO-PUMA algorithm was then used to identify the JCA model parameters corresponding to the measured values. The results showed excellent agreement with an error of less than 1% compared to the experimental data. The identified values of the physical parameters can be used to design polyurethane foams with desired acoustic properties, which confirms the proposed GWO-PUMA hybridization algorithm as a valuable tool in designing acoustic materials.

2nd International Conference on Mathematical Modelling in Mechanics and Engineering
Mathematical Institute SANU, 12-14. September, 2024.

A GEOMETRY PROJECTION METHOD WITH LENGTH CONSTRAINT FOR DESIGNING MONOLITHIC STRUCTURES MADE OF CONTINUOUS FIBER-REINFORCED COMPOSITES

Yogesh Gandhi[1], Ana Pavlovic[2], Julián Norato[3] and Giangiacomo Minak[4]

[1,2,4] *Department of Industrial Engineering, University of Bologna,47121 Forlì, Italy*

[3]*School of Mechanical, Aerospace, and Manufacturing Engineering, University of Connecticut, CT 06269 Storrs, USA*

[1]yogesh.gandhi@unibo.it; [2]ana.pavlovic@unibo.it; [3]julian.norato@uconn.edu; [4]giangiacomo.minak@unibo.it

ORCID iD: [1]0000-0002-8330-8515; [2]0000-0003-2158-1820; [3]0000-0002-2677-3090; [4]0000-0003-4961-0961

Keywords: geometry projection, variable stiffness composite laminates, length constraint, continuous fiber fused filament.

ABSTRACT

Continuous fiber fused filament fabrication (CF4) is a layer-by-layer printing technique that produces continuous carbon fiber-reinforced polymers (CCFRPs) with in-plane spatial varying material distribution and orientations. This allows for fabricating variable-stiffness composite laminates (VSCLs) with great flexibility. However, designing VSCLs can be challenging due to the complexity of the design space and the various design parameters involved. As a result, advanced computational design tools are necessary to utilize the design freedom offered by CF4 fully [1].

One such computational design procedure is topology optimization based on the geometry projection (GP) method [2]. This method uses geometric primitives such as bars and/or plates described by geometric parameters; these primitives are then mapped onto a density field---discretized via a fixed finite element mesh---for analysis. GP has been successfully used to optimize the layout of FRBs for maximum structural stiffness, both in 2D and 3D [3], and the technique was later advanced to consider primitives made of fiber-reinforced plates [4]. However, GP has mainly been used to design structures as assemblies of individual fiber-reinforced components. Thus, its application in designing monolithic composite structures, in which fiber-reinforced components form out-of-plane overlaps (or stacks), has yet to be demonstrated. This is essential because stacking at angles that are not parallel can be crucial in lowering the strain energy by optimizing the orthotropic ratio (E_2/E_1) so that the stiff fiber direction aligns with all the intersecting load paths. This challenges the current GP methodology because the smooth maximum function (i.e., softargmax) implementation pushes the design to attain a discrete component choice instead of aligning the primitives with all intersecting load paths. In current GP techniques, points that lie at the intersection of two or more primitives (i.e., joints) are assigned the material of one of the primitives, which means they do not capture the mechanical behavior at joints that would be obtained from overlapping components.

We present a GP method to enable the design of VSCLs. Using FRBs as features significantly enriches the GP methodology. First, by employing theories that describe composite laminates, we endow the GP technique with the ability to model overlapping FRBs

in the design, thus allowing for stacks of unidirectional plies or layers. These overlapping regions are then represented in the density field by exploiting the dual nature of GP. Specifically, the equivalent single-layer model based on first-order shear deformation theory is used to compute the reduced-order stiffness of FRBs. Second, we formulate a simple material interpolation approach to consider the effect of overlapping primitives. This is contrary to previous GP techniques that employ a softargmax interpolation for which regions of intersecting primitives are assigned the material of one overlapping primitive. Finally, to ensure that GP yields print-ready designs, we define a minimum length constraint for the bars by assigning a length-dependent weight to each component, computed using a sigmoid function, and effectively removing the bar from the design if its length does not attain the specified minimum value. Several minimal-compliance examples demonstrate the proposed methodology's applicability and effectiveness.

ACKNOWLEDGMENT

Financed by the European Union—NextGenerationEU (Italian Ministry of University and Research 2022NW83RE_002 - CUP J53D23002320006 – 28/09/2023, Advanced Structural Composites for Easily Reconfigurable Applications - ASCENT).

REFERENCES

[1] Y. Gandhi and G. Minak, “A review on topology optimization strategies for additively manufactured continuous fiber-reinforced composite structures .,” Appl. Sci., vol. 12, no. 21, pp. 1–26, 2022, doi: 10.3390/app122111211.
[2] J. A. Norato, B. K. Bell, and D. A. Tortorelli, “A geometry projection method for continuum-based topology optimization with discrete elements,” Comput. Methods Appl. Mech. Eng., vol. 293, pp. 306–327, Aug. 2015, doi: 10.1016/j.cma.2015.05.005.
[3] H. Smith and J. A. Norato, “Topology optimization with discrete geometric components made of composite materials,” Comput. Methods Appl. Mech. Eng., vol. 376, p. 113582, Apr. 2021, doi: 10.1016/J.CMA.2020.113582.
[4] H. Smith and J. Norato, “Topology optimization of structures made of fiber-reinforced plates,” Struct. Multidiscip. Optim., vol. 65, no. 2, pp. 1–18, Feb. 2022, doi: 10.1007/s00158-021-03164.

2nd International Conference on Mathematical
Modelling in Mechanics and Engineering
Mathematical Institute SANU, 12-14. September, 2024.

DYNAMIC SIMULATION OF HIGH-PRESSURE ANGLE SPUR GEARS

G. Vasileiou[1], N.Rogkas[2], L. Gkimisis[3] and V. Spitas[4]

[1]*School of Mechanical Engineering, National Technical University of Athen NTUA, Athens, Greece,*
e-mail: gvasileiou@mail.ntua.gr ORCID ID: 0000-0003-3496-0619

[2]*School of Mechanical Engineering, National Technical University of Athen NTUA, Athens, Greece,*
e-mail: nrogkas@mail.ntua.gr ORCID ID: 0000-0002-4581-5639

[3]*Max Planck Institute for Dynamics of Complex Technical Systems, Magdeburg, Germany*
e-mail: gkimisis@mpi-magdeburg.mpg.de

[4]*School of Mechanical Engineering, National Technical University of Athen NTUA, Athens, Greece,*
e-mail: vspitas@mail.ntua.gr ORCID ID: 0000-0003-3999-7752

Keywords: Spur gears, high pressure angle, dynamic simulation

ABSTRACT

Modelling and simulation of the highly non-linear dynamic response of gear pairs is an essential part of understanding dynamic phenomena such as rattling. Such analyses can be typically performed using extensive tooth contact analysis algorithms, noise vibration and harshness simulations or simplified models. Numerous works have been published on the dynamic simulation of standard gear geometries.

The present work aims at the dynamic modeling of high-pressure angle spur gears ranging from 30 to 35 degrees. The benefits and potential of such gears have been previously presented by the authors. However, although high-pressure angles are used extensively in asymmetric gearing, very few works can be traced to the dynamic simulation of such geometries. In the context of the present work, custom, optimized spur gear tooth geometries are used to evaluate the mesh stiffness of high-pressure angle gears employing analytical calculations and finite element analysis data. The non-linear load and position dependent mesh stiffness is formulated in closed form and used in a single DOF dynamic model predicting the transmission error of a gear pair as well as meshing nonlinearities including contact reversal and loss of contact.

The results are presented both in the time domain (time series) and in phase diagrams providing comprehensive understanding of the dynamic response of the examined gear pairs. Moreover, the results are also compared versus standard ISO geometries in order to further evaluate the performance of the proposed non-standard tooth profiles.

Finally, the contribution of the material properties on the dynamic response is also presented and discussed upon.

REFERENCES

[1] Sakaridis, E., Spitas, V., & Spitas, C. (2019). Non-linear modeling of gear drive dynamics incorporating intermittent tooth contact analysis and tooth eigenvibrations. Mechanism and Machine Theory, 136, 307-333.

[2] Gkimisis, L., Vasileiou, G., Sakaridis, E., Spitas, C., & Spitas, V. (2021). A fast, non-implicit SDOF model for spur gear dynamics. Mechanism and Machine Theory, 160, 104279.

[3] Spitas, C., & Spitas, V. (2016). Coupled multi-DOF dynamic contact analysis model for the simulation of intermittent gear tooth contacts, impacts and rattling considering backlash and variable torque. Proceedings of the Institution of Mechanical Engineers, Part C: Journal of Mechanical Engineering Science, 230(7-8), 1022-1047.

[4] Parker, R. G., Vijayakar, S. M., & Imajo, T. (2000). Non-linear dynamic response of a spur gear pair: modelling and experimental comparisons. Journal of Sound and vibration, 237(3), 435-455.

[5] Theodossiades, S., & NATSIAVAS, S. (2000). Non-linear dynamics of gear-pair systems with periodic stiffness and backlash. Journal of Sound and vibration, 229(2), 287-310.

[6] Faggioni, M., Samani, F. S., Bertacchi, G., & Pellicano, F. (2011). Dynamic optimization of spur gears. Mechanism and machine theory, 46(4), 544-557.

[7] Yu, W., Mechefske, C. K., & Timusk, M. (2016, August). A comparison of several sdof models of gear dynamics. In International Design Engineering Technical Conferences and Computers and Information in Engineering Conference (Vol. 50206, p. V008T10A023). American Society of Mechanical Engineers.

[8] Litvin, F. L., Lian, Q., & Kapelevich, A. L. (2000). Asymmetric modified spur gear drives: reduction of noise, localization of contact, simulation of meshing and stress analysis. Computer methods in applied mechanics and engineering, 188(1-3), 363-390.

[9] Thomas, B., Sankaranarayanasamy, K., Ramachandra, S., & Kumar, S. P. (2019). Selection of Pressure Angle-based on Dynamic Effects in Asymmetric Spur Gear with Fixed Normal Contact Ratio. Defence Science Journal, 69(3).

[10] Karpat, F., Ekwaro-Osire, S., Cavdar, K., & Babalik, F. C. (2008). Dynamic analysis of involute spur gears with asymmetric teeth. International Journal of Mechanical Sciences, 50(12), 1598-1610.

[11] Pleguezuelos, M., Sánchez, M. B., & Pedrero, J. I. (2021). Analytical model for meshing stiffness, load sharing, and transmission error for spur gears with profile modification under non-nominal load conditions. Applied Mathematical Modelling, 97, 344-365.

[12] Sánchez, M. B., Pleguezuelos, M., & Pedrero, J. I. (2017). Approximate equations for the meshing stiffness and the load sharing ratio of spur gears including hertzian effects. Mechanism and Machine Theory, 109, 231-249.

[13] Vasileiou, G., Rogkas, N., Markopoulos, A., & Spitas, V. (2024). Fully ceramic versus steel gears: Potential, feasibility and challenges. Proceedings of the Institution of Mechanical Engineers, Part C: Journal of Mechanical Engineering Science, 238(3), 775-784.

CHEMICAL ANALYSIS OF BLACK POWDER AS USEFUL DIAGNOSTIC TOOL OF GAS PIPELINE SYSTEM

Siniša M. Bikić[1], Sebastian S. Baloš[2], Milivoj T. Radojčin[3] and Ivan S. Pavkov[4]

[1,3,4]*Faculty of Agriculture, University of Novi Sad, 21000 Novi Sad, Serbia*

[2]*Faculty of Technical Sciences, University of Novi Sad, 21000 Novi Sad, Serbia*

[1]*bika@uns.ac.rs*; [2]*sebab@uns.ac.rs*; [3]*milivoj.radojcin@polj.edu.rs*; [4]*ivan.pavkov@polj.uns.ac.rs*

ORCID iD: [1]https://orcid.org/0000-0002-1641-8546; [2]https://orcid.org/0000-0002-3828-8500; [3]https://orcid.org/0000-0002-2864-7872, [4]https://orcid.org/0000-0002-6472-5209

Keywords: Internal corrosion, Black power, Gas pipeline

ABSTRACT

Internal corrosion of steel gas pipelines occurs due to the presence of water in natural gas. Water chemically reacts with carbon dioxide (CO_2), hydrogen sulfide (H_2S) and oxygen (O_2), creating unwanted internal corrosion products such as iron carbonate ($FeCO_3$), iron sulfide (FeS) and iron oxide (Fe_3O_4, FeOOH). Black powder was formed from internal corrosion products mixed with salt, sand, liquid hydrocarbons and metal residues [1].

Black powder can cause various problems at gas pipeline systems: reduce flow efficiency; clog and collapse filters; make deposition on gas measurement devices; clogging of instrumentation and valves and accelerated deterioration of valves due to erosion [2]. For example, the contamination of the orifice meter can influence the parameters of gas flow through the orifice meters [3].

In order to prevent the appearance of black powder in the gas pipeline system, the legal regulations of countries limit the content of certain components in natural gas. For instance, according to legislation in Republic of Serbia, the natural gas which is taken into system and delivered from the system must not contain water and the content of the following components in natural gas must be limited to: 1 mol% CO_2, 2 mol% H_2S and 0.02 mol% O_2 [4].

For the purpose of this work the samples of contaminants were removed from the filters of the four main gas metering and regulating stations. The chemical characterization of samples was performed using an energy dispersive spectrometer (EDS). Chemical analysis showed that tested samples mainly contain iron Fe, carbon C and oxygen O. These elements are indicators of formation of internal corrosion products as iron oxide (Fe_3O_4, FeOOH) and iron carbonate $FeCO_3$. This is also confirmation of black powder presence in the natural gas transmission system. The presence of black powder at the filter of main gas metering and regulating station points out that water exist in the natural gas transmission system. Analysis of the chemical contaminants that are periodically removed from the filter can be a useful diagnostic tool of the gas pipeline system from the point of view of prevention of internal corrosion.

REFERENCES

[1] Sherik, A.M., Lewis, A.L. and Duval, S. (2008), "Managing Black Powder in Sales Gas Transmission Pipelines", *Saudi Aramco Journal of Technology*, 42-46

[2] Tsochatzidis, N.A and Maroulis, K.E. (2007), "Methods help remove black powder from gas
pipelines", *Oil & Gas Journal*, 105(10)

[3] Hasečić, A., Imamović, J., Bikić, S., Džaferović, E. (2021), "Investigation of the contamination influence on the parameters of gas flow through multi-hole orifice flow meter", *IEEE Transactions on Instrumentation and Measurement*, 70(2021), 1-8, DOI:10.1109/TIM.2021.3063198

[4] Uredba o uslovima isporuke i snabdevanja prirodnim gasom ("Službeni glasnik RS", br. 49/22)

2nd International Conference on Mathematical
Modelling in Mechanics and Engineering
Mathematical Institute SANU, 12-14. September, 2024.

ON ROBUST STABILIZATION OF MOTION OF A QUADROTOR WITH SLUNG PAYLOAD

Yury D. Selyutskiy[1], Andrei P. Holub[2], Boris Ya. Lokshin[3] and Valery B. Zudov[4]

Institute of Mechanics of Lomonosov Moscow State University, 119192, Moscow, Russia

[1]seliutski@imec.msu.ru; [2]holub.imech@gmail.com; [3]blokshin@imec.msu.ru;
[4]golikov_valera@mail.ru

ORCID iD: [1]0000-0001-8477-6233; [2]0000-0001-8982-4097; [3]0000-0002-5818-6704

Keywords: Stabilization, Control, Quadrotor.

ABSTRACT

One of important tasks, for which quadrotors can be used, is transportation of payloads suspended with strings or ropes. The fact that the payload can move with respect to the quadrotor body and thus disturb the motion of the quadrotor requires developing the dedicated control algorithms. In literature, there were discussed various aspects of dynamics and control of such systems (e.g., [1-3]). However, usually, the payload is supposed a mass point of a sphere, and its aerodynamics is either neglected or reduced to the drag force only. The aim of the present work is more detailed consideration of the aerodynamic forces acting upon the payload.

We consider a copter (quadrotor) with suspended payload (see Fig. 1). The load is attached to the center of masses *G* of the quadrotor with a massless string. The payload is a symmetrical body with a plane of symmetry perpendicular to the plane of drawing and passing through the line *PG* (where *P* is the center of mass of the payload). The system can move in the vertical plane.

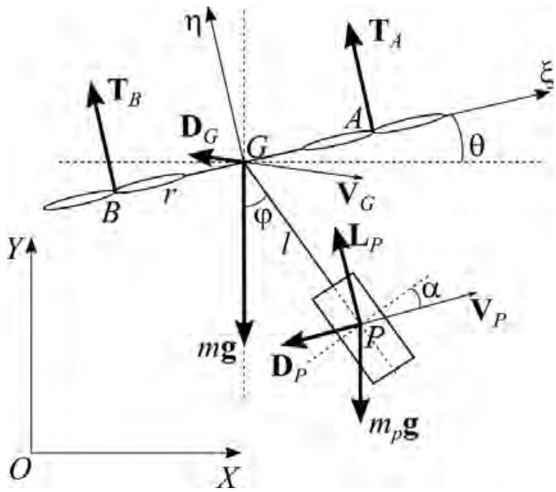

Fig. 1. A quadrotor with a slung payload

It is supposed that the payload is subject to aerodynamic forces that can be reduced to the lift force $\boldsymbol{L}_P$ and drag force $\boldsymbol{D}_P$ applied in the center of mass of the payload. In order to describe these forces, we use the quasi-steady approach, which implies that they depend only upon the instantaneous angle of attack α and instantaneous velocity $\boldsymbol{V}_P$ of the point P.

It should be noted that in real life the aerodynamic characteristics of the payload might be unknown. However, for a wide class of payload shapes, values of aerodynamic coefficients lie to certain intervals. Thus, a question arises, whether (and under which conditions) it is possible to construct a robust control that would ensure stabilization of the desired motion of the system (such as steady upward/downward motion, or steady horizontal flight) for any aerodynamic characteristics belonging to the predefined range.

In this work, the area in the space of parameters is determined where robust (in the above sense) stabilization of the upward/downward steady motion is impossible. For the cases when it is possible, different strategies for constructing the robust stabilizing control are proposed and discussed, and their advantages and drawbacks are outlined.

The study is supported by the Russian Science Foundation (Project No. 24-29-00151).

REFERENCES

[1] Homolka, P., Hromčík, M., Vyhlídal, T. (2017), "Input shaping solutions for drones with suspended load: First results," *Proceedings of the 21st International Conference on Process Control,* Strbske Pleso, Slovakia, pp. 30-35, doi: 10.1109/PC.2017.7976184.

[2] Cabecinhas, D., Cunha, R., Silvestre, C. (2019), "A trajectory tracking control law for a quadrotor with slung load," *Automatica*, Vol. 106, pp. 384-389, doi: 10.1016/j.automatica.2019.04.030.

[3] Dalwadi, N., Deb, D., Muyeen, S.M. (2022) "Observer based rotor failure compensation for biplane quadrotor with slung load," *Ain Shams Engineering Journal*, Vol. 13, No. 6, pp. 101748, doi: 10.1016/j.asej.2022.101748.

ANALYSIS OF HEAT TRANSFER IN A PERISTALTIC DIVERGING TUBE WITH SURFACE ROUGHNESS

Ashvani Kumar[1] *; Dharmendra Tripathi[2]

[1,2]*Department of Mathematics, National Institute of Technology, Uttarakhand, Srinagar-246174, India*

[1]*kashvani14@gmail.com*; [2]*dtripathi@nituk.ac.in*

ORCID iD: [1]0009-0000-4420-3297; [2]0000-0003-4798-1021

Keywords: Heat Transfer. Entropy Generation, Surface Roughness, Peristalsis.

ABSTRACT

The natural pumping mechanism known as peristalsis is crucial for driving biological fluids through bodily systems. However, the surface roughness of physiological vessels significantly impacts fluid slip and resistance within these systems. This study utilizes specialized equations designed for low Reynolds numbers and extended wavelengths to explore how wall surface roughness affects fluid flow and heat transfer. Through an analytical approach supported by MATLAB simulations, the research generates visual representations that provide valuable insights. The findings indicate that various parameters, including surface roughness, non-uniformity, Grashof number, Nusselt number, and heat source parameter, significantly influence pressure gradients, velocity fields, stream function, and entropy generation distributions within the microchannel. The study shows that surface roughness can either enhance or impede fluid movement, affecting overall efficiency and heat transfer rates in peristaltic systems. By understanding these effects, the research sheds light on the complex interactions between fluid dynamics and thermal properties in peristaltic flows. Additionally, the study highlights potential areas for further investigation, particularly focusing on non-Newtonian rheological effects in peristaltic pumping combined with heat transfer and surface roughness. These insights are essential for advancing our comprehension of peristaltic mechanisms in biological and industrial applications, where precise control of fluid flow and heat transfer is necessary. The enhanced understanding from this study could lead to improved designs and operational strategies for systems relying on peristaltic pumping, particularly in medical and engineering fields where surface roughness and heat transfer are critical factors.

REFERENCES

[1]. R. Shukla, S. S. Bhatt, A. Medhavi and R. Kumar, "Effect of surface roughness during peristaltic movement in a Nonuniform channel," Math. Probl. Eng., vol. 2020, pp. 1–8, 2022.

[2]. M. Irfan, I. Siddique, M. Nazeer and W. Ali, "Theoretical study of silver nanoparticle suspension in electroosmosis flow through a nonuniform divergent channel with compliant walls: a therapeutic application," Alex. Eng. J., vol. 86, pp. 443–457, 2024.

[3]. D. S. Bhandari and D. Tripathi, "Study of entropy generation and heat flow through a microtube induced by the membrane-based thermofluidic systems," Thermal Sci. Eng. Prog., vol. 34, pp. 101395, 2022.

2nd International Conference on Mathematical
Modelling in Mechanics and Engineering
Mathematical Institute SANU, 12-14. September, 2024.

DESIGN AND OPTIMIZATION OF SHELL AND TUBE HEAT EXCHANGER AT HADITHA HYDRO POWER PLANT

Abdulmuttalib MUHSEN[1], Natalya Kizilova[2] and Bashar Hassan Attiya[3]

[1] *Warsaw University of Technology, Warsaw, Poland*

[2] *Haditha Hydropower Station, Ministry of Electricity, Haditha, Iraq*
[3] *Imam Ja'afar Al-Sadiq University, Kirkuk, Iraq*
[1]abdulmuttalib.muhsen.dokt@pw.edu.pl

Keywords: Shell and tube heat exchanger, Design and optimize, CFD, Haditha Hydro Power Plant.

ABSTRACT

To design and optimize a shell and tube heat exchanger at Haditha Hydro Power Plant, it is essential to understand the background of the study. Developing an efficient heat exchanger involves minimizing costs while ensuring optimal heat transfer performance. As such, accurately determining the required minimum heat transfer area for a specific heat duty is crucial, as it directly influences the overall cost of the heat exchanger. The main issue faced by the industry is the excessive heat generated by the primary transformer at the Haditha hydro power plant, leading to overheating concerns. Therefore, the aim of this project is to design a Shell and Tube Heat Exchanger for oil cooling that optimizes performance and addresses the overheating problem. Various optimization techniques, including altering flow direction, utilizing finned tubes, and combining these methods, are evaluated to identify the most effective solution that achieves the highest average thermal efficiency and meets the necessary temperature change requirements.

REFERENCES

[1] D. Priyanto, Chikako Wada, N. Sato, S. Ueno, K. Mae. (2018). Fly Ash Transformation and Fouling Tendency during Co-firing Biomass with Coal.
[2] P. Gómez. (2017). Design and dynamic analysis of steam generators of concentrating solar power plants. p. 1.
[3] Dheeraj Shriwas, Mr. Jagdeesh Saini. (2018). Heat Transfer Enhancement Technique in Heat Exchanger: An Overview.
[4] D. Priyanto, Chikako Wada, N. Sato, S. Ueno, K. Mae. (2018). Fly Ash Transformation and Fouling Tendency during Co-firing Biomass with Coal.
[5] Berkowitz, B. J., Hare, R. C., Hausz, W. Conceptual design of thermal energy storage systems for near term electric utility applications. Volume 1: Screening of concepts.

APPLICATION OF ANN MODEL IN MECHANICAL ENGINEERING EDUCATION TO ENHANCE COGNITIVE SKILLS IN CHILDREN THROUGH CHESS AND LOGICAL GAMES

Dragan A. Milošević[1], Dragoljub Ilić[2] and Dragana Trnavac[3]

[1] *University Business Academy in Novi Sad, Faculty of Economics and Engineering Management, Cvećarska 2, 21000 Novi Sad, Serbia*

[2] *University Business Academy in Novi Sad, Faculty of Economics and Engineering Management, Cvećarska 2, 21000 Novi Sad, Serbia*

[3] *Faculty of Business and Law, "MB" University, Teodora Drajzera 27, 11000 Belgrade, Serbia*

[1]dragan.milosevic@fimek.edu.rs; [2]dragoljub.ilic@fimek.edu.rs ; [3]dragana.trnavac@mb.edu.rs
ORCID iD: [1]0000-0003-0244-5196

Keywords: ANN model, Chess Education, Mechanical Engineering, Children Development, Cognitive Skills.

ABSTRACT

Building on the experience of applying the Artificial Neural Network (ANN) model in mechanical engineering education at the Faculty of Economics and Engineering Management (FIMEK) in Novi Sad, this paper explores the innovative extension of these models to enhance cognitive skills in children through structured chess education and logical games. Utilizing 20 years of expertise from Chess Emporium, the largest chess education company in Arizona, based in Scottsdale and currently operating in approximately 500 schools, the ANN model originally designed for mechanical engineering courses is adapted to personalize learning experiences for children. This model optimizes the selection of chess problems and logical games based on individual skill levels. Data from chess tournaments organized by Chess Emporium serve as the foundation for this model, demonstrating its potential to develop logical thinking, problem-solving abilities, and overall cognitive functions in young learners. The interdisciplinary application of mechanical engineering principles to educational technology highlights significant improvements in children's logical reasoning and academic performance. The integration of empirical data analysis, machine learning techniques, and practical implementation in educational settings underscores the model's efficacy and scalability.

REFERENCES

[1] Milosevic, D. et al. (2022), "A Practical Model of the Application of Information Technology in Various Fields of Online Education during the COVID-19 Pandemic," Sustainability, 14(23), 16164.

[2] Ilic, D. et al. (2022), "MLP ANN Condition Assessment Model of the Turbogenerator Shaft A6 HPP Đerdap 2," Proceedings of the Symposium, 291-296.

[3] Zhong, M. and Li, Z. (2023), "Enhancing Education Performance through Machine Learning: A Study of Student Learning Outcomes Prediction Using GANs and ANNs," Proceedings of the 2023 IEEE International Conference on Control, Electronics and Computer Technology (ICCECT), Jilin, China, 28-30 April, pp. 123-130, DOI: 10.1109/ICCECT57938.2023.10140769.

[4] Klein, D. (2022), "Neural Networks for Chess," arXiv preprint arXiv:2209.01506, 3 September, pp. 1-150, DOI: 10.48550/arXiv.2209.01506.

[5] Munteanu, D. and Munteanu, N. (2020), "Sentiment Analysis Based on Deep Learning Techniques Applied to Children in Logical Games from Nonformal Education," Proceedings of the eLearning & Software for Education Conference, Bucharest, Romania, 14-15 May, pp. 57-64, DOI: 10.12753/2066-026X-20-007.

[6] Ma, W., Zhao, X. and Guo, Y. (2021), "Improving the Effectiveness of Traditional Education Based on Computer Artificial Intelligence and Neural Network System," Journal of Intelligent & Fuzzy Systems, Vol. 40, No. 2, pp. 2565-2575, DOI: 10.3233/JIFS-189249.

[7] Thangaramya, K., Logeswari, G., Sudhakaran, G., Aadharsh, R., Bhuvaneshwar, S., Dheepakraaj, R. and Sunny, P. (2024), "Predicting Optimal Moves in Chess Board Using Artificial Intelligence," in Cognitive Analytics and Reinforcement Learning: Theories, Techniques and Applications, edited by R. Elakkiya and V. Subramaniyaswamy, Wiley, pp. 67-89, DOI: 10.1002/9781394214068.ch4.

ROGUE WAVE CLUSTERS OF THE HIGHER-ORDER NONLINEAR SCHRÖDINGER EQUATION

Stanko N. Nikolić[1,2] and Milivoj R. Belić[2]

[1]*Institute of Physics Belgrade, University of Belgrade, Pregrevica 118, 11080 Belgrade, Serbia*

[2]*Division of Arts and Sciences, Texas A&M University at Qatar, P.O. Box 23874, Doha, Qatar*

[1]stankon@ipb.ac.rs; [2]milivoj.belic@qatar.tamu.edu

[1]ORCID ID: 0000-0002-2082-9954

Keywords: Quintic nonlinear Schrödinger equation, Darboux transformation, Rogue wave clusters.

ABSTRACT

We analyze three types of rogue wave (RW) clusters for the quintic nonlinear Schrödinger equation (QNLSE) on a flat background. The exact QNLSE solutions are generated using the Darboux transformation (DT) scheme and they are composed of the higher-order Akhmediev breathers (ABs) and Kuznetsov-Ma solitons (KMSs) [1]. We analyze the dependence of their shapes and intensity profiles on the eigenvalues and evolution shifts in the DT scheme and on three real quintic parameters. The first type of RW clusters, characterized by the periodic array of peaks along the evolution or transverse axis, is obtained when the condition of commensurate frequencies of DT components is applied. The elliptical RW clusters are computed from the previous solution class when the first *m* evolution shifts in the DT scheme of order *n* are equal and nonzero. For both AB and KMS solutions a periodic structure is obtained with the central RW and *m* ellipses, containing the first-order maxima that encircle the central peak. We show that RW clusters built on KMSs are significantly more vulnerable to the application of high values of QNLSE parameters, in contrast to the AB case. We next present non-periodic long-tail KMS clusters. They are characterized by the rogue wave at the origin and *n* tails above and below the central point containing the first-order KMSs. We also show that the breather-to-soliton conversion can transform the shape of RW clusters by careful adjustment of the real parts of DT eigenvalues, while remaining parameters are left unchanged.

REFERENCES

[1] Stanko N. Nikolić, Najdan B. Aleksić, Milivoj R. Belić. (2024), "Akhmediev and Kuznetsov-Ma rogue wave clusters of the higher-order nonlinear Schrödinger equation". Accepted for publication in the *Optical and Quantum Electronics*.

2nd International Conference on Mathematical
Modelling in Mechanics and Engineering
Mathematical Institute SANU, 12-14. September, 2024.

MULTI-CRITERIA ESTIMATION OF DOUBLE-ELLIPSOIDAL HEAT SOURCE PARAMETERS FOR NUMERICAL SIMULATION OF WELDING PROCESS

Mišo B. Bjelić[1], Branko S. Radičević[2], Mladen S. Rasinac[3] and Vladan R. Grković[4]

[1,2,3,4]*Faculty of Mechanical and Civil Engineering, University of Kragujevac, 36000 Kraljevo, Serbia*

[1]*bjelic.m@mfkv.rs*; [2]*radicevic.b@mfkv.rs*; [3]*rasinac.m@mfkv.rs*; [4]*grkovic.v@mfkv.rs*

ORCID iD: [1]0000-0002-6148-1982; [2]0000-0002-4182-4095; [3]0000-0003-4933-3765; [4]0000-0003-1229-4678

Keywords: Welding simulation, Multi-criteria estimation, Double-ellipsoidal heat source.

ABSTRACT

The results of welding simulation models depend heavily on the input parameters, particularly on the parameters of the heat source model. In this study, we present a method for estimation of the heat source parameters for a three-dimensional quasi-stationary heat transfer model for gas metal arc welding. In the case of a double-ellipsoidal heat source, five parameters are commonly used, the values for which are primarily determined by the researcher's experience. This approach can be a source of error; to estimate these values and to reduce computational time, we applied a calibration procedure using a Taguchi-based set of simulation results from the numerical model. In combination with grey relational analysis and two objective functions based on weld geometry, this approach showed very good results considering the matching between simulation and experimental results.

REFERENCES

[1] Gu, Y., et al. (2019), "Determination Of Parameters Of Double-Ellipsoidal Heat Source Model Based On Optimization Method," Welding in the World, 63(2), pp. 365-376.

[2] Farias, R.M., et al. (2021), "An Efficient Computational Approach For Heat Source Optimization In Numerical Simulations Of Arc Welding Processes," Journal of Constructional Steel Research, 176(106382), pp. 1-13.

[3] Bjelić, M. B., et al. (2022), "Multi-objective calibration of the double-ellipsoid heat source model for GMAW process simulation," Thermal Science, 26(3), pp. 2081–2092.

2nd International Conference on Mathematical
Modelling in Mechanics and Engineering
Mathematical Institute SANU, 12-14. September, 2024.

CASCADED ILC-MPC CONTROLLER FOR ROBOT MANIPULATORS

Nikola LJ. Živković[1], Mihailo P. Lazarević[2], Jelena Z. Vidaković[3] and Andrija C. Dević[4]

[1,3,4]Lola Institute, Kneza Višeslava 70a 11030 Belgrade, Serbia

[2]Faculty of Mechanical Engineering, University of Belgrade, Kraljice Marije 16, Belgrade, Serbia

[1]nikola.zivkovic@li.rs; [2]mlazarevic@mas.bg.ac.rs; [3]jelena.vidakovic@li.rs; [4]andrija.devic@li.rs
ORCID iD: [1]0000-0002-2276-2933; [2]0000-0002-3326-6636; [3]0000-0002-3363-8807; [4]0000-0002-5773-1635

Keywords: Trajectory tracking, Robots, Iterative Learning Control, Model Predictive Control.

ABSTRACT

Trajectory tracking is one of the key aspects of robot control system design. High-precision trajectory under disturbances, unmodeled dynamics, and parametric uncertainties of robotic systems is a highly challenging task for multiple DoFs. Many different control approaches, from simple PID controllers to advanced controllers such as Sliding Mode Control, Adaptive Control, Robust Control, Fuzzy Control, and Model Predictive Control (MPC), are used within trajectory tracking problems for robotic systems [1]. One of the control strategies suitable for trajectory tracking problems for systems executing repetitive tasks is Iterative Learning Control (ILC) [2]. The ILC is an intelligent, memory-based control method aimed at improving the transient response performance of the system that operates repetitively over a fixed time interval [3]. Several papers tackle improving the MPC with iterative learning controllers [4], [5]. This research presents the integration of MPC and ILC using a simple structure consisting of a cascaded ILC and MPC controller (Fig. 1.a) for position control of the robot manipulator. The motivation for the cascaded structure is that the ILC controller does not interfere with the MPC controller's nonlinear optimization solver since the parallel structure of the ILC and MPC would make MPC's objective function more complex.

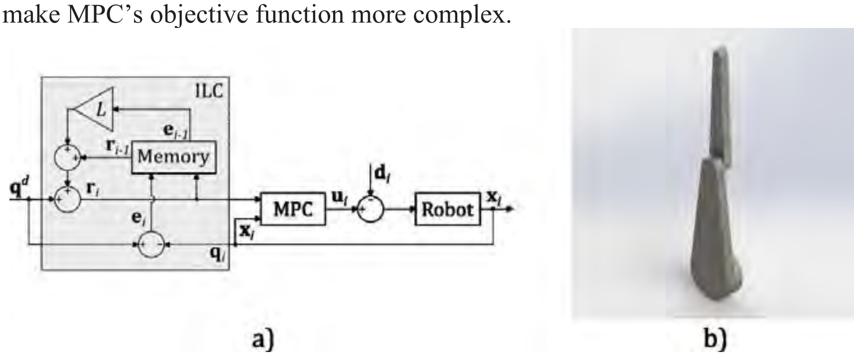

Fig. 1. a) Block diagram of the proposed cascaded ILC-MPC control strategy; b) Planar manipulator model.

The proposed control system is verified via numerical simulation on a two-degree-of-freedom planar manipulator (Fig. 1.b). The constant disturbance (time and iteration-wise) is considered in the simulation model. The reference trajectory in joint space is set to be a cubic polynomial. The performance of the proposed control system is evaluated using Maximal Absolute Error (MAE).

For each iteration, MAE is calculated and plotted as shown in Fig. 2.a, from which it can be concluded that the ILC controller reduces the tracking error for both joints in approximately four iterations. Fig. 2.b shows that the first joint tracks the reference trajectory almost perfectly while the second joint has a larger tracking error, although still significantly reduced in comparison to the sole MPC controller.

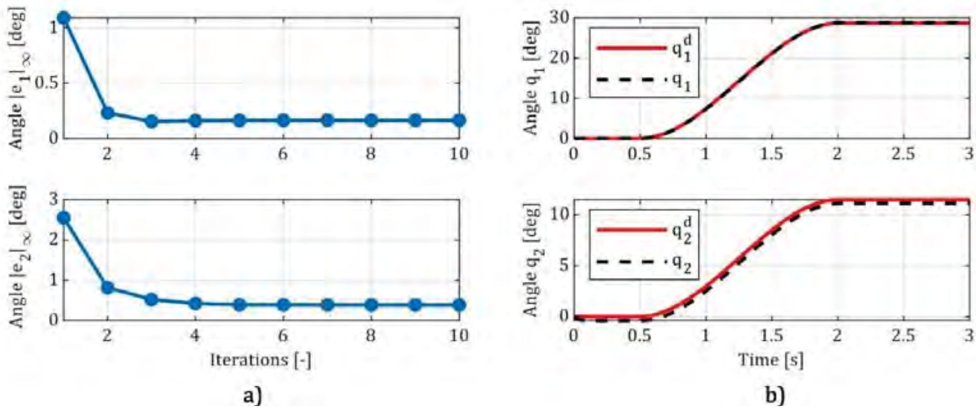

Fig. 2. a) Maximal absolute error over 10 iterations per robot joint; b) Reference q_j^d versus actual q_j joint trajectories pre joint ($j = 1, \dots, n$, n – degrees of freedom).

The proposed Cascaded ILC-MPC control solution for robotic systems shows promising results. Further investigation should encompass the reduced dynamics model in the MPC and the fractional derivative in the ILC.

ACKNOWLEDGMENT:

This research has been supported by the research grants of the Serbian Ministry of Science, Technological Development and Innovations, grant No. 451-03-65/2024-03/200105 from 5.2.2024 and No. 451-03-66/2024-03/200066

REFERENCES

[1] Li D., Du L., (2021) AUV Trajectory Tracking Models and Control Strategies: A Review. Journal of Marine Science and Engineering. 9(9) pp. 1020.

[2] Ahn, H. S., Moore, K. L., Chen, Y. (2007), Iterative learning control: robustness and monotonic convergence for interval systems. London: Springer.

[3] Moore, K. L., (1993), Iterative learning control for deterministic systems, Advances Industrial Control, New York: Springer-Verlag.

[4] Rosolia, U., Zhang, X., Borrelli, F. (2017), "Robust learning model predictive control for iterative tasks: Learning from experience," *56th Annual Conference on Decision and Control (CDC) Proceedings*, Melbourne, Australia, 12-15 December, pp. 1157-1162.

[5] Tang, Z. Q., Heung, H. L., Tong, K. Y., Li, Z. (2019). "A Novel Iterative Learning Model Predictive Control Method for Soft Bending Actuators," *2019 International Conference on Robotics and Automation (ICRA) Proceedings*, Montreal, QC, Canada, 2019, pp. 4004-4010.

2nd International Conference on Mathematical
Modelling in Mechanics and Engineering
Mathematical Institute SANU, 12-14. September, 2024.

GALERKIN MODELS FOR TIME SUPER-SAMPLING OF PIV MEASUREMENTS

Qihong L. Li-Hu[1*], Patricia García-Caspueñas[2], Andrea Ianiro[3] and Stefano Discetti[4]

Department of Aerospace Engineering, University Carlos III of Madrid, Avda. Universidad 30, 28911, Madrid, Spain

*qihonglorena.li@uc3m.es

ORCID iD: [1]0009-0008-5601-9970; [2]0000-0002-0735-4579; [3]0000-0001-7342-4814; [4]0000-0001-9025-1505

Keywords: Galerkin model, Data-Driven method, POD, PIV, Jet flow, Time super-sampling.

ABSTRACT

We propose a data-driven method to enhance the time resolution of snapshot Particle Image Velocimetry (PIV). The method consists of the time integration of empirical Galerkin models based on Proper Orthogonal Decomposition (POD) modes of the flow field, as developed by Noack et al. 2005 [1]. The objective is to extract time-resolved (TR) flow dynamics from non- time-resolved (NTR) velocity datasets.

PIV is an experimental technique to measure instantaneous flow velocity fields. Time-resolved PIV measurements enable capturing the dynamics of turbulent flows. However, it is highly constrained by the cost of equipment, and technological limits as the maximum sampling rate of cameras, pulsation frequency of light sources, and lowest signal/noise ratio due to the limited laser-pulse intensity and camera sensitivity. Snapshot PIV (i.e. delivering instantaneous fields without time resolution) is on the other hand a consolidated and widespread technique. It is however limited in the description of the dynamics of the flow. Increasing time resolution of snapshot PIV up to the level of describing the dynamics of the flow would be an enabler for flow description in configurations where TR PIV is unfeasible.

Despite their chaotic behaviour, turbulent flows show inherent patterns with dynamics often evolving on low-dimensional manifolds. This enables the development of simplified models that capture the main dynamical features of the flow. This approach has been studied previously in works exploiting physical constraints, such as Taylor's Hypothesis (Kar & Ganapathisubramani, 2012 [2]; Scarano & Moore, 2012 [3]) or advection of vorticity (Schneiders et al. 2016 [4]). However, the main constraint of these approaches is the validity of the hypothesis behind them.

This work focuses on the application of the Galerkin model for time super-sampling of NTR velocity measurements that can be obtained from PIV experiments. This Galerkin approximation is based on the projection of the incompressible Navier-Stokes equation on a domain spanned by an orthogonal basis obtained through a POD (Berkooz et al. 1993 [5]) of the fluctuation velocity fields, obtained from an SVD of the snapshot matrix $\boldsymbol{u}'$

$$\boldsymbol{u}'=\boldsymbol{\Phi}\boldsymbol{\Sigma}\boldsymbol{\Psi}^*=\boldsymbol{\Phi}\boldsymbol{a} \tag{1}$$

Note that the snapshot matrix, $\boldsymbol{u}'$, has dimension $N_p\times N_t$, with N_p the number of points per snapshot, N_t the total number of snapshots, and most often $N_t < N_p$. $\boldsymbol{\Phi}\in\mathbb{R}^{N_p\times N_t}$, $\boldsymbol{\Sigma}\in\mathbb{R}^{N_t\times N_t}$, and $\boldsymbol{\Psi}\in\mathbb{R}^{N_t\times N_t}$, are matrices of the spatial modes, the singular values, and the temporal modes, respectively. $\boldsymbol{a}=\boldsymbol{\Sigma}\boldsymbol{\Psi}^*\in\mathbb{R}^{N_t\times N_t}$ are the temporal coefficients. Projecting

the incompressible Navier Stokes equations on a set of N spatial modes it is obtained a set of N ordinary differential equations:

$$\frac{d}{dt}a_i = \frac{1}{Re}\sum_{j=0}^{N} l_{ij}\,\boldsymbol{a_j} + \sum_{j=0}^{N}\sum_{k=0}^{N} q_{ijk}\;\boldsymbol{a_j}\,\boldsymbol{a_k} \tag{2}$$

$\boldsymbol{l_{ij}}$ and $\boldsymbol{q_{ijk}}$ are the coefficients of the viscous and convective terms which describe the interaction between modes. The Galerkin model allows to represent the flow system with a relatively small set of ordinary differential equation that can be integrated in time describing the dynamics. Consider a certain NTR PIV sequence the flow dynamics between two snapshots can be reconstructed integrating backwards and forward the set of equations (2).

To test the method, we employ planar PIV measurements of a water jet flow at Reynolds number equal to 3300. A set of 40000 TR velocity snapshots measured with a time separation of dt=0.0011s is subsampled taking 1 snapshot every 40 from the TR dataset, being D=0.03m the jet diameter and Ub=0.11m/s the bulk velocity, and fed to the Galerkin model, which reconstructs the flow with 80% of the total energy (92 modes). *Figure (1)* shows a comparison of the streamwise velocity fields of the jet flow reconstructed at two instants of time. The Low Order Reconstruction (LOR) from the original time-resolved sequence is included for comparison. The first one is a snapshot within the NTR training dataset and the second one corresponding to a snapshot equispaced between two snapshots of the input dataset. Preliminary results show that the velocity fields are effectively reconstructed, suggesting the usefulness of the proposed methodology.

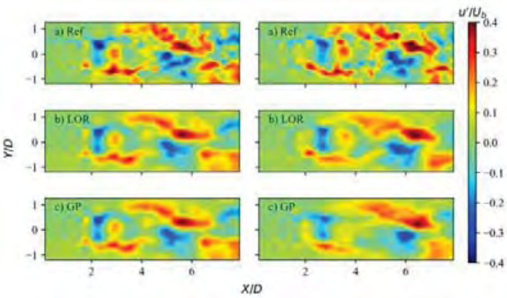

Figure 1: Low-order reconstruction with 92 modes of streamwise velocity fluctuation contours. Left: snapshot used as initial condition. Right: reconstructed snapshot located in the middle between two snapshots of the subsampled sequence. From top to bottom: reference field, LOR, and result from Galerkin model.

This project has received funding from the European Research Council (ERC) under the European Union's Horizon 2020 research and innovation program (grant agreement No 949085).

REFERENCES

[1] B. R. Noack, P. Papas, y P. A. Monkewitz, "The need for a pressure-term representation in empirical Galerkin models of incompressible shear flows", J. Fluid Mech., vol. 523, pp. 339- 365, ene. 2005.

[2] R. De Kat y B. Ganapathisubramani, "Pressure from particle image velocimetry for convective flows: a Taylor's hypothesis approach", Meas. Sci. Technol., vol. 24, n.o 2, p. 024002, feb. 2013.

[3] F. Scarano y P. Moore, "An advection-based model to increase the temporal resolution of PIV time series", Exp. Fluids, vol. 52, n.o 4, pp. 919-933, abr. 2012.

[4] A. Laskari, R. De Kat, y B. Ganapathisubramani, "Full-field pressure from snapshot and time-resolved volumetric PIV", Exp. Fluids, vol. 57, n.o 3, p. 44, mar. 2016.

[5] G. Berkooz, P. Holmes, y J. L. Lumley, "The Proper Orthogonal Decomposition in the Analysis of Turbulent Flows", Annu. Rev. Fluid Mech., vol. 25, n.o 1, pp. 539-575, ene. 1993.

2nd International Conference on Mathematical Modelling in Mechanics and Engineering
Mathematical Institute SANU, 12-14. September, 2024.

SCHEFFLER BASED HOUSEHOLD SOLAR COOKING SYSTEM FOR REMOTE LOCATIONS IN INDIA: DESIGN AND DEVELOPMENT

Hemant Raj Singh[1*], Dilip Sharma [2], Vishnu Agarwal[3]

[1]*Department of Mechanical Engineering, Manipal University Jaipur, Rajasthan 303007, India*

[2,3]*Department of Mechanical Engineering, Malaviya National Institute of Technology Jaipur, Rajasthan 302017, India*

[1*]hemant.singh@jaipur.manipal.edu

ORCID iD: [1]0000-0002-1662-4411; [2]0000-0003-2348-8961; [3]0009-0009-3428-2409

Keywords: Cooking stove, Renewable Energy, Scheffler Dish, Solar Concentrator, Receiver, Rural Household, Cooking, Thermosiphon.

ABSTRACT

The objective of the present work is to provide a comprehensive cooking solution for a single rural household of western India. A Scheffler type solar concentrator-based cooking system is conceptualized for the above requirement due to its unique feature of stationary Receiver. Prime attributes of the proposed system are stationary cooking place, thermosiphon-based system and low cost which makes this suitable for rural applications. The proposed system consists of a Scheffler dish operated Stove (rectangular box of 55 cm × 35 cm × 20 cm) having two customized vessels viz. cooking vessel 2.5-liter capacity and a cooking pan(griddle) of 25 cm diameter made of SS 304 and cast iron respectively. Thermosiphon effect is used to carry the heat from the receiver to the stove using thermic fluid (Shell Thermia 'S2'). Based on the mathematical model developed, the approximate thermosiphon flow rate comes out to be 0.80 LPM or 2.63 cm/s for a pipe diameter of 1 inch. To check thermosiphoning and thermal feasibility of the system, CFD analysis was done for four different configurations to find the optimum configuration using ANSYS Fluent. After finalizing the design, a prototype experimental setup was developed and tested using an induction heater to ensure proper thermosiphon of HTF and boiling process in the cooking vessels. Experimental results showed close resemblance to the simulation results of thermosiphon for a thermosiphon height of 0.63 m.

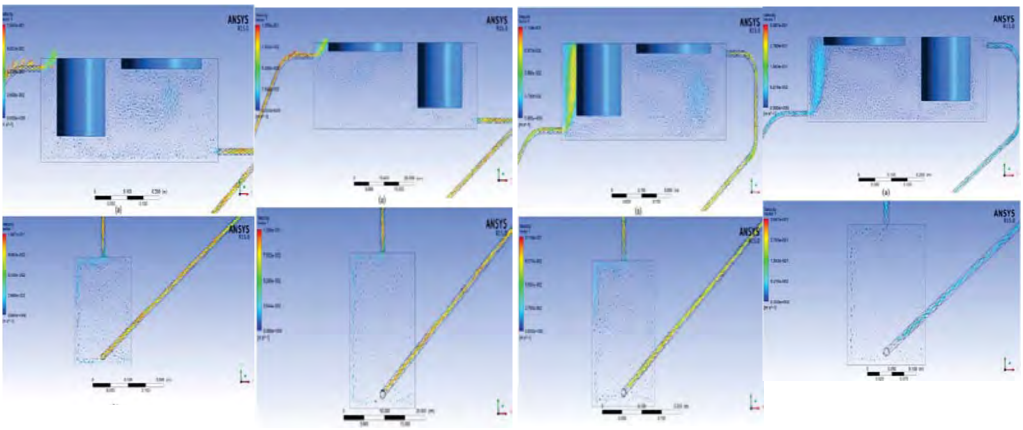

Figure 1 Simulation of Configuration A, B, C, and D

REFERENCES

[1] Daioglou, Vassilis, Bas J. van Ruijven, and Detlef P. van Vuuren. 2012. "Model Projections for Household Energy Use in Developing Countries." Energy 37 (1): 601–615.Gross, A. W.: Gas film lubrication, John Wiley and Sons, New York.

[2] Pohekar, S. D., Dinesh Kumar, and M. Ramachandran. 2005. "Dissemination of Cooking Energy Alternatives in India - A Review." Renewable and Sustainable Energy Reviews 9 (4): 379–93.

[3] Bansal, Mohit, R. P. Saini, and D. K. Khatod. 2013. "Development of Cooking Sector in Rural Areas in India - A Review." Renewable and Sustainable Energy Reviews 17: 44–53.

[4] "Energy Demand." 2014. In TERI Energy & Environment Data Directory and Yearbook 2013/14, 263–285. TERI.

[5] Singh, et al.,2021, "A new methodology to find out cooking energy needs for a rural household", Int. J. Environ. Sustain. Dev., 20 (3/4) (2021), pp.255-263,10.1504/IJESD.2021.116854.

[6] Kalogirou, Soteris A. 2004. "Solar Thermal Collectors and Applications." Progress in Energy and Combustion Science 30 (3): 231–295.

[7] Rural folk of Village Dhab ka nala, Jaipur, interview by Hemant Raj Singh. 2016. Survey done at Village Dhab ka nala, Jaipur.

[8] Hannani, S. K., E. Hessari, M. Fardadi, and M. K. Jeddi. 2006. "Mathematical Modeling of Cooking Pots' Thermal Efficiency Using a Combined Experimental and Neural Network Method." Energy 31 (14): 2633–49.

[9] Santhi Rekha, S.M., and S. Sukchai. 2018. "Design of Phase Change Material Based Domestic Solar Cooking System for Both Indoor and Outdoor Cooking Applications." Journal of Solar Energy Engineering, Transactions of the ASME 140 (4): 1–8.

[10] Kuhnke, Klaus; Reuber, and Detlef; Marianne; Schwefel. 1997, "Solar Cookers in the Third World: Evaluation of the Prerequisites, Prospects and Impacts of an Innovative Technology". 1st ed. Springer.

[11] Santhi Rekha, S.M., and S. Sukchai. 2018. "Design of Phase Change Material Based Domestic Solar Cooking System for Both Indoor and Outdoor Cooking Applications." Journal of Solar Energy Engineering, Transactions of the ASME 140 (4): 1–8.

[12] Ruelas, José, Gabriel Pando, Baldomero Lucero, and Juan Tzab. 2014. "Ray Tracing Study to Determine the Characteristics of the Solar Image in the Receiver for a Scheffler-Type Solar Concentrator Coupled with a Stirling Engine." Energy Procedia 57: 2858–2866.

[13] Scheffler, W., 2006. Introduction to the revolutionary design of Scheffler. In: SCIs International Solar Cooker Conference, Granada, Spain

[14] Munir, A., O. Hensel, and Wolfgang Scheffler. 2010. "Design Principle and Calculations of a Scheffler Fixed Focus Concentrator for Medium Temperature Applications." Solar Energy 84: 1490–1502.

[15] Singh, H.R., Sharma, D,; "Thermal Performance Assessment Review of the Solar Concentrator System's Receiver Utilized for High-Temperature Applications" Advancements in Nanotechnology for Energy and Environment; ISBN: 978-981-19-5200-5, Ch:7,(2022), Springer Singapore; https://link.springer.com/book/9789811952036.

[16] Habib, Gazala, Chandra Venkataraman, Manish Shrivastava, Rangan Banerjee, J. W. Stehr, and Russell R. Dickerson. 2004. "New Methodology for Estimating Biofuel Consumption for Cooking: Atmospheric Emissions of Black Carbon and Sulfur Dioxide from India." Global Biogeochemical Cycles 18 (3): 1–11.

[17] Muthusivagami, R. M., R. Velraj, and R. Sethumadhavan. 2010, "Solar Cookers with and without Thermal Storage-A Review." Renewable and Sustainable Energy Reviews 14 (2): 691–701.

[18] Ogie, Nosa Andrew, Ikponmwosa Oghogho, and Julius Jesumirewhe, 2013. "Design and Construction of a Solar Water Heater Based on the Thermosiphon Principle." Journal of Fundamentals of Renewable Energy and Applications 3: 1–8. https://doi.org/10.4303/jfrea/235592.

[19] Purohit, Pallav. 2009, "Economic Potential of Biomass Gasification Projects under Clean Development Mechanism in India." Journal of Cleaner Production 17 (2): 181–93.

[20] Holman, J. P.,2012, "Experimental Methods for Engineers", McGraw Hill. https://doi.org/10.1016/0894-1777(94)90118-x.

[21] Lassahn, G. D., 1985, "Uncertainty Definition," ASME J. Fluids Eng.,107(2), p. 179.

[22] Kalogirou, 2013. "Solar Energy Engineering Processes and Systems": Academic Press.

2nd International Conference on Mathematical Modelling in Mechanics and Engineering
Mathematical Institute SANU, 12-14. September, 2024.

SCIENTIFIC APPROACH OF FOUR-DIMENSIONAL PRINTING OF CITY WIND TURBINES

Nikolay Zlatov[1], Krastimir Popov[2] and Georgi Hristov[3]

[1] *Institute of Mechanics – BAS, Acad. G. Bontchev St., bl. 4, 1113 Sofia, Bulgaria*
[2]*-Institute of Mechanics – BAS, Acad. G. Bontchev St., bl. 4, 1113 Sofia, Bulgaria*
[3]*-University of Ruse, 8 Studentska Str., POB 7017, Ruse, Bulgaria*
[1]zlatovn@hotmail.com; [2]krastimirp@yahoo.com; [3] ghristov@uni-ruse.bg
ORCID iD: [1]0000-0003-4063-8730

Keywords: Renewable energy, Mechanics, Simulations, Engineering.

ABSTRACT

This studies have focused on enhancing and ensuring maximum efficiency and commercial viability of city wind turbines, including Savonius, Darrieus, Ugrinksy, and their hybrid combinations. To address this, the present research explores a novel approach incorporating design, optimization, and 4D printing (which combines 3D printing with a fourth-time dimension, enabling independent printed components to self-assemble after agitation) for selected city-appropriate wind turbine types. The research objective is to outline a methodology that facilitates the design and preparation of wind turbines for successful 4D printing. This sustainable approach aims to improve wind turbine efficiency by utilizing smart blades and hybrid models.

By employing this new methodology, we can foster the production, testing, and viability assessment of wind turbines in urban settings, paving the way for greater sustainable energy generation in cities.

2nd International Conference on Mathematical Modelling in Mechanics and Engineering
Mathematical Institute SANU, 12-14. September, 2024.

APPLICATION OF MANIFOLD LEARNING TECHNIQUES TO SEVERAL ACTUATED FLOW CONFIGURATIONS

Alicia Rodríguez-Asensio[1*], Stefano Discetti[2] and Andrea Ianiro[3]

[1,2,3]*Department of Aerospace Engineering, Universidad Carlos III de Madrid, Av. de la Universidad 30, Leganés, 28911, Madrid, Spain*

[*]*alirodri@pa.uc3m.es*

ORCID iD: [1]0009-0001-3848-4691; [2]0000-0001-9025-1505; [3]0000-0001-7342-4814

Keywords: Dimensionality Reduction, Manifold Learning, PCA, kPCA, MDS, ISOMAP, LLE.

ABSTRACT

The complex and turbulent dynamics of three-dimensional flows represent a challenge for real-time sensing and control strategies. The importance of turbulence in fields like automotive or aviation motivated numerous research activities focused on drag reduction, unsteady loads, or mixing-enhancing, in an attempt to develop simplified models for engineering control applications for problems of unbounded shear flows, such as jets and wakes.

Despite their inherent multi-scale nature and high dimensionality, turbulent flows exhibit recurrent patterns known as coherent structures. This observation hints at the possibility of representing some important flow dynamics as evolving on a low-dimensional attractor, thereby enabling the dimensionality reduction into simpler dynamics. Special attention has been paid to manifold learning, which aims to identify a low-dimensional surface, referred to as the manifold, in close proximity to where the dataset is located. Farzamnik *et al.* 2023 demonstrated that many shear flows can be effectively described with a low-dimensional manifold.

However, while these techniques have proven successful for flow estimation in the absence of control actions, it must be recognized that the introduction of control inputs alters the flow dynamics, thereby affecting the manifold itself. Consequently, any data-driven model must be trained within the context of such control actuation to accurately identify the state of the actuated system. This presents a significant challenge for manifold-based control strategies, as the presence of control inputs complicates the utilization of low-order models or manifolds to discern control dynamics, given that the control inputs modify the system dynamics itself.

The present work serves as a comparison between some key data-driven linear and nonlinear manifold learning techniques. The following techniques are highlighted: standard and kernel Principal Component Analysis (kPCA, Schölkopf *et al*. 1997), Multidimensional Scaling (MDS, Cox and Cox 2008), isometric featuring mapping (ISOMAP, Tenenbaum *et al*. 2000) and Local Linear Embedding (LLE, Roweis and Saul 2000). For this purpose, the fluidic pinball (Noack and Morzynki 2017) is chosen as a test case. The fluidic pinball is a configuration of three cylinders invested by a uniform flow, whose rotation can be controlled independently to manipulate the flow. This test case represents an excellent multiple-input multiple-output benchmark due to its simple dynamics. Nonetheless, the wide range of control possibilities makes this approach more intricate, being able to produce an extensive span of flow configurations.

In this document, a simplified dataset of the fluidic pinball is utilized. None of the cylinders rotate and the Reynolds number is set to $Re = 130$, entering into the chaotic regime. The low-dimensional manifolds obtained with PCA, kPCA, MDS and ISOMAP are gathered in Figure 1. We anticipate that non-linear manifold learning techniques allow to obtain a clearer representation of the flow evolution.

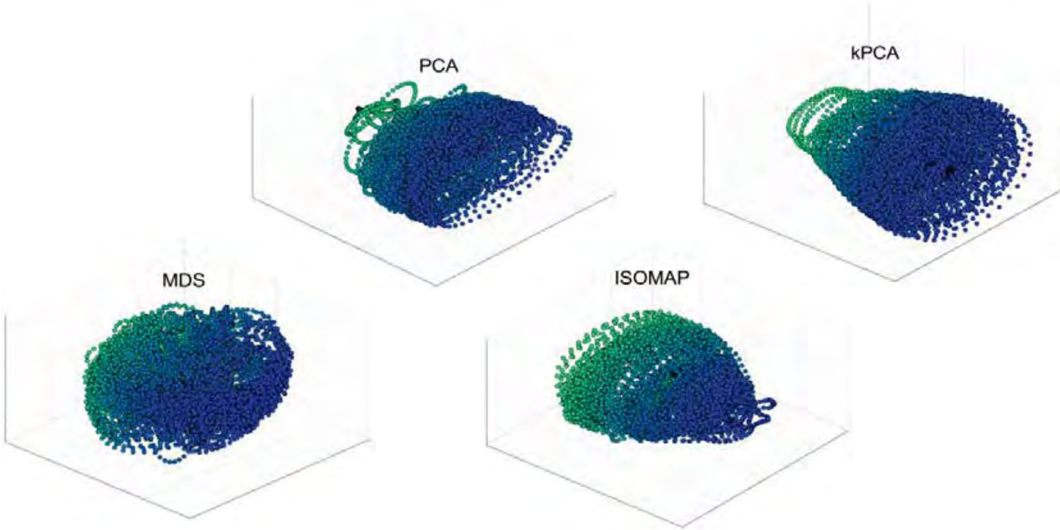

Figure 4. Three-dimensional embedded manifolds of the fluidic pinball at Re=130 for PCA, kPCA, MDS and ISOMAP

ACKNOWLEDGEMENTS

This work is part of the project EXCALIBUR (Grant No PID2022-138314NB-I00), funded by MCIU/AEI/ 10.13039/501100011033 and by “ERDF A way of making Europe”

REFERENCES

[1] Chen, C. H., Härdle, W., Unwin, A., Cox, M. A., & Cox, T. F. (2008). “Multidimensional scaling” (pp. 315-347). *Springer Berlin Heidelberg*.
[2] Farzamnik, E., Ianiro, A., Discetti, S., Deng, N., Oberleithner, K., Noack, B. R., & Guerrero, V. (2023). “From snapshots to manifolds–a tale of shear flows”. *Journal of Fluid Mechanics*, 955, A34.
[3] Noack, B. R., & Morzynski, M. 2017 “The fluidic pinball– a toolkit for multiple-input multiple-output flow control (version 1.0)”. Tech. Rep. 02/2017 Chair of Virtual Engineering, Institute of Combustion Engines and Transport, Poznan University of Technology, Poland.
[4] Roweis, S. T., & Saul, L. K. (2000). “Nonlinear dimensionality reduction by locally linear embedding”. *science*, 290(5500), 2323-2326.
[5] Schölkopf, B., Smola, A., & Müller, K. R. (1997, October). “Kernel principal component analysis. In International conference on artificial neural networks” (pp. 583-588). Berlin, Heidelberg: *Springer Berlin Heidelberg*.
[6] Tenenbaum, J. B., Silva, V. D., & Langford, J. C. (2000). “A global geometric framework for nonlinear dimensionality reduction”. *science*, 290(5500), 2319-2323.

2nd International Conference on Mathematical
Modelling in Mechanics and Engineering
Mathematical Institute SANU, 12-14. September, 2024.

ROBUST BIO-INSPIRED SHAPE OPTIMIZATION OF STRUCTURES

Chunmei Liu[1], Renata Troian[1] and Eduardo Souza de Cursi[1]

[1]*LMN, INSA Rouen Normandy, 76800 Rouen, France*

[1]*liu_chunmei05@163.com*

Keywords: bio-inspired design, shape optimization, robust design, IGA, uncertainties.

ABSTRACT

Biological structures typically generate a uniform strain field to avoid overloading or underutilizing material. Inspired by the branching architecture of trees in nature, we formulated bio-inspired criteria for uniform strain distribution, which are used as objective functions in the shape optimization process[1-4].

We developed a framework for robust bio-inspired shape optimization of statically loaded structures, based on isogeometric analysis (IGA)[5], which accounts for geometrical uncertainties arising during manufacturing. As shown in the figure, the key steps include:

(1) design variables are about some control points of the geometric model;
(2) computer-aided design model is established based on IGA;
(3) the Latin hypercube sampling[6] is adopted to obtain the geometrical uncertainties sampling points;
(4) IGA method is employed to analyze the structure model of each sampling case based on the sampling data, obtaining the strain values of each node of the discretized element in the physical space through numerical simulation;
(5) bio-inspired criteria are applied as objective functions;
(6) the non-dominated sorting genetic algorithm-II (NSGA-II)[7] is chosen as the optimization algorithm to update design variables to obtain the Pareto front;
(7) the level diagrams method[8] is regarded as the technique for visualization to select the optimal design.

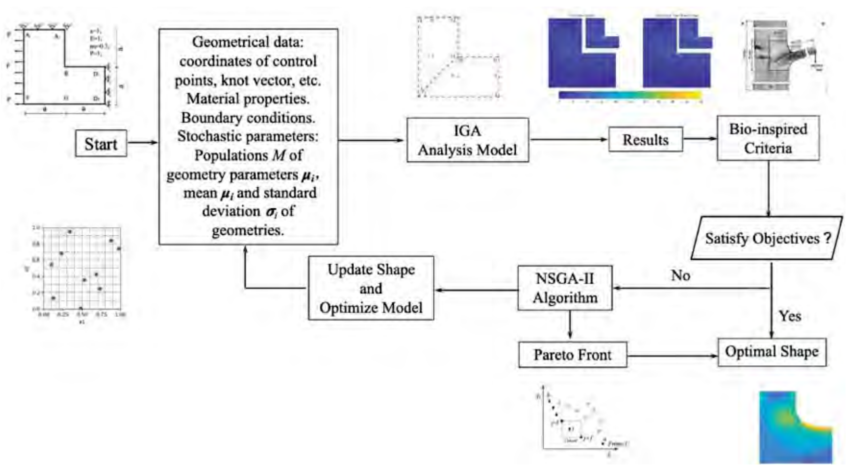

Fig. The framework for robust bio-inspired shape optimization.

Finally, we compare the bio-inspired criteria for uniform strain distribution with classical criteria for strain minimization. The results show that bio-inspired criteria achieve a more uniform strain distribution and reduced strain in each element. While classical criteria provide acceptable results, bio-inspired criteria offer a more preferable outcome for designers. This research provides new criteria for structural robust design.

REFERENCES

[1] C. Mattheck. Design in nature: learning from trees. Springer Science & Business Media, 1998.
[2] U. Müller, W. Gindl, and G. Jeronimidis. Biomechanics of a branch-stem junction in softwood. Trees 2006; 20, 643 – 648.
[3] B. Wilson, B and R. Archer. Tree design - some biological solutions to mechanical problems. Bioscience 1979; 29, 293 – 298.
[4] T. Dean, S. Roberts, D. Gilmore, D. Maguire, J. Long, K. O'Hara, and R. Seymour. An evaluation of the uniform stress hypothesis based on stem geometry in selected North American conifers. Trees; 2002; 16, 559-568.
[5] V. Agrawal, S S. Gautam. IGA: a simplified introduction and implementation details for finite element users[J]. Journal of The Institution of Engineers (India): Series C, 2019, 100(3): 561-585.
[6] Anders MJ Olsson and Göran E Sandberg. Latin hypercube sampling for stochastic finite element analysis. Journal of Engineering Mechanics, 128(1):121–125, 2002.
[7] K.Deb, A. Pratap, S. Agarwal, et al. A fast and elitist multiobjective genetic algorithm: NSGA-II[J]. IEEE transactions on evolutionary computation, 2002, 6(2): 182-197.
[8] Xavier Blasco, Juan M Herrero, Javier Sanchis, and Manuel Martínez. A new graphical visualization of n-dimensional pareto front for decision-making in multiobjective optimization. Information Sciences, 178(20):3908–3924, 2008.

COMPUTATIONAL STUDY OF COMBINED FUEL INJECTION APPROACHES IN SUPERSONIC COMBUSTOR

Gautam Choubey[1], Gurkreetkaur Brar[2]

[1]*Department of Mechanical Engineering, NIT Silchar, Assam 788010, India*

[2] *Department of Mechanical and Aerospace Engineering, IITRAM Ahmedabad, 380026, India*

[1]*gautamchoubey@mech.nits.ac.in*; [2] *gurkreetkaur.brar.19m@iitram.ac.in*

Keywords: Scramjet combustor; combined fuel injection approaches; H_2 fuel; mixing augmentation

ABSTRACT

The aviation sector employs various air-breathing engines for propulsion. The adoption of scramjet engines holds significant promise for high-speed air and space travel innovation. However, optimizing the combustion process within scramjet engines poses a complex challenge due to the extreme flow conditions. This study focuses on understanding the combustion mechanism within a scramjet combustor, specifically concentrating on designing and enhancing the fuel injection system. Using 2D-RANS reactive flow simulations and a simplified chemical kinetics model, the research investigates the impact of different strut + cavity injection configurations as potential flame stabilizers on supersonic reacting flow. The simulations indicate that scramjets employing strut + cavity configurations generate stronger shockwaves compared to those without cavities, leading to pronounced recirculation zones. Moreover, the presence of cavities prolongs air residence time within the combustor, promoting stable combustion.

Computational modelling

Unsteady RANS simulations were performed using the governing equations and species transport equations. An implicit formulation and the advection upstream splitting method (AUSM) were utilized in a density-based solver, employing a second-order upwind discretization technique to solve the governing equations [1]. The *SST K-ω* model was chosen as the turbulence model [2]. To ensure standard acceptable stability, the Courant number was set to 0.5.

Results and Discussion

In the preliminary study, computational simulations were carried out to comprehend various flow parameters and their effects. This involved analyzing the boundary layer separations, recirculation region, mixing and total pressure losses. This enables an analysis of the impact of different combined fuel injector's effects on supersonic combustion. These insights can contribute to the effective design of engines under working conditions. A detailed analysis can be further conducted by examining the various contours produced by the simulations.

Outlook for Complete Paper

The potential outcomes of the complete paper involve offering in-depth insights into turbulent combustion and fuel injection strategies within supersonic combustors. Additionally, it aims to provide a thorough examination of the effectiveness of passive mixing mechanisms in combined strut and cavity-based designs. These findings are anticipated to improve engine efficiency and offer valuable guidance for the development of future practical scramjet engines.

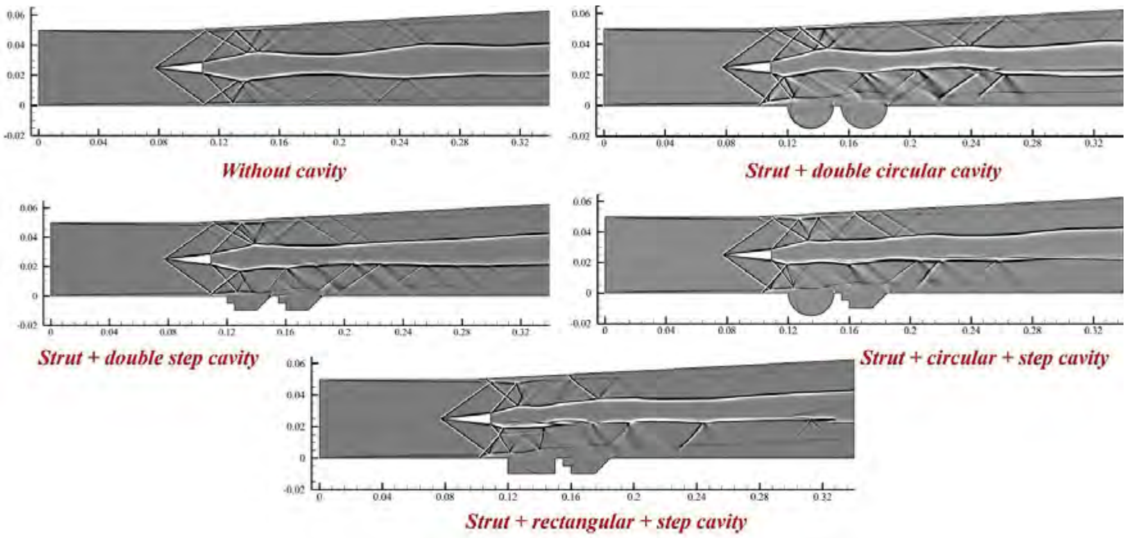

***Fig. 1** Numerical schlieren for different fuel injectors*

REFERENCES

[1] Choubey G, et al (2023), "Effect of different strut design on the mixing performance of H2 fueled two-strut based scramjet combustor, Fuel, 351, pp.128972.
[2] Menter F R, (1994), "Two-equation eddy-viscosity turbulence models for engineering applications", AIAA J, 32 (8), pp. 1598-1605

3D FINITE ELEMENT ANALYSIS OF FRICTION BETWEEN PDMS MICRO-PILLAR BIOMIMETIC TEXTURE AND SIO2

Nikolaos Rogkas[1,2], Anna Maniou[1], Dimitrios Skondras-Gousios[1], Georgios Vasileiou[1], Pavlos Zalimidis[2] and Vasilios Spitas[1]

[1]*School of Mechanical Engineering, National Technical University of Athen NTUA, Athens, Greece, e-mail: nrogkas@mail.ntua.gr ORCID ID: 0000-0002-4581-5639*

[1]*School of Mechanical Engineering, National Technical University of Athen NTUA, Athens, Greece, e-mail: annamaniou07@gmail.com ORCID ID: 0009-0009-0081-418X*

[1]*School of Mechanical Engineering, National Technical University of Athen NTUA, Athens, Greece, e-mail: di-sko@hotmail.com ORCID ID: 0000-0001-8770-0568*

[1]*School of Mechanical Engineering, National Technical University of Athen NTUA, Athens, Greece, e-mail: gvasileiou@mail.ntua.gr ORCID ID: 0000-0003-3496-0619*

[2]*Department of Mechanical Engineering Educators, School of Pedagogical and Technological Education, Athens, Greece, email: pzalimidis@aspete.gr ORCID ID:-*

[1]*School of Mechanical Engineering, National Technical University of Athen NTUA, Athens, Greece, e-mail: vspitas@mail.ntua.gr ORCID ID: 0000-0003-3999-7752*

Keywords: Surface texturing, biomimetics, micro-pillar, friction, finite element analysis

ABSTRACT

Surface texturing plays a crucial role in tribology, impacting various engineering applications [1] and the use of biomimetic surface texturing in areas where friction is significant, is an ongoing field of research [2]. Nature provides numerous examples that inspire these advancements, such as the textured surfaces of snakeskin for reduced friction [3], shark skin for drag reduction [4], gecko feet for enhanced adhesion and friction [5], frog legs for optimized movement in water [6], and lotus leaves for their water-repellent properties that can reduce drag [7]. These natural surfaces offer insights and solutions that enhance human technology and efficiency, leading to innovations that improve performance, durability, and sustainability across various industries.

This study investigates the potential of tapered micro-pillars, inspired by gecko feet, to enhance friction control properties on textured surfaces. Specifically, it examines the contact interaction between a textured PDMS surface and a curved SiO_2 surface, aligning with the work presented in [8]. This research is part of the research project “WerSURF: From Micro to Macro Scale: Nature-Inspired Hierarchical Surfaces for Tribology”, funded by the Basic Research Program of National Technical University of Athens. To investigate this, a 3D numerical model was developed using COMSOL software employing the Finite Element Method (FEM). Initially, the texture surface geometry was parametrized using CAD tools, allowing for the examination of a sufficient number of design points (different aspect ratio, number of pillars, etc.). The analysis was conducted as a time-dependent study, utilizing the structural mechanics solver. The computational domain was defined as a square with dimensions of 500 x 500 μm while the pillar height was equal to 150 μm and its diameter was varying between 75 μm and 40 μm. Several assumptions were made, including a constant friction coefficient throughout

the simulation. The boundary conditions involved the application of axial pretension to induce the required normal load, along with a specified relative velocity of 10 μm/s imposed to the curved SiO_2 surface.

Figure 1. illustrates the response of the x-component of the total reaction force on the fixed PDMS surface. It showcases the overall behavior of a one-pillar case study, involving the engagement, deflection and disengagement of the pillar which leads to an almost constant force of increase magnitude throughout this timespan, emphasizing the significant impact of the investigated texture on the friction coefficient.

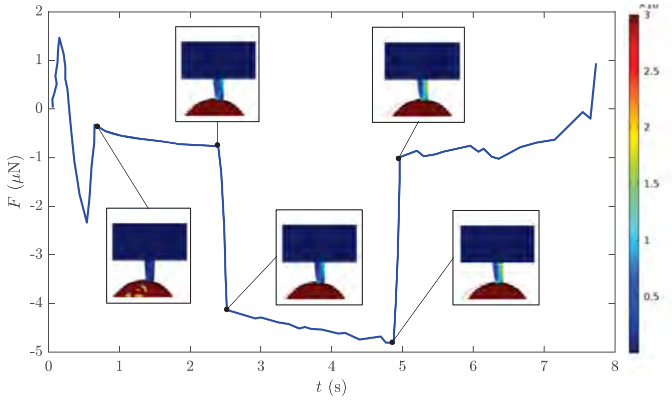

Figure 1. Reaction force (x-component) response along with Von Mises stress contours at characteristic timesteps.

REFERENCES

[1] Lu P, Wood RJK. Tribological performance of surface texturing in mechanical applications—A review. Surface Topography: Metrology and Properties. 2020;8:043001.

[2] Sharma SK, Grewal HS. Tribological Behavior of Bioinspired Surfaces. Biomimetics. 2023;8:62.

[3] Greiner C, Schäfer M. Bio-inspired scale-like surface textures and their tribological properties. Bioinspiration & biomimetics. 2015;10:044001.

[4] Bixler GD, Bhushan B. Fluid drag reduction with shark-skin riblet inspired microstructured surfaces. Advanced Functional Materials. 2013;23:4507-28.

[5] Tian Y, Pesika N, Zeng H, Rosenberg K, Zhao B, McGuiggan P, et al. Adhesion and friction in gecko toe attachment and detachment. Proceedings of the National Academy of Sciences. 2006;103:19320-5.

[6] Meng F, Liu Q, Wang X, Tan D, Xue L, Barnes WJP. Tree frog adhesion biomimetics: opportunities for the development of new, smart adhesives that adhere under wet conditions. Philosophical Transactions of the Royal Society A. 2019;377:20190131.

[7] Lu Y. Fabrication of a lotus leaf-like hierarchical structure to induce an air lubricant for drag reduction. Surface and Coatings Technology. 2017;331:48-56.

[8] Skondras-Giousios D, Karkalos NE, Markopoulos AP. Finite element simulation of friction and adhesion attributed contact of bio-inspired gecko-mimetic PDMS micro-flaps with SiO2 spherical surface. Bioinspiration & Biomimetics. 2020;15:066004.

2nd International Conference on Mathematical Modelling in Mechanics and Engineering
Mathematical Institute SANU, 12-14. September, 2024.

AVERAGE VELOCITY FIELD DOWNSTREAM DISTRIBUTIONS IN THE FREE TURBULENT SWIRLING JET GENERATED BY THE AXIAL FAN IMPELLER WITH TWISTED BLADES

Novica Z. Janković[1], Đorđe S. Čantrak[2] and Dejan B. Ilić[3]

Faculty of Mechanical Engineering, University of Belgrade, 11000 Belgrade, Serbia

[1]njankovic@mas.bg.ac.rs; [2]djcantrak@mas.bg.ac.rs; [3]dilic@mas.bg.ac.rs

ORCID iD: [1]0000-0003-2645-8602; [2]0000-0003-1841-9187; [3]0000-0003-4562-8881

Keywords: Turbulence, Swirling Flow, Jet, Axial Fan, three-component LDV

ABSTRACT

Some contributions to the research of the turbulent swirling flow in jet behind the axial fan impeller with twisted blades is presented in this paper. Numerous measurements and profound analysis are presented in [1]. Experimental investigation is performed by use of the three-component laser Doppler velocimetry (LDV) system [1, 2]. Previous optical based measurements of the turbulent swirling flow in pipe and diffuser have been performed and presented in [3, 4], respectively. A good overview of the literature is provided in [1, 3, 4].

The generated turbulent swirling flow is three-dimensional, inhomogeneous and anisotropic. Complex experimental, numerical and theoretical approaches were applied. Here is analyzed three dimensional time-averaged velocity field c (U, V, W), where c is total velocity, while U is axial, V radial and W circumferential velocity components. This velocity field is very complex, characterized by inhomogeneity and distinct gradients, especially in the radial direction.

Axial fan impeller has blades with variable angle and here is adjusted angle 30° at the axial fan outer diameter which is 0.399 m. This is denoted as the ZP30. Measurements have been performed in ten measurement sections along vertical directions [1, 2]. Measuring sections along the axial fan rotating axis are x = 300, 400, 600, 800, 1000, 1200, 1400, 1600, 1800 and 2000 mm. Here are presented measurements for the axial fan rotation speed n = 1500 rpm.

In Figure 1.a are presented experimentally obtained distributions of the total velocity c along the axis and radius, i.e. $c=c(r, x)$. The development of the flow is observed and continuous deformation of the velocity profile with gradients in the radial and axial directions occur.

Circumferential velocity (W) significantly deforms profile of the axial velocity (U), which is thoroughly discussed in this paper. Radial velocity (V) development and distribution are also correlated with the presence and distribution of the circumferential velocity, what will be also analyzed in the paper.

In Figure 1.b are presented distributions of all three velocity components $U_i = U$, V and W for ZP30 and the same fan rotation speed in section III, where x = 600 mm. U_m is average velocity, which is for this III measuring section and fan rotation speed n = 1500 rpm, U_m = 12.57 m/s. Reynolds number is Re = 358951. Average circulation is calculated after the following equation:

$$\Gamma = 4\pi^2 R^3 \int_0^1 k^2\, UW \mathrm{d}k / Q, \text{ where } k = r/R.$$

It has value Γ = 4.93 m^2/s.

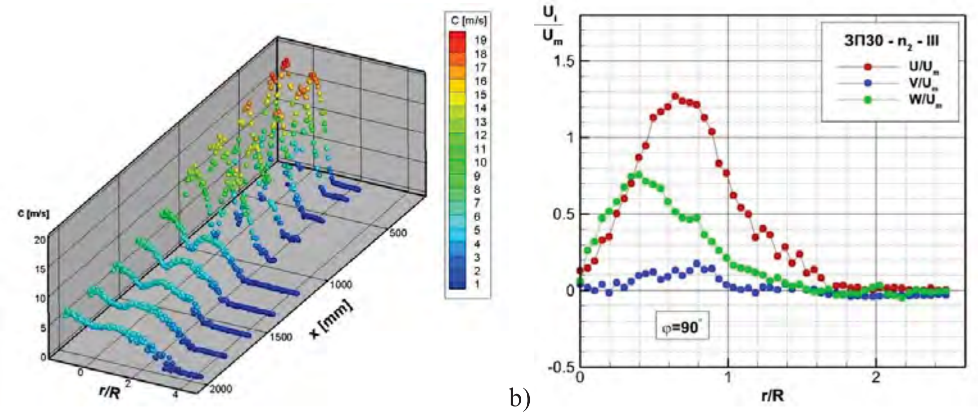

a) b)

Figure 1. a) Total velocity distributions c = c(r, x) for ZP30 and n = 1500 rpm and b) all three velocities (U_i = U, V and W) distributions in the III section, i.e. x = 600 mm.

The presented empirical profiles of all three velocities show that in addition to the global maxima (within the respective sections), for example for section III (Figure 1.b), U_{max} is reached for $r/R \approx 0.65$ and W_{max} for $r/R \approx 0.4$, there is also a significant number of local maxima for all three velocity components. The complexity of the structure of the averaged velocity field becomes even more obvious when to the previous elements is added the presence of heterogeneous changes of the $\partial_r U_i$ for all three components in the radial direction of the turbulent swirling jet, what will be, also, discussed in the paper.

Ackwnoledgments

The results presented in this paper are the result of the research supported by the Ministry of Science, Technological Development and Innovation of the Republic of Serbia under the Agreement on financing the scientific research work of teaching staff at accredited higher education institutions in 2024, no. 451-03-65/2024-03/200105 dated on February 5th, 2024.

REFERENCES

[1]Janković, N.Z. (2020), “Experimental and theoretical research of the structure of turbulent swirl flow in axial fan jet”, *Doctoral dissertation,* Faculty of Mechanical Engineering, University of Belgrade, Belgrade, Serbia.

[2]Janković, N.Z. (2017), “Investigation of the free turbulent swirl jet behind the axial fan”, *Thermal Science,* Vol. 21, Suppl. 3, Belgrade, Serbia, pp. S771-S782.

[3]Čantrak, Đ.S. (2012), “Analysis of the vortex core and turbulence structure behind axial fans in a straight pipe using PIV, LDA and HWA methods”, *Doctoral dissertation,* Faculty of Mechanical Engineering, University of Belgrade, Belgrade, Serbia.

[4] Ilić, D.B. (2013), “Swirl flow in conical diffusers”, *Doctoral dissertation,* Faculty of Mechanical Engineering, University of Belgrade, Belgrade, Serbia.

MULTI-MEMBRANES-BASED PUMPING FLOW OF NANOFLUIDS: APPLICATION IN THERMOFLUIDS SYSTEM

Anjali Bhardwaj *; Dharmendra Tripathi

Department of Mathematics, National Institute of Technology, Uttarakhand, Srinagar-246174, India

[1]anjalibhardwaj183@gmail.com; [2]dtripathi@nituk.ac.in

ORCID iD: [1]0009-0000-4420-3297; [2]0000-0003-4798-1021

Keywords: Nanofluid, Heat Transfer and mass transfer, Entropy Generation, membrane pumping mechanism, phase(time) lag parameter.

ABSTRACT

Objective

The microscale heat transfer is now very much essential to analyse and applicable in various smart thermal devices like microchannel heat sinks, micro heat pipes, thermosyphon, and micro heat exchangers, etc. The present analysis discussed the heat and mass transfer in nanofluids flow driven by multi-membranes pumping mechanisms (Ghost-Valve model).

Methodology

Analytical solutions have been obtained for governing equations (continuity, momentum, energy and concentration equation) through dimensional analysis and the lubrication technique, and MATLAB software has been employed for graphical results. The results demonstrate the impact of operational parameters on axial velocity, transverse velocity, stream function, pressure gradient, temperature profile, nanoparticle fraction profile, volumetric flow rate and wall shear stress.

Key Outcomes

A larger time phase lag diminishes the contraction for the first membrane as compared to the second membrane, which alleviate the reverse flow and promoting forward fluid movement. It is further reported that the membrane-based pump can effectively control micro level fluid flow and heat transfer in microchannel.

Applications and Future Scope

This model explores the applications in various fields where precise control of fluid flow and heat transfer is essential, such as electronics cooling, energy conversion, desalination, and biomedical devices.

REFERENCES

[1] Iverson, Brian D., and Suresh V. Garimella. "Recent advances in microscale pumping technologies: a review and evaluation." Microfluidics and nanofluidics 5 (2008): 145-174.

[2] Aboelkassem, Yasser, and Anne E. Staples. "A bioinspired pumping model for flow in a microtube with rhythmic wall contractions." Journal of Fluids and Structures 42 (2013):

[3] Aboelkassem, Yasser. "A ghost-valve micropumping paradigm for biomedical applications." Biomedical Engineering Letters 5 (2015): 45-50.

[4] Jakeer, Shaik, and S. R. R. Reddy. "Electrokinetic membrane pumping flow of hybrid nanofluid in a vertical microtube with heat source/sink effect." The European Physical Journal Plus

NUMERICAL SEISMIC RESPONSE EVALUATION OF CHEVRON BRACED FRAME WITH TADAS DAMPER

Marin Grubišić

University of Osijek, Faculty of Civil Engineering and Architecture Osijek, Osijek, Croatia

marin.grubisic@gfos.hr, ORCID: 0000-0001-8674-0082

Keywords: steel frames, seismic strengthening, TADAS dissipative element, numerical modelling, *OpenSees*

ABSTRACT

The aim of this study is to evaluate the feasibility of seismically strengthening existing steel frames. Through computational analysis of a bare frame, two methods of seismic strengthening were proposed. The expected behaviour of each of the three tested steel frames was determined through initial iterative calculations using numerical models. The dimensions for the two strengthening methods were derived from the numerical analysis of the bare frame: one employing a specialised inverted V-bracing (Chevron) system, and the other using a dissipative TADAS connection. The study explored two seismic strengthening methods for steel frames: Inverted V-bracing (Chevron) system and Dissipative TADAS connection. These methods were designed to improve the load-bearing capacity while maintaining or enhancing ductility. Computational models helped establish the dimensions for both strengthening techniques. The strengthened frames, along with a bare frame, were subjected to static reversed cyclic displacement control tests up to failure, following FEMA 461 standards.

- Bare Frame (BF): The testing of the BF and TADAS frame (TF) was halted due to significant global out-of-plane instability. The ductility and stiffness of the BF were used as benchmarks for comparison.
- Chevron Frame (CF): Testing was discontinued following brace tensile failure. The CF showed 0.6 times lower ductility and 5 times higher initial stiffness compared to the BF.
- TADAS Frame (TF): The TF exhibited 1.4 times higher ductility and 2 times higher initial stiffness compared to the BF. Notably, the TF dissipated 4 times more energy at the point of failure than the CF, indicating superior performance in energy dissipation.

The cyclic responses of all specimens displayed symmetrical behaviour. The maximum lateral load capacity for the CF was twice as high as the BF, and for the TF, it was three times higher. The study concluded that both Chevron and TADAS strengthening methods significantly enhance the seismic performance of steel frames. The CF provided higher stiffness but lower ductility, while the TF offered a balanced improvement in both stiffness and ductility. The TF's ability to dissipate energy was notably higher, making it a preferable choice for seismic strengthening.

Key findings include:

- The CF achieved twice the lateral load-bearing capacity compared to the BF.
- The TF achieved almost three times the load-bearing capacity compared to the BF.
- The TF exhibited 32% greater displacement capacity than the CF.
- The TF dissipated 4 times more energy than the CF at the point of failure.

The study underscores the importance of careful design in maintaining the plasticization hierarchy, particularly for the TADAS element. The enhanced load-bearing capacity and energy dissipation characteristics of the TADAS frame make it an effective method for seismic strengthening of steel structures. In summary, both strengthening techniques significantly improved the seismic response of the steel frames, with the TADAS connection offering superior overall performance, which is confirmed by numerical models in *OpenSees*, covering all failure mechanisms. This research highlights the potential for applying these methods to existing structures to enhance their earthquake resilience effectively.

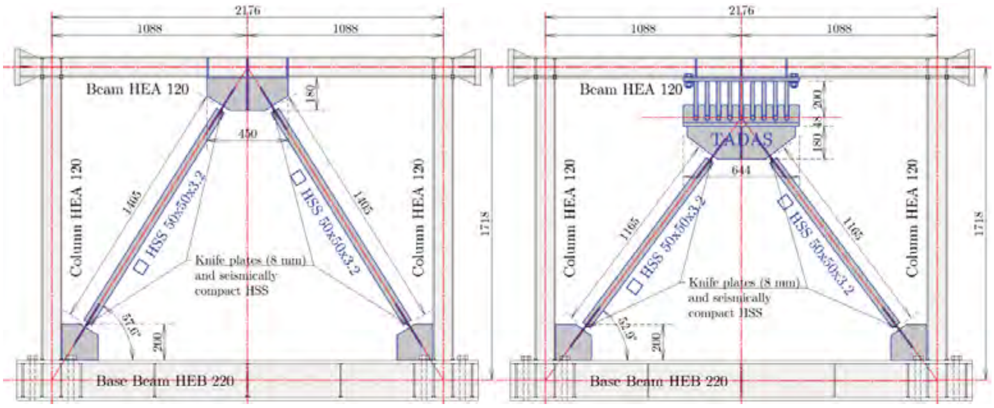

Figure 1. Geometries of steel frames: Inverted V-braced/Chevron (left) and TADAS frame (right)

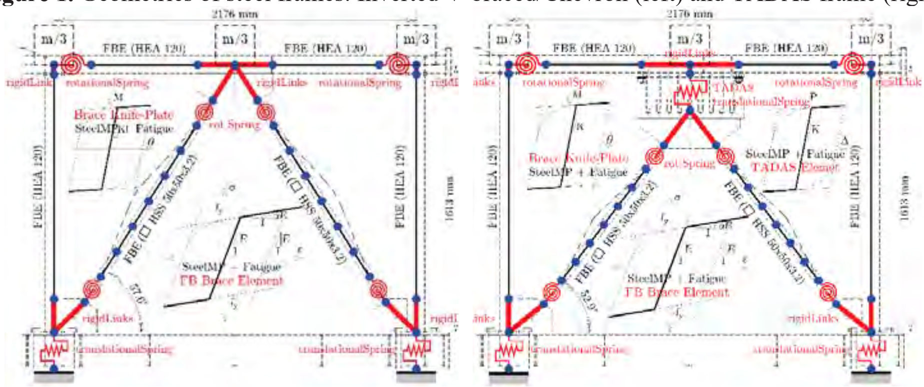

Figure 2. Representation of numerical models: Inverted V-braced/Chevron (left) and TADAS frame (right)

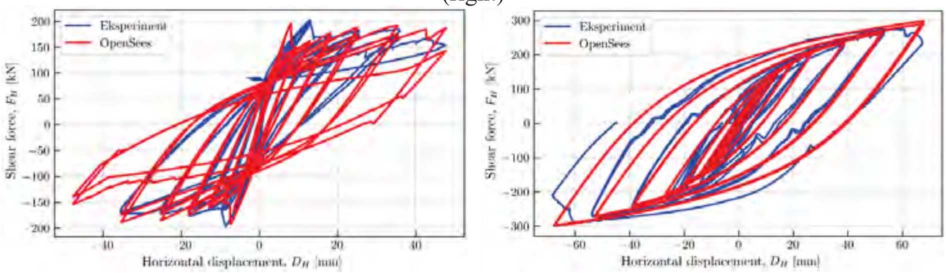

Figure 3. Global hysteresis responses: Inverted V-braced/Chevron (left) and TADAS frame (right)

REFERENCES

[1] Whittakar, A., Bertero, V., Alonso, J., Thompson, C. (1989) *Earthquake Simulator Testing of Steel Plate Added Damping and Stiffness Elements. Report No. UCB/EERC-89/02*. Earthquake Eng. Res. Centre Univ. California, Berkely, URL: https://nehrpsearch.nist.gov/static/files/NSF/PB92192988.pdf

[2] Tsai, K., Chen, H., Hong, C., Su, Y. (1993) *Design of Steel Triangular Plate Energy Absorbers for Seismic Resistant Construction.* Earthquake Spectra; 9(3): 505-28., DOI: https://doi.org/10.1193/1.1585727

[3] McKenna, F., Fenves, G. L, and Scott, M. H. (2000) *Open System for Earthquake Engineering Simulation (OpenSees)*. University of California, Berkeley, http://opensees.berkeley.edu

2nd International Conference on Mathematical
Modelling in Mechanics and Engineering
Mathematical Institute SANU, 12-14. September, 2024.

OPTIMIZATION OF CAPACITATED OPEN LOOP STOCHASTIC SUPPLY CHAIN NETWORKS UNDER UNCERTAIN DEMAND USING MODIFIED BEES ALGORITHM

Dr. Mohammad Rizwanullah[1]

[1]*Department of Mathematics and Statistics, Manipal University Jaipur, Jaipur, 303007, Rajasthan, India*

[1]rizwansal@yahoo.co.in

ORCID iD: [1]0000-0002-6270-5562

Keywords: Open Loop Supply Chain, Bee Algorithm, Stochastic Optimization, Networks.

ABSTRACT

A supply chain is a system of complex networks that connects suppliers and customers through products, services, and information flows. Its goal is to find the best route for a specific vehicle to serve a group of customers in a predetermined amount of time. In an open-loop supply chain, decisions are made at the beginning of the planning horizon without the possibility of revising them based on future information. This contrasts with closed-loop systems, where feedback and real-time information can adjust operations dynamically. A Capacitated Open Loop Stochastic Supply Chain Network (COLSSCN) refers to a supply chain model that incorporates various complexities such as capacity constraints, open-loop structure, and stochastic elements. A Modified Bee Algorithm (MBA) for Capacitated Open Loop Supply Chain Network Problem (COLSCNP) is presented in this article. This algorithm is used to find shortest path such that a distributor visits each city exactly once. The COLSCNP is an extension form of SCNP. In COLSCNP, the aim is to reduce overall transportation costs.

As a numerical problem, considered supply chain network system of a biscuit industry. The company primarily produces a wide range of biscuit products and operates in a highly competitive environment, as producers attempt to enter the biscuit business under investigation. It provides a small number of large chain store industries, and on the other, it continues to serve a lot of small retailers. As a result, the company has to deal with a number of lean SCNs. The chain store industries have a leading role in such partnerships. It was found that the goods cost, on-time delivery, and flexibility are critical metrics for the company in question. We have proposed a general optimization-based methodology to address the problem of optimally controlling a supply chain with a cost-cutting objective. The proposed work can further be extended to areas in various industrial problems including transportation, logistics, and semiconductors.

Conclusion:

In this paper, the proposed Bees Algorithm (BA) for the Capacitated Open Loop Supply Chain Network Problem (COLACNP) is able to perform good quality solutions. The result shows that algorithm has reduced cost and enhanced performance for SCNP. BA is used to obtain best fit result of a probabilistic operations research problem in this paper. This study concludes that introduced methodology is a best to obtain optimal route for distributed products from manufacturer points to customers. It is a best route for a certain vehicle with its minimum value according to demands. The algorithm's main strength is that it uses scout bees to conduct global explorations and recruiter bees to conduct local exploitation. The algorithm's main flaw, on the other hand, is that it is decision variable dependent, which means that every instance may require distinct values. The use of automatic parameter tuning strategies is something we intend to do in the future.

REFERENCES

[1] Abdel-Basset, M., Mohamed, R., Zaied, A. E. N. H., Gamal, A., & Smarandache, F. (2020). Solving the supply chain problem using the best-worst method based on a novel Plithogenic model, In Optimization Theory Based on Neutrosophic and Plithogenic Sets, pp. 1-19.

[2] Alzaqebah, M., Jawarneh, S., Sarim, H. M., & Abdullah, S. (2018). Bees' algorithm for vehicle routing problems with time windows, International Journal of Machine Learning and Computing, 8(3), pp. 236-240.

[3] Farooq, M. U., Salman, Q., Arshad, M., Khan, I., Akhtar, R., & Kim, S. (2019). An artificial bee colony algorithm based on a multi-objective framework for supplier integration, Applied Sciences, 9(3), pp. 1-14.

[4] Goodarzian, F., Shishebori, D., Nasseri, H., & Dadvar, F. (2021). A bi-objective production-distribution problem in a supply chain network under grey flexible conditions, Operations Research, 55, pp. 1287-1316.

[5] Jamhuri, J., Norizah, K., Mohd Hasmadi, I., & Azfanizam, A. S. (2021). Bee's algorithm for Forest transportation planning optimization in Malaysia.

[6]Mastrocinque, E., Yuce, B., Lambiase, A., & Packianather, M. S. (2013). A multi-objective optimization for supply chain network using the bee's algorithm, International Journal of Engineering Business Management, 5(38), pp. 1-11.

[7] Mondal, A., & Roy, S. K. (2021). Multi-objective sustainable opened-and closed-loop supply chain under mixed uncertainty during COVID-19 pandemic situation, Computers & Industrial Engineering, 159, pp.1-20.

[8] Pham, D. T., Negm, M., & Otri, S. (2008). Using the Bees Algorithm to solve a stochastic optimization problem, In 4th International Virtual Conference on Intelligent Production Machines and Systems (IPROMS), pp. 1-8.

2nd International Conference on Mathematical
Modelling in Mechanics and Engineering
Mathematical Institute SANU, 12-14. September, 2024.

MASS OPTIMIZATION OF TIMOSHENKO BEAMS BY USING THE PONTRYAGIN MAXIMUM PRINCIPLE

M. Veg [1], A. Obradović [2] and A.Tomović[3]

[1]*Faculty of MechanicalEngineering, University of Belgrade, 11000 Belgrade, Serbia*
[2]*Faculty of Mechanical Engineering, University of Belgrade, 11000 Belgrade, Serbia*
[3]*Faculty of Mechanical Engineering, University of Belgrade, 11000 Belgrade, Serbia*
[1] *mveg@mas.bg.ac.rs*; [2]*aobradovic@mas.bg.ac.rs*; [3]*atomovic@mas.bg.ac.rs*
ORCID iD: [1]0000-0002-5308-6122; [2]0000-0001-8808-6627; [3]0000-0002-8462-8086

Keywords: Vibrations, Optimal control theory, Functionally graded materials.

ABSTRACT

The mass optimization of axially functionally graded (AFG) circular Timoshenko beams is considered in this paper for a given fundamental natural frequency. The case of coupled longitudinal, bending and torsional vibrations is considered based on given boundary conditions. The Pontryagin maximum principle is applied for shape optimization with respect to the limited diameter under the constraints of structural integrity and Timoshenko beam theory. Governing equations are transformed into a system of ODEs and the problem is formulated as the TPBVP. For the self-adjoined systems all coupled variables except one, are expressed through state variables, thus the numerical solution is more approachable.

Theoretical considerations are illustrated with a numerical example. In the example, different boundary conditions and mechanical characteristics of materials are implemented. The mass reduction is compared for beams with constant cross-sectional profiles and beams with optimized profiles for the given fundamental natural frequency.

REFERENCES

[1] Šalinić, S., Obradović, A., Tomović, A. *et al.* "Coupled axial-bending vibration of axially functionally graded Timoshenko cantilever beams of non-uniform cross-section with an attached rigid body." *Meccanica* 58, 1233–1248 (2023). https://doi.org/10.1007/s11012-023-01672-3

[2] T.M. Atanackovic, A.P. Seyranian, "Application of pontryagin's principle to bimodal optimization problems." *Struct. Multidiscip. Optim.* 37, 1–12 (2008). https://doi.org/10.1007/s00158-007-0211-6

[3] A. Obradović, S. Šalinić, A. Grbović, "Mass minimization of an Euler-Bernoulli beam with coupled bending and axial vibrations at prescribed fundamental frequency." *Eng. Struct.* 228, (2021). https://doi.org/10.1016/j.engstruct.2020.111538

MATHEMATICAL MODELING OF SMART CHARGING OF ELECTRIC VEHICLES

Sonali Chadha[1*], Vaibhav Jain [2], Vinay Kumar Chandna [3]

[1,3]*Department of Electrical Engineering, JECRC, Rajasthan 302022, India*

[2]*Department of Electrical Engineering, JECRC University, Rajasthan 303905, India*

[1*]*sonalichadha.ee@jecrc.ac.in*; [2]*vaibhav.jain@jecrcu.edu.in; vkchandna.ee@jecrc.ac.in*

ORCID iD: 0000-0002-0568-4937[1]; 0000-0001-5641-6863[2]; 0000-0002-8400-2112[3]

Keywords: Electric Vehicle, Electric Grid, Mathematical Modeling, Demand Side Management, Smart Charging.

ABSTRACT

This study presents the charging impact of increasing electric vehicles on the grid. Electric vehicle charging during peak hours can cause stability issues, power quality issues, and overloading of the distribution network as the charging of electric vehicles burdens the grid. There are other factors that can be hampered due to increased electric vehicle charging, such as voltage fluctuations, harmonic injections, battery degradation, etc. Mathematical modeling (MATLAB) has been done using the bus system, and analysis of the impact of charging electric vehicles is carried out, thereby mitigating stability issues and power quality issues by integrating renewable energy resources. The mathematical study evaluates the influence of smart charging of electric vehicle on the grid. Integration of renewable energy resources reduce the overloading of distribution network.

2nd International Conference on Mathematical
Modelling in Mechanics and Engineering
Mathematical Institute SANU, 12-14. September, 2024.

POSITION CONTROL OF ROBOT MANIPULATOR USING OPTIMAL PID CONTROLLER

Petar D. Mandić[1], Tomislav B. Šekara[2] and Mihailo P. Lazarević[3]

[1,3] *University of Belgrade, Faculty of Mechanical Engineering, 11000 Belgrade, Serbia*

[2] *University of Belgrade, School of Electrical Engineering, 11000 Belgrade, Serbia*

[1]pmandic@mas.bg.ac.rs; [2]tomil@etf.rs; [3]mlazarevic@mas.bg.ac.rs

ORCID iD: [1]0000-0001-7004-2087; [2]0000-0001-8031-3135; [3]0000-0002-3326-6636

Keywords: Robot manipulator, Position control, PID controller, Optimization.

ABSTRACT

Due to increasing demands of productivity and accuracy in today's robotic applications, scientific community is under constant pressure to deliver more and more efficient control strategies. This is a challenging task considering the nonlinear nature of robotic structure, which is often accompanied with some degree of uncertainty of model parameters. Most of robots work in industrial surrounding and again, most of them are controlled through standard proportional-integral-derivative (PID) algorithms. The reason for this lies in the relatively simple structure of PID controller which can be easily implemented in practice, and the fact it can achieve desired position without steady-state error. However, tuning control gains of the regulator in order to guarantee transient performance is not an easy task, and deserves further research.

In our case, a robotic manipulator is actuated by electric motors with reduction gears of high ratios. The presence of gears tends to linearize system dynamics and nonlinear coupling effects between the joints can be neglected. This way, each robotic joint can be controlled independently by using a linear model of DC motor. In this paper we are revisiting the PID control of robot manipulators in the light of modern control theory, which assumes an inevitable trade-off between the performance and robustness of the closed loop system. Efficient load disturbance response is of primary concern when designing a control system. Also, system should be robust with respect to model uncertainties, i.e. it should possess a certain degree of relative stability when it comes to modeling errors. It is also important to have a good response to set point changes. More specifically, in this paper we are interested in achieving a set point response without overshoot, so that robot manipulator can approach the manipulated object without damaging it. Last but not least, the closed loop system should be able to cope with negative effects of measurement noise, and this is accomplished by incorporating derivative filter in the control design procedure.

All the above specifications are necessary to be captured in an appropriate mathematical form. For example, the efficiency of load disturbance rejection can be expressed in terms of the integrated absolute error (*IAE*) due to a unit step at the process (motor) input. Sensitivity to modeling errors can be evaluated by the largest value of the sensitivity function. A good set point response without overshoot can be achieved by placing dominant poles of the closed loop system in predetermined positions on the negative real axis of the complex *s* plane. Finally, noise attenuation can be adequately addressed by limiting the largest value of the sensitivity to measurement noise. So, having in mind everything stated above, the design specifications can be formulated as the following optimization problem: find controller parameters that maximize

proportional gain k subject to the constraints on robustness and sensitivity to measurement noise. In order to successfully cope with the given problem, it is required to solve four nonlinear algebraic equations. Some preliminary results of position control of a robot manipulator with three degrees of freedom are given in the figure below. Controller gains are determined based on the well-defined constrained optimization problem. Time response of every joint due to the unit step change of the set point value is shown. It can be seen that a zero overshoot set point response is obtained, which under a given robustness and performance constraints provides optimal load disturbance rejection.

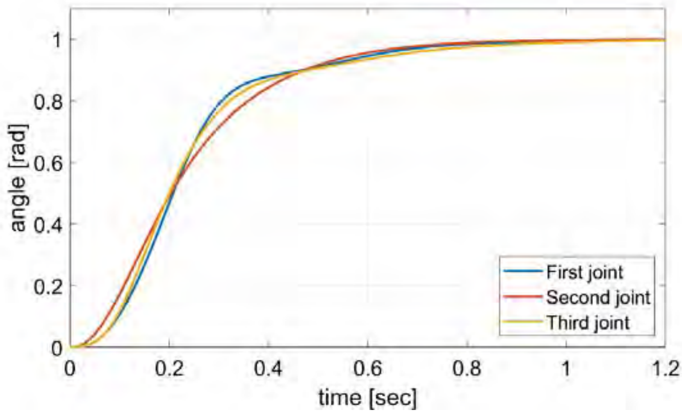

Acknowledgment. Authors gratefully acknowledge the support of Ministry of Education, Science and Technological Development of the Republic of Serbia under contract No. 451-03-65/2024-03/200105 from 5.2.2024, and 451-03-47/2023-01/200103 (T.B.Š.)

REFERENCES

[1] Šekara, T.B., Mataušek, M. R. (2009), "Optimization of PID controller based on maximization of the proportional gain under constraints on robustness and sensitivity to measurement noise", *IEEE Transactions on Automatic Control*, 54(1), pp. 184–189.

[2] Bošković, M., Rapaić, M.R., Šekara, T.B., Mandić, P.D., Lazarević, M.P. (2017), "Pole placement based design of PIDC controller under constraint on robustness", *Proceedings of Infoteh*, 16, pp. 664–668.

[3] Šekara, T.B., Rapaić, M.R. (2015), "A revision of root locus method with applications", Journal of Process Control, 34, pp. 26-34.

[4] Mandić, P.D., Bošković, M.Č., Šekara, T.B., Lazarević, M.P. (2024), "A new optimisation method of PIDC controller under constraints on robustness and sensitivity to measurement noise using amplitude optimum principle", *International Journal of Control*, 97, pp. 36-50.

[5] Mandić, P.D., Šekara, T.B., Lazarević, M.P. (2023), "Analytical design of resonant controller applied for solving robot arm tracking problema", *Proceedings of 9th International Congress of SSM*, pp. 275-282.

SPECIAL SESSION 1

Fluid Mechanics

Dedicated to Academician Prof. Dr. Vladan Djordjevic

2nd International Conference on Mathematical
Modelling in Mechanics and Engineering
Mathematical Institute SANU, 12-14. September, 2024.

RADIUS RATIO EFFECTS ON PRESSURE DISTRIBUTION OF GAS FLOW THROUGH ANNULAR MICROTUBE

Iva I. Guranov[1], Snežana S. Milićev[2] and Nevena D. Stevanović[3]
[1,2,3]*Faculty of Mechanical Engineering, University of Belgrade, 11000 Belgrade, Serbia*
[1]*iguranov@mas.bg.ac.rs*; [2]*smilicev@mas.bg.ac.rs*; [3]*nstevanovic@mas.bg.ac.rs*
ORCID iD: [1]0000-0002-2411-389X; [2] 0000-0003-3055-5544; [3]0000-0003-4385-3882

Keywords: Rarefied gas, Slip flow, Isothermal flow, Compressible flow, Annular microtube.

ABSTRACT

In this paper, we considered stationary isothermal compressible subsonic axisymmetric slip gas flow in annular microtubes. The gas flow occurs due to the pressure difference between the inlet and outlet cross-section. The length of the free path of the molecules is not negligibly small compared to the diameter of the microtube. Therefore the effect of gas rarefaction is taken into account. The level of rarefaction is determined by the Knudsen number. Here we consider slip flow regime, i.e. flow of low rarefied gas. This enables applying the macroscopic approach to solve the problems. Hence, the system of governing equations and boundary conditions is:

$$\tilde{\rho}\left(\tilde{v}\frac{\partial\tilde{u}}{\partial\tilde{r}}+\tilde{u}\frac{\partial\tilde{u}}{\partial\tilde{z}}\right)=\tilde{\mu}\left(\frac{\partial^2\tilde{u}}{\partial\tilde{r}^2}+\frac{\partial^2\tilde{v}}{\partial\tilde{r}\partial\tilde{z}}\right)-\frac{\partial\tilde{p}}{\partial\tilde{z}}-\frac{2}{3}\tilde{\mu}\left(\frac{\partial}{\partial\tilde{z}}\frac{1}{\tilde{r}}\frac{\partial(\tilde{r}\tilde{v})}{\partial\tilde{r}}\right)+\frac{4}{3}\tilde{\mu}\frac{\partial^2\tilde{u}}{\partial\tilde{z}^2}+\frac{\tilde{\mu}}{\tilde{r}}\left(\frac{\partial\tilde{u}}{\partial\tilde{r}}+\frac{\partial\tilde{v}}{\partial\tilde{z}}\right), \tag{1}$$

$$\frac{1}{\tilde{r}}\frac{\partial(\tilde{\rho}\tilde{r}\tilde{v})}{\partial\tilde{r}}+\frac{\partial(\tilde{\rho}\tilde{u})}{\partial\tilde{z}}=0, \tag{2}$$

$$\tilde{p}=\tilde{\rho}\tilde{R}_g\tilde{T}, \tag{3}$$

$$\tilde{u}|_{\tilde{r}=\tilde{R}_1}=-\frac{2-\sigma_v}{\sigma_v}\tilde{\lambda}\frac{\partial\tilde{u}}{\partial\tilde{r}}\bigg|_{\tilde{r}=\tilde{R}_1},\ \tilde{u}|_{\tilde{r}=\tilde{R}_2}=-\frac{2-\sigma_v}{\sigma_v}\tilde{\lambda}\frac{\partial\tilde{u}}{\partial\tilde{r}}\bigg|_{\tilde{r}=\tilde{R}_2}. \tag{4}$$

To convert the system of dimensional equations into dimensionless, non-dimensional variables are introduced:

$$u=\frac{\tilde{u}}{\tilde{u}_r},\ v=\frac{\tilde{v}}{\tilde{u}_r},\ p=\frac{\tilde{p}}{\tilde{p}_r},\ r=\frac{\tilde{r}}{\tilde{R}_r},\ z=\frac{\tilde{z}}{\tilde{L}},\ \mu=\frac{\tilde{\mu}}{\tilde{\mu}_r}, \tag{5}$$

where index r represents variables at the reference cross-section. As the gas flow is in subsonic and slip regime, we can assume:

$$\mathrm{Kn_r}=\eta\varepsilon^n,\ \kappa\mathrm{Ma_r^2}=\gamma\varepsilon^m,\ \kappa\mathrm{Ma_r^2}/\mathrm{Re_r}=\beta\varepsilon,\ \tilde{v}=\varepsilon\tilde{V}. \tag{6}$$

where small parameter ε is the ratio between the reference diameter $2(R_2-R_1)$ and length of the microtube L. Taking into account (5), (6) and assuming pressure p and velocity components u and V in the form of a perturbation series $f=f_0+\mathrm{Kn_r}f_1+O(\mathrm{Kn_r^2})$ equations (7)-(11) are obtained:

$$\int_{R_1}^{R_2}2p_0u_0rdr=R_1+R_2,\qquad p_0|_{z=1}=1, \tag{7}$$

$$4\beta\frac{\partial^2u_0}{\partial r^2}-\frac{\partial p_0}{\partial z}+\frac{4\beta}{r}\frac{\partial u_0}{\partial r}=0,\qquad u_0|_{r=R_1}=0,\qquad u_0|_{r=R_2}=0, \tag{8}$$

$$\int_{R_1}^{R_2}2(p_0u_1+p_1u_0)rdr=0,\qquad p_1|_{z=1}=0, \tag{9}$$

$$4\beta\frac{\partial^2u_1}{\partial r^2}-\frac{\partial p_1}{\partial z}+\frac{4\beta}{r}\frac{\partial u_1}{\partial r}=\frac{\gamma}{\eta}p_0\left(V_0\frac{\partial u_0}{\partial r}+u_0\frac{\partial u_0}{\partial z}\right), \tag{10}$$

$$u_1|_{r=R_1} = \frac{2-\sigma_v}{\sigma_v}\frac{2}{p_0}\frac{\partial u_0}{\partial r}\bigg|_{r=R_1}, \quad u_1|_{r=R_2} = -\frac{2-\sigma_v}{\sigma_v}\frac{2}{p_0}\frac{\partial u_0}{\partial r}\bigg|_{r=R_2}. \tag{11}$$

where the first system (7)-(8) represents the first approximation - continuum, while the second system (9)-(11) stands for the second approximation - influence of the slip. Systems of equations are solved successively and a solution for the pressure is attained [1]:

$$p = p_0 + \mathrm{Kn_r} p_1 = p_0 + \mathrm{Kn_r}\frac{2-\sigma_v}{\sigma_v}\left(1-\frac{1}{p_0}\right)C_2C_3. \tag{12}$$

Here p_0 is $\sqrt{1+64\beta(z-1)C_2}$. Constants C_1, C_2, C_3 are:

$$C_1 = R_1^2 - R_2^2, \quad C_2 = \left[(R_1-R_2)\left(C_1+(R_1^2+R_2^2)\ln\frac{R_2}{R_1}\right)\right]^{-1}\ln\frac{R_2}{R_1}, \tag{13}$$

$$C_3 = 2\left(C_1^2 + 4R_1R_2\left(C_1+(R_1^2-R_1R_2+R_2^2)\ln\frac{R_2}{R_1}\right)\ln\frac{R_2}{R_1}\right)\left[R_1R_2\left(\ln\frac{R_2}{R_1}\right)^2\right]^{-1}\ln\frac{R_2}{R_1}. \tag{14}$$

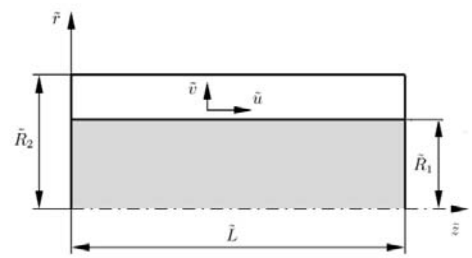

Fig. 1. Geometry of the annular microtube

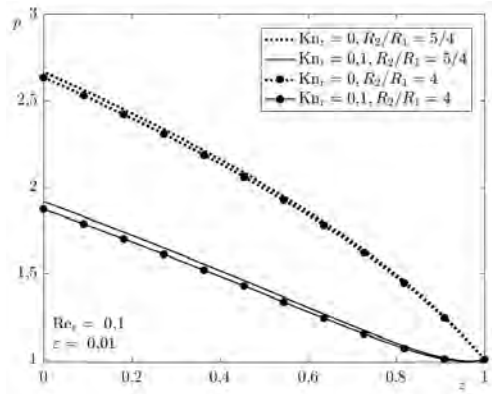

Fig. 2. The pressure distribution in annular microtube for continuum and slip, with radius ratio effect

Pressure distribution through annular microtube for continuum and slip is represented at Fig. 1. In the case of rarefied gas flow through annular tubes at low Reynolds numbers, it is shown that rarefaction leads to a decrease of pressure for the same mass flow. The influence of the ratio of the outer and inner radius of the microtube on the pressure distribution was also analyzed. It is shown that an increase of the ratio R_2/R_1 leads to a lower pressure along the microtube, both in the case of continuum and in the case of rarefied flow. The influence of the ratio R_2/R_1 is amplified at higher values of the Knudsen number.

REFERENCES

[1] Guranov, I. (2023), "Rarefied gas flow in microtubes", *Doctoral dissertation,* University of Belgrade - Faculty of Mechanical Engineering, Belgrade, Serbia.

ON THE POSSIBILITIES OF OBTAINING ANALYTICAL SOLUTIONS FOR GAS FLOW OF DIFFERENT LEVELS OF RAREFACTION

Snežana S. Milićev[1], **Nevena D. Stevanović**[2]

[1,2]*Faculty of Mechanical Engineering, University of Belgrade, 11000 Belgrade, Serbia*

[1]*smilicev@mas.bg.ac.rs*; [2]*nstevanovic@mas.bg.ac.rs*

ORCID iD: [1]0000-0003-3055-5544; [2]0000-0003-4385-3882

Keywords: analytical solution, rarefied gas, channels, micro/nanochannels, Knudsen number, Mach number, Reynolds number.

ABSTRACT

The analytical results are important in all science disciplines as they are explicit and can be benchmarks in solving problems in those domains. Here we focus on gas flow through the channels of variable cross sections (constant height, convergent or divergent). We consider steady, viscous, compressible and pressure-driven gas flow. The rarefaction is included as we intend to consider both the continuum and the rarefied gas flow. It is assumed that the flow is fully developed and that all the variables change slowly in the streamwise direction.

The correlation between Mach, Knudsen and Reynolds numbers:

$$\mathrm{Kn} = \sqrt{\frac{\kappa\pi}{2}}\frac{\mathrm{Ma}}{\mathrm{Re}}$$

enables defining the characteristic domains according to these dimensionless parameters (Fig. 1).

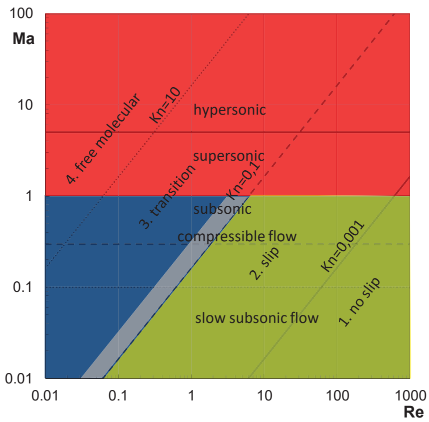

Figure 1 *Domains according to Knudsen, Mach and Reynolds number values*

We showed in previous research that the perturbation theory gives the analytical results for both isothermal [1] and non-isothermal gas flow [2] in channels and microchannels. These solutions were obtained macroscopically, by assuming pressure, velocity and temperature in the form of perturbation series in the Knudsen number, and then solving the corresponding systems of equations and boundary conditions. The continuum equations (the continuity and Navier-Stokes for isothermal flow, and energy equation, if gas flow is non-isothermal) are order of Knudsen number and correspond to the first order boundary conditions for gas velocity and temperature. We used the first-order Maxwell boundary condition for the slip velocity at the channel walls in the case of isothermal gas flow, and Smoluchowski boundary condition for the gas temperature jump at the channel walls in the case of non-isothermal gas flow. Except for the rarefaction, the perturbation method enables including the other effects depending on the case under consideration: inertia, convection, dissipation, and rate at which work is done in compressing the element of fluid. According to the Knudsen number values, the perturbation method covers the continuum and slip gas flow regions, i.e. Kn≤0.1 (green area in Fig. 1). Even though we can use the higher-order boundary conditions here, there is a limit zone in the beginning part of the transition area (0.1<Kn<0.4), colored grey in Fig. 1. The obtained analytical results correspond to the subsonic gas flow (Ma<1) and in terms of the Reynolds number values it is viscous, but laminar gas flow.

Is there any possibility of macroscopic analytical analyses of the gas flow in the transition and free molecular domains or, in other words, for all Knudsen number values? Can we get the solutions that hold for channels, microchannels and nanochannels?

The unified approach that was proposed by Beskok and Karniadakis [3] includes the general velocity slip boundary condition. Besides, it generalizes the dynamic viscosity by using the rarefaction correction parameter. These two steps enable the analytical solutions for the velocity and pressure distribution along the channels, which are appropriate for all rarefaction degrees (channels, micro and nanochannels). The downsides of this approach are using only tabulated correction parameter values for the discrete Knudsen number values, and the fact that the analytical results are possible only if inertia is excluded (only for subsonic gas flow). This approach gives the solutions that correspond the green, grey and blue areas in Fig. 1. Both the perturbation method and the unified approach used a two-dimensional mathematical model for the gas flow in channels.

At last, we proposed a one-dimensional model that compensate the drawbacks of the previous ones [4]. Firstly, we got the explicit correlation between the rarefaction correction parameter and the Knudsen number. Furthermore, our system of continuum equations included inertia effect, so its solutions covered both subsonic (green, grey and blue areas in Fig. 1) and supersonic gas flow (red area in Fig. 1). Finally, the friction factor used in the momentum equation was specially modelled and made the solutions applicable in the entire Knudsen number domain. In the case when gas molecules reflect diffusely at channel walls the friction factor is:

$$f\,\mathrm{Re} = \frac{12(1+\mathrm{Kn})}{(1+\alpha\mathrm{Kn})(1+7\mathrm{Kn})}.$$

Here, the Reynolds number is constant along the channel and defines the mass flow rate. The obtained solution holds for all levels of rarefaction, i.e. for the gas flow through the channels, microchannels and nanochannels of variable cross sections (constant height, convergent or divergent).

REFERENCES

[1] Stevanović, N. (2007), “A new analytical solution of microchannel gas flow,” *J. Micromech. Microeng,* 17, pp. 1695-1702.

[2] Milićev, S. (2024), “*Nonisothermal Compressible Gas Flow in Micrichannels*,” Faculty of Mechanical Engineering, University of Belgrade, ISBN 978-86-6060-181-2.

[3] Beskok, A., Karniadakis, G. E., (1999), “Report: A model for Flows in Channels, Pipes, and Ducts at Micro and Nano Scales,” *J. Microscale Thermophys. Eng.,* 3 (1), pp. 43-77.

[4] Milićev, S. Stevanović, N., (2021), “Gas Flow in Microchannels and Nanochannels With Variable Cross Section for All Knudsen and All Mach number Values,” *ASME J. Fluids Eng.*, 143(2):021203.

MATHEMATICAL TRANSFORMATION FOR ANALYTICAL SOLUTION OF THE RAREFIED GAS FLOW IN A VARIABLE CROSS-SECTION MICROCHANNEL

Nevena D. Stevanović[1], Snežana S. Milićev[2]

[1,2]*Faculty of Mechanical Engineering, University of Belgrade, 11000 Belgrade, Serbia*

[1]*nstevanovic@mas.bg.ac.rs*; [2]*smilicev@mas.bg.ac.rs*

ORCID iD: [1]0000-0003-4385-3882; [2]0000-0003-3055-5544

Keywords: Analytical solution, Rarefied gas, microchannel, Variable cross-section, Knudsen.

ABSTRACT

In this paper the analytical solution for two-dimensional, isothermal, compressible and subsonic gas flow in a microchannel with slowly varying cross section is presented.

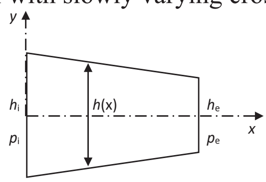

Fig. 1. Geometry of the variable cross-sectoion microchannel.

In order to achieve higher accuracy of the solution for gas flow in slip regime, as well as to obtain a solution for the initial part of the transition regime, second order boundary condition for the gas velocity slip at microchannel walls is applied. It requires implementation of the Burnett momentum equation that comprises the shear stress tensor of the second order. It was shown that for extremely subsonic gas flow through a channel with slowly varying cross sections where the height of the channel is much smaller than its length, Barnett's equations has the same form as the Navier-Stokes equations. Finally, for low Reynolds number flow (Re<1), which is mostly present in microchannels, the momentum equation is reduced to:

$$\frac{\partial^2 u}{\partial y^2} = \frac{1}{\mu}\frac{\mathrm{d}p}{\mathrm{d}x} \tag{1}$$

By applying a second-order boundary condition at the walls [1]

$$u\Big|_{y=\pm\frac{h(x)}{2}} = \mp \mathrm{A}_1\lambda\left(\partial u/\partial y\right)\Big|_{y=\pm\frac{h(x)}{2}} - \mathrm{A}_2\lambda^2\left(\partial^2 u/\partial y^2\right)\Big|_{y=\pm\frac{h(x)}{2}} \tag{2}$$

the stream-wise velocity component u is obtained:

$$u = \frac{h(x)^2}{2\eta}\frac{\mathrm{d}p}{\mathrm{d}x}\left(\frac{y^2}{h(x)^2} - \mathrm{A}_1 Kn - 2\mathrm{A}_2 Kn^2 - \frac{1}{4}\right) \tag{3}$$

Now, from the integral form of the continuity equation mass flow rate is determined:

$$\dot{m} = w\int_0^h \rho u \mathrm{d}y = -\frac{wph(x)^3}{12R_\mathrm{g}T\eta}\frac{\mathrm{d}p}{\mathrm{d}x}\left(1+6\mathrm{A}_1 Kn + 12\mathrm{A}_2 Kn^2\right). \tag{4}$$

In this differential equation, there are two dependent variables, $p(x)$ and $Kn(x)$, whereby there is a dependency between them. Since the mean free path of molecules under isothermal flow conditions is inversely proportional to pressure, the local Knudsen number ($Kn = \lambda/h$) can be expressed through the local value of the Knudsen number at the exit $\left(Kn_e = \lambda_e/h_e\right)$:

$$Kn = Kn_e p_e h_e/(ph). \tag{5}$$

It is shown that differential equation (4) could be solved by variable separation only by expressing pressure via Kn, i.e. by transforming equation into the following form:

$$\dot{m} = \frac{wh}{12R_g T\eta}\frac{\left(Kn_e p_e h_e\right)^2}{Kn^2}\left(\frac{1}{Kn}\frac{dKn}{dh} + \frac{1}{h}\right)\frac{\mathrm{d}h}{\mathrm{d}x}\left(1 + 6A_1 Kn + 12A_2 Kn^2\right), \quad \frac{\mathrm{d}h}{\mathrm{d}x} = -\frac{h_i - h_e}{L}. \tag{6}$$

Thus, in this case, the mathematical solution also carries a physical meaning. Namely, the main characteristic of the rarefied gas flow is the Knudsen number and here, in order to obtain the solution, it is necessary to express differential equation via Kn [2]. Hence, the Kn distribution in the channel is first determined, and then the pressure field can be find. Equation (6) can be written in the form in which variables Kn and h are separated:

$$\frac{\left(Kn_e p_e h_e\right)^2\left(1 + 6A_1 Kn + 12A_2 Kn^2\right)dKn}{\left(CKn^3 + \left(Kn_e p_e h_e\right)^2\left(Kn + 6A_1 Kn^2 + 12A_2 Kn^3\right)\right)} = -\frac{dh}{h}. \tag{7}$$

where $C = 12\dot{m}R_g T\eta L/(w\Delta h)$ is a constant for a certain flow regime. The boundary conditions at the inlet and exit of the microchannel are:

$$h = h_i: \quad Kn = Kn_i = Kn_e p_e h_e/(p_i h_i); \quad h = h_e: \quad Kn = Kn_e. \tag{8}$$

The mass flow contained in the constant C can now be determined by fitting:

$$ln\,h_i - ln\,h_e = \int_{Kn_i}^{Kn_e}\frac{\left(Kn_e p_e h_e\right)^2\left(1 + 6A_1 Kn + 12A_2 Kn^2\right)dKn}{\left(CKn^3 + \left(Kn_e p_e h_e\right)^2\left(Kn + 6A_1 Kn^2 + 12A_2 Kn^3\right)\right)} \tag{9}$$

Now, the distribution of the Knudsen number in the entire microchannel can be determined. Its value in the microchannel is in the range $Kn_i \le Kn \le Kn_e$ (in the case of a divergent channel it can also be $Kn_i \ge Kn \ge Kn_e$). The problem is solved by integrating the equation (7) from the arbitrary to the exit crossection:

$$ln\,h - ln\,h_e = \int_{Kn}^{Kn_e}\frac{\left(Kn_e p_e h_e\right)^2\left(1 + 6A_1 Kn + 12A_2 Kn^2\right)\mathrm{d}Kn}{\left(CKn^3 + \left(Kn_e p_e h_e\right)^2\left(Kn + 6A_1 Kn^2 + 12A_2 Kn^3\right)\right)}. \tag{10}$$

It is solved indirectly from eq. (10) by setting the value of the Kn in an arbitrary cross-section, and then determining the height h of the channel that corresponds to that value of the Knudsen number. For that cross section dp/dx follows from equation 4. Finally, the velocity profile could be defined (3).

REFERENCES

[1] Stevanović, N. (2014), "Fundamentals of microfluidics and nanofluidics", Faculty of Mechanical Engineering, Belgrade.
[2] Stevanović, N., Djordjevic V. (2012), "The exact analytical solution for the gas lubricated bearing in the slip and continuum flow regime", *Publications de l`Institute Matematique*, 91 (105), pp. 83-93.

Prof. Vladan Djordjevic award candidate

NON-AXISYMMETRIC DISPLACEMENT IN A COMPLIANT HELE-SHAW CELL

Ivana Cvetkovic[1], Draga Pihler-Puzovic[2], Snezana Milicev[3]

[1,3] *Faculty of Mechanical Engineering, University of Belgrade, 11000 Belgrade, Serbia*
[2] *Department of Physics and Astronomy*
University of Manchester, Oxford Road, Manchester M13 9PL, United Kingdom
[1] icvetkovic@mas.bg.ac.rs; [3] smilicev@mas.bag.ac.rs
ORCID iD: [1] 0000-0002-2773-5643, [3] 0000-0003-3055-5544

Keywords: Hele-Shaw cell, viscous fingering, choking, Saffman-Taylor instability, perturbation analysis

ABSTRACT

We consider a two-phase flow in a small gap between a rigid plate and a volumetrically confined elastomer, which form an elastic Hele-Shaw cell (see Fig. 1). Such set up is common in soft microfluidic devices which include deformable components that require no external actuation. When a radially outwards fluid flow is generated by displacing liquid occupying the cell with the same liquid (no interface), the elastic solid can deform in response to viscous pressure field so that the gap expands near the inlet of the cell (where the fluid is injected) and contracts near its rim [1]. If the flow rate exceeds a critical value, the cell outlet can even close completely, interrupting or "choking" the flow. Similar phenomena are seen when a liquid flows through a column of deformable hydrogel beads [2], and in the two-phased gas-driven displacement of a mixture of aqueous liquid and hydrophilic solid grains in a capillary tube [3]. It was also used to propose a design of a microfluid fuse, a device that can interrupt a flow in a microfluidic circuit if a critical flow rate is exceeded [1].

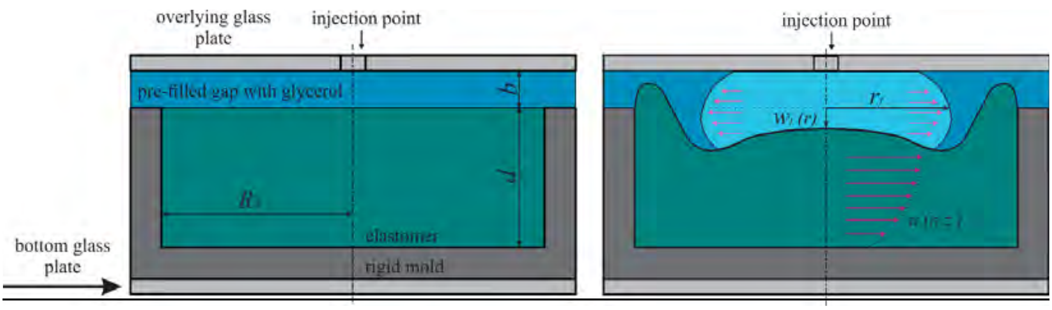

Figure 1: *Schematic diagram of an elasto-rigid Hele-Shaw cell: a narrow gap between a rigid horizontal top plate and an elastomer confined within a rigid mould (left); fluid injected into the compliant Hele-Shaw cell at a constant flow rate spreads outwards deforming the elastomer and displacing fluid resident in the cell (right); Adapted from [4]*

However, microfluidic applications often deal with multiphase flows, so a natural extension to this problem is that of a displacement flow in the soft Hele-Shaw cell when the flow is driven by expanding gas [4], a displacement flow that is suspectable to viscous fingering [5-7]. This interfacial instability develops when the fluid is injected at a sufficiently fast rate so that viscous forces exceed surface tension forces, causing the axisymmetric interface between the two fluids to become linearly unstable to non-axisymmetric perturbations, and grow non-linearly into complex disordered patterns (see Fig. 2). The choking phenomenon is still observed when the gas-liquid interface fingers, but it is highly dependent on the interfacial morphology [8]. Hence, we explore viscous fingering in the soft Hele-Shaw cells by focusing on its onset.

We consider a theoretical model that couples Reynolds lubrication equations and equations of linear elasticity. The inertia and gravity, as well as compressibility of both the solid and the fluids are neglected. To study development of the instabilities, we derive equations that allow us to assess the linear growth or decay of small-amplitude non-axisymmetric perturbations to the axisymmetric gas-liquid displacement studied in [4].

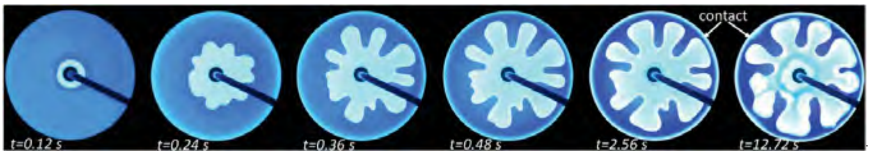

Figure 2: *Top view of viscous fingering developing in a radial elastic Hele-Shaw cell when air displaces glycerol (dyed blue, so that thicker liquid layers correspond to darker colours). In the final two images cell chokes, trapping the interface: a white band around the cell rim indicates contact between the soft slab and the glass plate near the rim located at 60 mm from the cell centre. From [8].*

REFERENCES

[1] Box, F., Peng, G. G., Pihler-Puzovic, D., Juel, A.: *Flow-induced choking of a compliant Hele-Shaw cell*; Proceedings of the National Academy of Science (PNAS) (2020); Vol. 117, Issue 48, pp. 30228-30233

[2] Hewitt, D. R., Niijer, J. S., Worster M. G., Neufeld, J. A.: *Flow-induced compaction of a deformable porous medium*; Physical Review E (2016), Vol. 93, Issue 2, 023116

[3] Dumazer, G., Sandnes, B., Ayaz, M., Måløy, K. J. and Flekkøy, E. G.: *Frictional fluid dynamics and plug formation in multiphase millifluidic flow*, Physical Review Letters (2016), Vol. 117, Issue 2, 028002

[4] Peng, G. G., Cuttle, C., MacMinn, C. W., Pihler-Puzovic, D.: *Axisymmetric gas-liquid displacement flow under a confined elastic slab*; Physical Review Fluids (2023), Vol. 8, Issue 9, 094005

[5] Couder Y.: *Viscous fingering as an archetype of growth patterns*; A Collective Introduction to Current Research (2000), edited by G. K. Batchelor, H. K. Moffatt, and M. G. Worster, Cambridge University Press, pp. 53-104

[6] Saffman, P. G., Taylor, G. I.: *The Penetration of a fluid into a porous medium or Hele-Shaw cell containing more viscous fluid*; Proc. R. Soc. Lond. A (1958), 1242(245), pp. 312-329

[7] Homsy, G. M.: *Viscous Fingering in Porous Media*; Ann. Rev. Fluid Mech. (1987); 19: 271-311

[8] Peng, G. G., Cuttle, C., Box, F., Guan, J. H., Juel, A., MacMinn, C. W., Pihler-Puzovic, D.: *Trapping and escape of viscous fingers in a soft Hele-Shaw cell*; Physical Review Fluids (2022), Vol. 7, Issue 6, L062001

2nd International Conference on Mathematical Modelling in Mechanics and Engineering
Mathematical Institute SANU, 12-14. September, 2024.

Prof. Vladan Djordjevic award candidate

THE ASSESSMENT OF INFLUENCE OF SHEAR FLOW ON THE RESULTS OF NUMERICAL SIMULATIONS OF TWO-PHASE BUBBLY FLOW

Milan M. Raković[1] and Aleksandar S. Ćoćić[2]

Faculty of Mechanical Engineering, University of Belgrade, 11000 Belgrade, Serbia
[1]mrakovic@mas.bg.ac.rs; [2]acocic@mas.bg.ac.rs
ORCID iD: [1]0000-0001-8879-552X, [2]0000-0002-2473-5226

Keywords: Two-phase bubbly flow, Shear flow, Drag coefficient.

ABSTRACT

Two-phase flow of liquid and gas can occur in several different regimes. A bubbly flow occurs at the beginning of the evaporation of water in the boiler tubes, but also in many other cases. This flow regime has often been investigated experimentally and numerically.

One of the main challenges in mathematical modeling of two-phase bubbly flow is how to represent the interfacial forces, i.e. the forces that describe the momentum transfer between phases. Among the forces at the interface, the drag force is of particular importance for two-phase bubbly flow. To calculate it, it is necessary to determine the bubble drag coefficient. There are several expressions for calculating the drag coefficient. However, it should be noted that they all correspond to the case when the bubble is in a uniform fluid flow. Legendre and Magnaudet [1] proved that there is an increase in the value of the drag coefficient when the bubble is in a fluid stream with a velocity gradient, i.e. in fluid shear flow. They made a proposal for the introduction of a correction in the calculation of the drag coefficient, which will take this influence into account.

Their proposal was verified during research conducted by Hosokawa and Tomiyama [2]. They performed an experimental investigation of two-phase bubbly flow inside a vertical pipe. They then performed two sets of numerical simulations, one with and one without the introduction of the drag coefficient correction proposed by Legendre and Magnaudet [1]. They showed that the results of numerical simulations, which were performed taking into account the effect of shear flow on the drag coefficient, have a better agreement with the experimental results.

Raković et al [3] showed that in certain cases, such as the use of low-Reynolds-number turbulent models (LRN), the correction proposed by Legendre and Magnaudet [1] can lead to instability and divergence of the numerical calculation. A modification of the Legendre and Magnaudet [1] correction was then proposed to eliminate this defect. The new correction of drag coefficient has been tested and its functionality has been proven, (Raković et al [3] and Raković [4]). The new correction leads to a more accurate calculation of the drag coefficient, which allows a better prediction of the velocity profiles.

During the testing of the new correction under different flow conditions, it was shown that there are cases in which it is necessary to take into account the effect of shear flow on the drag coefficient, as well as cases in which shear flow has no significant effect on the results of numerical simulations.

The main goal of the presented paper is to find a way to quantify the impact of shear flow, ie. to establish a criterion that indicates whether or not it is necessary to take into account the

influence of shear flow when performing numerical simulations of two-phase bubbly flow.

Both corrections proposed by Legendre and Magnaudet [1] and Raković et al [3] are a function of the dimensionless quantity shear rate Sr. The distribution of the shear rate Sr on the pipe cross section depends on several quantities and can be very different, as shown in the figure 1 for three different cases.

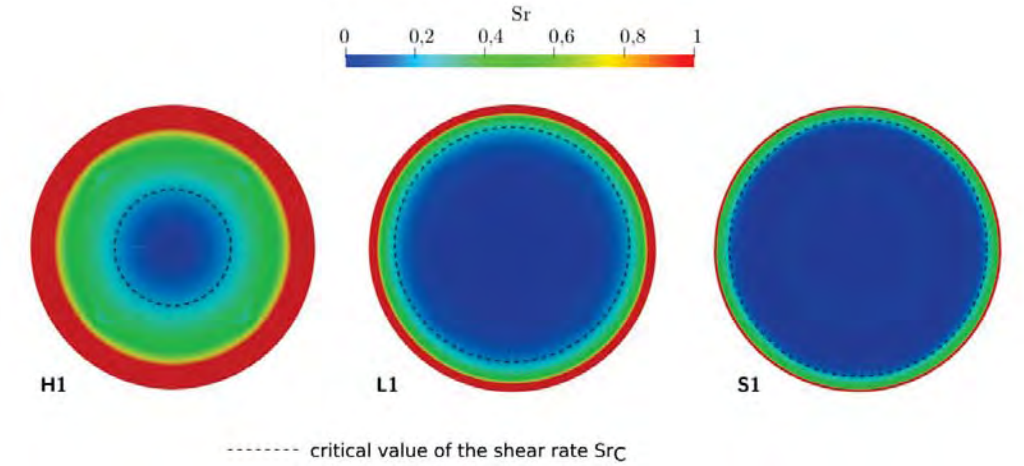

Figure 5: Distribution of the shear rate on the pipe cross-section for three different cases [4].

The task is to find the critical value of the shear rate Sr_C. In the area where $Sr>Sr_C$ is valid, it is necessary to use the drag coefficient correction, so that the numerical simulations can correctly predict the velocity profiles. In the area where $Sr<Sr_C$ is valid, the correction will not be used, and thus the complexity of the calculation procedure will not be unnecessarily increased. In this way, the correction will be used only in that part of the computation domain where it is necessary, but not in the entire computational domain. A similar approach is used when calculating other interfacial forces, such as the hydrodynamic lubrication force.

REFERENCES

[1] Legendre D, Magnaudet J. (1998.) "The lift force on a spherical bubble in a viscous linear shear flow." *J Fluid Mech* ; 368: 81–126.

[2] Hosokawa S, Tomiyama A. (2009.) "Multi-fluid simulation of turbulent bubbly pipe flows." *Chem Eng Sci*; 64: 5308–5318.

[3] Raković M, Radenković D, Ćoćić A, Lečić M. (2022.) "Euler-Euler numerical simulations of upward turbulent bubbly flows in vertical pipes with low-Reynolds-number model." *Advances in Mechanical Engineering*; 14(4). doi:10.1177/16878132221094909

[4] Raković, Milan M., (2023.) "Утицај смицања на коефицијент отпора мехура при двофазном мехурастом струјању" Univerzitet u Beogradu, Mašinski fakultet, Doktorska disertacija. https://phaidrabg.bg.ac.rs/detail/o:33194

Prof. Vladan Djordjevic award candidate

ANALYTICAL MODELING OF SQUEEZED AND ROTATING THIN FILMS

Nikolaos Rogkas[1]

[1]*School of Mechanical Engineering, National Technical University of Athen NTUA, Athens, Greece,*
e-mail: nrogkas@mail.ntua.gr
ORCID iD: 0000-0002-4581-5639

Keywords: squeeze film, rotating film, thin films, Reynolds Equation, analytical modeling

ABSTRACT

Squeeze films play a critical role in lubrication and damping applications, generating significant pressure to provide essential load support. In wet clutch systems, the unique dynamics of squeezed and rotating films have been extensively investigated. These films enhance torque transmission by ensuring a smooth response, mitigating overshoots, and improving cooling efficiency while reducing wear [1].

Various studies have attempted analytical calculations of pressure and velocity distribution, typically relying on assumptions related to the Reynolds Equation [2–5]. However, these assumptions only hold under specific operating conditions. As parameters such as squeeze velocity, rotating speed, or film thickness change, the validity of these analytical solutions diminishes. For example, the linear variation of circumferential velocity versus film thickness may transition to 2nd or even 3rd degree.

This paper extends the methodology outlined in [6] by introducing new criteria to assess the validity of Reynolds equation derivations through nondimensional analysis. Additionally, it presents and discusses modified analytical solutions aimed at better capturing flow characteristics, particularly under extreme values of the dominant variables. The study focuses on circular discs without grooves as a reference case, analyzing the problem from both quasi-static and transient perspectives. Finally, to demonstrate the accuracy of the findings, a comparison is made between the analytical results and Computational Fluid Dynamics (CFD) analysis.

REFERENCES

[1] Rogkas N, Vasilopoulos L, Spitas V (2023) A hybrid transient/quasi-static model for wet clutch engagement. Int J Mech Sci 256:. https://doi.org/10.1016/j.ijmecsci.2023.108507.

[2] Brunetière N, Wodtke M (2020) Considerations about the applicability of the Reynolds equation for analyzing high-speed near field levitation phenomena. J Sound Vib 483:115496. https://doi.org/10.1016/j.jsv.2020.115496

[3] Snyder T, Braun M (2018) Comparison of perturbed Reynolds equation and CFD models for the prediction of dynamic Coefficients of sliding bearings. Lubricants 6:. https://doi.org/10.3390/lubricants6010005

[4] Gong RZ, Li DY, Wang HJ, et al (2016) Analytical solution of Reynolds equation under dynamic conditions. Proceedings of the Institution of Mechanical Engineers, Part J: Journal of Engineering Tribology 230:416–427

[5] Temizer I, Stupkiewicz S (2016) Formulation of the Reynolds equation on a time-dependent lubrication surface. Proceedings of the Royal Society A: Mathematical, Physical and Engineering Sciences 472:. https://doi.org/10.1098/rspa.2016.0032

[6] Rogkas N, Vakouftsis C, Vasileiou G, et al (2020) Nondimensional characterization of the operational envelope of a wet friction clutch. Computation 8:. https://doi.org/10.3390/COMPUTATION8010021

Prof. Vladan Djordjevic award candidate

DYNAMICS OF A CATAMARAN WITH A SAVONIUS ROTOR AND WATER PROPELLER

Mikhail A. Garbuz[1]

[1]*Instituteof Mechanics of the LMSU, Moscow, Russia*

misha-garbuz@yandex.ru;

Keywords: Instructions, Mechanics, Engineering.

ABSTRACT

The dynamics of a catamaran with a Savonius rotor and a propeller installed on it is considered. Under the action of a stationary wind flow the rotor rotates and transmit it to the the propeller, which creates thrust. As a control, the angle of the catamaran's course relative to the wind flow is considered. The control task is to move the center of the masses of the hull from the starting point to a given endpoint located strictly upstream of the wind. The possibility of straight motion against the wind is shown. The dependence of the averege velocity in the stationary mode of movement against the wind on the radii of the Savonius rotor and propeller is analyzed.

REFERENCES

[1] Klimina L., Dosaev M., Selyutskiy Yu. Asymptotic Analysis of the Mathematical Model of a Wind-powered Vehicle // Appl. Math. Modelling. 2017 V. 46 P. 691–697. Doi: 10.1016/j.apm.2016.06.022.

[2] Garbuz M., Klimina L., Samsonov V. Wind Driven Plantigrade Machine Capable of Moving Against the Flow // Appl. Math. Modelling. 2022. V.110. P.17–27.

SPECIAL SESSION 2

Reanalysis and Simulation of Mechanical Systems

Session Chairs: **Nataša Trišović, Wei Li**

Plenary lecture

GAUSSIAN RBFNN METHOD FOR SOLVING FPK AND BK EQUATION IN A GVDP SYSTEM WITH FOPID CONTROLLER

Wei Li[1], Yu Guan[2] , Dongmei Huang[3] and Natasa Trisovic[4]

[1,2,3]*School of Mathematics and Statistics, Xidian University, Xi'an 710071, PR China*

[4]*Faculty of Mechanical Engineering, University of Belgrade, 11000 Belgrade, Serbia*

[1]liweilw@mail.xidian.edu.cn; [2]740565756@qq.com; [3]dmhuang@xidian.edu.cn;
[4]ntrisovic@mas.bg.ac.rs

ORCID iD: [1]0000-0002-4671-8785, [4]0000-0003-1043-5780

Keywords: FOPID controller, RBFNN, Transient probability density function, Reliability function

ABSTRACT

Solving the Fokker–Planck–Kolmogorov (FPK) equation and the Backward-Kolmogorov (BK) equation is a crucial task to obtain the transient response of stochastic dynamical systems[1]. Fractional order PID (FOPID) is a new efficient controller to change the system response to be the expected one. Therefore, in this paper, the Gaussian Radial Basis Functions Neural Network (RBFNN) is proposed to solve FPK and BK equations, to obtain the transient probability density function and the reliability function for a generalized Van der Pol system under a FOPID controller. The values of the different fractional orders are analyzed to discuss the performance of the FOPID controller. A data collection strategy is adopted to deal with the associated boundary conditions by way of a one-time Monte-Carlo simulation and uniform distribution in our Gaussian RBFNN method. The advantage of this method is that the solution process of FPK and BK equations is converted into solving algebraic equations. Numerical results with regard to the transient system response prove that the Gaussian RBFNN is efficient and accurate in getting the solutions of FPK and BK equations. The order of the fractional integration and the fractional derivative are critical parameters to control the system response. Moreover, we conclude that the fractional order parameters in a FOPID controller can indeed enhance the system's response to a certain extent and lead to bifurcation.

REFERENCES

[1] Li W., Guan Y., Huang D. M, Trisovic N. (2023), "Gaussian RBFNN method for solving FPK and BK equations in stochastic dynamical system with FOPID controller," *International Journal of Non-Linear Mechanics*, 153,104403.

2nd International Conference on Mathematical
Modelling in Mechanics and Engineering
Mathematical Institute SANU, 12-14. September, 2024.

RESPONSE ANALYSIS OF THE THREE-DEGREE-OF-FREEDOM VIBROIMPACT SYSTEM WITH AN UNCERTAIN PARAMETER

Guidong Yang[1]

[1]*School of Mathematics and Statistics, Xidian University, Xi'an, 710071, China*

[1]*gdyang@xidian.edu.cn;*

[1]ORCID: 0000-0002-9768-4802

Keywords: Vibroimpact system; bifurcation; Chebyshev polynomial; uncertain parameter.

ABSTRACT

The inherent non-smoothness of the vibroimpact system leads to complex behaviors and a strong sensitivity to parameter changes. Unfortunately, uncertainties and errors in system parameters are inevitable in mechanical engineering. Therefore, the investigations of dynamical behaviors for vibroimpact systems with stochastic parameters are highly essential. The present study aims to analyze the dynamical characteristics of the three-degree-of-freedom vibroimpact system with an uncertain parameter by means of the Chebyshev polynomial approximation method. Specifically, the vibroimpact system model considered is one with unilateral constraint. Firstly, the three-degree-of-freedom vibroimpact system with an uncertain parameter is transformed into an equivalent deterministic form by the Chebyshev orthogonal approximation. Then, the ensemble means responses of the stochastic vibroimpact system are derived. Numerical simulations are performed to verify the effectiveness of the approximation method. Furthermore, the periodic and chaos motions under different system parameters are investigated, and the bifurcations of the vibroimpact system are analyzed by the Poincaré map. The results demonstrate that both the restitution coefficient and the random factor can induce the appearance of the periodic bifurcation. It is worth noting that the bifurcations fundamentally differ between the stochastic and deter-ministic systems. The former has a bifurcation interval, while the latter occurs at a critical point..

REFERENCES

[1] Guo, Y.; Yin, X. ; Yu, B. ; Hao, Q. ; Xiao, X. et al. (2023) “Experimental analysis of dynamic behavior of elastic visco-plastic beam under repeated mass impacts”. *International Journal Of Impact Engineering*, 171: 104371.

[2] Yang, G. D. ; Xu, W. ; Feng, J. Q. ; Gu, X. D. (2015) “Response analysis of Rayleigh–Van der Pol vibroimpact system with inelastic impact under two parametric white-noise excitations”. Nonlinear Dynamics, 82: 1797-1810.

[3] Xu, Y. ; Liu, Q. ; Guo, G. ; Xu, C. ; Liu, D. (2017) Dynamical responses of airfoil models with harmonic excitation under uncertain disturbance. Nonlinear Dynamics,89: 1579-1590.

2nd International Conference on Mathematical
Modelling in Mechanics and Engineering
Mathematical Institute SANU, 12-14. September, 2024.

THEORETICAL ANALYSIS OF GALLOPING ENERGY HARVESTERS

Dongmei Huang[1]

[1]*School of Mathematics and Statistics, Xidian University, Xi'an, 710071, China*

[1]*dmhuang@xidian.edu.cn;*

[1] ORCID: 0000-0002-4832-7454

Keywords: Energy harvester, Theoretical solution, Wind energy.

ABSTRACT

With the rapid development of compact wind energy harvesting devices based on flow induced vibrations, more and more scholars are focusing on and studying vortex-induced vibration, galloping, flutter and wake galloping ones. The demands of applications such as wireless sensor networks, portable electronics, and implanted systems for power sources with high energy/power densities, low volumes, and long operating lives are promoting the rapid development of micro/nano-scale energy devices and systems via aerodynamic phenomena such as flutter, vortex-induced vibration, galloping. In our work, the response properties of galloping energy harvesters under stochastic excitation are studied theoretically.

Firstly, the performance of the galloping energy harvester under Gaussian white noise excitation is investigated. Using the equivalent linearization method and the method of moments in stochastic process theory, the exact closed expressions for the mean square voltage and the average output power are derived based on the distributed parameter model of the energy harvester, and the influence of dimensionless system parameters and noise parameters on the performance indexes are detailed. Monte Carlo numerical simulations verify the correctness of the theoretical predictions. The influence of the parameters and the noise intensity to the moment is studied.

Then, The complexification-averaging method is firstly used to derive the theoretical solutions and analyze the dynamical performance of the energy harvesters under galloping and base excitations. the critical condition for identifying the unstable region is obtained. And with the different system parameters, the critical unstable boundary can be identified. In order to improve the efficiency of energy harvesting, the parameters of the energy harvesters are optimized based on the purpose of maximum voltage amplitude. The results are predicted by means of the multilayer feedforward neural network, and the excellent prediction results can be found.

Finally, the design of an galloping energy harvester that incorporates an elastic structure to reconstructed the traditional GEH. The model is subsequently subjected to theoretical analysis to determine the joint probability density function (PDF) and the stationary PDF of displacement and
velocity. Due to the nonlinear properties of the model, the partial linearization technique and Fokker-Planck-Kolmogorov equation are used to further explore the probability density function of displacement and velocity. Monte Carlo simulation is used to illustrate the behavior of the theoretical results.The simulation results show that, under different conditions, the stationary PDF exhibits different shapes: of double-peak or single-peak, primarily caused by the different states of spring: compression or elongation, respectively.

REFERENCES

[4] Han, J., Huang, D., Li, W., et al. (2023) "Moment analysis of galloping energy harvesters with a parallel circuit under stochastic excitation". *International Journal of Non-Linear Mechanics,* 157: 104518.

[5] Huang, D., Han, J., Li, W., et al. (2023) "Responses, optimization and prediction of energy harvesters under galloping and base excitations". C*ommunications in Nonlinear Science and Numerical Simulation,* 119: 107086.

[6] Yan, Z, Abdelkefi A. (2014) Nonlinear characterization of concurrent energy harvesting from galloping and base excitations. Nonlinear Dynamics, 77(4): 1171-1189.

[7] Abdelmoula H, Abdelkefi, A. Investigations on the presence of electrical frequency on the characteristics of energy harvesters under base and galloping excitations. Nonlinear Dynamics, 2017, 89: 2461-2479.

[8] Li, H., Dong B., Cao, F., et al. (2022) Homoclinic bifurcation for a bi-stable piezoelectric energy harvester subjected to galloping and base excitations. Applied Mathematical Modelling,104: 228-242.

[9] Xu, C., Zhao, L. (2022) Investigation on the characteristics of a novel internal resonance galloping oscillator for concurrent aeroelastic and base vibratory energy harvesting. Mechanical Systems and Signal Processing, 173: 109022.

2nd International Conference on Mathematical
Modelling in Mechanics and Engineering
Mathematical Institute SANU, 12-14. September, 2024.

BENFORD'S LAW WITH APPLICATION IN DYNAMICAL SYSTEMS

Vesna Rajić[1], Jelena Stanojević[2], Nataša Trišović[3]

[1,2]*Faculty of Economics and Business, University of Belgrade, 11000 Belgrade, Serbia*

[3]*Faculty of Mechanical Engineering, University of Belgrade, 11000 Belgrade, Serbia*

[1]*vesna.rajic@ekof.bg.ac.rs*; [2]*jelena.stanojevic@ekof.bg.ac.rs;* [3]*ntrisovic@mas.bg.ac.rs*

[1]ORCID 0000-0002-4566-0147; [2]ORCID 0000-0001-5668-5297, [3]ORCID 0000-0003-1043-5780

Keywords: Benford's law, Manipulations, Dynamical systems.

ABSTRACT

Benford's law, also known as a first digit law, gives a monotonically decreasing distribution of the first digit in the considered data set. In a contradiction with our intuition of appearing of first digit with uniform distribution, this is decreasingly logarithmic law, where the digit 1 is appearing with 30% chance and the digit 9 is appearing with 4.58% chance. It is expected that data, such as: the sizes of events, populations of cities, the flow rates of rivers, the sizes of heavenly bodies, market values, companies' revenues, daily trading volumes follow Benford's law. Also, there are some limitations of the law application, like: coded data, the numbers used as identification numbers, psychologically rounded numbers or natural bounded data with minimum or maximum. The law is also a test of the diversity of data and gives an answer on the question of possible manipulation of the data.

The purpose of this paper is to consider does the Benford's law can be applied on different dynamical systems. These dynamical systems have been employed to describe the broad range of applications in the natural and social sciences, like in mathematics, chemistry, physics, engineering, economics, etc. They are fundamental part of chaos theory and the edge of chaos concept, logistic map dynamics, bifurcation theory, the self-assembly and self-organization processes. As a procedure, we analyze the frequency of the first digit of the coordinates of the trajectories generated by some dynamical systems. We conclude that some trajectories follow Benford's law, some don't follow the law, and some results depend of the choise of the parameters of the model. As the main point is that natural data will follow Benford's law, and we have shown that for the some dynamical systems the distinction between the trajectories that follow Benford's law and that do not follow Benford's law may be very small. Conclusion is that the application of Benford's law in order to make a difference between "natural" data and "artificial" data may require much more careful consideration.

REFERENCES

[1] Benford, F. (1938), "The law of anomalous numbers," *Proc. Am. Philos. Soc. 78*, pp. 551-572.

[2] Hill, T. P. (1998), "The first digit phenomenon," *Am. Sci. 86*, pp. 358–363.

[3] Newcomb, S. (1881), "Note on the frequency of use of the different digits in natural numbers," *Am. J. Math. 4*, pp. 39–40.

[4] Nigrini, M. (1996), "A taxpayer compliance application of Benford's law," *J. Amer. Tax. Assoc. 18*, pp. 72–91.

[5] Kaplan, D. and Glass, L. (1995), *Understanding Nonlinear Dynamics*, Springer-Verlag, New York.
[6] Raimi, R. A. (1976), “The first digit problem,” *Am. Math. Monthly 83*, pp. 521–538.
[7] Strogatz, S. H. (1994), *Nonlinear Dynamics and Chaos: With Applications to Physics, Biology, Chemistry, and Engineering*, (Addison Wesley, Reading, PA).
[8] S. Wolfram, S. (1986), “Random sequence generation by cellular automata,” *Adv.Appl. Math. 7*, pp.123–169.

2nd International Conference on Mathematical
Modelling in Mechanics and Engineering
Mathematical Institute SANU, 12-14. September, 2024.

THE INFLUENCE OF THE CHEMICAL COMPOSITION ON THE FINISH OF THE GRANULATION OF THE ALUMINUM ALLOYS 6082

C. Birtok Baneasa[1], D. Sapta[2] and A. Socalici[3]

[1] *Politehnica University of Timişoara, Faculty Engineering of Hunedoara, 331128, Hunedoara, Romania*

[2] *Politehnica University of Timişoara, Faculty Engineering of Hunedoara, 331128, Hunedoara, Romania*

[3] *Politehnica University of Timişoara, Faculty Engineering of Hunedoara, 331128, Hunedoara, Romania*

[1]*corneliu.birtok@fih.upt.ro*; [2]*saptad94@gmail.com*; [3]*virginia.socalici@fih.upt.ro*

ORCID iD: [1]0000-0002-7239-9597; [2]0009-0001-1358-0660; [3]0000-0002-1854-882X

Keywords: Aluminum alloy, Rims, Microstructure.

ABSTRACT

The work presents the results obtained from the experimental researches carried out at an aluminum alloys. Aluminum alloy was developed 6082 from which semi-finished products were poured. The elaboration of the aluminum alloy is done using different types of aluminum waste in the load. For the correction of the chemical composition, maximum 15% primary aluminum can be used. The elaboration of the aluminum alloy takes place in two-room melting furnaces. The addition of titanium and bor alloy performed for the finishing of grains leads to 0.002 - 0.004%B and 0.022 - 0.042%Ti. The casting is performed using a semi-continent casting system, and the semi-finished products are subjected to thermal homogenization treatment. On the casting flow, the addition of the alloying elements in the form of wire takes place with the role of finishing the structure and filtering of the alloy with the help of a ceramic filter. In order to correlate the refinement and determine the dimensions of the grains, on the production flow, samples are taken. These are analyzed at the XJP-6A microscope and by the optical measurement method, the limits for the size of the grains are determined.

The experimental data were collected and processed statistically. It was sought to establish correlations between the size of the grains (considered dependent parameter) and the elements of the chemical composition with influence on the granulation finish. The data were processed in the Excel calculation program in order to obtain addiction correlations between the analyzed parameters.

By processing the data in the Excel program, simple correlations were obtained, expressed by polynomial functions of grade 1 and 2. Analyzing the correlations obtained in the Excel program, from the point of view of the correlation coefficient and the graphic representation, it turns out that they are technologically significant. It is found that the elements of silicon, manganese, magnesium and titanium, used to finish the granulation, have a positive influence on the mechanical characteristics taking into account the limits between which these elements vary. As for titanium, its growth leads to granulation finishing, which also ensures increased values for mechanical characteristics.

The use of a quality load, leads to small variations for the elements in the chemical composition and following the allying, there are small differences of chemical composition, from one batch to another [1-3]. The limits of limited variation for the chemical elements have led to acceptable variations of the qualitative characteristics of the alloy. The correlations obtained in the Excel program allow the determination of optimal fields of the analyzed parameters. It is found that the alloying elements used finish the granulation. Interest for industrial practice presents the size of the gangs in the finished semi-finished product.

REFERENCES

[1] Bularda, N. (2015), "Metal alloys used for the manufacture of rims intended for road vehicles", *PhD Thesis*, University Politehnica of Timisoara.

[2] Mròvka-Nowotnik, G. (2010), "Influence of chemical composition variation and heat treatment on microstructure and mechanical properties of 6xxx alloys", *Archives of Materials Science and Engineering*, 46(2), pp. 98-107.

[2] Xia, E., Ye, T., Qiu, S., Liu, J., Luo, J., Sun L. and Wu, Y. (2024), "Mechanical Properties and Microstructural Evolution of 6082 Aluminum Alloy with Different Heat Treatment Methods", *Coatings*, 14, p.602.

2nd International Conference on Mathematical
Modelling in Mechanics and Engineering
Mathematical Institute SANU, 12-14. September, 2024.

LARGE AMPLITUDE THERMO-ELASTIC VIBRATION OF CIRCULAR PLATES: PARAMETRIC STUDY AND STABILITY ANALYSIS

Simona Doneva

Institute of Mechanics, Bulgarian Academy of Sciences, Sofia, Bulgaria
s.doneva@pollub.pl
ORCID iD: 0000-0002-5386-9063

Keywords: Nonlinear vibration, Stability, Circular plates.

ABSTRACT

Introduction and main goals

Plates, as main structural components, are often subjected to dynamic loading and temperature influence. The implementation of these fundamentals elements in engineering practice relies heavily on problems of stability and other nonlinear processes.

The nonlinear thermo-elastic vibrations of a circular plate are studied in this work. The plate model is based on the geometrically nonlinear Reissner-Mindlin plate theory assuming that the plate gets elevated temperature instantaneously and it is subjected to harmonic loading. The focus of this study is to investigate the nonlinear behavior of the plate and conduct a detailed parametric analysis of the structure's response in time and parametric domains. The stability analysis of the solutions is performed and its bifurcation is also investigated. Analytical and numerical techniques are used to achieve the main goals of the study.

Methods and models

The mathematical model is founded on the geometrically nonlinear version of Mindlin plate theory. The Galerkin technique reduces the governing partial differential equations that describe the plate motion to ordinary differential equations. The obtained nonlinear reduced model with cubic nonlinearity and temperature effect is studied analytically by Harmonic Balance Method (HBM). The reduced model allows to obtain efficiently the response of the plate in time and frequency domains. Using HBM the influence of the amplitude of the loading and the elevated temperature on the frequency response functions is studied and selected bifurcation diagrams are computed.

Results

The analytical solutions allow performing a parametric study of the response of the structures in the frequency and parameters domains. The stability of the solutions is studied and stable and unstable solutions are detected. The resonance curves around the selected resonance zones, buckling of the structure and other bifurcation points are studied and presented. Detailed parametric study is done.

The resonance curves at different temperatures and fixed amplitude P of the loading obtained analytically by HBM are shown in Fig. 1. The analytical solution is computed for three different values of the temperature: $\Delta T = 40$, $\Delta T = 30$ and $\Delta T = 20$. The strong

stiffening effect of the resonance curves due to the geometrical nonlinearity is clearly visible. The temperature change causes a shifts of the curves.

An example, illustrating the analysis of the stability of the solutions is shown in Fig. 2. A program in MATHEMATICA is created allowing to compute roots of the characteristic equation of the system and to classify the obtained fixed points (Fig. 2).

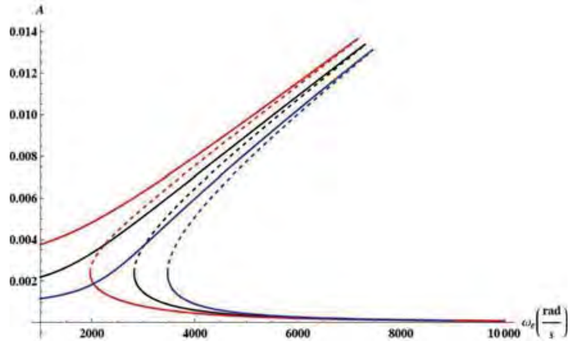

Fig. 1 Resonance curves by HBM for ΔT = 40 - red colour, ΔT = 30 -black colour, ΔT = 20 -blue colour, P = 15 000N / m^2

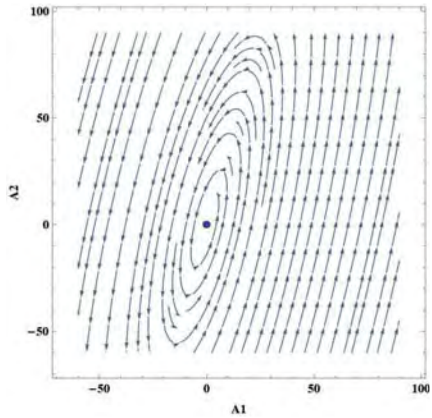

Fig. 2 Trajectories in the vicinity of stable focus for ω_e = 4000 rad / s

Conclusions

The obtained results and their verification by different methods confirm the applicability of the suggested model and approach. It enables getting information about the plate's behavior at different loading parameters - amplitude of the load, excitation frequency, temperature variations without complex computations. It is possible to obtain valuable information for the analysis of the solution stability. The study proofs that the suggested methods can be effectively used for analyzing the nonlinear dynamic behavior of thermally loaded structures**.**

REFERENCES

[1] Doneva, S., Warminski, J., Manoach, E. (2021) Dynamics of Circular Plates Under Temperature and Mechanical Loadings, Springer Proceedings in Mathematics and Statistics, 363, 215-226.

2nd International Conference on Mathematical
Modelling in Mechanics and Engineering
Mathematical Institute SANU, 12-14. September, 2024.

KINEMATIC ANALYSIS OF SCISSOR LIFT STEM TOY

Alma Žiga[1], Amra Talić-Čikmiš[2] and Adnan Barlov [3]

[1,2,3]*University of Zenica , Faculty of Mechanical Engineering, 72000 Zenica, B&H*

[1]alma.ziga@unze.ba; [2]amra.talic.cikmis@unze.ba; [3]ba.adnan123@gmail.com

[1]ORCID iD: 0000-0002-1019-7543

Keywords: STEM model, kinematics, design software.

ABSTRACT

Mechanical toys can be seen as STEM models. At the toy core is a mechanism whose mystic movement arouses children's curiosity. Then there is the level of design and simulation of the mechanism in the design software. When creating a design, it is necessary to know the properties of the material. This project is focused on plywood and PLA plastic. Plywood can be seen as a composite where alternately glued layers are composed of cellulose fibers in a lignin matrix. When designing mechanism, it is necessary to analyze the kinematics and dynamics of movement. At the end, there is the aspect of obtaining the toy parts itself using laser cutting and 3D printing, where the necessary assembly tolerances and tolerances of the parts manufacturing process must be taken into account.

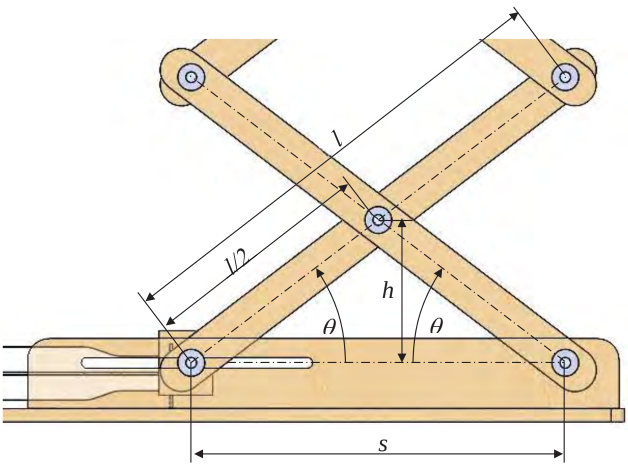

Fig. 1. Scissor lift mechanism

The task is to create a 3D model of a scissor lift mechanism based on an existing toy, perform a software kinematic analysis, and then compare results with analytical kinematic analysis. In the scissor lift mechanism, the linear movement of the piston (Fig. 1.) is converted into a floating movement of the levers, which leads to the vertical movement of the platform. The velocity of piston movement function will be set. Based on it, the distance function s and the height function h will be determined. Based on the obtained functions, the displacement and velocity of the scissor lift platform can be determined.

REFERENCES

[1] Dengiz, G. C., Şenel, M. C., & Yıldızlı, K. (2018). Design and analysis of scissor lifting system by using finite elements method. Universal Journal of Materials Science, 6(2).

[2] Rea, P., & Ottaviano, E. (2016). Analysis and mechanical design solutions for sit-to-stand assisting devices. American Journal of Engineering and Applied Sciences, 9(4).

[3] Saxena, A. (2016). Deriving a Generalized, Actuator Position-Independent Expression for the Force Output of a Scissor Lift. arXiv preprint arXiv:1611.10182.

[4] Toufiqul Islam, M., Yin, C., Jian, S., & Rolland, L. (2014). Dynamic analysis of scissor lift mechanism through bond graph modeling. 2014 IEEE/ASME International Conference on Advanced Intelligent Mechatronics.

[5] Žiga, A., & Begic-Hajdarevic, D. (2021). Rolling ball sculpture as a mechanical design challenge. International Conference "New Technologies, Development and Applications. Sarajevo.

[6] Žiga, A., Ćaro, A., & Mešeljević, L. (2024). 3D printed toy watch with mechanical iris. International Conference "New Technologies, Development and Applications. Sarajevo.

SPECIAL SESSION 3

Mechanics of Materials

Session Chair: **Marina Trajković Milenković**

Invited lecture

MODELING OF PHYSICAL PROBLEMS OF HYSTERESIS

Dragoslav M. Sumarac[1], Zoran B. Perovic[2], Ismail A. Nurkovic[3], Demir Vatic[4], Timur A. Curic[5] and Maosen Cao[6]

[1,3,4,5]*Department of Technical Sciences, State University of Novi Pazar, 36300 Novi Pazar, Serbia*
[2]*Faculty of Cl Engineering, University of Belgrade, 11000 Belgrade, Serbia*
[6]*Department of Engineering Mechanics, Hohai University, Nanjing, 210098, China*
[1]dsumaracl@np.ac.rs; [2]zperovic@grf.rs; [3]inurkovic@np.ac.rs; [4]dvatic@np.ac.rs; [5]tcuric@np.ac.rs; [6]cmszhy@hhu.edu.cn
ORCID iD: [1]0000-0002-4045-5582; [2]0000-0002-4633-954X; [3]0000-0003-3755-0535; [4]0000-0001-7746-7213; [5]0000-0001-5897-4279; [6]0000-0001-6640-1905

Keywords: Hysteresis phenomena, Cyclic plasticity, Adsorption.

ABSTRACT

Hysteretic nonlinear phenomena occur in many physical processes: ferromagnetism [1], adsorption, cyclic plasticity in mechanics, phase transformations, economics etc. It is characterized by the fact that the same instantaneous values of input can give different outputs depending on the history of the input applied. It means that relationship is not only nonlinear, but also multivalued making it very difficult to model and control. In this paper account was given to the application to mechanics i.e. to cyclic plasticity and adsorption.

Application of the Preisach model to cyclic behavior of elasto-plastic material was introduced in 1993 by Lubarda, Sumarac and Krajcinovic [2], [3].One of the most important properties of the Preisach operator is the so called memory map [4][5], but in addition, it is shown in [6] that suggested Preisach model also posses congruency and wiping out property, which makes this model [7]–[9] appropriate to describe hysteretic behavior of elastoplastic material. It was also shown that Preisach model can be defined In purely geometric terms, without any reference to analytic definition.

According to Mayergoyz [6], the Preisach model implies the mapping of an input *u(t)* on the output *f(t)* in the integral form

$$f(t) = \iint \boldsymbol{P}(\alpha,\beta)\boldsymbol{G}_{\alpha,\beta}\boldsymbol{u}(t)d\alpha d\beta \tag{1}$$

The domain of integration is right-hand triangle shown in Fig.1.

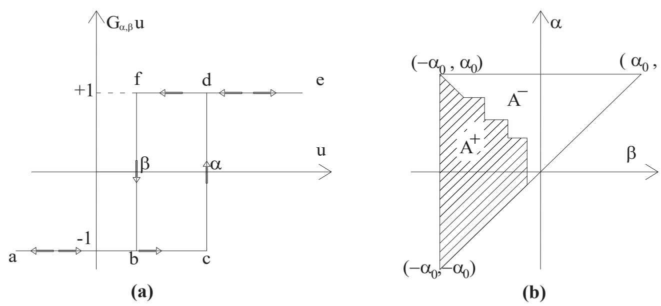

Fig.1. Elementary hysteretic operator and the Preisach triangle

In this paper, besides application to cyclic plasticity, attention will be paid to adsorption. According to [10] the same analogy as in mechanics can be applied for adsorption. A single bar element of elastoplastic bar, will be replaced by a single cylinder on micro level of material that undergoes adsorption. The Preisach function will be defined in this case.

REFERENCES

[1] Visintin, A. (2002) “On hysteresis in elasto-plasticity and in ferromagnetism,” Int. J. Non. Linear. Mech., vol. 37, pp. 1283–1298, doi: 10.1016/S0020-7462(02)00032-X.

[2] Lubarda, A. V, Sumarac, D, Krajcinovic, D.(1992) “Hysteretic Response of Ductile Materials Subjected to Cyclic Loads,” Recent Adv. Damage Mech. Plast., vol. 123, pp. 145–157, 1992.

[3] Lubarda, A. V, Sumarac, D, Krajcinovic, D. (1993). “Preisach model and hysteretic behaviour of ductile materials”, Eur. J. Mech, A&Solida 12(4), 445-457.1.

[4] Al-Bender, F, Symens, W, Swevers, J, Van Brussel, H. (2004) “Theoretical analysis of the dynamic behavior of hysteresis elements in mechanical systems,” Int. J. Non. Linear. Mech., vol. 39, pp. 1721–1736, doi: 10.1016/j.ijnonlinmec.2004.04.005.

[5] Sumarac, D, Knezevic, P, Dolicanin C, Cao, M. (2021) “Preisach elasto-plastic model for mild steel hysteretic behavior-experimental and theoretical considerations,” Sensors, vol. 21, no. 10, doi: 10.3390/s21103546.

[6] Mayergoyz, I. (1991) Mathematical Models of Hysteresis and their Applications. Elsevier..

[7] Sumarac, D, Petraškovic, Z. (2012) “Hysteretic behavior of rectangular tube (box) sections based on Preisach model,” Arch Appl Mech, vol. 82, no. 10, pp. 1663–1673, doi: 10.1007/s00419-012-0663-z.

[8] Sumarac, D, Stosic, S. (1996) “The Preisach Model for the Cyclic Bending of Elasto-plastic Beams,” Eur. J. Mech., A/Solids , vol. 15, no. 1, pp. 155–172,

[9] Sumarac, D, Perovic, Z. (2015) “Cyclic plasticity of trusses”, Arch. Appl. Mech., vol. 85, pp. 1513–1526, 2015, doi: 10.1007/s00419-014-0954-7.

[10] Mitropoulos, A. C, Favvas, E. P, Stefanopoulos, K. L, Vansant, E. F. (2016) “Scanning of adsorption hysteresis in situ with small angle x-ray scattering,” PLoS One, vol. 11, no. 10, doi: 10.1371/journal.pone.0164636.

2nd International Conference on Mathematical
Modelling in Mechanics and Engineering
Mathematical Institute SANU, 12-14. September, 2024.

Invited contribution

PARAMETRIC MODELLING OF BUILDING'S VULNERABILITY INDEX FOR URBAN SCALE RISK ASSESSMENT IN DUBROVNIK'S OLD CITY POST-1979 MONTENEGRO EARTHQUAKE

Penava, Davorin[1], Uzair, Aanis[2], Doctor Arastooye Marandi, Mahdi[3], Beinersdorf, Silke[4], Abrahamczyk, Lars[5]

[1]*Faculty of Civil Engineering and Architecture Osijek, Josip Juraj Strossmayer University of Osijek, 3 Vladimir Prelog Street, 31000 Osijek, Croatia*

[2,3,4,5]*Bauhaus-Universität Weimar, Faculty of Civil and Environmental Engineering, Marienstraße 13c, 99423 Weimar, Germany*

[1]davorin.penava@gfos.hr;[2]aanis.uzair@uni-weimar.de; [3]Mahdi.Arastoo@uni-weimar.de;
[4]silke.beinersdorf@uni-weimar.de; [5] lars.abrahamczyk@uni-weimar.de

ORCID iD: [1]0000-0001-7539-4639; [2]0000-0002-4003-9378; [3]0009-0000-3540-082X;
[4]0000-0001-7844-2739; [5]0000-0002-1217-3844

Keywords: Building Vulnerability Index, Parametric Modelling, Urban Seismic Risk, Dubrovnik's Old City, post-1979 Montenegro Earthquake; GIS mapping

ABSTRACT

Following the 1979 M6.9 Montenegro Earthquake, Dubrovnik's Old City gained significant attention due to its architectural significance and the impact of the seismic event. The earthquake highlighted the vulnerability of its historic structures, prompting increased efforts towards conservation and preservation. Recognizing its cultural importance and the need for protection, Dubrovnik's Old City was inscribed as a UNESCO World Heritage Site in 1979, shortly after the earthquake. This designation not only acknowledges its architectural and historical significance but also underscores the imperative of safeguarding this unique heritage against seismic risks.

The Dubrovnik region and its adjacent areas stand out as Croatia's most seismically active zone. Although recent decades have witnessed relatively mild seismic activity, historical data reveal occurrences of significantly potent earthquakes. The notable Dubrovnik Earthquake of 1667, with an intensity of I_{MCS}=IX-X within the city, resulted in widespread devastation and loss of life. Documented in the Croatian Earthquake Catalogue (CEC), there have been over 28,500 recorded earthquakes within a 100 km radius of Dubrovnik until the end of 2020. Among these, 59 earthquakes exceeded a magnitude of 5.0, with 28 occurring after 1900. Within a 50 km radius, 9708 earthquakes were recorded, with seven earthquakes above magnitude 5 occurring after 1900.

The primary objective of this study was to conduct comprehensive urban-scale eq. risk assessments for Dubrovnik's Old City. This entails evaluating eq. hazard, building vulnerability, and exposure, recognizing the critical role of vulnerability assessments in mitigating seismic impact [1]. Employing the EMS-98 [2] scale, assessments were conducted for about 930 buildings using the Vicente method [3]. Various scenarios were explored to address uncertainties, revealing the importance of precise building information obtained

through meticulous inspections.

Challenges in this regard underscored the need for enhanced precision through detailed surveys of the old masonry buildings. Additionally, analysis highlighted a seismic vulnerability area in the city center, consistent with observations from the 1979 Montenegro earthquake, prompting significant retrofitting efforts. By using GIS tools detailed maps were generated to facilitate urban-scale analysis and presentation of results. Utilizing the comparative analysis conducted, an analytical correlation was established between the vulnerability indexes of the two methods as follows, and the correlation was further detailed based on EMS 98 classification. Considering rehabilitation efforts alongside Best/Worst-Case scenarios, we delineate four distinct Cases: the Best/ Worst-Case before and after rehabilitation. The reconstruction endeavors subsequent to the 1979 earthquake are depicted in a map presented in the figure 1a,b.

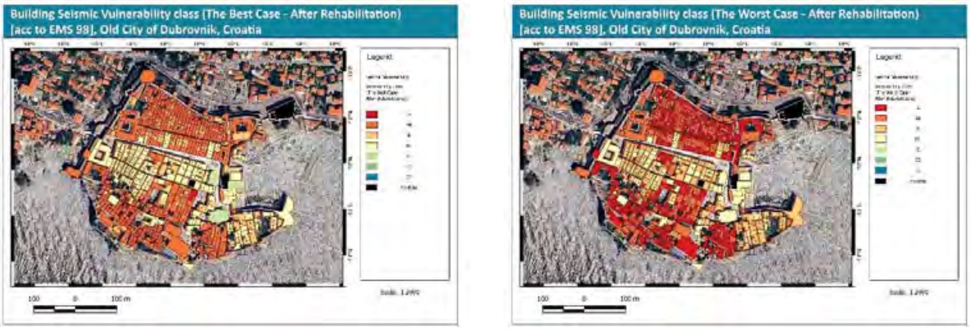

(a) (b)

Figure 1. Seismic vulnerability class after rehabilitation of buildings for: (a) the best-case and (b) the worst-case

Detailed formulations for assessing mean damage grades and subsequent mapping of damages using the EMS-98 scale are presented, with a comparison drawn between predicted and actual damage outcomes within the cultural heritage context.

ACKNOWLEDGMENTS

This study was developed in the framework of the research project entitled “Seismic risk assessment of cultural heritage buildings in Croatia – SeisRICHerCRO” (IP-2020-02-3531) supported by Croatian Science Foundation (HrZZ).

REFERENCES

[1] Stanko, D., Korbar, T., & Markušić, S. (2023). *Evaluation of the Local Site Effects and Their Implication to the Seismic Risk of the UNESCO World Heritage Site Old City of Dubrovnik (Croatia)*. Journal of Earthquake Engineering, 28(3), 731–759.

[2] Grünthal, G., Musson, R.M.W., Schwarz, J. & Stucchi, M. (1998), “*European Macroseismic Scale 1998*”, European Seismological Commission, Brussels, Luxembourg.

[3] Vicente, R. (2008), “*Strategies and methodologies for urban rehabilitation interventions. The vulnerability assessment and risk evaluation of the old city centre of Coimbra*”, Ph.D. thesis, University of Aveiro, Aveiro, Portugal.

2nd International Conference on Mathematical
Modelling in Mechanics and Engineering
Mathematical Institute SANU, 12-14. September, 2024.

Invited contribution

FINITE ELEMENT MODELING FOR STRUCTURAL OPTIMIZATION OF FIXATORS USED IN PROXIMAL FEMUR FRACTURES HEALING

Nikola D. Korunović[1], Jovan Z. Aranđelović[2]

[1]*Faculty of Mechanical Engineering, University of Niš, 18000 Niš, Serbia*

[1]*nikola.korunovic@masfak.ni.ac.rs*; [2]*jovan.arandjelovic@masfak.ni.ac.rs*;
ORCID iD: [1]0000-0002-9103-9300; [2]0000-0001-9653-4119;

Keywords: Orthopedic, Fixator, Parametric CAD model, Finite element method (FEM), Structural optimization.

ABSTRACT

Most long bone fractures require some kind of fixation to heal properly. Depending on the patient's condition, fracture type and fracture complexity, external or internal fixation may be used. Biological internal fixation, which requires the mutual mobility of fractured segments, is a widely recognized method for managing long bone fractures, particularly in the proximal femur [1]. Although this mobility is frequently advantageous for callus formation, it causes significant loading on the fixation device, potentially leading to concerns regarding its stability, strength, or durability. Structural analysis and optimization are commonly employed to mitigate these issues.

This work summarizes the efforts of the research team of LIPS laboratory, Faculty of Mechanical Engineering in Niš, in creating flexible and robust finite element (FE) models of bones mounted with fixation devices and using these in structural analysis and optimization. The object of the presented research is the Selfdynamisable Internal Fixator (SIF), patented by Prof. Mitkovic [1]. Similar to other fixation devices, it is engineered to endure the required load throughout the entire healing period of the fracture, thereby reducing the risk of mechanical failures such as screw breakage or bar bending, and other associated complications.

During the research, the issues that typically had to be addressed were generating CAD models of the femur using medical imaging data, developing flexible and robust parametric CAD models of the femur-fixator assemblies, addressing material modeling concerns specific to the femur, constructing appropriate finite element models for structural analysis, conducting sensitivity analyses, and performing structural optimization studies.

The most reliable basis for creation of CAD models of long bones are computational tomography (CT) images. Medical imaging software is used to separate bone tissue from surrounding soft tissue, resulting in the creation of a polygonal model. Further operations required to obtain a solid CAD model based on the polygonal one, include cleaning, healing, smoothing, surface fitting and solidifying, as described in [2]. An alternative approach implies creating a generic bone model, utilizing parametric modeling and statistics, which can be calibrated to represent a patient specific model based on simple measurements taken from x-ray images [4]. In this way a much less radiation dose is received by patients.

One of the most important issues related to the creation of FE models of long bones is material modeling. Different approaches may be used for this purpose, as detailed in [3]. The two main methods applied are the separation of bone models to internal zones followed by

assignment of constant values of material constants and material mapping. In material mapping, each finite element is assigned a specific material property, based on correlation with bone density indirectly calculated from grey values acquired from medical images.

This paper focuses on the original approach to creation of a CAD model of SIF and the associated FE model, which may be used in sensitivity studies and structural optimization. Here, the main goal of modeling is to create a flexible and robust pair of models, which can faultlessly represent any possible configuration of SIF and any possible placement of SIF in relation to the femur. The two main challenges in achieving this goal are the creation of anatomical landmarks on the bone [3] and appropriate definition of assembly mates (i.e. conversion of fixator placement criteria descriptively defined by surgeons to mathematical constraints [5]).

Created CAD and FE models of femur-fixator assembly were successfully used in sensitivity studies and structural optimization studies, as shown in [2]. Based on these, a number of trends considering the influence of fixator configuration and placement on fixator stress were identified, and the optimal values of corresponding design variables were found.

Future studies will prioritize defining the loads and boundary conditions that impact the femur. This remains a research area with ongoing exploration, given the complexity of determining the forces generated by femoral muscle action, necessitating multi-body simulations.

REFERENCES

[1] Mitkovic, M., Milenkovic, S., Micic, I., Mladenovic, D., Mitkovic, M. (2012), "Results of the femur fractures treated with the new selfdynamisable internal fixator (SIF)", *European journal of trauma and emergency surgery*, 38, pp. 191-200.

[2] Korunovic, N., Arandjelovic, J. (2022), "Structural Analysis and Optimization of Fixation Devices Used in Treatment of Proximal Femoral Fractures", *In Personalized Orthopedics: Contributions and Applications of Biomedical Engineering*, *Cham: Springer International Publishing*, pp. 503-533.

[3] Vitković, N., Milovanović, J., Trajanović, M., Korunović, N., Stojković, M., Manić, M. (2012), "Different approaches for the creation of femur anatomical axis and femur shaft geometrical models", *Strojarstvo: časopis za teoriju i praksu u strojarstvu*, 54(3), pp. 247-255.

[4] Korunovic, N., Trajanovic, M., Stevanovic, D., Vitkovic, N., Stojkovic, M., Milovanovic, J., Ilic, D. (2013), "Material characterization ISSUES in FEA of long bones", *Proceedings of the SEECCM III 3rd South–East European Conference on Computational Mechanics—An ECCOMAS and IACM Special Interest Conference*, Kos Island, Greece, June, pp. 12-14.

[5] Korunovic, N., Marinkovic, D., Trajanovic, M., Zehn, M., Mitkovic, M., Affatato, S. (2019), "In silico optimization of femoral fixator position and configuration by parametric CAD model", *Materials*, 12(14), 2326.

2nd International Conference on Mathematical
Modelling in Mechanics and Engineering
Mathematical Institute SANU, 12-14. September, 2024.

RHEOLOGICAL MODELS OF FRACTIONAL TYPE AND PIEZOELECTRIC PROPERTY FOR NEW BIOMATERIALS

K. (Stevanovic) Hedrih[1,2] and A. Hedrih[1]

[1]*Mathematical Institute of the Serbian Academy of Sciences and Arts, 11000 Belgrade, Serbia*

[2]*Faculty of Mechanical Engineering, University of Nis, 18000 Nis, Serbia*

[1]khedrih@sbb.com; [2]handjelka@mi.sanu.ac.rs

ORCID iD: [1]0000-0002-9773-892X; [2]0000-0001-7598-900X

Keywords: Rheological models, Fractional derivatives, Biomaterials.

ABSTRACT

To study mechanical properties of biological materials mathematical models of viscoelastic and viscoplastic properties of polymers, suspensions and gels might be very useful [1]. Implementation of fractional order derivatives in modelling viscoelastic and plastic properties of materials is new trend in science [2,3]. The general fractional-order Kelvin-Voigt and Maxwell models are used to describe rheological phenomena of real materials with the memory effect in [4]. As biological materials are very complex and include both mechanical and electrical properties in this paper will be present a new rheological model of biomaterial with piezoelectrical and viscoelastic properties using fractional order derivatives [5]. In the first model Kelvin-Voight-Faraday viscoelastic element of fractional type is coupled in parallel with Faraday's ideally piezoelectric element; in second model Maxwells' viscoelastic element of fractional type is coupled in series with Faraday's ideally piezoelectric element. Constitutive relations between normal stress and strain/strain rates, are given for each model. Two rheological models of biomaterial with piezoelectrical and viscoelastic properties are presented in Figure1.

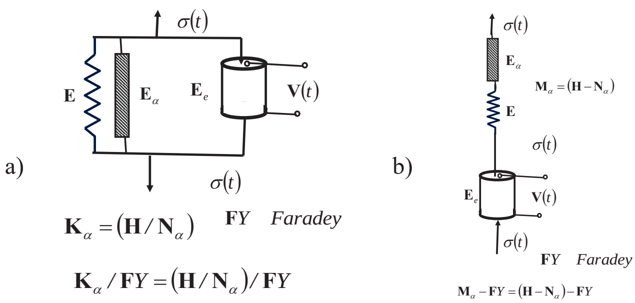

Figure 1. Two complex rheological models of a fractional type with piezoelectric properties. a) The Kelvin-Voight-Faraday's viscoelastic element of fractional type for solids is coupled in parallel Kelvin-Voight with Faraday's ideally piezoelectric element; b) second model The Maxwell-Faraday's viscoelastic fluid element of fractional type is coupled in series modified Maxwell's fractional type element with Faraday's ideally piezoelectric element

To find the relation between strain and time in case presented in a Figure 1 when biomaterial is under sudden constant stress, we apply Laplace transformation and inverse Laplace transformation on equation of constitutive relations between normal stress and strains. Approximatively analytical solutions for strain of material as a time function for both models are given. Dielectrically displacement D, $D_z(t)=b\sigma_z(t)$ and $D_z(t)=e\varepsilon_z(t)$ for a case in Figure 1a) (The Kelvin-Voight-*Faraday's* viscoelastic element of fractional type for solids) is:

$$D_z(t)=e\varepsilon_z(t)=e\frac{\sigma_{z,0}}{(\mathbf{E}+\mathbf{E}_e)}\cdot\cdot\left\langle 1+\sum_{k=}^{\infty}(-1)^k\left(\frac{\mathbf{E}_\alpha}{(\mathbf{E}+\mathbf{E}_e)}\right)^k\frac{t^{(2-\alpha)k+1}}{\Gamma(2k+2-\alpha k)}\right\rangle \tag{1}$$

and for a case Figure 1b, (The Maxwell-*Faraday*'s viscoelastic fluid element of fractional type):

$$D_z(t)=b\sigma_z(t)\approx b\mathbf{E}_\alpha\left\{\mathsf{D}_t^\alpha[\varepsilon_z]_{z,,0}\right\}\cdot\left\{1+\sum_{k=}^{\infty}(-1)^k\left(\frac{\mathbf{E}_\alpha}{\mathbf{E}_e}+\frac{\mathbf{E}_\alpha}{\mathbf{E}}p\right)^k\frac{t^{(2-\alpha)k+1}}{\Gamma(2k+2-\alpha k)}\right\} \tag{2}$$

The material modeled in a Figure 1a) exhibits the property of subsequent elasticity, where dilation lags behind stress.

The models presented serve as the foundation for the construction of more complex structures of ideal materials, with programmed stress relaxation properties and subsequent elasticity. Complex models also possess properties related to the occurrence of internal degrees of freedom that must be taken into account when studying rheological dynamical systems like oscillators or crawlers or forced pulsator of fractional type with piezoelectric properties.

Acknowledgement

We are grateful to the financial support from Ministry of Science, Technological Development and Innovation of Republic of Serbia trough Mathematical Institute of Serbian Academy of Sciences and Arts.

REFERENCES

[1] Verdier, C. (2003), Review: "Rheological properties of living materials. From cells to tissues", *Journal of Theoretical Medicine,* 5 (2), pp.67-91.

[2] Hedrih (Stevanović), K. R, Machado, J. T. (2015), "Discrete fractional order system vibrations," *International Journal Non-Linear Mechanics,* 73, 2–11

[3] Hedrih (Stevanović), K. R, Hedrih, A. N. (2023), "The Kelvin–Voigt visco-elastic model involving a fractional-order time derivative for modelling torsional oscillations of a complex discrete biodynamical system," *Acta Mechanica,* 234, pp. 1923–1942.

[4] Yang, X-J. (2018), "New rheological problems involving general fractional Derivatives with nonsingular power-law kernels", *Proceedings of the romanian academy,* Series A, 19(1), pp. 45–52.

[5] Hedrih (Stevanović), R. K, Milovanović, V. G. "Elements of mathematical phenomenology and analogies of electrical and mechanical oscillators of the fractional type with finite number of degrees of freedom of oscillations: linear and nonlinear modes" (under review).

2nd International Conference on Mathematical
Modelling in Mechanics and Engineering
Mathematical Institute SANU, 12-14. September, 2024.

APPLICATION OF NUMERICAL ANALYSIS IN DETERMINATION OF FRACTURE RESISTANCE OF PIPELINE MATERIALS

Isaak D. Trajković[1], Walid M. Musrati[2], Miloš S. Milošević[3], Aleksandar S. Sedmak[4], Bojan I. Medjo[5]

[1,3]Innovation center of faculty of Mechanical Engineering in Belgrade, Kraljice Marije 16, 11000 Belgrade, Serbia

[2]University of El Mergib, Faculty of Engineering, Khoms, Libya

[4]University of Belgrade, Faculty of Mechanical Engineering, Kraljice Marije 16, 11000 Belgrade, Serbia

[5]University of Belgrade, Faculty of Technology and Metallurgy, Karnegijeva 4, 11000 Belgrade, Serbia

[1]trajkovicisaak@gmail.com

ORCID iD: [1]0000-0001-6671-4733; [3]0000-0002-2418-1032; [5]0000-0001-8100-7519

Keywords: Pipeline Materials, Finite element analysis, Fracture Mechanics Specimens

ABSTRACT

Fracture mechanics analysis of pressurized pipelines is crucial to ensure the safety and durability of infrastructure, especially in industrial facilities where pipelines are exposed to high pressures and extreme conditions. Traditional methods and standards such as ASTM E1820 and ISO 12135 for fracture mechanics testing may not always be applicable or effective for thin-walled pipelines, necessitating the development of new approaches. Their disadvantages are reflected in the fact that the specimens must satisfy precisely defined dimensions in order for the test results to be relevant. In this context, experimental and numerical analysis of non-standard ring-shaped specimens with a sharp stress concentrator - PRNB (Pipe Ring Notched Bending) or PRNT (Pipe Ring Notched Tension) offers an insight into the behavior of pipeline materials. The pipe structure is not significantly changed during the preparation of specimens for measurement and enables the determination of pipeline material fracture resistance.

Fig. 1 contains the geometry of both considered specimens; they are both shaped as rings, and are obtained by cutting from the pipe. Also, the finite element models of these specimens are shown on the right-hand side of the figure. The loading is introduced through the contact with additional tools, which are designed to emulate the three-point bending in the case of PRNB specimen, or internal pressure in the case of PRNT specimen.

In this work, different aspects of failure assessment of these geometries which include the application of the finite element method will be considered, such as micromechanical analysis of crack growth and determination of the parameters necessary for calculation of the J integral. Application of numerical analysis in this context provides a detailed view of the material failure behaviour and enables calculation of quantities which are otherwise difficult or impossible to determine. Such combination of experimental and numerical examination enables a proper integrity assessment of pressure pipelines. This approach not only overcomes the limitations of existing standards, but also enables further innovations in the field of materials testing, thus contributing to greater safety and efficiency.

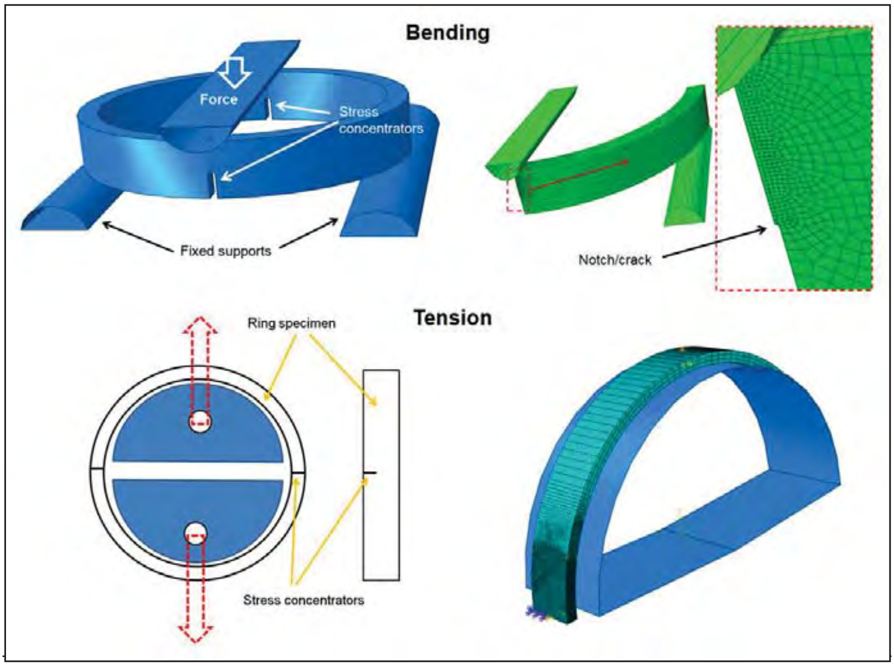

Fig. 1. Geometry and finite element models for PRNB and PRNT specimens

Acknowledgements:

The authors would like to acknowledge the contribution of late Prof. Dr. Marko Rakin, who was an integral part of this research in the previous period. The work was supported by the Ministry of Science, Technological Development and Innovation of the Republic of Serbia (contr. 451-03-66/2024-03/200213 and 451-03-65/2024-03/200135).

REFERENCES

[1] Musrati, W., Međo, B., Gubeljak, N., Štefane, P., Veljić, D., Sedmak, A., Rakin, M. (2019), "Fracture assessment of seam and seamless steel pipes by application of the ring-shaped bending specimens". *Theoretical And Applied Fracture Mechanics*, Vol. 103, Paper No. 102302

[2] Trajković, I., Rakin, M., Milošević, M., Mitrović, N., Travica, M., Sedmak, A., Međo, B. (2023), "Selective laser sintered pipe ring notched tension specimens for examination of fracture properties of pipeline materials". *Engineering Fracture Mechanics*, Vol. 292, Paper No. 109573

2nd International Conference on Mathematical
Modelling in Mechanics and Engineering
Mathematical Institute SANU, 12-14. September, 2024.

MODELS FOR UNIAXIAL AND MULTIAXIAL FATIGUE FAILURE

Zoran B. Perovic[1], Coric B. Stanko[2] and Sumarac M. Dragoslav[3]

[1,2]Faculty of Civil Engineering, University of Belgrade, 11000 Belgrade, Serbia

[3]Department of Technical Sciences, State University of Novi Pazar, 36300 Novi Pazar, Serbia

[1]zperovic@grf.rs; [2]cstanko@grf.rs; [3]dsumarac@np.ac.rs

ORCID iD: [1]0000-0002-4633-954X; [2]0000-0002-7383-6154; [3]0000-0002-4045-5582

Keywords: Cumulative damage, Arbitrary loading, Fatigue life, Critical plane.

ABSTRACT

The service life of various engineering components and structures can be substantially reduced if subjected to fatigue loading. This paper presents a study that proposes models for both uniaxial and multiaxial stress states in fatigue damage modeling. Since analyzed data for uniaxial fatigue considers mainly phenomena of low-cycle fatigue loading, the energy-based approach is defined using plastic energy as the governing parameter. Moreover, the material model is constructed as an assembly of N cells that can provide computationally efficient outputs of stress and hysteretic energy loss [1], for a strain as input. These cells [2] are distributed according to their different fracture energy values. As a result, a cumulative damage model is formed [3] since cells are eliminated from the global model gradually. The measure of damage D actually represents a point on the cumulative distribution function defined according to the probability density function (Fig.1(a))

$$\sigma = N \cdot \tilde{\sigma}(1 - D), \quad E = N \cdot \tilde{E}(1 - D) \tag{1}$$

σ and E are variables of the global model, while parameter D quantifies ruptured elements. Parameter D can be regarded as a scalar damage variable [4] that has a range from 0 (undamaged state) to 1 (total failure). For each cell, stress $\tilde{\sigma}$ and modulus of elasticity $\tilde{E}$ can also represent degraded values of the initial undamaged state, since these elements can depict elastoplastic damage behavior in function of strain input, which is quantified with another damage variable. Additionally, the model is expanded to consider the mean strain effect, enabling a numerically efficient model for arbitrary loading. As can be seen from Fig.1(a), the group n_{el} of different unit elements have varying fracture limits according to which corresponding distribution can usually be defined with several parameters. They are grouped according to equal fracture energy $Q_{f,i}$ which probability density function is defined from minimum to maximum fracture energy $Q_{f,max}$. Active cells have higher fracture energy than current achieved total energy loss $Q_f(t)$, while this value exceeds the limit for other cells that fail and consequently change material properties (Eq.1). Further, this distribution fluctuates depending on the strain level (Fig.1(b)), while the damage equivalence principle ensures the transition. Parameters for constructional steel S355 are determined based on experimental results, and used in the numerical example of random variable amplitude loading with different mean strain values (Fig 1(b)).

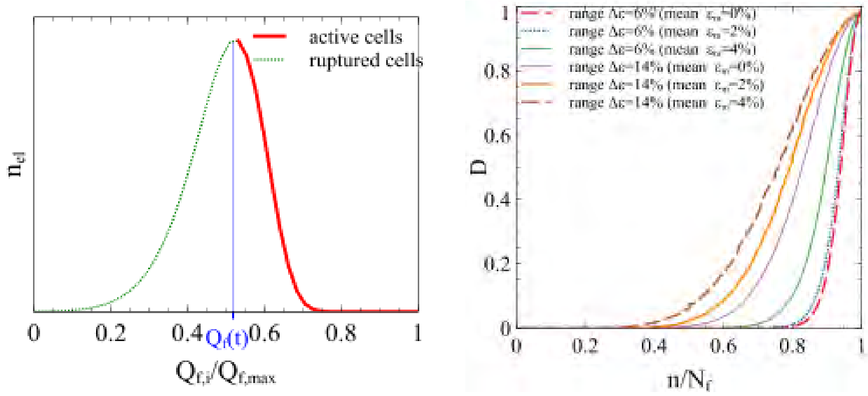

(a) (b)

Fig 1(a) Cells` fracture energy distribution; (b) Damage evolution for random loading

Further, the complex problem of multiaxial fatigue is tackled by similar tools. For a more realistic and complex multiaxial analysis, fatigue damage is usually defined up to crack initiation as an ultimate limit for failure ($D \ll 1$), in contrast to the theoretical limit of total degradation. One of the most efficient methods in multiaxial fatigue analysis is the critical plane approach [5], although often equivalent strain [6] and equivalent stress methods also consider the critical plane. Since multiaxial fatigue damage evaluation is a demanding task, especially under variable and nonproportional loading, the ultimate goal is to reduce the multiaxial strain or stress state to an equivalent damage condition. Similarly, most models transform irregular loading history into multiaxial regular fatigue by various counting algorithms. In the critical plane method, material volume analysis is remodeled by analyzing the expected location of the fatigue fracture plane based on the criteria of maximum shear stress, normal stress, principal stress, etc. In this case, the calculation of accumulated damage could be performed by the uniaxial cycle counting method. Therefore, this paper shows how particular features of the presented approach for uniaxial cumulative damage can be extended to a multiaxial stress state.

REFERENCES

[1] Mayergoyz I. (1991) Mathematical Models of Hysteresis and their Applications. Elsevier.
[2] D. Šumarac, Z. Perović, (2015) “Cyclic plasticity of trusses”, Arch. Appl. Mech., vol. 85, pp. 1513–1526, 2015, doi: 10.1007/s00419-014-0954-7.
[3] Perović Z., Šumarac D., Ćorić S. (2023) “Low-Cycle Fatigue Damage Model For Ductile Materials.” MS7-08, Fourth International Conference on Damage Mechanics (ICDM4), Louisiana State University, 15-18. May 2023.
[4] Kachanov L. M. (1958) “On time to rupture in creep conditions (in Russian),” Izviestia Akad. Nauk SSSR, Otd. Tekhnicheskikh Nauk, vol. 8, pp. 26–31.
[5] Carpinteri A., Kurek M., Łagoda T., Vantadori S. (2017) “Estimation of fatigue life under multiaxial loading by varying the critical plane orientation,” Int. J. Fatigue, vol. 100, pp. 512–520, Jul. 2017, doi: 10.1016/j.ijfatigue.2016.10.028.
[6] Zhu P. N., Gao J. X., Yuan Y. P., Wu Z. F., Xu R. X. (2023) “An Improved Multiaxial Low-Cycle Fatigue Life Prediction Model Based on Equivalent Strain Approach,” Metals (Basel)., vol. 13, no. 3, Mar. 2023, doi: 10.3390/met13030629.

2nd International Conference on Mathematical
Modelling in Mechanics and Engineering
Mathematical Institute SANU, 12-14. September, 2024.

MORTARS WITH MARBLE POWDER AS PARTIAL REPLACEMENT FOR CEMENT – EXPERIMENTAL AND NUMERICAL ANALYSIS

Merima Šahinagić-Isović [1], Marko Ćećez[2], Andrija Zorić[3], Marina Trajković-Milenković[4]

[1,2]*Faculty of Civil Engineering, Džemal Bijedić University of Mostar, 88000 Mostar, B&H*
[3,4]*Faculty of Civil Engineering and Architecture, University of Niš, 18000 Niš, Serbia*
[1]*merima.sahinagic@unmo.ba*; [2]*marko.cecez@unmo.ba*; [3]*andrija.zoric@gaf.ni.ac.rs*;
[4]*marina.trajkovic@gaf.ni.ac.rs*
ORCID iD: [1]0000-0002-3975-0824; [2]0000-0002-5938-2985; [3]0000-0002-3107-9204;
[4]0000-0001-6874-758X

Keywords: Mortar, Marble powder, Sustainability, Experiment, Finite element analysis.

ABSTRACT

In recent years much attention has been paid to investigate replacement of cement with some industrial waste materials in order to reduce the cement production [1], considering that it provides about 7-8% of total world CO_2 emission [2]. Industrial waste materials that are in focus have promising chemical composition and favorable particle size distribution [3]. Besides several most researched materials for this purpose, marble powder has drawn attention, due to accessibility and potentially compatible chemical composition. World production of marble in 2019 was about 319 million of metric tons, while about 53% was considered as waste [4]. However, marble waste as cement replacement in mortar is not sufficiently researched.

In this paper, experimental tests of compressive and flexural tensile strength of cement mortar incorporating marble powder as partial replacement for cement are presented. The numerical finite element analysis model for determination of flexural tensile strength is proposed as well.

The cement mortar 1:3 is prepared with cement CEM II/A-M (S-V) 42,5N and crush-separated limestone. In total 5 mixtures (marked as CM1 to CM5) are prepared, where marble powder replaces the cement at ratios 0%, 5%, 10%, 15% and 20% by weight of cement. Marble powder and cement are considered as binders and water/binder ratio of 0,52 is constant in all mixtures. Compressive strength and flexural tensile strength tests are performed on prismatic 40x40x40 mm and 40x40x160 mm samples, respectively. All tests are conducted after 28 days. Average experimental results of three samples for each mixture are presented in Table 1.

Finite element analysis models for flexural tensile strength determination of CM1 and CM5 have been created according to the experimental setup. The concrete damage plasticity model has been used in order to indirectly track crack propagation. Modulus of elasticities have been defined based on the experimental compressive strength [5], while characteristic axial tensile strengths have been calculated according to concrete standard [6]. Stress-strain relationship in compression and tension has been idealized as bilinear diagram due to the lack of exact data, and based on available test results [5, 7], while damage parameters have been determined accordingly to the adopted stress-strain diagrams [8]. Considering damage parameter in tension as crack propagation, it can be concluded that specimen failure occurs due to one dominant crack in midspan, which is fully in concordance with the experimental results (Figure 1).

Numerically obtained ultimate forces for models CM1 and CM5 are approximately 5-6% lower than experimentally obtained values.

Table 1. Experimental test results

Mixture	Strength [MPa]	
	Compressive	Flexural
CM1	49,21	9,03
CM2	47,72	8,91
CM3	51,41	8,67
CM4	48,09	7,97
CM5	36,32	8,83

a) b)

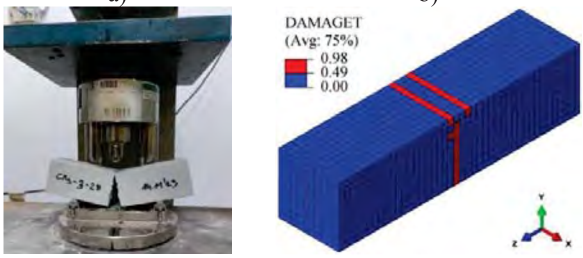

Figure 1. Flexural tensile strength sample CM5: a) Experiment test, b) Numerical simulation

Based on the experimental results it can be concluded that satisfactory compressive and flexural tensile strength are obtained by replacing cement with marble powder up to 15%. The proposed finite element analysis model and material model can be considered as validated and reliable, considering good agreement of numerical and experimental results.

REFERENCES

[1] Serdar, M., Biljecki, I., Bjegović, D. (2017), "High performance concrete incorporating locally available industrial by-products", *Journal of Materials in Civil Engineering*, 29(3), 04016239, https://doi.org/10.1061/(ASCE)MT.1943-5533.0001773

[2] Winnefeld, F., Leemann, A., German, A., Lothenbach, B. (2022), "CO_2 storage in cement and concrete by mineral carbonation", *Current Opinion in Green and Sustainable Chemistry*, 38, 100672, https://doi.org/10.1016/j.cogsc.2022.100672.

[3] Vladić Kancir, I., Serdar, M. (2022), "Contribution to Understanding of Synergy between Red Mud and Common Supplementary Cementitious Materials", *Materials*, 15(5), 1968, https://doi.org/10.3390/ma15051968

[4] Khorshed, E. A. E., El-Naggar, S. A., El-Gohary, S. S., Awad, A. M. B., Ahmed, A. S. (2022). "Occupational ocular health problems among marble workers at Shaq El Tho'ban industrial area in Egypt". *Environmental Science and Pollution Research*, 29(25), pp. 37445-37457. https://doi.org/10.1007/s11356-021-18410-5.

[5] Aocharoen, Y., Chotickai, P. (2021), "Compressive mechanical properties of cement mortar containing recycled high-density polyethylene aggregates: Stress-strain relationship", *Case Studies in Construction Materials*, 15, e00752, https://doi.org/10.1016/j.cscm.2021.e00752.

[6] European Committee for Standardization CEN (2004), "EN 1992-1-1:2004, Eurocode 2: Design of concrete structures - Part 1-1: General rules and rules for buildings".

[7] Zhou, J., Qian, P., Chen, X. (2014), "Stress-Strain Behavior of Cementitious Materials with Different Sizes", *The Scientific World Journal*, Hindawi Publishing Corporation, 2014, 919154, https://doi.org/10.1155/2014/919154.

[8] Ranković, S., Zorić, A., Vacev, T., Petrović, Ž. (2023), "Numerical Analysis of an Innovative Double-Strap Joint for the Splicing of Near-Surface Mounted Fiber-Reinforced Polymer Bars for Reinforced Concrete Beam Strengthening", *Applied Sciences*, 13(22), 12387, https://doi.org/10.3390/app132212387.

2nd International Conference on Mathematical
Modelling in Mechanics and Engineering
Mathematical Institute SANU, 12-14. September, 2024.

NUMERICAL ESTIMATION OF SPRING-BACK EFFECT IN BENDING PROCESSES

Marina Trajković-Milenković[1], Saša Ranđelović[2], Andrija Zorić[3], Katarina Slavković[4]

[1,3,4]Faculty of Civil Engineering and Architecture, University of Niš, 18000 Niš, Serbia
[2]Faculty of Mechanical Engineering, University of Niš, 18000 Niš, Serbia

[1]marina.trajkovic@gaf.ni.ac.rs; [2]sasa.randjelovic@masfak.ni.ac.rs; [3]andrija.zoric@gaf.ni.ac.rs;
[4]slavkovic.katarina3@gmail.com

ORCID iD: [1]0000-0001-6874-758X; [2]0000-0002-2334-8929; [3]0000-0002-3107-9204;
[4]0009-0009-9231-2856

Keywords: Bending, Spring-back, Objective Jaumann rate, Numerical elastoplastic analysis.

ABSTRACT

Until recently, the design of metal forming has been based on the knowledge gained through a long practical experience or expensive experimental try-outs. Nowadays, using a finite element analysis from an early stage of a production process, the errors can be corrected and avoided before the actual manufacturing, making the production process less expensive.

In this paper, the authors perform a numerical analysis of the V shape bending of a thin plate in order to properly predict the elastic deformations during unloading in bending processes, known as a spring-back effect. The aim of this work is to define the amount of an elastic spring-back of the thin plate during its metal forming process by plastic deformation only. Also, the possible corrections of this effect are proposed. Different parameters can influence the amount of spring-back effect such as a change in the thickness of the metal sheet, eventual heat treatment and change of material strength during the production process, the chemical composition of the material, and the direction of rolling of the sheet in comparison with the direction of its bending. In this work, only the influence and possible correction of the geometry of the die and punch are considered. The obtained results for the same material are compared mutually and with the relevant literature. The influence of the sheet thickness and other parameters on the spring-back problem remains for further analysis. The Abaqus/Standard software procedure completes a nonlinear finite element analysis. The numerical models are tested using a built-in elastoplasticity material model which is based on the objective Jaumann stress rate.

In Figure 1 the initial bending shape of the steel sheet (black solid line) and the shape of the tested material after elastic recovery (gray solid line) are presented. The final shape of the thin plate is not obtained in the initial trial, due to the elastic unloading. Therefore, several numerical iterations are performed to tune up the geometry of the tool in order to achieve the desired shape of the thin plate. The final iteration gave satisfactory geometry of the metal sheet and consequently, the die and punch geometry in that iteration are assumed to be final.

The special attention in this work is paid to the stress and strain state analysis of the chosen material during the shaping processes (Figure 2), especially the development of the zone of plastic deformation through the cross-section of the sheet.

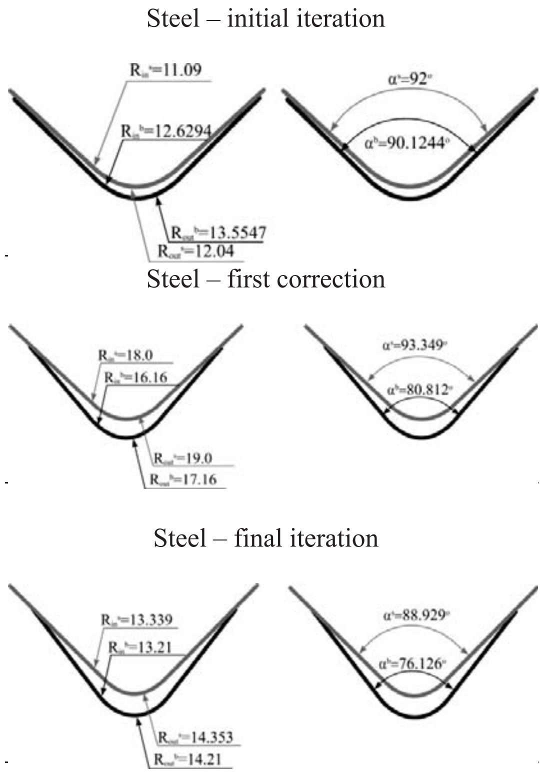

Figure 1. Shape of the steel metal sheets before (b) and after the spring-back (s) in several numerical iterations

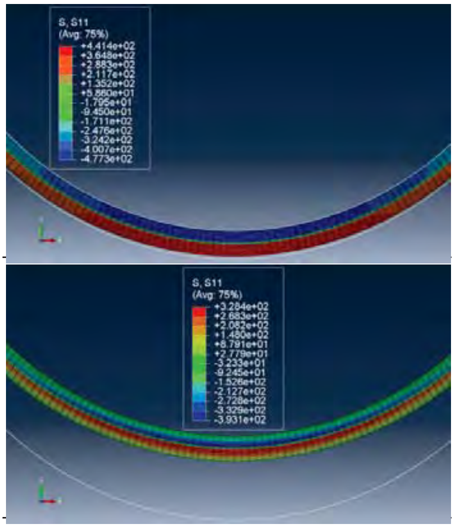

Figure 2. The normal stress distribution at the bottom of V shape in the steel sheet at the bending stage and after the spring-back

Based on the obtained and presented numerical results, the significant difference between the desired shape of the metal sheet obtained by the pure bending process and the one obtained due to the recovered elastic deformation, i.e. the spring-back, of the tested material can be observed. This work confirms that the extensive numerical analysis can be useful for properly identifying the spring-back effect in the metal forming process by plastic deformation prior to the actual manufacturing processes. In order to obtain the desired shape of the profiles, the proposed approach can make the production process significantly less costly. The additional parameters stated above, which also influence the spring-back effect, have to be considered as well.

REFERENCES

[1] Chan, W.M., Chew, H.I., Lee, H.P., Cheok, B.T. (2004),“ Finite element analysis of spring-back of V-bending sheet metal forming processes”, *Journal of Materials Processing Technology*, 148(1), pp.15-24, https://doi.org/10.1016/j.jmatprotec.2003.11.038.

[2] Damtew, AW, Gebresenbet, T. (2017), “Study the Effects of Spring Back on Sheet Metal Bending using Mathematical Methods”, *Journal of Material Sciences & Engineering*, 6(5), doi:10.4172/2169-0022.1000382.

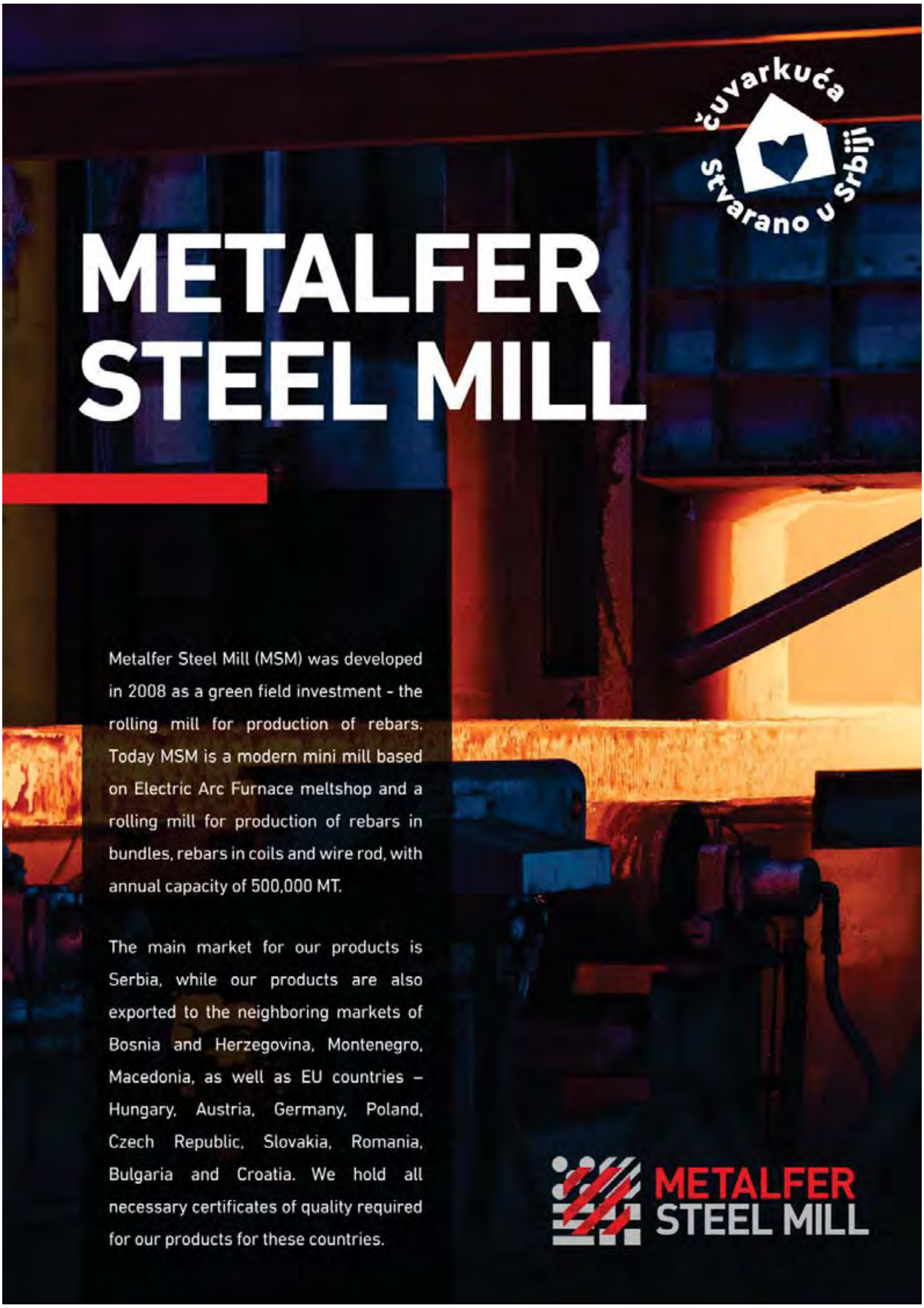
čuvarkuća
Stvarano u Srbiji
METALFER
STEEL MILL
Metalfer Steel Mill (MSM) was developed in 2008 as a green field investment - the rolling mill for production of rebars. Today MSM is a modern mini mill based on Electric Arc Furnace meltshop and a rolling mill for production of rebars in bundles, rebars in coils and wire rod, with annual capacity of 500,000 MT.
The main market for our products is Serbia, while our products are also exported to the neighboring markets of Bosnia and Herzegovina, Montenegro, Macedonia, as well as EU countries – Hungary, Austria, Germany, Poland, Czech Republic, Slovakia, Romania, Bulgaria and Croatia. We hold all necessary certificates of quality required for our products for these countries.
METALFER
STEEL MILL


SHIMADZU
Doprinos društvu kroz znanost i tehnologiju
Svrha je služiti i štititi temelj života čovečanstva i prirode.
Shimadzu nudi veliki broj različitih proizvoda, od analitičke i merne opreme do naprednih medicinskih uređaja te je jedan od vodećih svetskih proizvođača analitičkih instrumenata kao i opreme za praćenje okoliša. Shimadzu analitički instrumenti su idealna rešenja za farmaciju, hemiju, petrohemiju, biogoriva, energiju, hranu, pića, poljoprivredu, okoliš, zdravlje, biomedicinske nauke, industriju i automobile.
Slogan Excellence in Science (Izvrsnost u nauci) odražava težnju i stav da na zahteve korisnika odgovaramo ponudom superiorne tehnologije svetske klase.
Održivost
Inovacija
Kvaliteta
Shimadzu d.o.o. Beograd - Milutina Milankovića 23 - 11 070 Novi Beograd
T: +381 11 711 54 46, +381 11 711 54 49 - F: +381 11 711 54 51
shimadzu@shimadzu.rs

"PROJEKTINŽENJERING TIM" D.O.O Niš
Privredno društvo za projektovanje, inženjering, konsalting i nekretnine
18000 Niš, ul. Prešernova br. 8, lokal 1;
tel: 018/522-177; mob.tel.: (+381) 69-194-1280;
E: office@projektinzenjering.com;
www.projektinzenjering.com;
PIB: 108 142 547; Mat. br. 20938927; Šif. del. 7112

Projektinženjering Tim is a design, engineering, consulting and real estate company, active in the areas of residential, public, commercial and infrastructure construction.

As a trusted partner, we offer our clients diverse services in all phases of their investments – from concept design to building acceptance, as well as in adaptation of existing buildings and the improvement of their energy efficiency.

Based in Niš, Serbia, Projektinženjering Tim was founded in 2013 to channel the decades-long experience of our engineers, architects and other associates, and offer it to our clients, according to the needs of each individual project.

With strong ties to the academic community, we also innovate in the field of structural design. We are especially proud of our patent "Adaptive system for seismic protection of buildings against the effects of strong earthquakes through structurally ensured global optimization of the seismic-energy balance", realized with assistance from the Republic of Serbia Innovation Fund.

For more details about our activities and for potential cooperation in any form, it would be our pleasure if you would get in touch.

Deo referenci / Some reference

Proizvodni objekat fabrike “IMI”, Niška Banja
Production facility of the “IMI” factory, Niška Banja

Proizvodni objekat fabrike “Ergomade”, Merošina
Production facility of the “Ergomade” factory, Merošina

Naučno-istraživački institut “BioSense”, Novi Sad, projekat konstrukcije
Scientific Research Institute "BioSense", Novi Sad, structural design

Pešački most preko Prolomske reke, Prolom Banja
Pedestrian bridge over the Prolomska river, Prolom Banja

ANA MILANOVIĆ JOVANOVIĆ PR BIRO ZA PROJEKTOVANJE
AMING PROJEKT KNJAŽEVAC,
ul. Knjaza Miloša 75/12, 19350 Knjaževac, tel.069/618331,
E: aming.projekt@gmail.com;
PIB: 110 045 226; Mat.br. 64607880; Šif. del. 7112

Agencija za projektovanje AMING PROJEKT iz Knjaževca je osnovana\ 2017. godine.

Stručan kadar sa značajnim iskustvom u oblasti projektovanja građevinskih konstrukcija zadužen je za realizaciju različitih projekata, a sve na zadovoljstvo klijenata. Iako mlada, agencija poseduje impozantne reference, koje se ogledaju u projektovanju građevinskih konstrukcija objekata bruto površine oko 200.000,00 m^2.

The agency AMING PROJEKT from Knjaževac was founded in 2017.

Personal staff with considerable experience in the field of structural design is responsible for the implementation of various projects, all to the satisfaction of the clients. Although young, the agency has impressive references, which are reflected in the design of building structures with a gross area of approximately 200.000,00 m^2.

Deo referenci / Some reference

Stambeno-poslovni objekat, ul. Cara Dušana, Niš
Residential and office building, Cara Dušana st., Niš

Stambeno-poslovni objekat, ul. Obilićev venac bb, Niš
Residential and office building, Obilićev venac st., Niš


SIMULATION, TESTING, VIRTUAL PROTOTYING
FOR PRODUCT DEVELOPMENT
econ ENGINEERING
Founded in 2002
100+ engineers
Serbia | Croatia | Hungary Germany | U.S.A.
ISO 9001 | ISO/IEC 27001 | EN 9100 TISAX Level 3 | GE IT-Security
Advanced RDI competencies
In-house material testing lab
SOFTWARE DISTRIBUTION
LICENSE | LEASE | SUPPORT | TRAINING
Ansys / CHANNEL PARTNER
Moldex3D
CFturbo
Particleworks
AnalySwift
dante
CAST-DESIGNER
CAE SERVICES
FEA I CFD I EMS I MBS I 1D
AREAS OF EXPERTISE
Aerospace | Space | Automotive
Composite | Military | Energy (Oil & Gas)
Healthcare | Railway | Construction
Pharma | Food & Beverage | Agriculture
CONTACT US
www.econengineering.com
/econengineering
/econengineeringkft
/@econengineering932

SVECOM doo, Preduzeće za inženjering, spoljni u unutrašnji promet,

Ustanička 128a/III, Beograd

Kompanija SVECOM DOO BEOGRAD osnovana je 1991. godine u Beogradu sa aktivnostima u oblasti energetike, rudatsva, ekologije ,gasne detekcije i drugim granama industrije.

Ukupan broj zaposlenih je oko 30 od čega je 25 u stalnom odnosu, dok je 5-6 eksperata angažovano na raznim projektima. Najveći broj zaposlenih su inženjeri različitih profila ,zatim ekonomisti i menadžeri.

U oblasti energetike sa češkim partnerima **ZVVZ** kao i **PSP** realizovali smo isporuku i ugradnju elektrofiltera na TE Kostolac,TE Ugljevik, kao i isporuku I ugradnju drobiličnih postrojenja u REIK Kolubara i Kostolac.

U oblasti rudarstva u saradnji sa jednim od najvećih svestskih proizvođača specijalnih čeličnih konstrukcija **ArcelorMittal** i **Liberty Ostrava** (Češka) opremamo rudnike sa podzemnom eksploatacijom čeličnim lučnim profilima (rudarska podgrada).

U oblasti gasne detekcije saradjujemo sa kompanijama **Teledyne-Oldham Simtronics** Francuska vodećim svetskim proizvođačem stabilnih sistema gasne detekcije za industriju , **Trolex** Engleska-vodećim svetskim proizvođačem stabilnih sistema za detekciju gasova u rudnicima sa podzemnom eksploatacijom kao i sa **Industrial Scientific** USA. Vodećim svestskim proizvođačem u oblasti mobilnih gasnih detektora.

Oblast delovanja je detekcija eksplozivnih i toksičnih gasova u rudnicima sa podzemnom eksploatacijom, industrijskim postrojenjima , čeliščanama, pogonima za proizvodnju veštačkog đubriva kao i skladištima tečnog naftnog gasa.

Iz oblasti gasne detekcije posedujemo sertifikat o akreditaciji izdat od ATS a kao i rešenje MUP a koji nam omogućava kontrolisanje instalacija posebnih sistema za detekciju eksplozivnih i zapaljivih gasova.

Bregava d.o.o.

Dunavska BB, 11158 Palilula, Beograd
Kontakt telefon: +38163445253
E-mail: bregavabg@sezampro.rs

Firma je osnovana 1995. godine i na početku svog poslovanja preduzeće se bavilo prodajom građevinskog materijala. U kasnijoj fazi poslovanja, preduzeće je počelo da se bavi obradom gvožđa i proizvodnjom armaturnih mreža u skladu sa zahtevima tržišta. Osnivač i vlasnik firme je Saša Kresović čije dugogodišnje iskustvo i znanje predstavlja siguran oslonac za budući razvoj. Preduzeće Bregava doo posvećeno je očuvanju konstantnog kvaliteta svojih proizvoda, tehnološkom unapređenju proizvodnog procesa, kao i održavanju dobrih poslovnih odnosa sa kupcima i dobavljačima. Svoju reputaciju gradili smo na kvalitetu svojih proizvoda i na pouzdanim i dugoročnim poslovnim odnosima. Nakon više od 25 godina uspešnog poslovanja na tržištu, možemo se pohvaliti učešćem u velikom broju projekata kao što su Delta City, Ada Mall, TC Galerija, Skyline, Termoelektrana Nikola Tesla, više objekata u sklopu naselja Belgrade Waterfront i Airport city kao i u velikom broju stambenih objekata.

Ponosimo se učešćem na svim dosadašnjim projektima, ali pre svega poslovnim odnosima koje smo gradili dugi niz godina jer su oni odlika naše pouzdanosti, profesionalizma i kvaliteta.

CIP - Каталогизација у публикацији
Народна библиотека Србије, Београд

531/534(048)
51-7(048)
62(048)

INTERNATIONAL Conference on Mathematical Modelling in Mechanics and Engineering (2 ; 2024 ; Beograd)
Booklet of Abstracts / "2nd International Conference on Mathematical Modelling in Mechanics and Engineering", Belgrade, 2.-14. September 2024. ; organized by Mathematical Institute of the Serbian Academy of Science and Arts ... [et al.] ; editor Ivana Atanasovska. - Belgrade : Mathematical Institute SASA, 2024 (Belgrade : CopyPlanet). - 263 str. : ilustr. ; 25 cm

Tiraž 130. - Str. 5: Preface / Ivana Atanasovska. - Bibliografija uz većinu apstarakata.

ISBN 978-86-80593-77-7

a) Механика -- Апстракти б) Примењена математика -- Апстракти в) Инжењерство -- Апстракти

COBISS.SR-ID 148683017